

Università degli Studi di Milano

Department of Chemistry



Doctorate School in Chemical Science and Technologies

Ph.D Course in Chemical Sciences - XXIX Cycle

**REDUCTIVE TRANSFORMATIONS OF THE
NITRO GROUP: FROM HOMOGENEOUS TO
HETEROGENEOUS CATALYSIS**

Ph.D Thesis of:

Dario Formenti

Matr. n. R10642

Advisor: Prof. Dr. Fabio Ragaini

Coordinator: Prof. Dr. Emanuela Licandro

Academic Year 2016/2017

A Sissi, Alessandra e Flavia

Summary

Chapter I - Introduction	1
1. Background and general considerations	1
2. Work described in this thesis.....	3
3. References	4
Chapter II - Reductive cyclization of nitro compounds using CO surrogates	5
1. Background.....	5
2. Results and discussion.....	12
2.1. N,N-Dimethylformamide as CO source	12
2.2. Formate esters as CO sources: alkyl formates.....	14
2.3. Formate esters as CO sources: phenyl formate.....	22
3. Synthesis of the starting materials	35
4. Experimental section	38
4.1. General consideration.....	38
4.2. General analysis methods.....	38
4.3. General protocol for catalytic reactions conducted in a pressure tube and using Schlenk glassware	39
4.4. General protocol for catalytic reactions conducted in autoclave.....	39
4.5. GC quantitative analysis for catalytic reactions	39
4.6. Isolation of reaction products	40
4.7. General protocol for FT-IR investigation under standard catalytic conditions (pressure tube)...	40
4.8. General protocol for FT-IR investigation under Schlenk conditions (kinetics)	40
4.9. CV procedure.....	40
4.10. Synthesis of phenyl formate	41
4.11. Preparation of Pd and Ru precursors	41
4.12. Preparation of substrates.....	43
4.13. Indoles and other heterocycles	58
4.14. NMR Spectra.....	66
Chapter III - Co and Fe Doped-Carbon-Based Heterogeneous Catalysts for the Selective Hydrogenation of Nitroaromatics	117
1. Background.....	117
2. Transition-metal based heteroatom-doped carbon catalysts: general overview and introduction to the presented work.....	121
3. Fe ₂ O ₃ /NGr@C- and Co-CO ₃ O ₄ /NGr@C-catalysed hydrogenation of nitroarenes under mild conditions	125

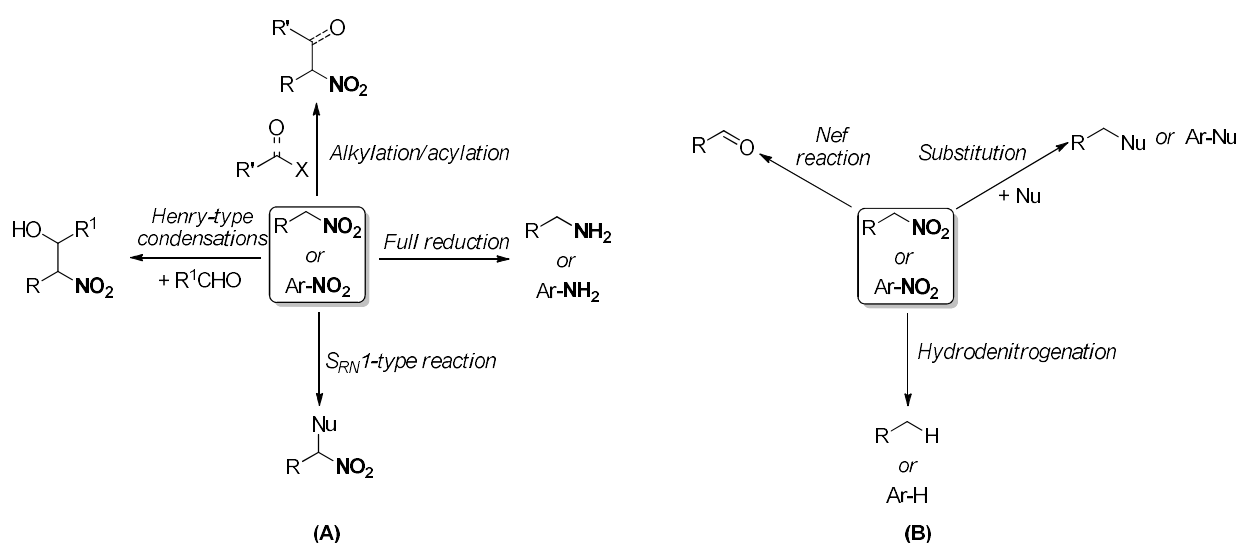
4. Ar-BIANs and related α -diimine Co complexes as precursors for heterogeneous catalysts: on the role of nitrogen	132
5. Conclusion.....	150
6. Supplementary catalytic data and experimental section.....	151
6.1. General methods – reagents, solvents and manipulations	151
6.2. General methods - analysis and characterisation.....	151
6.3. General methods - catalysts preparation.....	152
6.4. General methods –catalytic reactions in the autoclave.....	152
6.5. General methods - recycling experiments	153
6.6. Preparation of Ar-BIANs and related α -diimine complexes	153
6.7. Additional catalytic data, catalysts characterisations, control experiments and characterisation of the catalytic reduction products.....	156
6.7.4. Additional characterisation data (STEM, EDX and XPS) for Co/L1, Co/L2, Co/L3 and Co/L7 catalysts	160
6.7.5. MS spectra of side-products detected in the catalytic run employing 1n as substrate.....	163
6.7.6. Isolated products: 2-aminoresorcinol and aminoflutamide (2aa and 2ab).....	164
6.8. NMR.....	165
References	175
Chapter IV - Appendix	178

Chapter I

Introduction

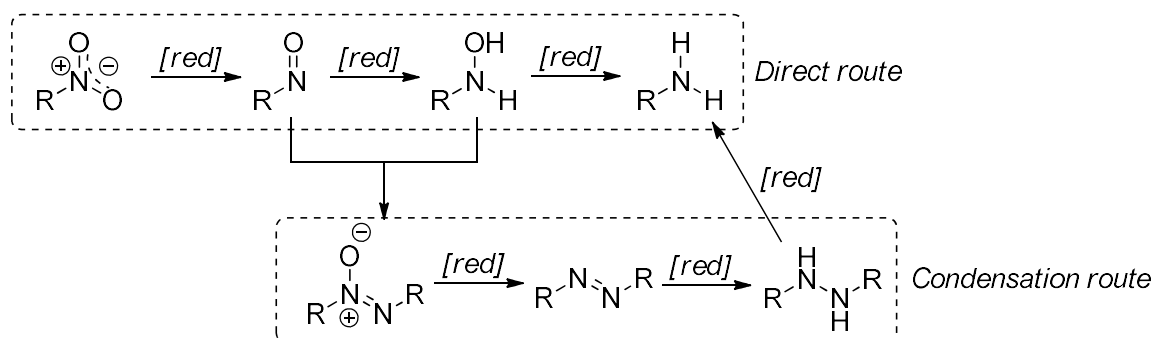
1. Background and general considerations

Nitro group and related compounds occupy a prominent place in chemistry. Although the presence of the nitro group in naturally-occurring compounds is rare (Chloramphenicol and 3-nitropropanoic acid), both aliphatic and aromatic nitro compounds are used as such for the preparation of dyes, energetic molecules (explosives) and, more recently, materials. However, the peculiarity of nitro group is represented by its flexibility of transformations, both from alkyl^[1] and aryl derivatives,^[2] that cover many field of organic synthesis.^[3] These reactions can be primarily divided into two main categories: in the first one fall all the reactions in which the N atom of the nitro group still remains bound in the target molecule (maintaining or not its oxidation state) whereas in the second category nitro group is replaced by other moieties thus missing the N atom. These transformations are depicted in Scheme 1 (A) and (B), respectively.



Scheme 1. Transformations of nitro compounds: general overview.

Owing to the high oxidation state of nitrogen in the nitro group (+3), it is possible to transform it into reduced forms. A classic reaction in this field is represented by the well-known reduction of nitro group to the corresponding amine (a 6-electron process). Several detailed mechanistic studies revealed that many intermediates are involved in this transformation (both in the *direct* or in the *condensation route*) namely nitroso, hydroxylamine, azoxybenzene, azobenzene and diphenylhydrazine (Scheme 2).



Scheme 2. Reduction of nitro compounds to amines: direct and condensation route.

Although they are detected as intermediates, their role does not terminate here. In fact, owing to their unique reactivity, they are useful compounds that find applications in many fields^[4] and they can serve as starting point for the preparation of other molecules, in particular heterocycles. The rich chemistry of nitroso compounds and azobenzenes is a valuable example as reviewed by Gowenlock^[5], Zuman^[6], Krebs^[7] and Miller^[8].

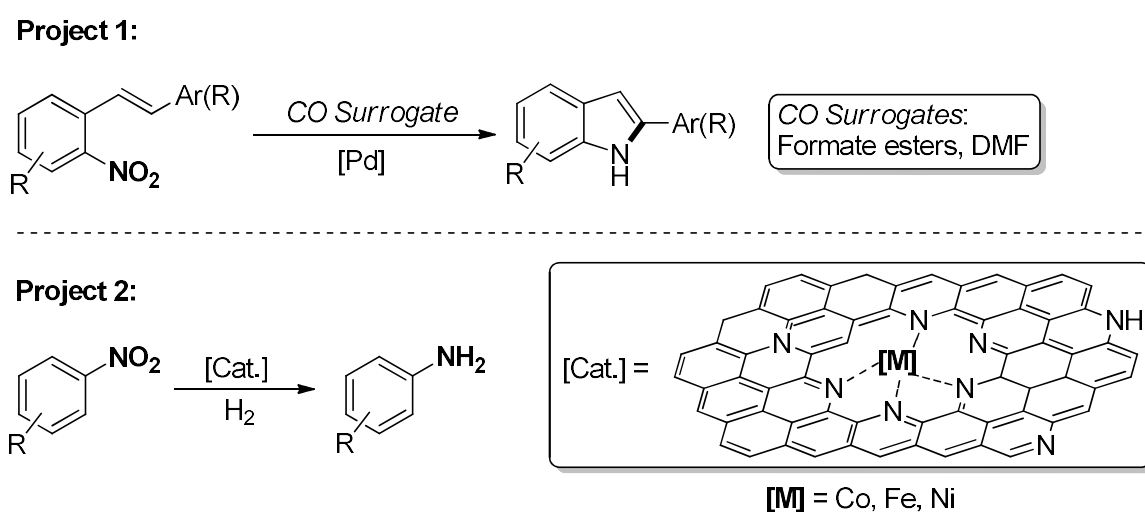
Many of the transformation described in Scheme 1 were developed as stoichiometric processes. However, especially during the last century, many of these reactions reborn as catalytic (both homogeneous or heterogeneous) transformations. Catalysis is a key-technology for a virtuous manufacturing of bulk and fine chemicals. It allows producing chemicals avoiding the formation of undesired and useless stoichiometric side products that requires energy and money for their wasting. By using the correct catalyst, it is possible not only to accelerate the target reaction but also to direct the selectivity towards the desired product. Almost 90 % of all the produced chemicals involves, in at least one step, a catalytic transformation. From an economical point of view, the value of goods which is annually produced by catalytic processes amounts to 400 billion € whereas the current catalyst market is estimated to be 10 billion €. Catalysis is applied for the production of bulk (ammonia, acetic acid, methanol, polyethylene, refinery processes), fine and specialty chemicals (agrochemicals, pharmaceuticals, flavors), energy processing, food processing and environmental chemistry. The center role of catalysis science is further demonstrated by the great number of Noble Prizes that were awarded to scientists working in this field.

Catalysis can be mainly divided into two different types: homogeneous and heterogeneous. Although the differences between these categories are well-known, it has to be underlined that in the last years the gap between them was partially filled. The need for such marriage derived from the fact that whilst homogeneous catalysts are difficult to separate, heterogeneous ones mostly exhibit moderate activities and/or selectivities

with respect to the homogeneous counterparts. In the light of this, the manufacture of active and selective catalysts (especially if based on abundant and biocompatible first-row transition metals) that can be easily recovered and reused (a key-factor in industry), is one of the major goals in the catalysts field and, in general, in synthetic chemistry. During the last decades, a large number of catalysts or catalytic materials that belonging to the latter category appeared in the literature. Examples include well-defined complexes supported on polymeric matrix or inorganic solids, soluble or supported nanoparticles, nanoclusters, metal-organic frameworks (MOFs) or immobilized enzymes. Despite the excellent results that in some cases were achieved, industry still uses “classic” catalysts to obtain bulk and fine chemicals. The cause of this reticence should not be found in a low quality of the published works but in an industrial attitude that is composed by a plethora of factors in which innovation sometimes does not occupy a privileged place. In fact, money, amortization and several technological features are usually at the base of the implementation of new chemical processes.

2. Work described in this thesis

This thesis focuses its attention into two different aspects of catalysis. In the first part (Project 1, Scheme 3), transition-metal complexes were used as homogeneous catalysts for the preparation nitrogen-containing heterocycles (especially indoles) using liquid sources of carbon monoxide. In the second part (Project 2, Scheme 3), in collaboration with Prof. Matthias Beller (Leibniz Institute for Catalysis-LIKAT, Rostock), doped-carbon heterogeneous non-noble metal catalysts were employed as catalytic materials in the hydrogenation of nitroaromatics. In both cases, nitro compounds were used as valuable starting materials corroborating their central role in organic chemistry. Equally, mechanistic aspects (especially kinetics) were taken into account showing how they can play a pivotal role in understanding not only the specific reaction mechanism but also how a catalytic system can be further improved.



Scheme 3. Projects presented in this thesis.

3. References

- [1] For reviews in the field see: (a) R. Ballini, S. Gabrielli, A. Palmieri, M. Petrini, *Curr. Org. Chem.* **2011**, *15*, 1482-1506; (b) R. Ballini, S. Gabrielli, A. Palmieri, CRC Press, **2011**, pp. 53-78; (c) R. Ballini, A. Palmieri, L. Barboni, *Chem. Commun. (Cambridge, U. K.)* **2008**, 2975-2985.
- [2] For review in the field see: (a) G. Booth, in *Ullmann's Encyclopedia of Industrial Chemistry*, Wiley-VCH Verlag GmbH & Co. KGaA, **2000**; (b) M. Dugal, in *Kirk-Othmer Encyclopedia of Chemical Technology*, John Wiley & Sons, Inc., **2000**.
- [3] N. Onu, *The Nitro Group in Organic Synthesis*, John Wiley & Sons, Inc., **2001**.
- [4] (a) R. Raue, J. F. Corbett, in *Ullmann's Encyclopedia of Industrial Chemistry*, Wiley-VCH Verlag GmbH & Co. KGaA, **2000**; (b) E. Merino, *Chem. Soc. Rev.* **2011**, *40*, 3835-3853.
- [5] B. G. Gowenlock, G. B. Richter-Addo, *Chem. Rev.* **2004**, *104*, 3315-3340.
- [6] P. Zuman, B. Shah, *Chem. Rev.* **1994**, *94*, 1621-1641.
- [7] W. Adam, O. Krebs, *Chem. Rev.* **2003**, *103*, 4131-4146.
- [8] B. S. Bodnar, M. J. Miller, *Angew. Chem. Int. Ed.* **2011**, *50*, 5630-5647.

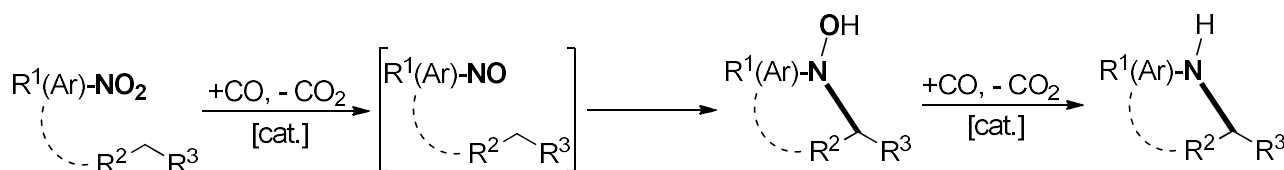
Chapter II

Reductive cyclization of nitro compounds using CO surrogates

1. Background

As discussed in the previous chapter, the reduction of nitro compounds to the corresponding amines proceeds smoothly under the action of a large variety of both stoichiometric reagents (based on low-valent sulfur, titanium, tin, selenium or iron compounds) and catalysts (see Chapter III for further information). However, the selective conversion of nitro groups into the intermediates of the latter transformation is a much more challenging goal. Around the half of the previous century, the use of pressurized CO as the selective reductant towards nitro group became an emerging strategy for converting aromatic nitro compounds into azo- or azoxyarenes.^[1] These transformations employ both homogeneous and heterogeneous catalysts. The use of CO as the reductant offers many advantages in terms of selectivity with respect to hydrogen. In fact, hydrogen is able to reduce almost all the unsaturated functional groups (nitro included) in the presence of numerous transition metals (both homogeneous complexes and supported metals). Moreover, hydrogen is typically not selective in interrupting the reaction at the stage of azo- or azoxybenzene, leading to the unavoidable formation of the fully reduced product (aniline). Unfortunately, the selective transformation of aromatic nitro compounds into nitroso ones is very problematic because of the further facile consecutive reduction of the target nitroso derivative. In confirmation of this, to the best of our knowledge, no example of transformation of nitroarenes to nitrosoarenes are present in the literature. In fact, the most viable route for the preparation of the latter is represented by amine oxidation. However, nitroso compounds are very powerful aminating agent towards C(sp³)-H and C(sp²)-H bonds enabling the construction of C-N bonds that are central to many biologically-relevant molecules.^[2] Owing to the high reactivity of nitroso derivatives, significant efforts have been made in order to produce them *in-situ* by reduction of nitro compounds with CO followed by a rapid trapping by C-H bonds through amination

reactions. Adopting this strategy, many research groups reported the synthesis of N-containing compounds starting from readily available nitro derivatives (Scheme 1).

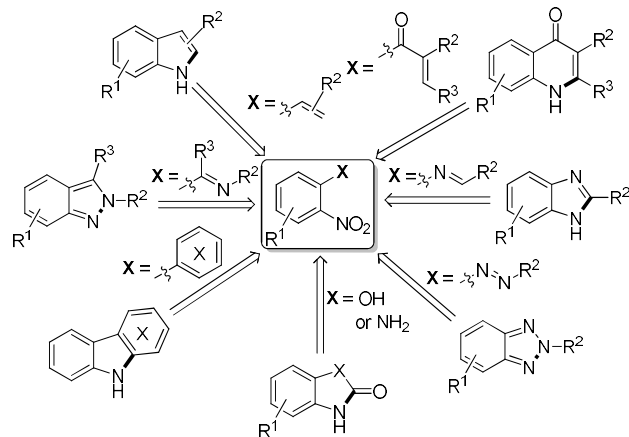


Scheme 1. Catalytic reductive cyclization of nitro compounds using CO as the stoichiometric reductant.

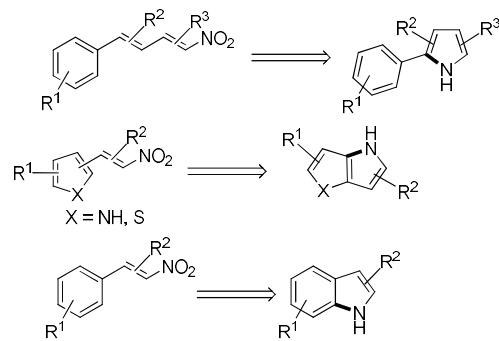
It should be underlined that this transformation is not a metal-mediated C-H activation, since no interaction between the metal catalyst and the C-H bond occurs at any stage of the catalytic cycle. The most employed catalysts are constituted by complexes of Fe, Ru, Rh and especially Pd, coupled with N- or P-based ligands, using CO as the stoichiometric reductant towards the nitro group. Moreover, several examples were reported using S,^[3] Se,^[4] Sn,^[5] low-valent Ti^[6] and especially P-based compounds (Cadogan chemistry)^[7] as stoichiometric reductants. In addition, Peters and co-workers developed a synthetic method based on the cathodic electrochemical reduction of *ortho*-nitrostyrenes leading to the formation of substituted indoles.^[8] Nevertheless, apart for isolated examples,^[9] the latter transformations exhibit low or moderate reactivity and/or selectivity.

During the years, in the field of N-containing heterocycles, the preparation of a large number of molecules has been reported following different approaches, both *intra*- or *inter*-molecular (Scheme 2). The large spectra of accessible compounds clearly demonstrate the broad applicability of substituted nitro derivatives in the preparation of molecules having remarkable biological activity. By using suitable substituted nitro compounds, quinolones, benzimidazoles, carbazoles, indazoles and indoles can be prepared in good yields (*a* in Scheme 2). Recently, we demonstrated that β -nitroolefins and γ -nitrodienes are convenient starting materials for the synthesis of pyrroles, indoles and fused heterocycles (*b* in Scheme 2). Finally, the *inter*-molecular cyclizations of simple nitroarenes with dienes or alkynes paves the way for the preparation of oxazines, N-substituted pyrroles and again indoles (*c* in Scheme 32).^[10]

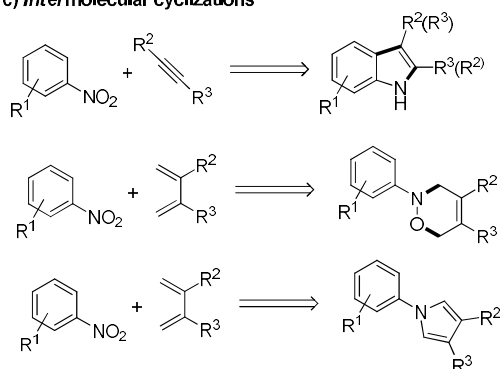
a) *Intramolecular cyclizations from ortho-substituted nitrobenzene*



b) *Intramolecular cyclizations from nitroalkenes and nitrodienes*

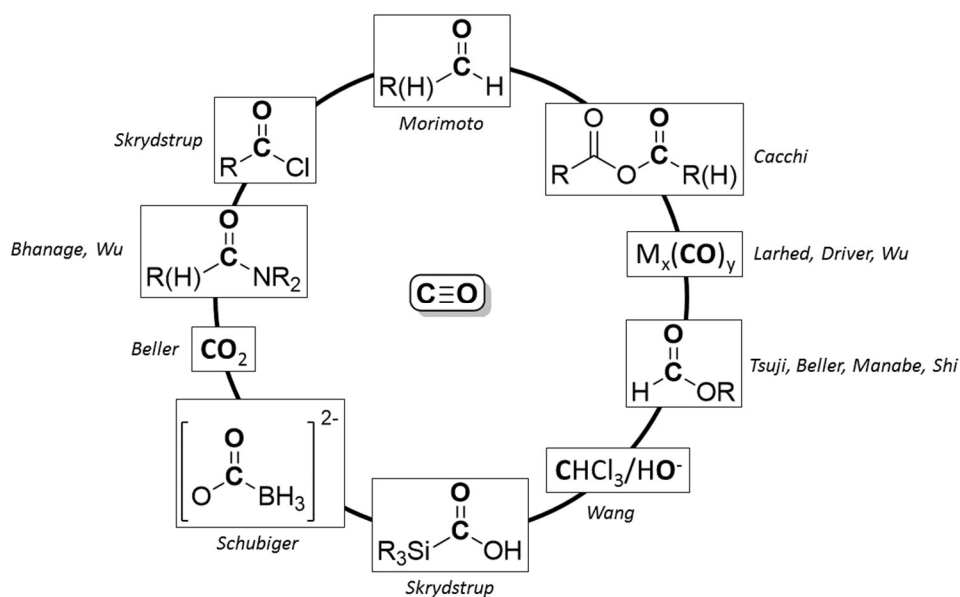


c) *Intermolecular cyclizations*



Scheme 2. Inter- and intra- molecular cyclization of substituted nitro compounds using CO and transition-metal complexes: reactions survey.

Although these reactions exhibited good conversions and selectivities, the use of gaseous and pressurized CO is often a drawback for applications in small or medium scale productions (especially on a laboratory-scale). In fact, CO is a highly toxic, odorless, colorless, tasteless and non-irritating gas. Owing to this features, it is often called *silent killer*. As the consequence, its handling requires the installation of expensive safety measures (sensors) and, in the case of pressurized reactions, special high-pressure equipment such as CO lines and/or autoclaves. In order to circumvent these issues, many research groups in the chemical community described the development and use of organic molecules capable to release one equivalent of carbon monoxide *in-situ*. These molecules were named *CO sources* or *CO surrogates*. Examples include metal carbonyls, formate esters, amides (especially *N,N*-dimethylformamide, DMF), aldehydes (mainly formaldehyde) and carbon dioxide. Along these, other uncommon systems were developed by the group of Skrydstrup (silacarboxylic acids and acyl chlorides, named *COgen* and *SilaCOgen* respectively), Cacchi (mixed formic-acid anhydride) and others (Scheme 3).^[11]



Scheme 3. Examples of CO surrogates.

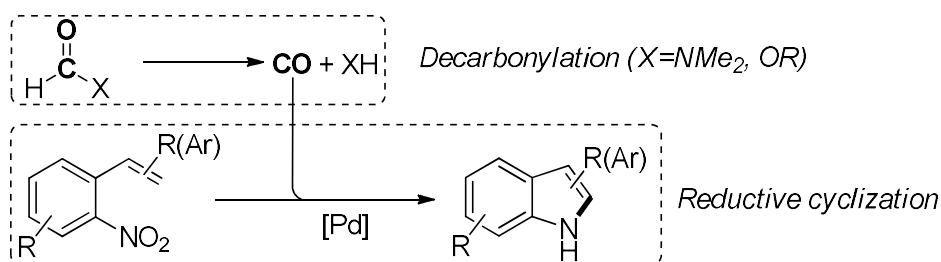
Despite extensive efforts have been made in the field, some of them present intrinsic drawbacks such as toxicity, functional group incompatibility, high cost, demanding procedures for their obtaining or complex reactor configurations (*i.e.*, double chamber reactors). For example, metal carbonyls (especially $\text{Mo}(\text{CO})_6$, one of the most employed CO sources) are very toxic solid compounds. Moreover, at the end of the reaction, the employed metal has to be totally removed from the mixture (and also separated from the catalytically active metal, if present), particularly in the case of pharmaceutically important target molecules. This fact not only rises the whole costs, but requires finding technical solutions for the waste disposal. Despite the use of CO_2 as CO source (both using the Reverse Water Gas Shift Reaction or stoichiometric selective reductants such as silanes) can be assessed as a part of a CO_2 -valorisation vision, its practical employment still necessitates for high-pressure equipment. The CO surrogates developed by Skrydstrup and co-workers, although perform well in many kind of carbonylation reactions, are not commercially available at a low price and otherwise have to be prepared. In addition, owing to their incompatibility with many functional groups (acyl chlorides are sensitive to almost all the known organic and inorganic nucleophiles) two-chamber systems^[12] have to be used thus increasing the costs and posing problems at the stage of scaling-up. Finally, anhydrides can act as CO sources only in the form of the mixed formic-acetic anhydride. Because of its low stability, the latter has to be prepared *in situ*, therefore lowering the appealing of the whole process. Other CO surrogates such as boranocarbonates^[13] and chloroform/alkali^[14] systems were developed during the years. However, in the first case the CO surrogate has to be synthesized from BH_3 and KOH under low-temperature conditions ($-78\text{ }^\circ\text{C}$) using demanding apparatus. Although chloroform and inorganic hydroxides are very cheap chemicals, the reaction between them led to the formation of highly reactive dichlorocarbene, which can interfere with the target carbonylation reaction.

Within the class of formic acid derivatives, formate esters and DMF play a significant role.^[11c, 15] Both of them are commercially available, cheap and stable compounds that exhibit good functional group tolerance.

Furthermore, DMF is one of the most employed solvent in organic chemistry, even in carbonylation reactions. From the 1920s, it is known that formate esters can be decarbonylated to give CO and the corresponding alcohol using strong bases (inorganic hydroxides or metal alkoxides) or strong acids (chlorosulfonic acid, sulfuric acid).^[16] Nevertheless, only at the end of the '80s, the attention of many research groups was focused on the decarbonylation of formate esters under catalytic conditions. The pioneering independent works of Jenner,^[17] Watanabe^[18] and Alper^[19] demonstrated that the decarbonylation reaction of alkyl formates can be catalyzed by metal complexes. $\text{Rh}_6(\text{CO})_{16}$, $\text{Ir}(\text{CO})(\text{Cl})(\text{PPh}_3)_2$ (Vaska's complex) and especially $\text{Ru}_3(\text{CO})_{12}$ were employed as catalysts often in combination with phosphines as ligands. Noteworthy, more than 15 year earlier, Sandner and Hall demonstrated for the first time that Raney®-Ni^[20] and Pd on charcoal^[21] can be effective catalysts in the decarbonylation of many alkyl formates, respectively. Starting from the '90s, the appealing of formate esters as CO alternative for conducting carbonylation reactions in the absence of pressurized carbon monoxide was evaluated. Hydroesterification of alkenes,^[22] carbonylation of alkyl and aryl halides,^[23] hydroformylations,^[24] Pauson-Khand reaction^[25] and nitroarene reductions^[26] were demonstrated to be feasible with alkyl formates (especially using methyl formate). At this stage, even Pd^[23c, 27] or Ni^[28] complexes were successfully employed as catalysts. More recently, aryl formates were reported to be valuable CO surrogates as demonstrated in the seminal paper of Tsuji.^[29] In the following years, many research groups directed their efforts to developing new aryl formates-based carbonylation protocols that avoid the use of free, gaseous or pressurized carbon monoxide. In fact, using the latter CO sources, it was possible to circumvent the severe reaction conditions required for the decarbonylation of alkyl formates. As the consequence, many of the aryl formate-based procedures involves mild reaction conditions and/or low catalyst loadings. The most active groups in the field are represented by M. Beller,^[30] Y. Shi,^[31] Y. Tsuji^[29, 32] and K. Manabe.^[33] Recently, the last author published a stimulating review that covered the field.^[11c] Concerning the chemical nature of the aryl moiety in the aryl formates, Manabe and co-workers demonstrated that EWG groups on the aryl ring led to faster decarbonylation rates. 2,4,6-Trichlorophenyl formate exhibits a complete decarbonylation in 30 minutes at room temperature using triethylamine as stoichiometric reactant (for the mechanistic discussion about the decarbonylation of aryl formates see below). As the comparison, 4-chlorophenyl formate and simple phenyl formate exhibited 24 % and 16 % conversion in 24 hours, respectively.^[34] Nevertheless, owing to its commercial availability and cheapness, phenyl formate is still considered the CO surrogate of choice in the field of formate esters. It has to be underlined that even formic acid itself can be used as CO surrogate. Strong mineral acids such as H_2SO_4 or solid acids such as zeolites can decarbonylate formic acid (in the case of H_2SO_4 , the dehydration reaction is known as Morgan reaction).^[35] However, the use of concentrated sulfuric acid and zeolites is incompatible with almost any type of transformations that involve organic compounds. Therefore, the use of double-chamber reactors is compulsory. In addition, the high corrosiveness of formic and sulfuric acid might be a problem if a non-glassware apparatus (such a metal reactor) has to be used.

DMF is widespread used as reaction solvent owing to its properties of polarity and aproticity accompanied by a high boiling point. However, in some cases DMF can act as a reactant and more specifically as a carbonylating agent. In 1965 Rusina and co-workers described for the first time this behavior demonstrating that if RhCl_3 and PPh_3 were refluxed in DMF, $\text{RhCl}(\text{CO})(\text{PPh}_3)_2$ was formed. Later, Buzina and co-workers described the same behavior of DMF with platinum halides. More recently, Gómez-Benitez and Serp showed that $\text{RuCl}_2(\text{CO})(\text{DMF})(\text{PPh}_3)_2$ and $[\text{PPN}]_2[\text{RuCl}_5(\text{CO})]$ (PPN = bis(triphenylphosphine)iminium chloride) can be prepared from $\text{RuCl}_2(\text{PPh}_3)_3$ and RuCl_3 in refluxing DMF, respectively. Based on these uncommon properties, DMF was evaluated as a CO source in carbonylation reactions, especially aminocarbonylations.^[36] Although the carbonyl group of the final target compound clearly derives from the carbonyl moiety of DMF, an explicit evidence for DMF decarbonylation was albeit never provided. However, the possibility to use DMF as a CO surrogate is still desirable due to its very low price and availability.

In continuation of the work on the synthesis of nitrogen heterocycles from substituted nitro compounds, we studied the feasibility of using DMF and formate esters as practical liquid CO surrogates in these transformations. Thus, the aim of the work is to combine in a one-pot protocol a decarbonylation and a reductive cyclization of *ortho*-nitrostyrene and other nitro compounds (Scheme 4).



Scheme 4. Aim of the work.

During the progress of our work, the group of Driver showed the first example of cyclization of nitro compounds using CO surrogates.^[37] However, toxic and expensive $\text{Mo}(\text{CO})_6$ was employed. As the consequence, this work describes for the first time the use of liquid CO surrogate for the production of heterocycles starting from nitro compounds.

Our attention was mainly focused on the synthesis of indoles. The indole scaffold is ubiquitous in natural, pharmaceutical, agrochemical and in general biologically active molecules (Figure 1).^[38]

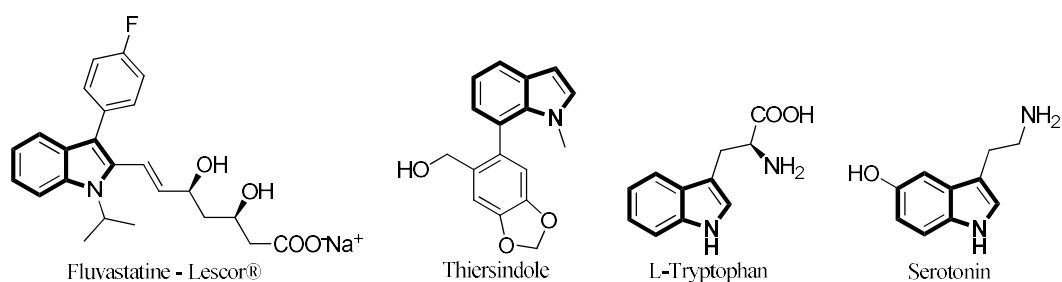
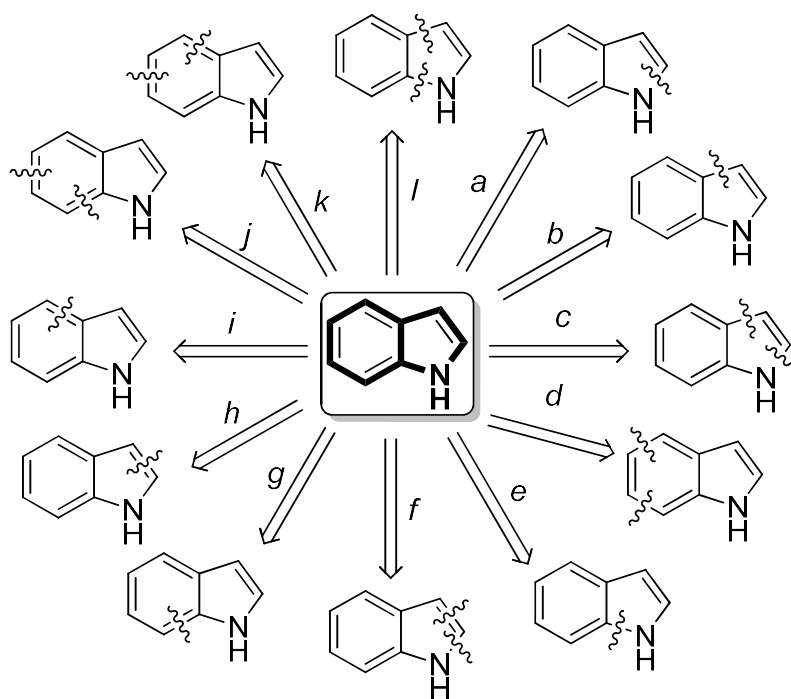


Figure 1. Examples of biologically-relevant molecules containing the indole scaffold.

Furthermore, substituted indoles are often described as *privileged structures* due to their ability of selectively bind biological receptors.^[39] Recently, indole-based functionalized molecules were successfully employed as materials in dyes or organic light emitting diodes (OLEDs).^[40] Starting from the well-known Fischer indole synthesis (first reported in 1883), during the last and the current centuries the literature has been enriched by a huge number of possible synthetic approaches.^[41] A multitude of both stoichiometric and catalytic processes were developed, some of which nowadays represent name reactions (Madelung, Nenitzescu, Bartoli, Batcho-Leimgruber, Larock, Madelung). Regarding catalytic processes, among the various transition metals, Pd represents a catalyst of choice for the synthesis^[42] and functionalization^[43] of indole rings. A general disconnection approach for the preparation of indoles is depicted in Scheme 5. The strategies presented in this thesis belongs to disconnection *a* and *e*.



Scheme 5. Indole synthesis: disconnection approach.

2. Results and discussion

Our investigation started with the selection of the target CO surrogates. We focused our attention to commercially available substances: four formate esters and *N,N*-dimethylformamide were chosen (Figure 2).

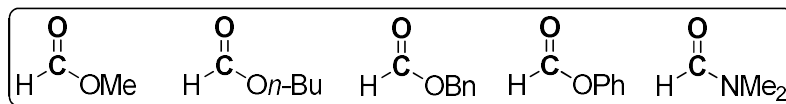
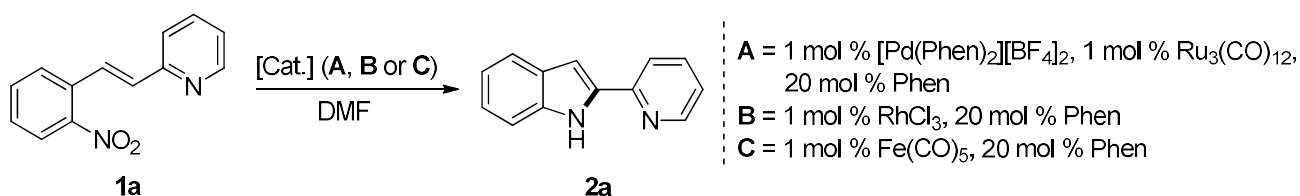


Figure 2

2.1. *N,N*-Dimethylformamide as CO source

Owing to the widespread use of DMF as solvent in many carbonylation reactions (included the reductive carbonylation of nitro compounds), our preliminary efforts have been devoted to evaluate its ability in releasing CO. Initial screening of conditions and metal sources embrace the use of various metal complexes, both alone or in bimetallic systems (Scheme 6).



Scheme 6. DMF as CO source: model reaction and the three employed catalytic systems.

Our preliminary efforts started with the evaluation of the couple $[\text{Pd}(\text{Phen})_2][\text{BF}_4]_2/\text{Ru}_3(\text{CO})_{12}$ as catalytic system for the reductive cyclization of **1a** (Table 1) using DMF both as the CO source and the reaction media.

Table 1. Use of DMF as CO source in the reductive cyclization of **1a** employing **A** (see Scheme 6) as the catalytic system.^a

Entry	Basic promoter	Conversion [%] ^b	Selectivity [%] ^b
1	-	17	56
2	DBU	24	43
3	KOH	96	19
4 ^c	-	36	18

^a Reaction conditions: 0.25 mmol **1a**, mol. ratio [Pd]:[Ru]:Phen:substrate = 1:1:20:100, DMF 10 mL, reaction time 6 h, temperature 143 °C. In entry 2 and 3, mol. ratio basic promoter:substrate = 1:1; ^b Conversion and selectivity were determined using GC (biphenyl as internal standard); ^c Reaction time was 12 h.

In order to avoid CO stripping from the reaction mixture, 143 °C was chosen as the reaction temperature (the boiling point of DMF is 153 °C). Although the catalytic system is active in the desired transformation, selectivities in the indole **2a** remains low or moderate without achieving complete conversion. The addition of a base to the reaction mixture turned out to be positive for the activity (Table 1, entry 2 and 3). Unfortunately, despite higher conversion were registered, selectivities decreased. An elongation of the

reaction time allowed for increasing the conversion (Table 1, entry 4), but a drop in the selectivity was detected.

Catalytic test in the presence of RhCl_3 were conducted under the same reaction conditions employed in the Pd/Ru system.

Table 2. Use of DMF as CO source in the reductive cyclization of **1a employing **B** (see Scheme 6) as the catalytic system.^a**

Entry	Basic promoter	Conversion [%] ^b	Selectivity [%] ^b
1	-	16	70
2^c	-	<1	<1
3^d	-	16	57
4^e	KOH	45	40

^a Reaction conditions: 0.25 mmol **1a**, mol. ratio [Rh]:Phen:substrate = 1:20:100, DMF 10 mL, reaction time 6 h, temperature 143 °C. In entry 4, mol. ratio basic promoter:substrate = 1:1; ^b Conversion and selectivity were determined using GC (biphenyl as internal standard); ^c Phen was omitted; ^d Reaction time was 18 h; ^e Reaction time was 12h.

Even in this case, we found that RuCl_3 is an active catalyst in the reductive cyclization of **1a** using DMF as the CO source (Table 2, entry 1). In order to increase conversion, reaction time was raised to 18 h (Table 1, entry 3). However, the conversion remains the same and a decreasing of the selectivity in the desired product occurred. The latter fact can be ascribed to the low stability of indoles at high temperature and in the presence of metallic species. Entry 2 demonstrated that Phen is an essential component for exploiting the activity of Rh. Following the results obtained in the case of Pd/Ru system in the presence of bases, we attempted to boost both conversion and selectivity adding KOH (Table 2, entry 4). Nevertheless, no significant improvements were obtained.

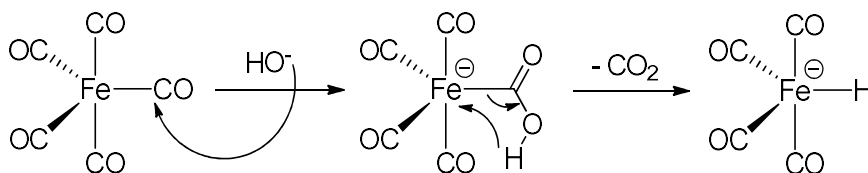
Finally, $\text{Fe}(\text{CO})_5$ were tested as catalyst in the transformation. The interest in the use of iron as catalyst in organic synthesis (both as homogeneous and heterogeneous) has shown an exponential growth in the last two decades due to the increasing demand for environmental friendly and sustainable chemical methods. In fact, Fe is one of the most abundant metals in the earth crust thus being one of the cheapest metal. In addition, its biocompatibility is in agreement with the implementation and development of benign chemical processes. For a more detailed discussion about metal prices, availability and use of Fe-based system in catalysis see Chapter III and references cited therein.

Table 3. Use of DMF as CO source in the reductive cyclization of 1a employing C (see Scheme 6) as the catalytic system.^a

Entry	Basic promoter	Conversion [%] ^b	Selectivity [%] ^b
1	-	<1	<1
2 ^d	KOH	45	7
3 ^{c, d}	KOH	>99	10
4 ^{c, e}	Et ₃ N	<1	<1
5 ^{c, d}	LiOH	23	34
6 ^{c, f}	Et ₃ N	9	96

^a Reaction conditions: 0.25 mmol **1a**, mol. ratio [Fe]:substrate = 1:100, DMF 10 mL, reaction time 6 h, temperature 110 °C. ^b Conversion and selectivity were determined using GC (biphenyl as internal standard); ^c Phen added (mo. ratio Phen: Fe(CO)₅ = 20:1); ^d Mol. ratio basic promoter:substrate = 2:1; ^e Mol. ratio Et₃N:substrate = 1:1; ^f Mol. ratio Et₃N:substrate = 29:1.

As demonstrated by the comparison between entry 1 and 2 in Table 3, the presence of a base is essential for the activity. In fact, it is generally known from the literature that Fe(CO)₅ could require a base for its activation.^[44] The reaction between Fe(CO)₅ and HO⁻ to give tetracarbonylhydridoferrates, HFe(CO)₄⁻, was discovered by Hieber in 1932 (Scheme 7).

**Scheme 7. The Hieber base reaction.**

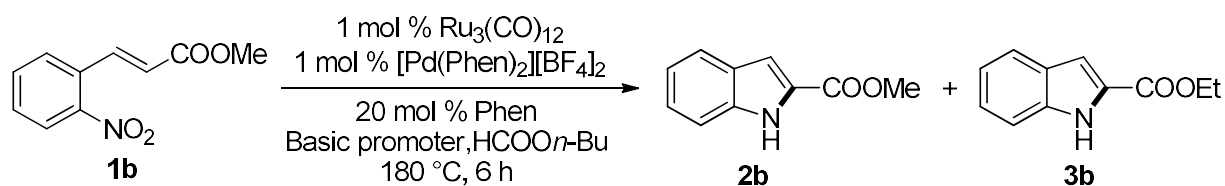
Moreover, the addition of Phen (Table 3, entry 3) doubled the conversion though maintaining the selectivity very low. Other organic (Table 3, entries 4 and 6) or inorganic (Table 3, entry 5) bases were evaluated as promoters. It is known that the couple Fe(CO)₅/Et₃N is able to reduce nitroarenes under catalytic conditions.^[45] However, in the examined reaction, the use of Et₃N did not lead to any conversion or, when used in large amount, only a slight activity was registered.

Despite we demonstrated that DMF can be used as CO source in our cyclization reactions, the obtained results remain overall poor. Thus, we focused our attention to the more promising formate esters.

2.2. Formate esters as CO sources: alkyl formates

As exhaustively described in the introduction of this chapter, alkyl formates were successfully employed as CO sources in many carbonylation reactions employing transition metal complexes as catalysts. Initially, the bimetallic system composed by Ru₃(CO)₁₂ and [Pd(Phen)₂][BF₄]₂ was investigated. In fact, [Pd(Phen)₂][BF₄]₂ was extensively used as catalyst in cyclization reactions using pressurized CO as the reductant whereas Ru₃(CO)₁₂ was found to be an active catalyst in the decarbonylation reaction of many alkyl formate esters. Using (*E*)-methyl-2-nitrocinnamate as the model substrate, various reaction conditions were evaluated (Table 4).

Table 4. [Pd]/[Ru]-catalyzed reductive cyclization of **1b using *n*-butyl formate as CO source: influence of various reaction parameters.^a**

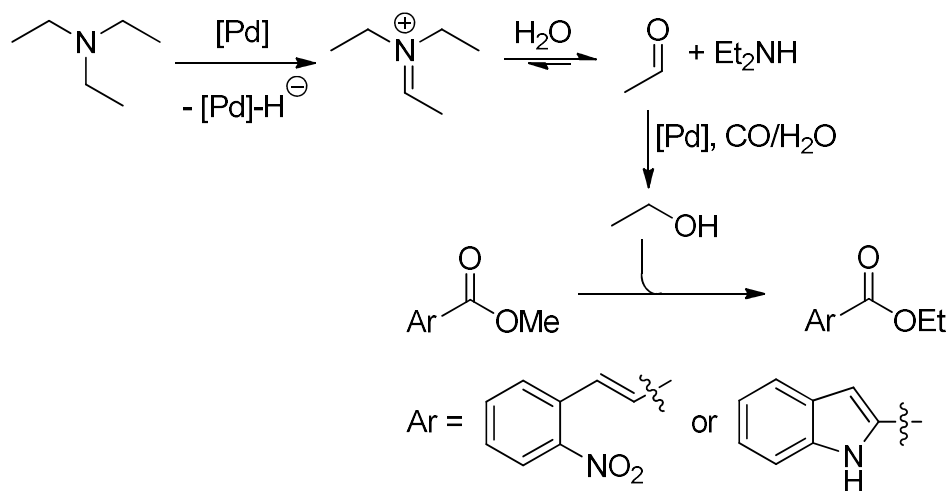


Entry	Basic promoter	1b Conversion [%] ^b	2b Selectivity [%] ^b	3b Selectivity [%] ^b	2b + 3b Selectivity	2b yield
1 ^c	-	<1	<1	<1	<1	<1
2 ^c	Et ₃ N	<1	<1	<1	<1	<1
3 ^d	-	<1	<1	<1	<1	<1
4 ^d	Et ₃ N	<1	<1	<1	<1	<1
5 ^e	Et ₃ N	15	traces	traces	<1	<1
6 ^f	Et ₃ N	72	45	2	47	32
7	Et ₃ N	85	40	8	48	34
8	-	53	23	<1	23	23
9 ^g	Et ₃ N	96	65	21	86	62
10	DBU	>99	29	<1	29	29
11	DABCO	97	24	<1	24	24
12	DIPEA	71	40	<1	40	29

^a Reaction conditions: 0.27 mmol **1b**, mol. ratio [Pd(Phen)₂][BF₄]₂:Ru₃(CO)₁₂:Phen:**1b** = 1:1:20:100; mol. ratio basic promoter:**1b** = 2:1; reaction solvent 10 mL. Reactions were performed into heavy-wall borosilicate glass tubes (ACE Pressure tube). ^b Conversion and selectivity were determined by GC analysis using biphenyl as the internal standard. ^c Reactions were performed in standard Schlenk glassware under N₂ atmosphere at the boiling point of *n*-butyl formate (106-107 °C). ^d CH₃CN was employed as reaction solvent instead of *n*-butyl formate. ^e Only [Pd(Phen)₂][BF₄]₂ was employed as catalyst. ^f Only Ru₃(CO)₁₂ was employed as catalyst. ^g Reaction time was 10 h

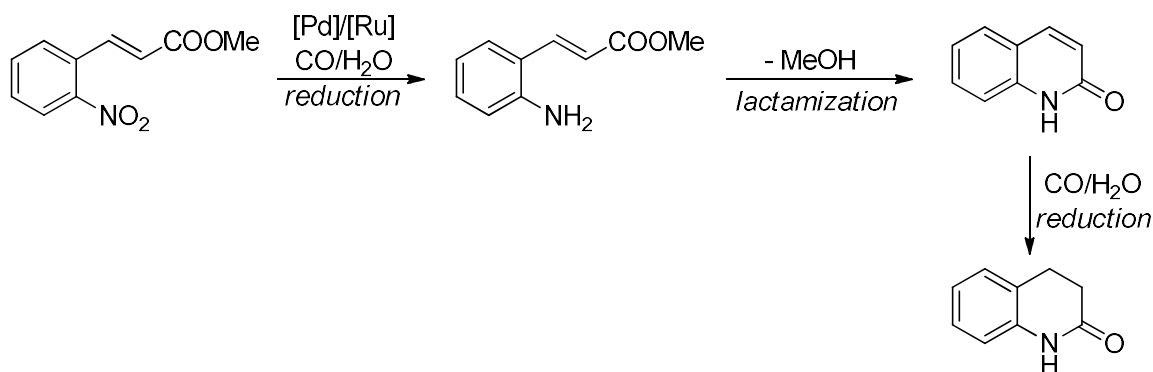
As our first attempt, we carried out the reaction under refluxing conditions in standard Schlenk glassware (Table 34, entries 1 and 2). However, the reaction did not proceed even in the presence of a basic promoter. As expected, if the transformations were carried out in a pressure tube but using a non-CO releasing solvent such as acetonitrile, still the reaction did not proceed. To our delight, the use of *n*-butyl formate both as CO source and reaction solvent, allowed to achieve moderate conversion of **1b** and good selectivity in the desired product. The reaction conducted with [Pd(Phen)₂][BF₄]₂ alone proceeded to a low extent. In fact, Pd complexes are not able to efficiently decarbonylate formate esters. In contrast, the use of Ru₃(CO)₁₂ alone was found to be effective showing a good selectivity but a low conversion in the desired indole. The use of Ru catalysts (and especially Ru₃(CO)₁₂) in the *intra*-molecular reductive cyclization of substituted nitro compounds has been known for years.^[46] The combination of the two metals allows for an increasing of the conversion (Table 4, entry 7). The best result was obtained in the case of 10-hours reaction (Table 4, entry 9): a nearly complete conversion and a satisfactory selectivity in the desired indole was achieved. The addition of Et₃N lead to an increasing of the selectivity in the indole. The use of other organic bases (stronger

than Et₃N) led to very high conversions but accompanied by a low selectivity. In these cases, relatively large amount of 2-aminocinnamic acid methyl ester were detected by GC-MS. The beneficial role of Et₃N in the reductive cyclization of nitro compounds was previously observed.^[47] However, it is noteworthy that, when Et₃N was employed in combination with Pd catalyst as the basic promoter, indole **3b** was detected as the side product. Although the mechanism of this transformation is still unclear, a Pd-mediated Et₃N dealkylation^[48] and a subsequently transesterification could be involved (Scheme 8). Complex [Pd] in Scheme 8 can result from the coordination of Et₃N to the Pd center after displacement of the acetonitrile ligand.^[49] However, owing to the presence of both Phen (that exhibit a stronger coordination ability than Et₃N) as ancillary ligand and acetonitrile as the reaction solvent, a large number of equilibria are contemporary present in the reaction mixture whose position is rather difficult to rationalize. In addition, very small amounts of the ethyl ester of the starting material was detected in the reaction, whose formation can be explained as in the case of **3b**.



Scheme 8. Pathway for the production of ethyl esters.

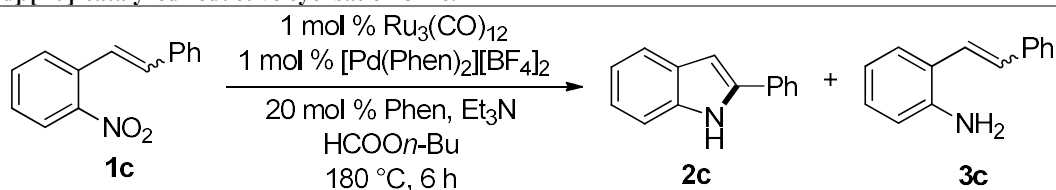
Other by-products of the reaction are by the corresponding amine and the cyclization product of the latter, namely a lactam (Scheme 9). The presence of 2-aminocinnamic acid methyl ester was detected only in the case of reactions conducted in the presence of Ru₃(CO)₁₂ (both alone or in combination with [Pd(Phen)₂][BF₄]₂). This fact can be explained by the ability of this cluster to catalyze the reduction of aromatic nitro compounds to amines using the couple CO/H₂O as the reductant.^[50] Traces of 3,4-dihydroquinolin-2(1*H*)-one were also detected that can arise from the reduction of the conjugated C=C double bond. In fact, despite the use of distilled solvents and dried glassware, adventitious traces of water may be present both in the solvents or in the gaseous nitrogen. However, one must also consider that alcohol dehydrogenation to yield aldehydes and a formal equivalent of dihydrogen (free dihydrogen does not need to be formed) is a well-known reaction, which is known to be catalyzed by several transition metals. Ruthenium is particularly effective in this respect and some butanol is obviously present in the reaction mixture as a byproduct of the formate decomposition. Thus, it is not surprising that some reduction processes occur, especially when ruthenium is present in the reaction mixture.



Scheme 9. Side reaction pathway for **1b**.

Using the reaction conditions previously employed in the case of (*E*)-methyl-2-nitrocinnamate, we extended the optimization study to 2-nitrostyrene for the synthesis of 2-phenylindole (Table 5). Since we obtained the starting material as a diastereomeric *E* and *Z* mixture, we examined the reactivity of both the pure diastereomers and their mixture. At variance with what observed with **1b**, in the current case the corresponding amine **3c** was detected as by-product to a much higher extent. As previously mentioned, the formation of this product can be explained by the ability of Pd and especially Ru in catalyzing the conversion of aromatic nitro compounds into the corresponding amines in the presence of CO and H₂O or alcohols. As expected, the catalytic system composed by Ru and Pd is active in the desired transformation. As demonstrated in the previous case, an elongation of the reaction time allowed for better conversions although a decrease in the selectivity in the desired indole **2c** occurred (Table 5, entry 2). However, the selectivity into **3c** did not significantly vary with the reaction time. This evidence can be attributed to the greater stability of **3c** with respect to **2c** under the reaction conditions. In entry 5, 6 and 7, other bases were evaluated. As demonstrated in the case of **1b**, despite complete (DBU and DABCO) or good (DIPEA) conversions, selectivities are lower than those obtained with Et₃N. It is worth noting that Et₃N is one of the best organic bases both in terms of cost (0.29 €·mL⁻¹) and easiness of removal from the reaction mixture owing to its relatively low boiling point (89 °C).

Table 5. [Pd]/[Ru]-catalyzed reductive cyclisation of **1c**.^a



Entry	<i>Z</i> : <i>E</i> mol. ratio	1c Conversion [%] ^b	2c Selectivity [%] ^b	3c Selectivity [%] ^b
1	2:1	65	69	27
2^c	2:1	>99	52	29
3	Only <i>Z</i>	61	74	20
4	Only <i>E</i>	81	63	19
5^d	2:1	>99	45	22
6^e	2:1	>99	32	31
7^f	2:1	41	23	32

^a Reaction conditions: 0.27 mmol **1c**, mol. ratio [Pd(Phen)₂][BF₄]₂:Ru₃(CO)₁₂:Phen:**1c** = 1:1:20:100; mol. ratio Et₃N:**1c** = 2:1; reaction solvent 10 mL. Reactions were performed into heavy-wall borosilicate glass tubes (ACE Pressure tube). ^b Conversion and selectivity were determined by GC analysis using biphenyl as the internal standard. ^c Reaction time was 10 h. ^d DBU was used instead Et₃N. ^e DABCO was used instead Et₃N. ^f DIPEA was used instead Et₃N.

A close look at the reaction outcomes in the case of pure *E* and pure *Z* isomers evidences that the reaction is slower in the case of the *Z* than in the case of *E* one. However, the selectivity followed an opposite trend. In both cases, the selectivity in the by-product **3c** was not affected by the configuration of the starting material. In order to better understand the observed outcomes, cyclic voltammetric studies were performed. As depicted in Figure 3, three cathodic peaks with peak potentials around -1.12 (A), -1.80 (B) and -2.30 V (C) were detected.

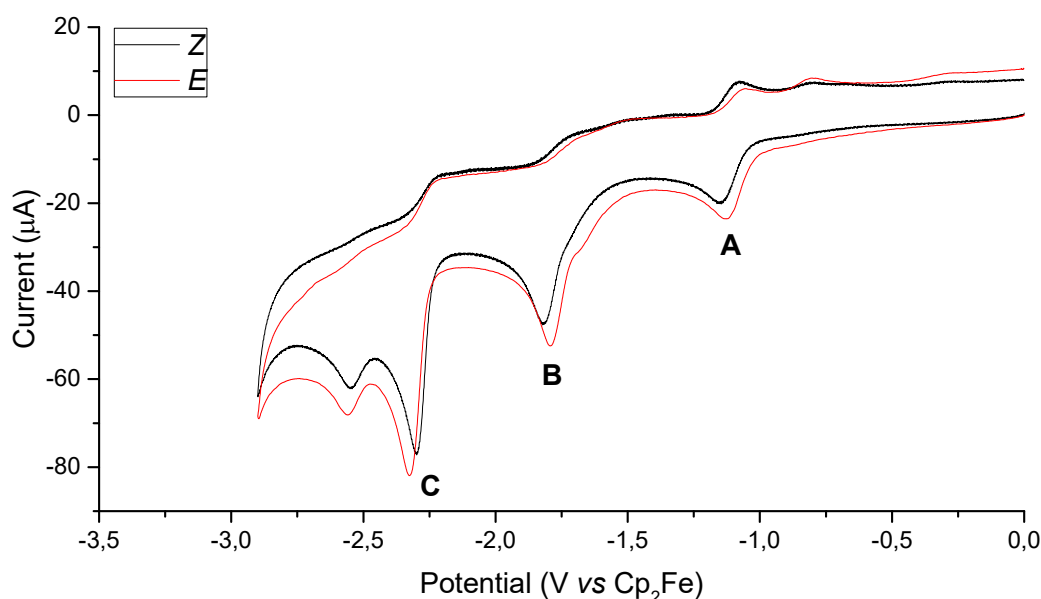
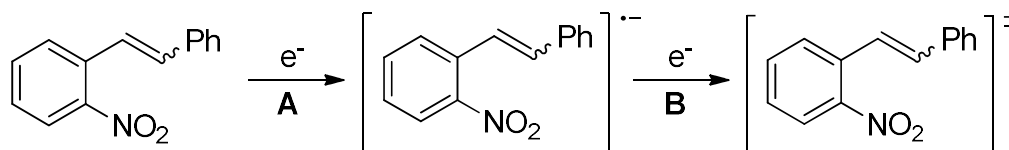


Figure 3. Cyclic voltammograms recorded of (*Z*)-**1c** and (*E*)-**1c**. The CV tests were conducted in anhydrous DMF with a substrate concentration of $6 \cdot 10^{-4}$ M + 0.1 M of TEATFB (= tetraethylammonium tetrafluoroborate) as supporting electrolyte, with a potential scan rate of $0.2 \text{ V} \cdot \text{s}^{-1}$.

According to the literature, the first peak (A in Figure 3) is attributed to the quasi-reversible one-electron reduction of the nitro group to its radical anion.^[8] At more negative potentials, the second peak (B in Figure 3) is attributed to the reversible one-electron reduction of the nitro radical-anion to the nitrodianion (Scheme 10). Finally, the third cathodic peak (C in Figure 3) at around -2.30 V arises from the irreversible reduction of the stilbene moiety. The involved species were depicted in Scheme 10 and the corresponding E_{pc} values are reported in Table 6.

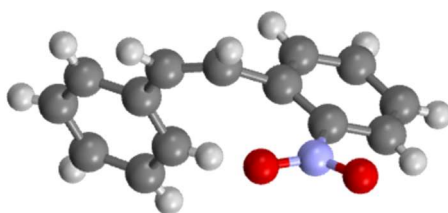


Scheme 10. Electrochemical reduction steps of **1c**.

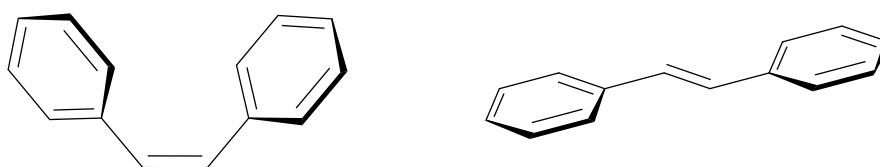
Table 6

Peak	E_{pc} for <i>Z</i> isomer [V]	E_{pc} for <i>E</i> isomer [V]	ΔE_{pc} [mV]
A	-1.15	-1.12	30
B	-1.83	-1.81	20

Analyzing the available data as a whole, it is clear that the *Z* isomer is more difficult to reduce than the *E* one. This is true for both the reduction steps attributed to the nitro moiety. The difference in reactivity can be explained as follows. If we assume that both the diastereoisomers follow the same reduction route for the nitro group, a radical anion is formed in the initial step. As any kind of radical species, the stability of the latter strongly depends on the extent of the electron delocalization. Owing to the steric hindrance in the *Z* isomer, the nitro group should be more tilted with respect to the aryl ring to which it is bound and, moreover, the latter may be located in a twisted position with respect to the central C=C double bond thus leading to a worst electron delocalization with respect to the *E* congeners (a flatter molecule). As confirmation of this, the crystal structure of (*Z*)-2-nitrostilbene clearly shows not only a twisting of the nitro group with respect to the aryl ring but even a remarkable twisting of the two aryl moieties (Figure 4).^[51] The twisting of the nitro group from the aryl plane has long been known to influence its reduction potential and *o*-nitrotoluene is reduced at a 0.07 V more negative potential than its *para* isomer.^[52]

**Figure 4. Crystal structure of (*Z*)-2-nitrostilbene.**

Unfortunately, the literature lacks of crystal structures of the *E* isomer. However, unsubstituted *trans*-stilbene showed a completely flat structure (Figure 5), which presumes an equal (or very similar) structure for the 2-nitro derivative.^[53] For the sake of completeness, *cis*-stilbene showed a distorted conformation in which the two sp^2 angles deviate from the canonical 120° (the actual value is 130°) and the two rings are tilted at a 43° angle with respect to the ethylene plane.^[54] In addition, not only the degree of delocalization in the *Z* isomer is minor than in the *E* one, but furthermore an isomerization is required prior to the amination step. On the contrary, in the *E* isomer the latter step is not necessary. These findings well correlate with the experimental outcomes.

**Figure 5. Structural conformation of *cis*-stilbene and *trans*-stilbene.**

In the aim of decreasing the amount of *n*-butyl formate, mixed reaction media were tested (Table 7). A volumetric ratio of 1:9 in favor of the second solvent was employed. Three solvents with different polarity were chosen. While polar aprotic solvents such as acetonitrile or DMF led to good conversions, the reaction using toluene proceeded very slowly. In every case, selectivities were moderate and lower than those achieved in the case of neat *n*-butyl formate.

Table 7. [Pd]/[Ru]-catalyzed cyclisation of 1b: mixed solvent effect.

Entry	Solvent	1b Conversion [%] ^b	2b Selectivity [%] ^b	3b Selectivity [%] ^b	2b + 3b Selectivity	2b yield
1	CH ₃ CN	53	18	5	23	10
2	DMF	70	40	<1	40	28
3	Toluene	28	21	traces	21	6

Other alkyl formate esters were tested in the desired transformations. Methyl formate was extensively used as CO source in a large variety of reactions.^[55] In addition, among all the tested CO surrogates depicted in Figure 2, it shows the highest value of atom economy because of the low molecular weight of methanol. Owing to the relatively low boiling point of methyl formate (32-34 °C), in order to avoid overpressure troubles (ACE pressure tubes are rated up to 11 bar), all the catalytic reaction that employed methyl formate were conducted in autoclave. Furthermore, benzyl formate was further employed.

Table 8. [Pd]/[Ru]-catalysed reductive cyclization of 1b using methyl and benzyl formates as CO sources.^a

Entry	CO Source	1b Conversion [%] ^b	2b Selectivity [%] ^b	3b Selectivity [%] ^b	2b + 3b Selectivity	2b yield
1	Methyl formate	48	52	-	52	25
2	Benzyl formate	>99	53	-	53	53

^a Reaction conditions: 0.27 mmol **1b**, mol. ratio [Pd(Phen)₂][BF₄]₂:Ru₃(CO)₁₂:Phen:**1b** = 1:1:20:100; mol. ratio basic promoter:**1b** = 2:1; reaction solvent 10 mL. Reaction in entry 2 was performed into heavy-wall borosilicate glass tubes (ACE Pressure tube). Reaction in entry 1 was performed into a 200 mL stainless-steel autoclave using a glass reaction vessel. ^b Conversion and selectivity were determined by GC analysis using biphenyl as the internal standard

As summarized in Table 8, these two CO sources did not allow for better results.

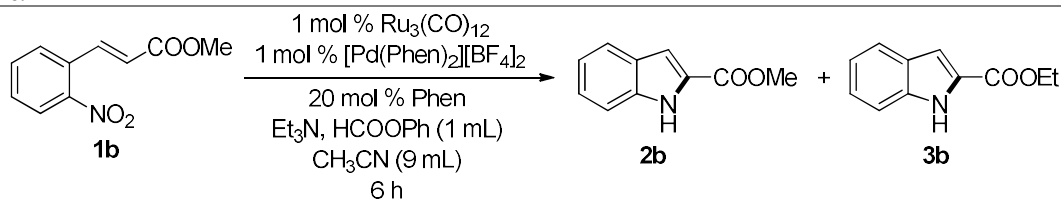
In this section, we demonstrated the feasibility of the use of alkyl formate esters as CO sources in the reductive cyclization of *o*-nitrostyrenes. A combined [Pd]/[Ru] catalytic system in combination with Et₃N under neat conditions of the CO surrogate, allowed for the preparation of indoles in moderate conversions and selectivities. Despite extensive efforts (that included the use of other alkyl formate esters-based CO

surrogates), the obtained results are far from achieving a useful protocol that can be substitute the ones based on gaseous CO. Thus, we proceeded in evaluating the use of phenyl formate as CO source.

2.3. Formate esters as CO sources: phenyl formate

In the last few years, the use of aryl formates as CO source was intensely investigated by many groups achieving very good results in many kind of carbonylation reactions. Thus, we explored the use of phenyl formate in our target transformation. Because of the relatively high cost of phenyl formate with respect to alkyl congeners, its amount was reduced to 1 mL using acetonitrile as the solvent. Firstly, different reaction temperatures were tested (Table 9).

Table 9. [Pd]/[Ru]-catalyzed reductive cyclization of **1b using phenyl formate as CO source: influence of the reaction temperature.^a**

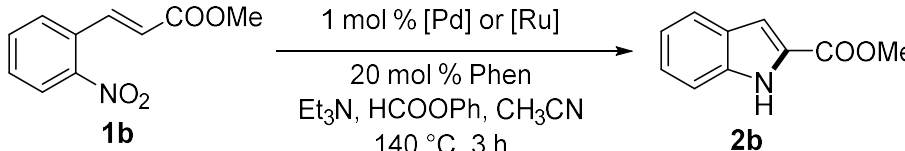


Entry	Reaction temperature [° C]	1b Conversion [%] ^b	2b Selectivity [%] ^b	3b Selectivity [%] ^b	2b + 3b Selectivity [%] ^b
1	180	>99	65	-	65
2	140	>99	92	-	92
3	120	>99	86	-	86
4	90	>99	76	-	76

^a Reaction conditions: 0.27 mmol **1b**, mol. ratio $[\text{Pd}(\text{Phen})_2][\text{BF}_4]_2:\text{Ru}_3(\text{CO})_{12}:\text{Phen}:\mathbf{1b} = 1:1:20:100$; mol. ratio basic promoter:**1b** = 2:1; reaction solvent: 1 mL HCOOPh + 9 mL CH_3CN . ^b Reactions were performed into heavy-wall borosilicate glass tubes (ACE Pressure tube). ^b Conversion and selectivity were determined by GC analysis using biphenyl as the internal standard

It is clear that, although conversion remains complete in all the cases, selectivity is severely influenced by reaction temperature. The highest selectivity was achieved at 140 °C. Temperature above or below this value led to lower values. This fact might be ascribed to two factors. The low selectivity achieved at 180 °C can be imputed to the low stability of indoles at high temperature whereas the relatively low selectivities registered at 120 °C and 90 °C can be attributed to the accumulation of a reaction intermediate. The latter can be *N*-hydroxyindole since the other possible intermediate (*o*-nitrostyrene) immediately reacts under the reaction conditions (see mechanistic investigations for further details). Gratefully, in every case, the formation of **3b** was completely suppressed. Encouraged by the results showed in Table 9, we focused our efforts to optimize the desired transformation using phenyl formate as the CO source. First of all, a screening of Pd and Ru precursors was performed at 140 °C, decreasing the reaction time to 3 h and diminishing the amount of phenyl formate to 0.5 mL (Table 10).

Table 10. Reductive cyclization of 1b: screening of Pd and Ru pre-catalysts.^a



Entry	Pd precursor	1b Conversion	2b Selectivity
		[%] ^b	[%] ^b
1	Pd(CH ₃ CN) ₂ Cl ₂	> 99 (19)	98 (17)
2	[Pd(Phen) ₂][BF ₄] ₂	> 99 (32)	94 (34)
3	Pd(OAc) ₂	> 99 (4)	92 (traces)
4	Pd(dba) ₂	86 (4)	93 (traces)
5	Ru ₃ (CO) ₁₂	23	79

^a Reaction conditions: 0.27 mmol **1b**, 1 mol % Pd catalysts or Ru₃(CO)₁₂, 20 mol % Phen, 500 μ L HCOOPh (that corresponds to 17 equiv. of **1b** or 8.5 equiv. of the CO required by the reaction), 2 equiv. Et₃N (80 μ L), 9.5 mL CH₃CN. Reactions were performed into heavy-wall borosilicate glass tubes (ACE Pressure tube) at 140 °C for 3 h. ^b Conversion and selectivity were determined by GC analysis using biphenyl as the internal standard. ^c Values in brackets refer to the reactions performed omitting Phen.

In all the cases, the employed Pd pre-catalysts were very effective in the transformation leading to complete conversion and almost complete selectivity in the case of Pd(CH₃CN)₂Cl₂. Notably, if the transformations were conducted in the absence of Phen, conversions were poor (Table 10, entries 1 and 2) or negligible (Table 10, entries 3 and 4). Conversely, Ru₃(CO)₁₂ does not provide satisfactory results. Apart specific cases, in many kind of intramolecular cyclization reactions of nitro compounds, Pd/Phen complexes are much more active than Ru-based catalytic systems. In contrast with the previously reported results in the case of alkyl formates, herein the bimetallic systems are not required and only Pd is sufficient to achieve excellent results in terms of both conversion and selectivity. Owing to the relatively high cost of phenyl formate compared to alkyl formates, its amount was optimized using Pd(CH₃CN)₂Cl₂ as pre-catalyst.

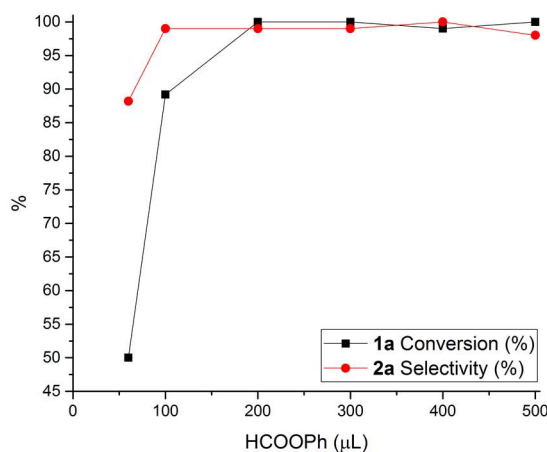


Figure 6. HCOOPh optimization. Reaction conditions: 0.27 mmol **1b**, 1 mol % Pd(CH₃CN)₂Cl₂, 20 mol % Phen, 2 equiv. Et₃N (80 μ L), 10 mL CH₃CN. Reactions were conducted into a sealed ACE Pressure Tube at 140 °C for 3 h. In the case of complete conversion at the end of the reaction, dispersed metallic Pd was observed into the reaction vessel. Conversion and selectivity were determined using GC (biphenyl as internal standard).

As demonstrated in Figure 6, the reaction maintains its efficiency down to 200 μ L, which corresponds to 3.4 times the stoichiometric amount with respect to the required CO (2 equivalents of CO are needed for a complete deoxygenation of a nitro group). Further diminishing of the HCOOPh amount lead to a slight

decreasing of the selectivity and a drop of the conversion. It should be noted that, both purchased phenyl formate (Sigma-Aldrich, code n. 06556) and that synthesized by us (see experimental section for its preparation) performed equally. We further proceeded in the optimization of the Et₃N amount, achieving complete conversion and selectivity with 1 equivalent to **1b** (Figure 7).

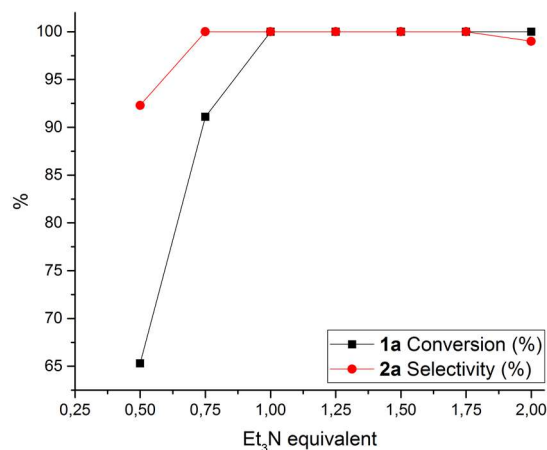


Figure 7. Et₃N optimization. Reaction conditions: 1 mol % Pd(CH₃CN)₂Cl₂, 0.27 mmol **1b**, 20 mol % Phen, 200 μL HCOOPh, 10 mL CH₃CN. Reactions were conducted into a sealed ACE Pressure Tube at 140 °C for 3 h. Conversion and selectivity were determined using GC (biphenyl as internal standard).

Finally, the Phen amount was optimized. Results depicted in Figure 8, showed that just a small amount of ligand (5 mol %) is necessary to achieve both complete conversion and selectivity. Although such low ligand:metal ratios are common in phosphine-based catalytic systems, in the case of nitrogen based ones, because of the general low coordination ability of the latter, relatively high ratio must be used. Thus, our current case represents an exception.

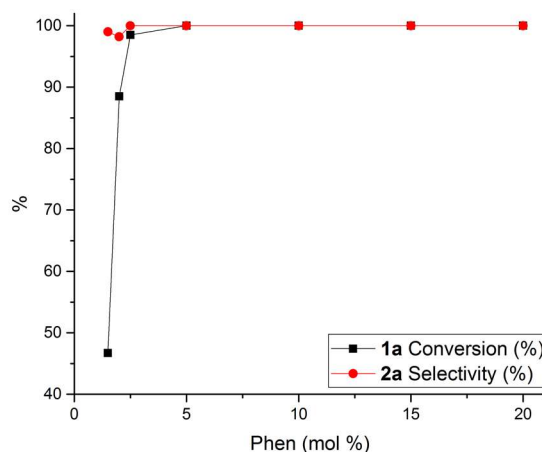


Figure 8. Phen optimization. 1 mol % Pd(CH₃CN)₂Cl₂, 0.27 mmol **1a**, 200 μL HCOOPh, 40 μL Et₃N (1 equiv.), 10 mL CH₃CN. Reactions were conducted into a sealed ACE Pressure Tube at 140 °C for 3 h. Conversion and selectivity were determined using GC (biphenyl as internal standard).

Owing to the relatively mild conditions employed in the case of phenyl formate with respect to the alkyl congeners, we were interested in testing if the reaction can be run in standard Schlenk glassware (note that when *n*-butyl formate was employed under these conditions no catalytic activity was registered at all). Catalytic experiments revealed that if the reaction was conducted into Schlenk glassware, poor conversion

was achieved (Figure 9). Indeed, after 9 h conversion was 8 %. However, if further 200 μL of HCOOPh were added, the reaction was speeded-up achieving 19 % of conversion. As a comparison, if the reaction was performed into a pressure tube, 65 % conversion and 97 % selectivity after 9 h were achieved. This experiment proves that the sluggish reactivity into an open vessel system cannot be imputed to a deactivation of the Pd catalyst but to a very low CO concentration in the liquid phase since it is free to move into the gas phase. As a matter of fact, the use of a pressure tube (or in general of a closed reaction vessel) is crucial for both maximizing the amount of CO in solution and increase the reaction rate.

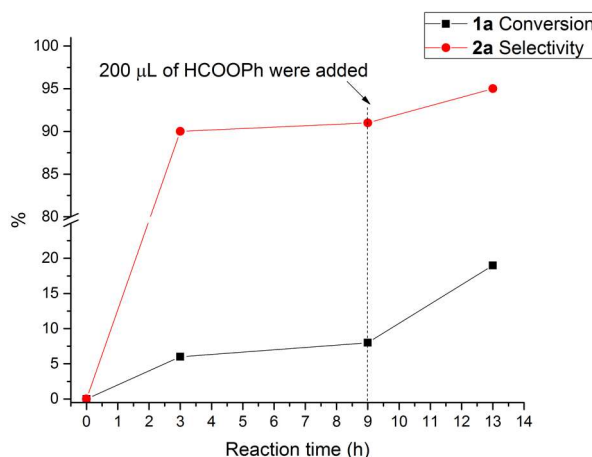
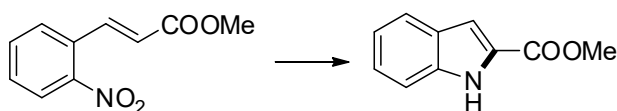


Figure 9. Reaction conditions: 0.27 mmol **1b**, 1 mol % Pd(CH₃CN)₂Cl₂, 20 mol % Phen, 1 equiv. Et₃N (40 μL), 10 mL CH₃CN. The reaction was conducted at reflux temperature. Conversion and selectivity were determined using GC (biphenyl as internal standard).

In order to handle suitable amount of both starting materials and reaction products, we decided to scale-up the reaction by a factor of two. In order not to shift the coordination equilibria in the system, the following variations were made: a) the catalyst and nitroarene amounts were doubled; b) the Phen, Et₃N and CH₃CN amounts were left unvaried; c) the amount of HCOOPh was varied in such a way that its excess with respect to the stoichiometrically required amount remained unchanged.



0.27 mmol - based protocol:

1 mol % Pd(CH₃CN)₂Cl₂
 5 mol % Phen
 6.8 equiv. HCOOPh
 1 equiv. Et₃N
 10 mL reaction solvent

0.54 mmol - based protocol:

1 mol % Pd(CH₃CN)₂Cl₂
 2.5 mol % Phen
 0.50 equiv. Et₃N
 4.4 equiv. HCOOPh
 10 mL CH₃CN

Having the optimized conditions in our hands, we proceeded with the exploration of the reaction scope. To this purpose, various *o*-nitrostyrenes were cyclized to the corresponding indoles. As showed in Figure 10, esters (**2a**, **2b**, **2c**) and amides (**2l**) derived from 2-nitrocinnamic acid were successfully cyclized providing

the corresponding indoles in yields from good to excellent. Indoles substituted in the 2 and/or 3 positions with aryl (**2n**), 2-pyridil (**2h**) and cyano group (**2i**, **2j**, **2k**) were obtained in excellent yields. Cyano groups, due to their synthetic versatility, can be further transformed into other functional groups such as thioamides, tetrazoles, amines or carboxylic acid derivatives. Labile, bromo (**2m**), chloro (**2s**, **2t**) and aldehydic (**2f**) groups were well tolerated affording the desired indoles in moderate to excellent yields. 2-Phenyl-6-azaindoles **2e** was synthesized in very high yield starting from **1e**. Azaindoles are a class of nitrogen rich molecules that found broad application in many fields such as pharmaceuticals, agrochemicals and natural products also exhibiting peculiar photophysical properties.^[56] Furthermore, double cyclization was feasible leading to the formation of a bisindole in good yields (**2o**). Compounds belonging to 2,6-bis(2'-indoyl)pyridine class have been successfully used as ligands in metal-based phosphorescent and electroluminescent devices.^[57] Trifluoromethyl groups on the aryl moiety were outstandingly tolerated leading to the formation of the corresponding indoles in almost quantitative yield. Indole **2r**, bearing a pyrrole moiety in position 2, represent a scaffold for a large family of novel estrogen receptor ligands.^[58] The moderate yield of **2r** can be ascribed to the very low stability of the compound under the reaction conditions. In fact, although the dried crude reaction was stored under nitrogen at low temperature (-20 °C) in the dark, after one night the solid became brown. In addition, when the pure compound was solubilized into distilled CDCl₃ under a nitrogen atmosphere, a black precipitate appeared after few hours. Unfortunately, the cyclization of bis-*o*-nitrostyrene **1v** failed due to the very scarce solubility of the starting material in both acetonitrile or chlorinated solvent (*o*-dichlorobenzene) at various reaction temperatures (up to 180 °C). Irrespective of the reaction time (up to 8 h), in all cases the substrate was recovered almost quantitatively at the end of the reaction without any trace of the desired product.

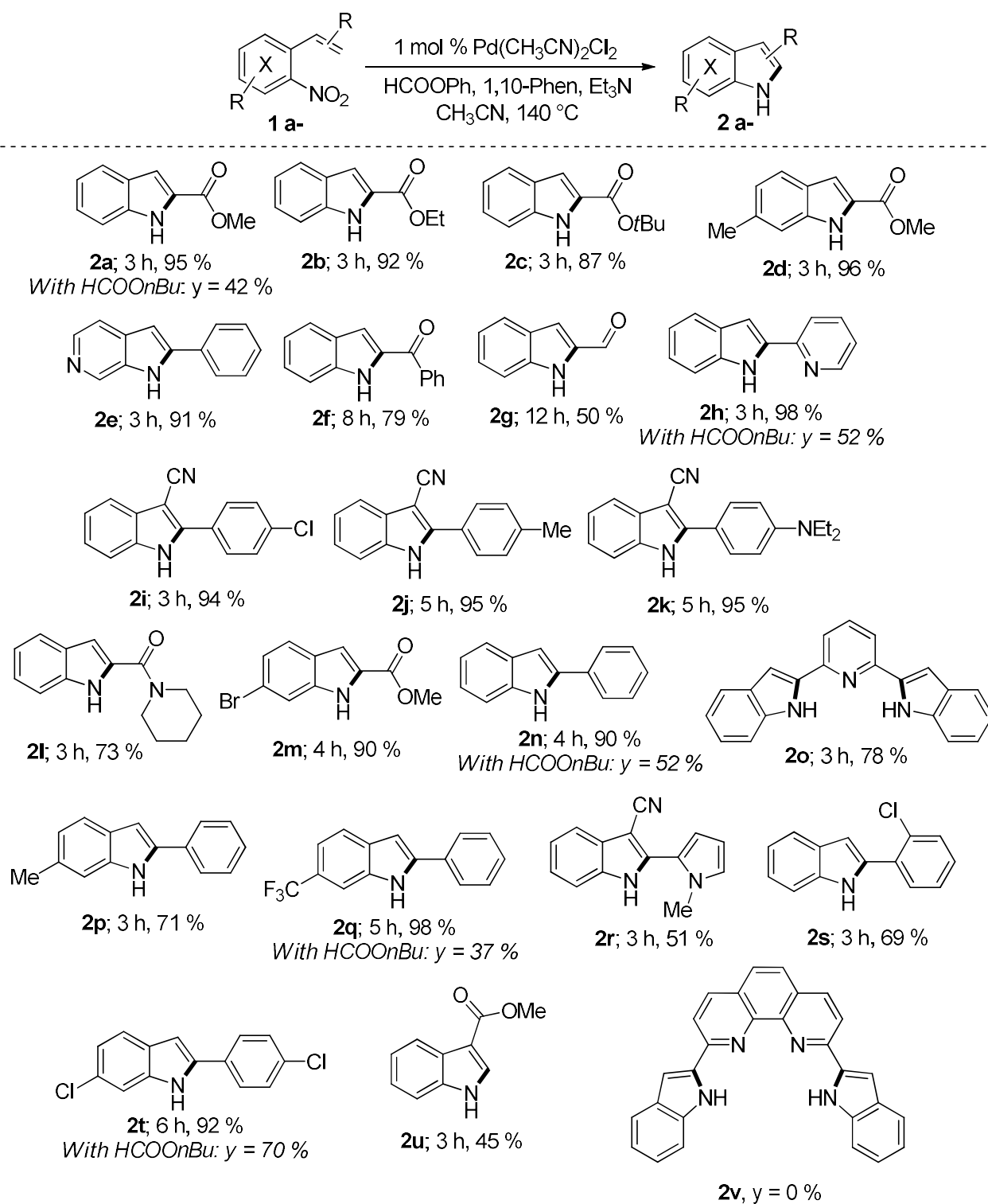
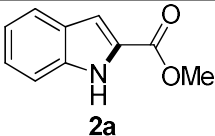
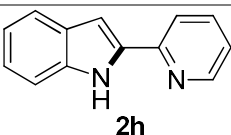
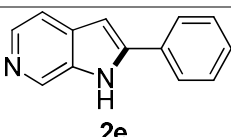
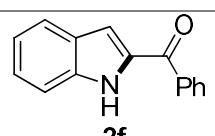
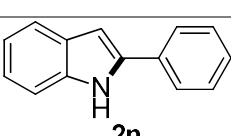
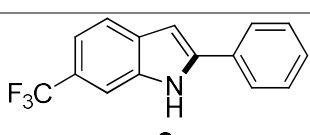


Figure 10. Substrate scope. Reaction conditions: 0.54 mmol nitro compound, 2.5 mol % Phen, 4.4 equiv. HCOOPh (260 μ L) with respect to the starting material, 0.50 equiv. Et₃N (40 μ L), 10 mL CH₃CN. All reactions were conducted into a sealed ACE Pressure Tube at 140 °C for the indicated time.

As the comparison, if the previously investigated protocol based on *n*-butyl formate was applied, lower yields were achieved (see **2a**, **2h**, **2n**, **2q** and **2t**) thus confirming the effectiveness of phenyl formate as CO source. Furthermore, it has to be highlighted that in several cases the achieved yields are larger than those previously reported in the literature using pressurized CO. As demonstrated by Table 11, in almost all the cases our protocol allowed for higher yields.

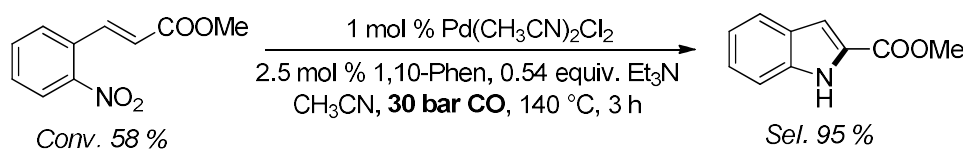
Table 11. Comparison with indoles synthesized from *o*-nitrostyrenes using gaseous CO: selected example from the literature. The maximum achieved yields for each compound are here reported.

Entry	Indole	Catalytic system	Yield [%]	Reference
1		[Rh] ^a , 7 bar CO, 100 °C, 20 h	83	[59]
2		Ru ₃ (CO) ₁₂ , 80 bar CO, 220 °C, 5 h	63	[60]
3		Pd(dba) ₂ /Phen 6 atm, 120 °C, 24 h	87	[61]
4		[Rh] ^a , 7 bar CO, 100 °C, 20 h	92	[59]
5		Pd(OAc) ₂ , PPh ₃ , 4 atm CO, 70 °C, 15 h	91	[62]
6		Pd(OAc) ₂ /TMPhen ^b Mo(CO) ₆ ^c , 100 °C, 10 h	55	[37b]

^a [Rh] = [Rh(CO)₂(TMEDA)]⁺[RhCl₂(CO)₂]⁻; ^b TMPhen = 3,4,7,8-tetramethyl-1,10-phenanthroline; ^c Mo(CO)₆ was employed as CO source instead of gaseous CO.

The latter outcomes clearly demonstrate that our procedure is a virtuous alternative to the free-CO based ones not only in terms of less dangerousness and costs, but even for synthetic purposes.

Moreover, if the model reaction was conducted under CO pressure under optimized conditions (but omitting the phenyl formate), a decreased activity was registered obtaining the desired product in very high selectivity but accompanied with a moderate conversion.



In order to broaden the scope of our protocol, we decided to extend our method to other reductive cyclization reactions of substituted nitro compounds. More specifically, carbazoles, quinolones and indoles from β -methyl- β -nitrostyrenes were produced in low to good yields (Figure 11). Despite the obtained results

are not comparable to those reported in the case of *ortho*-nitrostyrenes, it has to be underlined that we did not further optimized the reaction conditions.

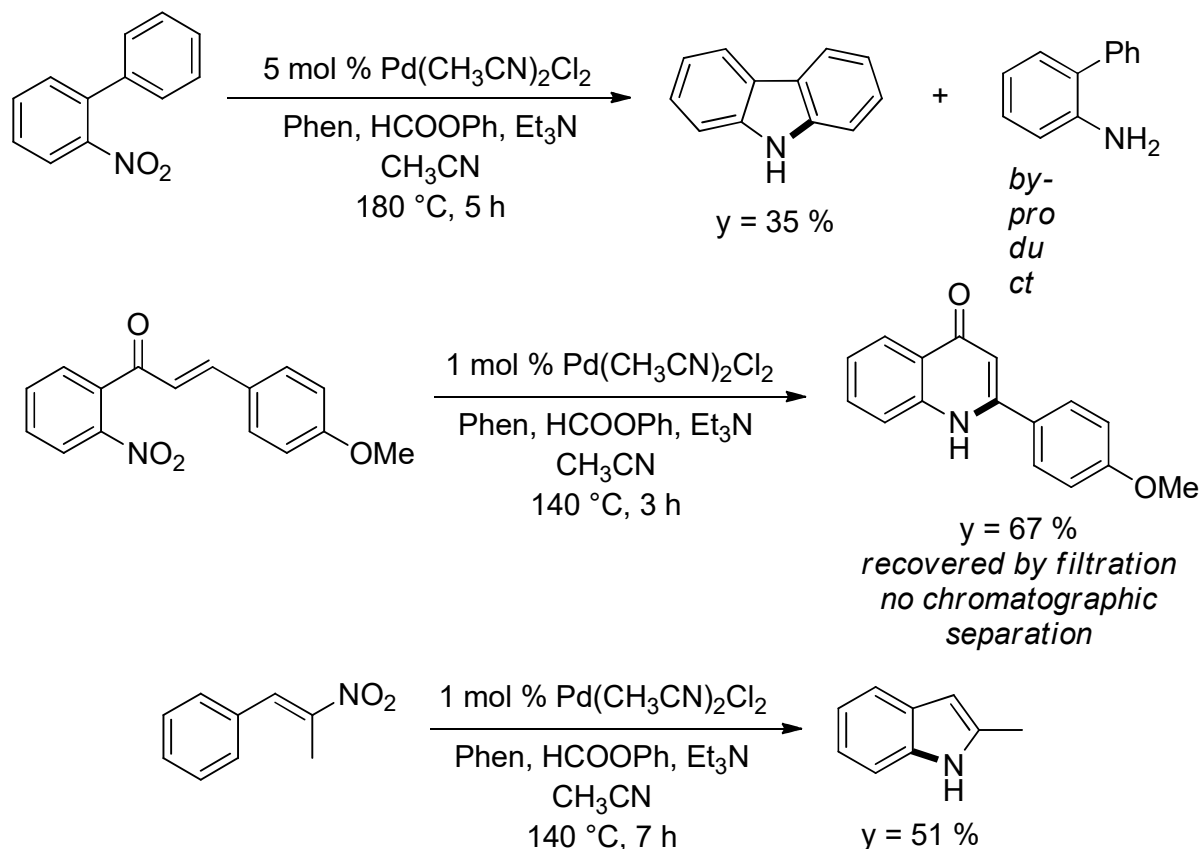


Figure 11. Other N-heterocycles from the Pd-catalysed reductive cyclization of substituted nitro compounds using HCOOPh as the CO source.

In order to gain insight into the reaction mechanism, the decarbonylation reaction was independently studied. Various previous works in the literature claimed that phenyl formate can be decarbonylated by bases, e.g. triethylamine.^[32, 34] On the contrary, to the best of our knowledge, only one work reported that $\text{Pd}(\text{OAc})_2$ in combination with P-based ligands (both chelating or not) is able to perform this transformation.^[29] In order to discriminate between this two kind of activations, as the first test, HCOOPh was subject to react with Et_3N or $\text{Pd}(\text{CH}_3\text{CN})_2\text{Cl}_2$ at 140 °C in a pressure tube (Figure 12 and Figure 13, respectively). After 3 h, in the first case complete conversion was achieved (the characteristic IR peaks at 1741 and 1761 cm^{-1} corresponding to the symmetric and asymmetric stretching of $\text{C}=\text{O}$ were used to detect the presence or the absence of HCOOPh into the reaction mixture) and a 3400 cm^{-1} broad band ascribed to phenol appeared. On the contrary, in the second case (reaction with $\text{Pd}(\text{CH}_3\text{CN})_2\text{Cl}_2$) no conversion was detected at all. A control experiment carried with HCOOPh alone in CH_3CN , rules out a thermally-driven decarbonylation reaction. In addition, Ph alone was found to be inactive in the same transformation.

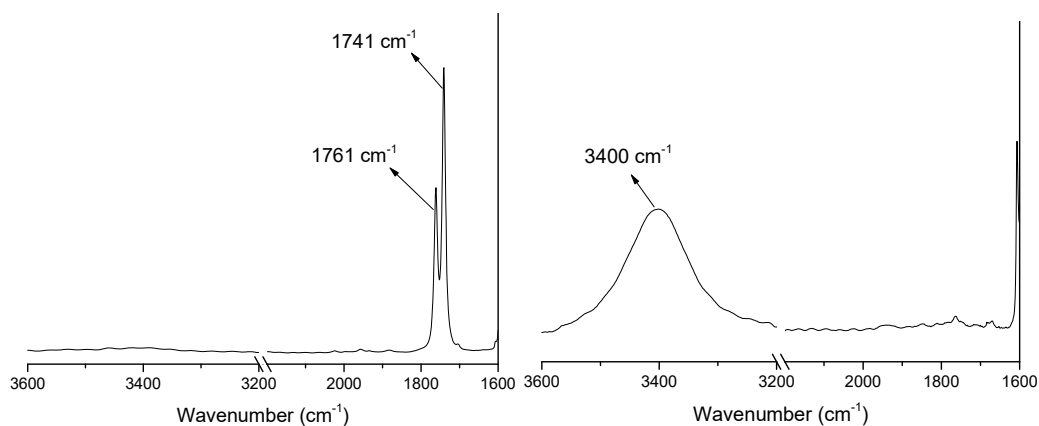


Figure 12. Reaction of HCOOPh with Et₃N at t=0 (left) and after 3 h (right). Reaction conditions: HCOOPh 1 mmol, Et₃N 1 mmol, CH₃CN 5 mL. Reaction was conducted into a sealed ACE Pressure Tube at 140 °C for 3 h.

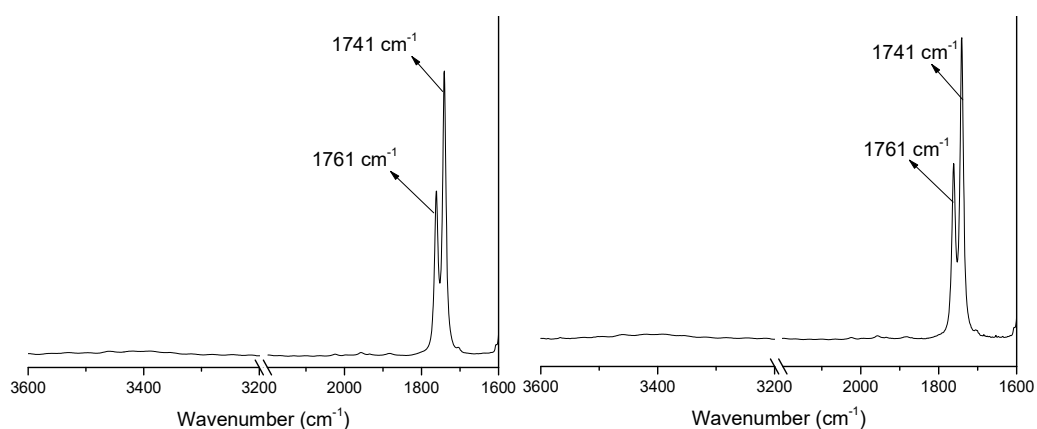
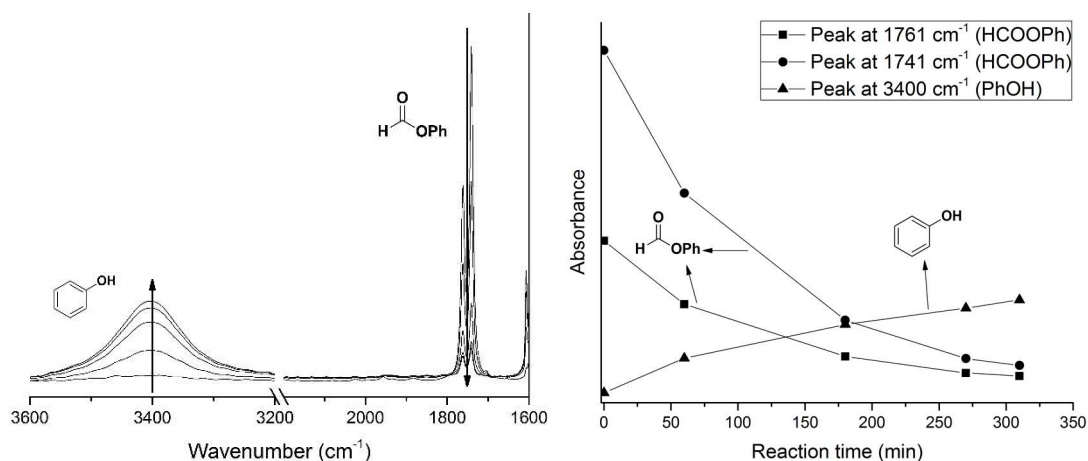


Figure 13. Reaction of HCOOPh with Pd(CH₃CN)₂Cl₂ at t=0 (left) and after 3 h (right). Reaction conditions: HCOOPh 1 mmol, 5 mol % Pd(CH₃CN)₂Cl₂, CH₃CN 5 mL. Reaction was conducted into a sealed ACE Pressure Tube at 140 °C for 3 h.

For the purpose of better following the course of the transformation, the reaction of HCOOPh with Et₃N was performed under refluxing conditions (CH₃CN as the solvent) and monitored by FT-IR spectroscopy (Figure 14). A clear decrease of the two peaks corresponding to the C=O bonds and a contemporary increase of the band at 3400 cm⁻¹ were detected during the time. Noteworthy, at all stages of the reactions, no other C=O stretching bands were detected. Kinetic studies revealed that the reaction follows a first kinetic order with respect to HCOOPh and Et₃N leading to a global second order ($r = k[\text{HCOOPh}][\text{Et}_3\text{N}]$).



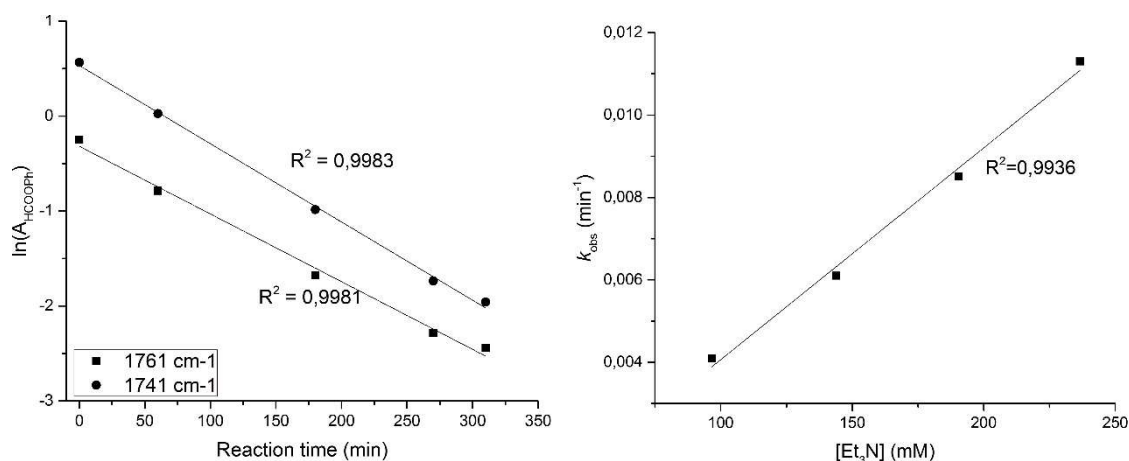
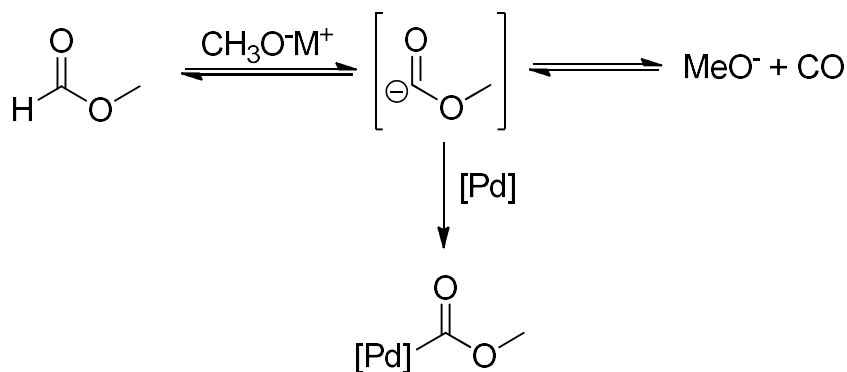


Figure 14. Decarbonylation of HCOOPh with Et₃N. Top left: superimposed FT-IR spectra at different times. Top right: HCOOPh and PhOH absorbance vs reaction time. Bottom left: first order kinetic plot for HCOOPh. Bottom right: first order kinetic plot for Et₃N.

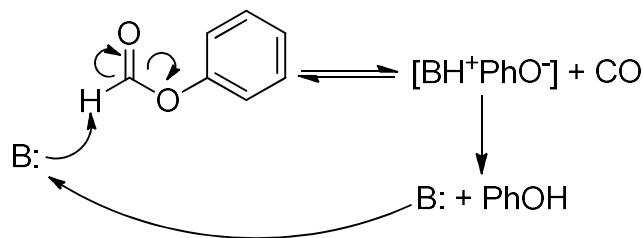
In the light of the obtained results, it is clear that a base (in the current case Et₃N) is able to decarbonylate phenyl formate without the assistance of any metal species (Et₃N-mediated decarbonylation of phenyl formate were performed in glass equipment with a new stirring bar in order to avoid any false positive provided by adventitious metal traces adsorbed on the stirring bar). Concerning the mechanism, in a recent paper, Müller, Lolli and co-workers described the carbonylation of phenol to methyl phenyl carbonate using methyl formate as the carbonylating agent and sodium or potassium methoxide as the catalysts.^[63] In the mechanistic proposal, the authors assumed that the alkoxide anion is able to deprotonate the formic proton generating an unusual carbonyl anion. Subsequently, CO and methanol can be formed. The formation of a methoxy-carbonyl palladium complex was also supposed (Scheme 11).



Scheme 11. Alkoxide-mediated decarbonylation of methyl formate.

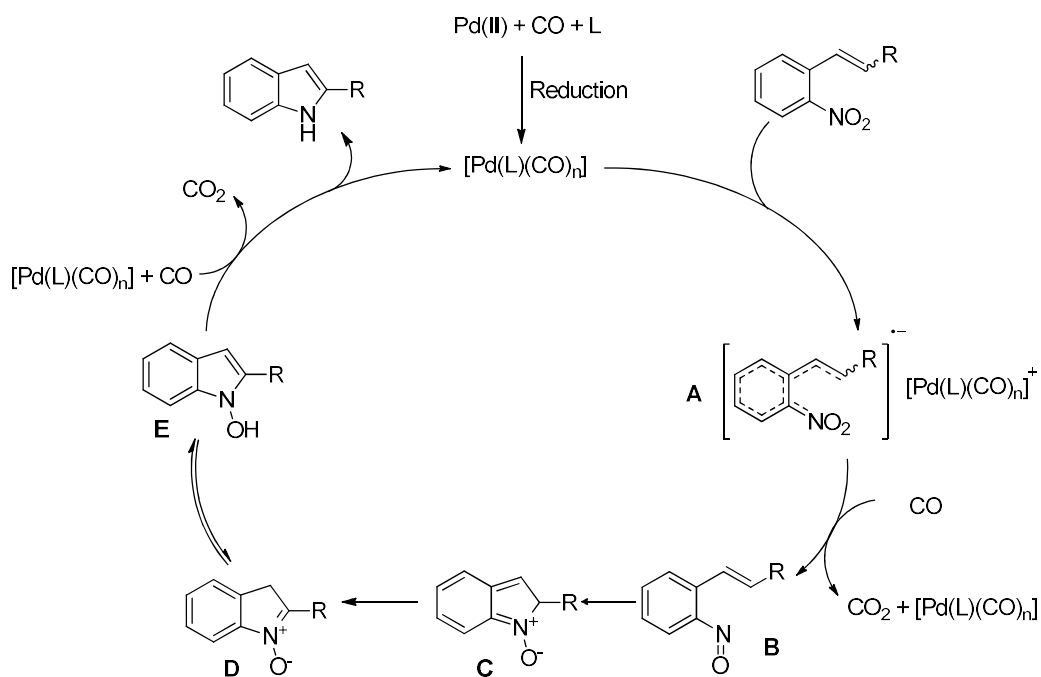
Despite methoxycarbonyl-type complexes are well known and stable,^[64] no evidence of their formation were provided in the mentioned paper. In addition, the carbonyl anion was never detected. Unfortunately, no other mechanistic investigations for the decarbonylation reaction have ever been published. However, we found that if pyridine was employed as the base, no reaction occurred (in refluxing CH₃CN) whereas DBU under the same reaction conditions is able to decarbonylate phenyl formate in less than 15 minutes (the reaction performs well even at room temperature). Thus, the decarbonylation mechanism can somehow be correlated with the strength of the employed base. This fact is an evidence that an acid-base reaction could occur.

Nevertheless, we can assume that since the carbonyl anion is rather unstable (no reports of its detection), a concerted process might be occurring (Scheme 12).



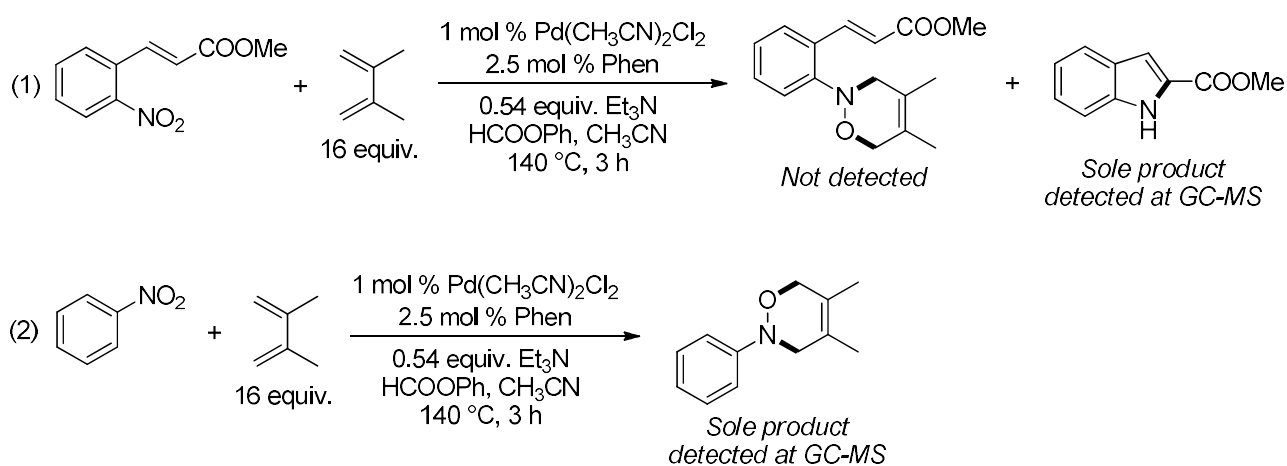
Scheme 12. Proposed decarbonylation mechanism of phenyl formate.

Finally, our attention focused on the mechanism of the reductive cyclization. It is generally accepted that any kind of transition-metal catalyzed reduction of nitroarene using CO as the reductant begins with a single electron transfer (SET) from the metal to the nitro group. This mechanism was demonstrated in the case of Ni,^[65] Ru,^[66] Fe^[67] and Rh^[68] complexes. Despite direct indications of such mechanism in the case of Pd-based systems were never reported, evidences for radical formations involving nitrosoarenes with Pd(0) species were described.^[69] It is thus clear that only metal species in low (zero or even negative) oxidation states are able to activate nitroarenes. The proposed cycle is depicted in Scheme 13. On the basis of the latter assumptions, we postulated that the Pd(II) pre-catalyst is converted into a Pd(0) specie that is able to transfer an electron to the substrate forming the radical anion **A**. It is generally agreed that nitrosoarenes are active intermediate in the reductive cyclization of nitro compounds using CO as the reductant. As the consequence, intermediate **A** is deoxygenated by a first equivalent of CO generating the nitroso intermediate **B**. Subsequently, a 1,5-electrocyclization occurs and the nitronate **C** is formed. The latter is then converted into the nitronate **D** by a 1,5-hydrogen shift reaction. Isomerization of **D** lead to the formation of the N-hydroxyindole, which finally is converted into the desired product by a second equivalent of CO in the presence of the catalyst. The intermediate reaction sequence **B-C-D-E** was theoretically studied by Houk and Davies.^[70] They concluded that, despite the latter reaction sequence does not involve any metal-mediated reaction, the 1,5-hydrogen shift (from **C** to **D**) could be promoted by metals and/or bases.



Scheme 13. Proposed mechanism for the presented transformation.

In order to intercept the supposed key-intermediate **B**, **1a** was reacted under optimized reaction conditions with 2,3-dimethyl-1,3-butadiene in the aim of trapping it in the form of a 2*H*-oxazine through a hetero-Diels-Alder (HDA) as probe reaction. Unfortunately, only the cyclization product was detected (eq. (1), Scheme 14). On the contrary, if nitrobenzene was subjected to the same reaction conditions, the corresponding 4,5-dimethyl-2-phenyl-3,6-dihydro-2*H*-1,2-oxazine was formed and detected as sole product at GC-MS (eq. (2), Scheme 14).



Scheme 14. Attempt to intercept the nitroso intermediate.

On the basis of these experiments, we can conclude that:

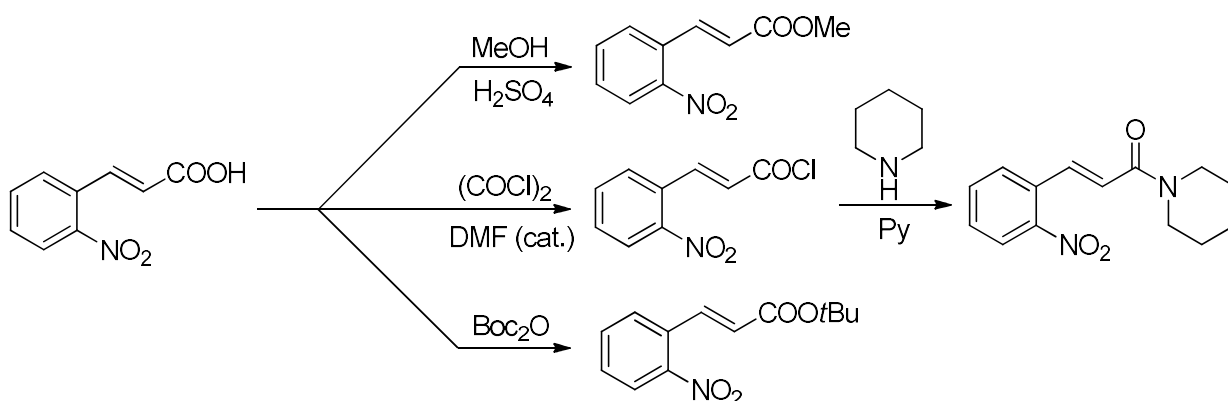
- Owing to the formation of the oxazine in eq. (2), it is very likely that nitroso intermediate of type **B** are generated during the catalytic cycle.

- 2) After *o*-nitrostyrene **B** has formed, the cyclization reaction occurs with a higher rate compared to the HDA. The inability of intercepting the *o*-nitrostyrene can be ascribed to the high reactivity of nitroso derivatives with alkenes (a marked phenomenon in the case of *intra*-molecular reactions), a fact known for years.^[2g, 71] In particular, Kuzmich and co-workers showed that when *o*-hydroxylamine were subjected to oxidations, *N*-hydroxyindoles were formed, failing in the isolation of the corresponding *o*-nitrostyrene.^[72] In support of this claim, any attempt by other authors to intercept *o*-nitrostyrenes were unsuccessful.^[9b, 73]
- 3) Our catalytic system coupled with HCOOPh is able to efficiently convert nitroaromatics into the corresponding oxazines paving the way for another synthetic application.

In conclusion, we have here presented an efficient and convenient synthetic procedure for the manufacture of nitrogen heterocycles from nitro compounds. In many cases, this CO-surrogate based protocol allows producing the desired products with selectivities and yields larger than those previously reported using hazardous pressurized CO. In addition, the catalytic system (based on Pd(CH₃CN)₂Cl₂ and Phen) and the CO surrogate are composed by commercially available compounds therefore avoiding tedious and elaborated synthesis of metal complexes or ligands thus increasing the feasibility of this protocol both in laboratory and in a larger scale production.

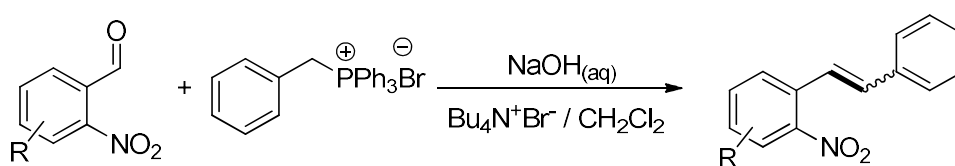
3. Synthesis of the starting materials

Since *ortho*-nitrostyrenes are not commercially available compounds, various strategies were employed for their preparation. Owing to the poor selectivity and sometimes harsh reaction conditions of nitration reactions, we decided to start from substrates already carrying the nitro group. Gratefully, 2-nitrocinnamic acid and 2-nitrobenzaldehyde are cheap commercially available compounds. Therefore, we used these molecules as key starting materials for the preparation of a large variety of substrates. Firstly, 2-nitrocinnamic acid was derivatized to the corresponding esters and amides by using conventional protocols (Scheme 15).



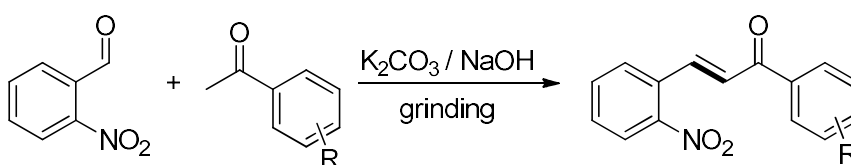
Scheme 15. Preparation of carboxylic acid derivatives starting from 2-nitrocinnamic acid.

As a classic tool in organic synthesis, Wittig reaction was employed for the synthesis of 2-nitrostilbene derivatives. Taking advantage of the commercial availability of substituted 2-nitrobenzaldehydes, several 2-nitrostilbenes were prepared. We employed a simple protocol that allowed for conducting the reaction in a biphasic water-CH₂Cl₂ system at room temperature (Scheme 16) using ammonium salts as phase-transfer agents.



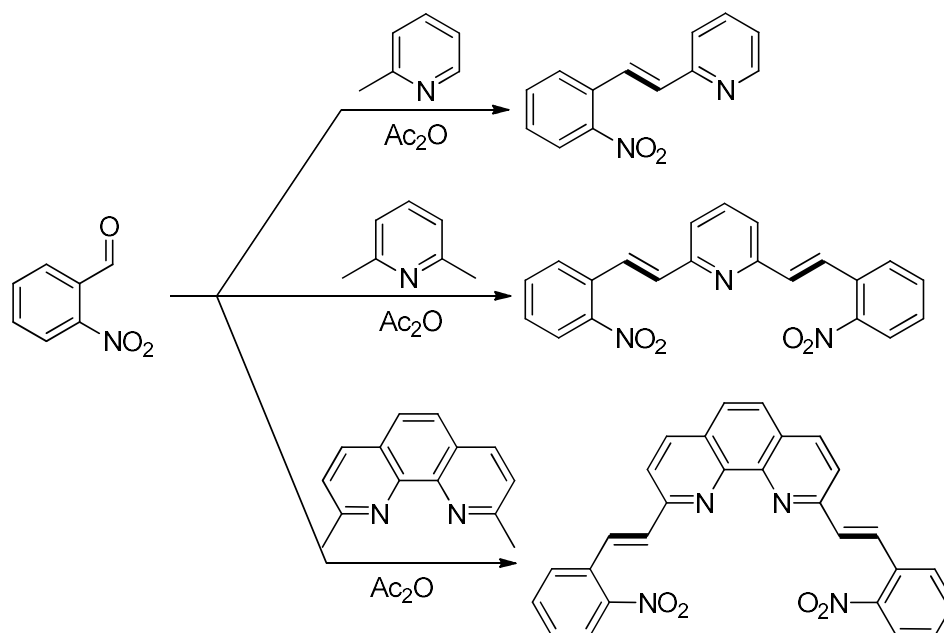
Scheme 16. The Wittig approach to the preparation of substituted 2-nitrostilbenes.

2-Nitrobenzaldehyde was employed as starting material for the preparation of 2-nitroalchones through Claisen-Schmidt condensation. The reaction was performed in the solid state grinding the starting materials and the alkali reactants in a mortar without the use of any solvents. Good yields were achieved with this protocol (Scheme 17).



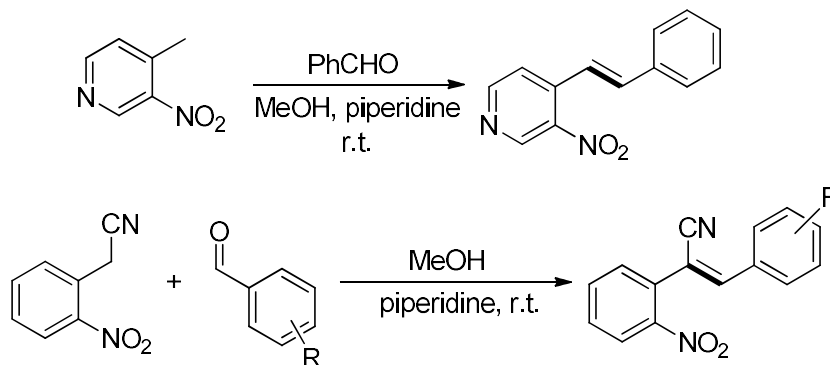
Scheme 17. Solid-phase Claisen-Schmidt condensation.

Knoevenagel and Knoevenagel-type condensations are versatile tools for the construction of C=C double bonds starting from activated C-H bonds. By following this strategy and using 2-nitrobenzaldehyde as starting material, pyridine and phenanthroline containing substrates were prepared (Scheme 18).



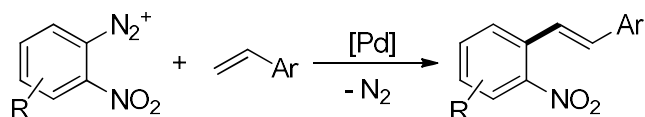
Scheme 18. Knoevenagel-type condensation of 2-nitrobenzaldehyde.

In addition, Knoevenagel-type condensations were further used for the preparation of nitrostyrylpyridine and of other *ortho*-nitrostyrenes substituted in position α with a cyano group. Notably, in the latter cases the products precipitate from the reaction media allowing for a ready recovering (Scheme 19).



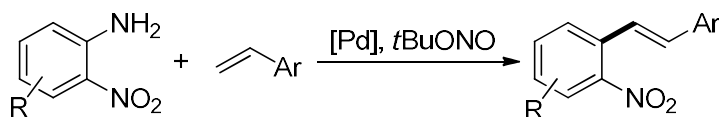
Scheme 19. Other Knoevenagel-type condensations for the preparation of substrates.

Finally, we focused our attention on transition metal catalyzed cross-coupling methodologies. One of the most valuable approach for the arylation of styrenes is represented by Mizoroki-Heck reaction. Unfortunately, very few examples for the arylation of styrenes with 2-halonitrobenzenes are present in the literature. Moreover, classic cross-coupling methodologies such as Suzuki-Miyaura, Stille and Negishi cross-couplings require the pre-functionalization of the starting materials with boron, tin or zinc moieties, increasing the cost and the overall steps of the transformation. Thus, we focused our attention to different methods. An alternative and feasible approach is represented by the Heck-Matsuda reaction (Scheme 20).



Scheme 20. Classic Heck-Matsuda approach for the preparation of *ortho*-nitrostyrenes.

This reaction has the benefit that only gaseous dinitrogen is produced as side product thus avoiding the formation of salts as wastes. On the other hand, diazonium salts must be prepared from the corresponding anilines and they generally suffer from poor thermal stability (in some cases they tend to explode, especially in the presence of a nitro group on the aryl ring). A great advance in this field was made when Matsuda demonstrated that this transformation can be performed directly from anilines and alkyl nitrite generating the diazonium salt *in situ* (Scheme 21).^[74] In addition, only dinitrogen, water and *tert*-butanol were produced as side products.



Scheme 21. Modified Heck-Matsuda approach: *in situ* formation of the diazonium salt.

Following reported protocols,^[74-75] we were able to synthesize various alkyl and aryl *ortho*-nitrostyrenes starting from cheap and commercially available *ortho*-nitroaniline derivatives in very good yields.

4. Experimental section

4.1. General consideration

Unless otherwise stated, all reactions and manipulations were performed under dinitrogen atmosphere using standard Schlenk apparatus. All glassware and magnetic stirring bars were kept in an oven at 120 °C for at least two hours and let to cool under vacuum before use. Solvents were dried and distilled by standard procedures and stored under dinitrogen atmosphere. Butyl and methyl formate was dried over MgSO₄, filtered by cannula techniques and then distilled under a dinitrogen atmosphere. Benzyl formate was degassed by three freeze-pump-thaw cycles but not distilled. Et₃N was distilled from CaH₂. DBU (1,8-diazabicyclo[5.4.0]undecen-5-ene) and DIPEA (N,N-diisopropylethylamine) were distilled from CaH₂ under vacuum and under atmospheric pressure, respectively. Phenyl formate was purchased from Sigma Aldrich or prepared following a procedure reported in the literature (*vide infra*). Deuterated solvents were purchased by Sigma-Aldrich: DMSO-d₆ (commercially available in 0.75 mL vials under dinitrogen atmosphere) was used as purchased while CDCl₃ was filtered on basic alumina and stored under dinitrogen over 4 Å molecular sieves. 1,10-Phenanthroline (Phen) was purchased as hydrate (Sigma-Aldrich). Before use, it was dissolved in CH₂Cl₂, dried over Na₂SO₄ followed by filtration under dinitrogen atmosphere and evaporation of the solvent in vacuum. Phen was weighed in the air but stored under dinitrogen atmosphere to avoid water uptake. All the Pd precursors employed in this work were prepared starting from commercially available PdCl₂ following procedures reported in the literature (*vide infra*). RhCl₃ and Fe(CO)₅ were purchased by Sigma Aldrich. Fe(CO)₅ was distilled under static vacuum, collecting the liquid in a liquid nitrogen cooled trap. All other reagents were purchased from Sigma-Aldrich or Alfa-Aesar and used without further purifications.

4.2. General analysis methods

¹H-NMR and ¹³C-NMR spectra were recorded at room temperature (at frequencies of 300MHz for the proton and 75MHz for the carbon) on a *Bruker AC 300 FT* or on an *Avance Bruker DPX 300* or on a *Avance Bruker 600 MHz*. Chemical shifts are reported in ppm relative to TMS; the data are reported as follows: proton multiplicities (s=singlet, d=doublet, t=triplet, q=quartet, m=multiplet and br=broad), coupling constants and integration.

GC-MS analyses were registered using a *Thermo Fisher ISQ™ QD* Single Quadrupole GC-MS equipped with a ZB-1MS 60m column or on a *Shimadzu GC-MS QP5050A* equipped with a Equity-5ms capillary column.

GC analyses were performed using a *Shimadzu GC - 17A / GCMS - QP5050* equipped with a Supelco SLB™-5ms capillary column. A standard analysis involves the preparation of a sample solution (conc. 0.1 mg·mL⁻¹ calculated respect to the internal standard amount) in CH₂Cl₂. The internal standard was biphenyl.

Elemental analyses were performed on a *Perkin Elmer 2400 CHN* elemental analyzer. IR spectra were registered on a *Varian Scimitar FTS-100* instrument.

4.3. General protocol for catalytic reactions conducted in a pressure tube and using Schlenk glassware

All the Ru, Pd, Rh and Fe catalysts were added to the reaction through stock solutions prepared in the appropriate alkyl formate, DMF or acetonitrile (in the case of phenyl formate). Every catalyst was weighted and stored in the air (except for Pd(OAc)₂ that was stored under nitrogen to avoid water uptake and Fe(CO)₅ that was stored under nitrogen and in the dark) whereas the solutions were prepared under dinitrogen atmosphere using distilled solvents. For catalytic runs that required an amount of Phen less than 10 mg, a stock solution was prepared.

In a typical catalytic reaction, the substrate was weighted in the air and placed in a heavy-wall borosilicate glass tube (ACE pressure tube, volumetric capacity of ~ 18 mL, purchased from Sigma Aldrich – code n. Z181064). Afterwards solvent, stock solutions of the catalysts and Phen, phenyl formate and triethylamine were added. In the case of alkyl formates, the reactions were conducted under neat conditions of the CO surrogate. Subsequently the pressure tube was plugged with a Teflon screw cap and immersed in a preheated oil bath. At the end of the reaction, the pressure tube was lifted and let to cool to room temperature.

Then, the screw cap was carefully removed, the excess of CO was vented and the content analyzed by GC, GC-MS or subject to column chromatography.

The same reaction protocol was employed for running the catalytic runs in standard Schlenk glassware.

4.4. General protocol for catalytic reactions conducted in autoclave

In a typical catalytic reaction 1,10-Phenanthroline and the substrate were weighed in the air in a glass liner and then placed inside a Schlenk tube with a wide mouth under a dinitrogen atmosphere. The catalyst solutions ([Pd(Phen)₂][BF₄]₂ and Ru₃(CO)₁₂ in freshly distilled methyl formate or Pd(CH₃CN)₂Cl₂ in CH₃CN) and Et₃N were added by volume and the liner was closed with a screw cap having a glass wool-filled open mouth which allows gaseous reagents to exchange. The Schlenk tube was immersed in liquid nitrogen until the solvent froze and evacuated and filled with dinitrogen three times. The liner was rapidly transferred to a 200 mL stainless steel autoclave equipped with magnetic stirring. The autoclave was then evacuated and filled with dinitrogen three times and subsequently immersed in a pre-heated oil bath. At the end of the reaction, the autoclave was quickly cooled with an ice bath and vented.

4.5. GC quantitative analysis for catalytic reactions

At the end of the catalytic reaction, the internal standard (biphenyl) was added to the reaction mixture (1/4 mass ratio with respect to the starting material) and an aliquot was diluted with CH₂Cl₂. The final solution must have a biphenyl concentration of 0.1 mg·mL⁻¹.

4.6. Isolation of reaction products

At the end of the catalytic run, the reaction mixture was quantitatively transferred into a round bottom flask and the solvent removed. Reaction products were isolated by column chromatography (silica gel) using hexane/CH₂Cl₂ or hexane/AcOEt as the eluent (in both the cases, from 1 to 2 % of Et₃N was added to the eluent in the aim of partially deactivate acidic sites of silica gel).

4.7. General protocol for FT-IR investigation under standard catalytic conditions (pressure tube)

HCOOPh (109 μL, 1 mmol) was dissolved in 5 mL of CH₃CN inside an ACE pressure tube. Subsequently, the desired reagent (Et₃N or Pd(CH₃CN)₂Cl₂) was added. The reaction vessel was plugged with a Teflon coated screw cap and immersed in a preheated oil bath (140 °C). At the end of the reaction, the pressure tube was lifted and let to cool to room temperature. Then, the screw cap was carefully removed and the content analyzed at FT-IR using a 0.1 mm CaF₂ cell.

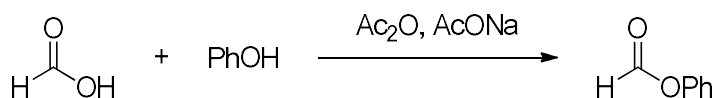
4.8. General protocol for FT-IR investigation under Schlenk conditions (kinetics)

HCOOPh (65.4 μL, 0.6 mmol) were dissolved in CH₃CN (3 mL) inside a Schlenk tube. Subsequently, the desired amount of Et₃N was added. The reaction vessel was immersed into a pre-heated oil bath reaching refluxing conditions. At the desired time, the Schlenk tube was lifted-up and after 5 minutes a very small aliquot was analyzed at FT-IR using a CaF₂ cell. The disappearing of HCOOPh was evaluated monitoring the decreasing of the two C=O stretching bands at 1741 and 1761 cm⁻¹.

4.9. CV procedure

Cyclic voltammetry (CV) investigations were carried out in a 25 cm³ conic glass cell, under conditions, on 6·10⁻⁴ M solutions of the investigated molecules. Tetraethylammonium tetrafluoroborate (0.1 M) was employed as the supporting electrolyte. The working electrode was a glassy carbon disk (GC2=AMEL, geometrical surface 0.05 cm²) cleaned by synthetic diamond powder (Aldrich, diameter=1 mm) on a wet cloth (STRUERS DP-NAP), and rinsed with the dry solvent employed afterwards to remove any moisture possibly remaining on the electrode after the cleaning (failure to do so can lead to irreproducible results); the counter electrode was a platinum wire or disk; the operating reference electrode was an aqueous saturated calomel electrode, but the potentials were ultimately referred to the Fc⁺/Fc couple (the intersolvental redox potential reference currently recommended by IUPAC). The experiments were carried out using an AUTOLAB PGSTAT potentiostat (EcoChemie, The Netherlands) run by a PC with GPES software. Potential scan rates typically ranged 0.05 to 2 V·s⁻¹, and ohmic drops were corrected with the positive feedback method. Since electron-transfer products tend to film the electrode surface thus conditioning its activity, the reported CV patterns consist of the combination of half cycles started from a central potential value at which no process takes place and proceeding in either positive or negative direction, on a freshly polished electrode surface.

4.10. Synthesis of phenyl formate



The synthesis was performed following the procedure reported in the literature.^[33a]

The reaction was performed under a dinitrogen atmosphere. In a 250 mL Schlenk flask formic acid (38 mL, 1 mol) was added to acetic anhydride (76 mL, 0.8 mol). The mixture was stirred at 60 °C for 1 h and then cooled to r.t. This mixture was transferred by using a cannula into a 500 mL flask containing phenol (18.8 g, 200 mmol) and sodium acetate (16.4 g, 200 mmol). (Attention: the reaction is rather exothermic. Maintain the flask into a water/ice cooling bath until it reaches RT.) The reaction was stirred for 3 h and then diluted with toluene (150 mL), washed with water (3x100 mL) and dried over MgSO₄. Then, it was filtered and concentrated affording phenyl formate as a pale yellow liquid (65 % yield).

¹H NMR (400 MHz, CDCl₃) δ 8.33 (s, 1H), 7.47 – 7.41 (m, 2H), 7.30 (t, *J* = 7.5 Hz, 1H), 7.18 (m, 2H).

¹³C NMR (101 MHz, CDCl₃) δ 159.33, 149.98, 129.73, 126.39, 121.16.

4.11. Preparation of Pd and Ru precursors

4.11.1. Pd(CH₃CN)₂Cl₂

The synthesis was performed following the procedure reported in the literature.^[76]

PdCl₂ (1.011 g, 5.70 mmol) were suspended into 70 mL of CH₃CN and refluxed for 2 h. In order to remove undissolved material, the hot solution was filtered by using a Teflon cannula. The solution was cooled at 0 °C to promote the precipitation of the desired complex. The so-formed orange solid was filtered through a Buchner funnel. (1.4706 g, 99.5 % yield).

Elemental analysis for C₄H₆Cl₂N₂Pd. Calc.: C 18.52; H 2.33; N 10.80. Found: C 18.80; H 2.28; N 10.80.

4.11.2. [Pd(Phen)₂][BF₄]₂

The synthesis was adapted from that reported in the literature.^[77]

PdCl₂ (1 g, 5.72 mmol) was suspended into 100 mL of water. HCOONa (2.051 mg, 30.2 mmol) and NaOH (1.624 g, 40.6 mmol) were subsequently added. After 30 min, metallic Pd in the form of finely divided powder appeared. Water was removed and the solid obtained washed with 3x30 mL of water. 12 mL of HNO₃ (65 % water solution) was dropwise added (attention: brow/red gases were released, use a well-ventilated fume hood). At the end of the gases releasing, the volume of the liquid phase was concentrated to around 1 mL. Water was added (2x3mL) and removed maintaining only 1 mL of it. In a 50 mL flask, the so-formed Pd(NO₃)₂ was dissolved into 75 mL of acetone and maintained under stirring for 30 min. The suspension was filtered. The solution was transferred into a 100 mL flask and Phen (2.052 g, 11.4 mmol) was added. Immediately a white solid precipitated. The mixture was maintained under stirring overnight. The

day after it was filtered through a Buchner funnel. The obtained solid was dissolved in methanol (170 mL). NaBF₄ (9.39 g, 85.5 mmol) was added and the suspension maintained under stirring for 2 days at room temperature. Subsequently, it was collected by filtration on a Buchner funnel and dried. 2.6203 g of [Pd(Phen)₂][BF₄]₂ were obtained (72 % yield).

Elemental analysis for C₂₄H₁₆B₂F₈N₄Pd. Calc.: C 45.01; H 2.52; N 8.75. Found: C 44.83; H 2.57; N 8.83.

4.11.3. Pd(dba)₂

The synthesis was adapted from that reported in the literature.^[78]

PdCl₂ (1.48 g, 8.35 mmol), and NaCl (492 mg, 8.41 mmol) were dissolved into 40 mL of freshly distilled methanol at room temperature for 16 hours. Afterwards, the mixture was heated at around 60 °C and dba (6.36 g, 27.1 mmol) was added. The solution was maintained at 60 °C until complete dissolution of all the material occurred. Then, AcONa (12.52 g, 152.6 mmol) was added and the mixture maintained under stirring at room temperature. A dark violet solid precipitated. It was collected by filtration on a Buchner funnel, washed with methanol and water, and finally dried in vacuo. Yield = 97 %.

Elemental analysis for C₃₄H₂₈O₂Pd. Calc.: C 71.02; H 4.91; N -. Found: C 71.32; H 4.88; N -.

4.11.4. Pd(OAc)₂

The synthesis was performed following the procedure reported in the literature.^[79]

PdCl₂ (1 g, 5.72 mmol) was suspended into 100 mL of water. HCOONa (1.6 g, 23.4 mmol) and NaOH (2 g, 50 mmol) were subsequently added. After 30 min metallic Pd in the form of finely divided powder appeared. Water was removed and the obtained solid washed with 3x30 mL of water. The solid was suspended in 40 mL of glacial acetic acid and 0.6 mL of concentrated nitric acid was slowly added under stirring. The mixture was refluxed for 30 min while nitrogen was bubbled inside the reaction solution. The volume of the reaction mixture was reduced to one third using gentle heating. After reaching RT, an orange powder precipitated. It was collected by filtration on a Buchner funnel affording the desired compound (86 % yield).

Elemental analysis for C₄H₆O₄Pd. Calc.: C 21.40; H 2.69; N -. Found: C 21.54; H 2.67; N -.

4.11.5. Ru₃(CO)₁₂

The synthesis was adapted to that reported in the literature.^[80]

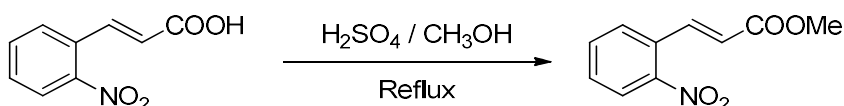
1.26 g of RuCl₃·nH₂O were dissolved in 50 mL of distilled methanol and placed into a glass liner. The latter was insert into a 200 mL stainless-steel autoclave that was charged with 50 bar of CO. Finally, it was heated to 125 °C for 8 hours. At the end of the reaction, the autoclave was vented and the reaction mixture contained an orange precipitate. The liner was maintained at -20 °C with the aim of maximizing the

precipitate. The solid was collected by filtration on a sintered disc filter funnel. The resulting solid was dissolved in inhibitor-free THF and filtered through Celite®. At the end, the solvent was removed affording a bright orange solid (939 mg, 72 % yield).

FT-IR (hexane): 2060.8 cm^{-1} , 2029.0 cm^{-1} , 2008.8 cm^{-1} .

4.12. Preparation of substrates

4.12.1. Synthesis of (*E*)-2-nitrocinnamate methyl ester



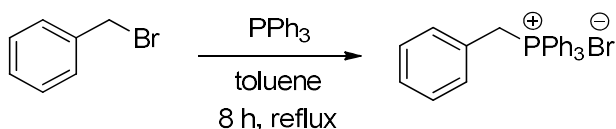
In a dried 100 mL round bottom Schlenk flask, *trans*-2-nitrocinnamic acid (2.02 g, 10.5 mmol) was dissolved in 60 mL of freshly distilled methanol and 187 μL of concentrated sulphuric acid (95 %) were added. The solution was refluxed under nitrogen atmosphere for 18 hours until the complete consumption of the reagent that was monitored by TLC (hexane:ethyl acetate = 8:2). The resulting mixture was allowed to reach room temperature and the methanol was removed in vacuo. The reaction raw material was suspended in 30 mL of a saturated solution of NaHCO_3 . The solution was extracted with CH_2Cl_2 (3 x 50 mL). Combined organic layers were washed three times with 30 mL of a saturated solution of NaHCO_3 and two times with 30 mL of water. The organic phase was dried over Na_2SO_4 , filtered and the solvent removed in vacuo. A pale yellow solid was collected (2.12 g, 10.2 mmol, 97 % yield).

^1H NMR (300 MHz, CDCl_3) δ 8.11 (d, $J = 15.8$ Hz, 1H), 8.03 (d, $J = 8.1$ Hz, 1H), 7.72 – 7.60 (m, 2H), 7.59 – 7.49 (m, 1H), 6.37 (d, $J = 15.8$ Hz, 1H), 3.83 (s, 3H).

^{13}C NMR (75 MHz, CDCl_3) δ 166.59, 148.71, 140.51, 133.93, 130.91, 130.72, 129.51, 125.28, 123.24, 96.97, 52.37.

Elemental analysis for $\text{C}_{10}\text{H}_9\text{NO}_4$. Calc.: C, 57.47; H, 4.38; N, 6.76. Found: C, 57.67; H, 4.50; N, 6.75.

4.12.2. Synthesis of benzyltriphenylphosphonium bromide for Wittig reactions



The procedure was adapted from those reported in the literature.^[81]

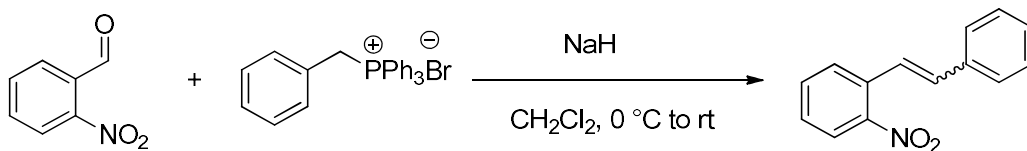
In a 50 mL Schlenk flask, PPh_3 (4.76 g, 18.15 mmol) was dissolved in toluene (15 mL). Then, benzyl bromide (1.96 mL, 16.15 mmol) was added. Immediately, a white solid precipitated. After 8 h of reflux, the solid was collected by filtration through a Büchner funnel. 6.648 g, 90 % yield.

^1H NMR (300 MHz, CDCl_3) δ (ppm) 7.77-7.56 (m, 15H), 7.19 (t, 2H), 7.16 (t, 2H), 7.07 (t, 2H), 5.32 (d, 2H).

$^{31}\text{P}\{^1\text{H}\}$ NMR (121.47 MHz, CDCl_3): δ (ppm) 23.14 (s).

Elemental analysis for $\text{C}_{25}\text{H}_{22}\text{BrP}$. Calc.: C 69.29; H 5.12 Found: C 69.27; H 5.08.

4.12.3. Synthesis of (*E*)- and (*Z*)-2-nitrostilbene



The procedure was adapted to those reported in the literature.^[82]

In a 1 L Schlenk flask, NaH (3.14 g, 78.5 mmol; 60 % dispersion in mineral oil) was placed inside and washed three times with hexane. Subsequently, 160 mL of CH_2Cl_2 were added. A solution of benzyltriphenylphosphonium bromide (8.74 g, 2.02 mmol) in CH_2Cl_2 (200 mL) was dropwise added while the flask was maintained at 0 °C. Afterward, a solution of 2-nitrobenzaldehyde (2.60 g, 17.2 mmol) in CH_2Cl_2 (110 mL) was dropwise added. Then, the reaction mixture was allowed to reach r.t. and maintained under stirring overnight. Water was then added and the two layers separated. The aqueous layer was extracted with CH_2Cl_2 (3x100 mL). The organic layers were washed with water and brine, dried over Na_2SO_4 and the solvent removed affording a yellow oil. In order to purify the desired product, a purification over a silica pad using toluene as eluent was performed. 3.17 g of the desired product were obtained (83 % yield). ^1H NMR analysis showed the presence of two isomers (*E* and *Z*) with a molar ratio 2:1 in favor of the *Z* isomer.

An aliquot of the product was purified by column chromatography (silica gel; hexane:AcOEt = 95:5 as the eluent) with the aim of separating the two isomers.

Characterization data for *Z* isomer:

^1H NMR (300 MHz, CDCl_3) δ 8.16 – 8.05 (m, 1H), 7.45 – 7.37 (m, 2H), 7.34 – 7.26 (m, 1H), 7.18 (m, 3H), 7.08 (m, 2H), 6.92 (d, $J = 12.1$ Hz, 1H), 6.79 (d, $J = 12.1$ Hz, 1H).

^{13}C NMR (75 MHz, CDCl_3) δ 136.27, 134.10, 133.48, 132.72, 132.27, 129.52, 128.66, 128.51, 127.93, 126.88, 125.11.

Elemental analysis for $\text{C}_{14}\text{H}_{11}\text{NO}_2$. Calc.: C 74.65; H 4.92; N 6.22. Found: C 74.42; H 4.69; N 6.01.

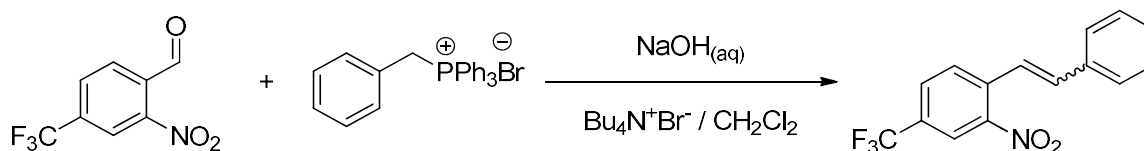
Characterization data for *E* isomer:

^1H NMR (300 MHz, CDCl_3) δ 7.99 (d, $J = 8.1$ Hz, 1H), 7.79 (d, $J = 7.9$ Hz, 1H), 7.67 – 7.54 (m, 4H), 7.49 – 7.30 (m, 4H), 7.11 (d, $J = 16.1$ Hz, 1H).

^{13}C NMR (75 MHz, CDCl_3) δ 143.15, 136.89, 134.28, 133.48, 129.22, 129.01, 128.58, 128.36, 127.49, 125.18, 123.93. One quaternary carbon is not detected.

Elemental analysis for $\text{C}_{14}\text{H}_{11}\text{NO}_2$. Calc.: C 74.65; H 4.92; N 6.22. Found: C 74.; H 4.69; N 6.01.

4.12.4. Synthesis of (*E*)-2-nitro-1-styryl-4-(trifluoromethyl)benzene



The procedure was adapted from a previous reported protocol.^[83]

In a 25 mL round-bottom Schlenk flask 2-nitro-4-(trifluoromethyl)benzaldehyde (234.5 mg; 1.07 mmol) was dissolved in 14 mL of CH_2Cl_2 . Then, benzyltriphenylphosphonium bromide (632.6 mg; 1.46 mmol) was added. After its solubilisation, NaOH solution (50 mg in 80 μL of water) and tetrabutylammonium bromide (1.7 g; 5.4 mmol) were added. The mixture was stirred at r.t. monitoring the disappearance of the starting aldehyde using TLC. At the end of the reaction 20 mL of water were added and extracted with 3x20 mL of CH_2Cl_2 . The combined organic layers were dried over Na_2SO_4 and concentrated under reduced pressure. In order to isolate the product a chromatographic column was carried out (hexane:AcOEt=9:1 as the eluent). A yellow oil was obtained. NMR analysis showed the presence of both the diastereoisomers in ratio *Z*:*E*=2:1.

Characterization data for *Z* isomer:

^1H -NMR (*cis* isomer) (400 MHz, CDCl_3) δ 8.37 (d, $J = 0.7$ Hz, 1H, *cis* 2), 7.63 (dd, $J = 8.4, 1.8$ Hz, 1H, overlap with *trans* 8), 7.45 - 7.41 (m, 1H, *cis*-5, overlap with *trans* 10-12), 7.21 - 7.25 (m, 3H, *cis* 11-12), 7.10-7.07 (m, 2H, *cis* 10), 6.91 (brs, 2H, *cis* 7-8).

^{13}C -NMR (*cis* isomer) (100 MHz, CDCl_3) δ 137.3, 135.9, 135.2, 133.7 (*cis* 8), 133.4 (*cis* 5), 129.1 - 129.5 (CF_3), 129.1 (*cis* 4 and *trans* 4), 128.1 (*cis* 11 or *cis* 12), 128.5 (*cis* 11 or *cis* 12), 125.0 (*cis* 7), 122.3 - 122.1 (m, *cis* 2, overlap with *trans* 2). Three quaternary carbon signals were detected but not assigned.

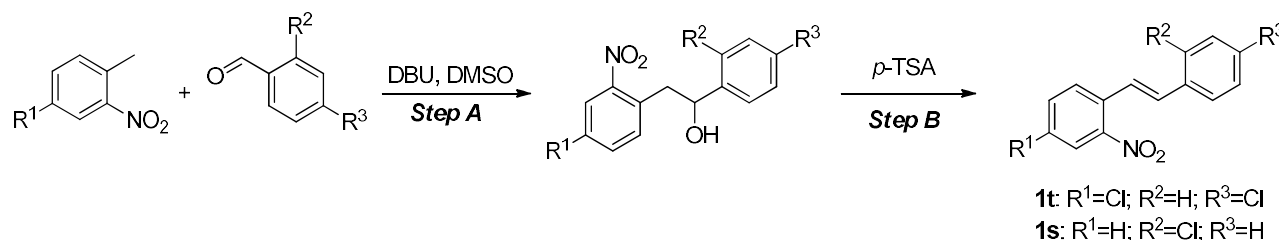
Characterization data for *E* isomer:

^1H -NMR (*trans* isomer) (400 MHz, CDCl_3) δ 8.26 (d, $J = 0.7$ Hz, 1H, *trans* 2), 7.95 (dd, $J = 8.3$, 1H, *trans* 5), 7.86 (dd, $J = 8.3, 0.6$ Hz 1H, *trans* 4), 7.64 (d, $J = 16.1$ Hz, 1H, *trans* 8), 7.59 (m, 2H, *trans* 11), 7.46 - 7.36 (m, 3H, *trans* 10-12), 7.21 (d, $J = 16.1$ Hz, 1H, *trans* 7, overlap with *cis* 11-12). Three quaternary carbon signals were detected but not assigned.

^{13}C -NMR (*trans* isomer) (100 MHz, CDCl_3) δ 137.3, 136.3 (*trans* 8), 135.9, 135.2, 129.1 – 129.5 (m, $\underline{\text{CF}}_3$), 129.1 (*cis* 4 and *trans* 4), 128.9 (*trans* 5 and *trans* 10-12), 127.4 (*trans* 11), 122.3 – 122.1 (m, *trans* 2 overlap with *cis* 2), 122.1 (*trans* 7).

^{19}F -NMR (both isomers) (282 MHz, CDCl_3) δ -63.13, -63.19.

4.12.5. Synthesis of (*E*)-4-chloro-1-(4-chlorostyryl)-2-nitrobenzene and (*E*)-1-chloro-2-(2-nitrostyryl)benzene



The procedure was adapted to those reported by the literature.^[73]

Step A. 4-Chloro-2-nitrotoluene (4.88 g, 28.4 mmol), 4-chlorobenzaldehyde (3.32 g, 23.6 mmol) were dissolved in 30 mL of DMSO. Then, DBU (4.2 mL, 28.1 mmol) was added. The mixture was maintained under stirring for 4 days. At the end of the reaction, 60 mL of AcOEt were added and the organic layer washed with brine (3x60 mL). The organic layer was dried over Na_2SO_4 , filtered and the solvent removed affording a yellow oil. The latter was purified using column chromatography (silica gel, hexane:AcOEt=9:1+3% *i*PrOH). The alcohol was obtained as dark yellow oil (2.85 g, 39 % yield).

Step B. The reaction was performed under air. 2.85 g (9.15 mmol) of the intermediate alcohol was dissolved in 60 mL of toluene. Subsequently, 348.3 mg (1.83 mmol) of *p*-toluenesulfonic acid was added. The mixture was refluxed for 3 h. At the end of the reaction, the acid was neutralized with a saturated solution of NaHCO_3 (3 x 40 mL). The organic layer was dried over Na_2SO_4 and the solvent removed affording a yellow solid. In order to isolate the product in a pure form, the obtained solid was subjected to recrystallation from hexane/toluene (2:1 by volume). 1.09 g of a yellow solid was obtained (41 % yield).

Characterization data for 1t

^1H NMR (300 MHz, CDCl_3) δ 7.98 (d, $J = 2.1$ Hz, 1H), 7.70 (d, $J = 8.5$ Hz, 1H), 7.63 – 7.53 (m, 1H), 7.50 – 7.43 (m, 3H), 7.35 (d, $J = 8.5$ Hz, 2H), 7.02 (d, $J = 16.1$ Hz, 1H).

^{13}C NMR (75 MHz, CDCl_3) δ 143.16, 135.08, 135.01, 134.21, 133.70, 133.52, 131.64, 129.62, 129.48, 128.69, 125.34, 123.43.

Elemental analysis for $\text{C}_{14}\text{H}_9\text{Cl}_2\text{NO}_3$. Calc.: C 57.17; H 3.08; N 4.76. Found: C 57.15; H 3.01; N 4.69.

The same procedure was employed for the preparation of **1s**.

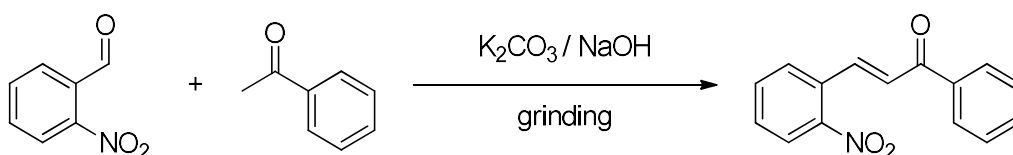
Characterization data for **1s**

^1H NMR (300 MHz, CDCl_3) δ 8.01 (d, $J = 8.1$ Hz, 1H), 7.82 (d, $J = 7.8$ Hz, 1H), 7.74 (dd, $J = 7.5, 1.6$ Hz, 1H), 7.65 (dd, $J = 9.5, 5.3$ Hz, 1H), 7.55 (d, $J = 17.8$ Hz, 2H), 7.50 – 7.39 (m, 2H), 7.36 – 7.21 (m, 2H).

^{13}C NMR (75 MHz, CDCl_3) δ 148.44, 135.03, 134.17, 133.67, 133.25, 130.25, 130.15, 129.88, 129.03, 128.78, 127.55, 126.62, 125.20.

Elemental analysis for $\text{C}_{14}\text{H}_{10}\text{ClNO}_2$. Calc.: C 64.75; H 3.88; N 5.39. Found: C 64.76; H 3.99; N 5.61.

4.12.6. Synthesis of (*E*)-3-(2-nitrophenyl)-1-phenylprop-2-en-1-one



The procedure was adapted to those reported by the literature.^[84]

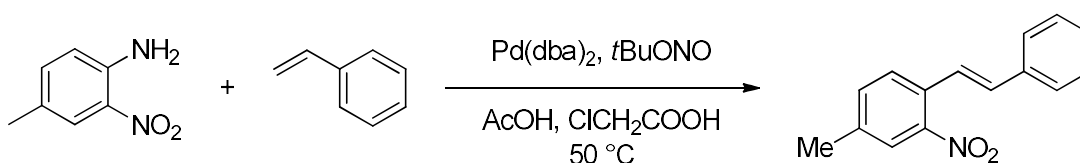
In a mortar, 2-nitrobenzaldehyde (377.8 mg; 2.5 mmol), acetophenone (292 μL ; 2.5 mmol), K_2CO_3 (1.7 g; 12.3 mmol) and NaOH (100 mg; 2.5 mmol) were placed. They were grounded for about 20 minutes. The mixture was extracted with 3x20 mL of AcOEt and the extracts were washed with water (3x20 mL) and concentrated. A brown solid was obtained. The latter was purified using column chromatography (gradient eluent, from hexane:AcOEt=8:2 to hexane:AcOEt=1:1) affording the product as a pale yellow solid (538.2 mg, 85 %).

^1H NMR (300 MHz, CDCl_3) δ 8.16 (d, $J = 15.7$ Hz, 1H), 8.10 (d, $J = 7.9$ Hz, 1H), 8.04 (d, $J = 7.1$ Hz, 2H), 7.81 – 7.67 (m, 2H), 7.58 (m, 4H), 7.34 (d, $J = 15.7$ Hz, 1H).

^{13}C NMR (75 MHz, CDCl_3) δ 190.89, 148.95, 140.54, 137.79, 133.89, 133.49, 131.73, 130.68, 129.61, 128.98, 128.40, 127.80, 125.36.

Elemental analysis for $\text{C}_{15}\text{H}_{11}\text{NO}_3$. Calc.: C 71.14; H 4.38; N 5.53. Found: C 71.46; H 4.19; N 5.31.

4.12.7. Synthesis of (*E*)-4-methyl-2-nitro-1-styrylbenzene



The procedure was adapted to those reported by the literature.^[74]

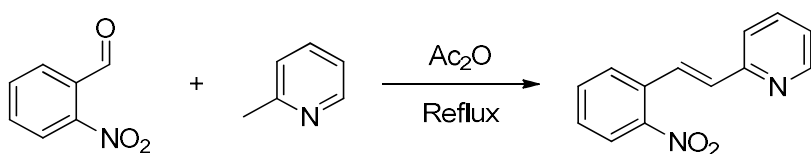
4-Methyl-2-nitroaniline (1.52 g, 10 mmol), styrene (2.3 mL, 20 mmol) and monochloroacetic acid (20 g) were dissolved into 20 mL of glacial acetic acid. Finally, Pd(dba)₂ (287.5 mg, 0.5 mmol) was added. The resulting mixture was heated to 50 °C. A solution of *t*BuONO in acetic acid (1.3 mL of *t*BuONO in 10 mL of glacial acetic acid) was dropwise added over a 15 min period. Gas evolution was immediately detected. The reaction mixture was maintained under stirring for additional 30 minutes. The mixture was neutralized with saturated aqueous solution of sodium carbonate. Then, it was extracted with dichloromethane (3x50 mL). The combined organic layers were washed with brine and dried over Na₂SO₄. Solvent, *t*BuOH and excess of styrene were removed under vacuum for at least 1 day. The resulting crude was purified by column chromatography (hexane:AcOEt = 97:2). A yellow solid was obtained (1.43 g, 60 % yield).

¹H NMR (300 MHz, CDCl₃) δ 7.77 (s, 1H), 7.65 (d, *J* = 8.0 Hz, 1H), 7.59 (m, 3H), 7.44 – 7.27 (m, 4H), 7.05 (d, *J* = 16.1 Hz, 1H), 2.44 (s, 3H).

¹³C NMR (75 MHz, CDCl₃) δ 148.28, 138.97, 137.06, 134.34, 133.39, 130.58, 129.18, 128.82, 128.31, 127.39, 125.38, 123.85, 21.30.

Elemental analysis for C₁₅H₁₃NO₂. Calc.: C 75.30; H 5.48; N 5.85. Found: C 75.41; H 5.62; N 5.86.

4.12.8. Synthesis of of (*E*)-2-(2-nitrostyryl)pyridine



The procedure was adapted from a previous reported protocol.^[85]

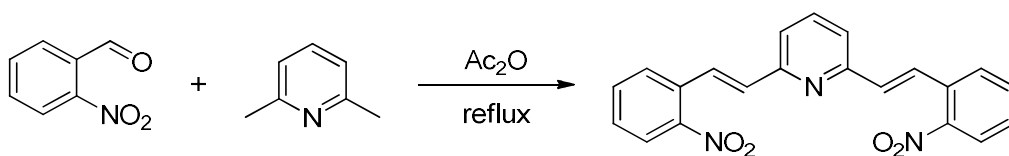
A 25 mL round-bottom Schlenk flask was charged with 2-nitrobenzaldehyde (1g; 6.62 mmol), acetic anhydride (2 mL) and 2-picoline (914 μL; 9.26 mmol). The mixture was refluxed for 20 hours and monitored by TLC (hexane:AcOEt = 3:7). The mixture turned from yellow to dark and the end of the reaction. The solvent was evaporated to afford the crude product. The dark brown powder was purified by filtration over silica pad using CH₂Cl₂ as the eluent. A yellow solid was obtained (1.11 g; 74 % yield).

¹H NMR (300 MHz, CDCl₃) δ 8.66 (d, *J* = 4.1 Hz, 1H), 8.04 (d, *J* = 16.0 Hz, 1H), 8.01 (dd, *J* = 8.1, 1.2 Hz, 1H), 7.83 (d, *J* = 7.8 Hz, 1H), 7.73 (td, *J* = 7.7, 1.7 Hz, 1H), 7.65 (t, *J* = 7.5 Hz, 1H), 7.53 (d, *J* = 7.9 Hz, 1H), 7.48 (t, *J* = 7.8 Hz, 1H), 7.26 (d, 1H, overlap with CDCl₃), 7.20 (d, *J* = 16.1 Hz, 1H).

¹³C NMR (75 MHz, CDCl₃) δ 155.16, 150.01, 148.71, 137.22, 133.59, 133.38, 132.79, 129.05, 128.93, 128.31, 125.18, 123.28, 122.50.

Elemental analysis for C₁₃H₁₀N₂O₂. Calc.: C 69.02; H 4.46; N 12.38. Found: C 69.31; H 4.53; N 12.49.

4.12.9. Synthesis of of 2,6-bis((*E*)-2-nitrostyryl)pyridine



The procedure was adapted from a previous reported protocol.^[85]

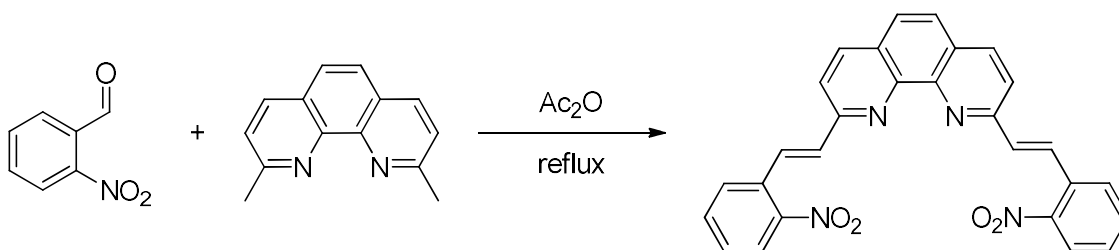
In a 25 mL Schlenk flask *o*-nitrobenzaldehyde (1.43 g, 9.46 mmol) and 2,6-lutidine (330 μL , 2.85 mmol) were dissolved in 2 mL of acetic anhydride. After 24 h of reflux a yellow solid precipitated. It was filtered through a Buchner funnel and washed with cold hexane. 725.5 mg of a yellow solid were obtained (68 % yield).

^1H NMR (300 MHz, $\text{DMSO}-d^6$) δ 8.09 – 7.96 (m, 6H), 7.88 (t, $J = 7.7$ Hz, 1H), 7.78 (t, $J = 7.6$ Hz, 2H), 7.64 – 7.51 (m, 4H), 7.41 (d, $J = 15.8$ Hz, 2H).

^{13}C NMR (75 MHz, $\text{DMSO}-d^6$) δ 154.90, 149.14, 138.82, 134.35, 133.67, 131.88, 130.13, 129.26, 127.62, 125.37, 123.41.

Elemental analysis for $\text{C}_{21}\text{H}_{15}\text{N}_3\text{O}_4$. Calc.: C 67.56; H 4.05; N 11.25. Found: C 67.82; H 4.19; N 10.90.

4.12.10. Synthesis of of 2,9-bis((*E*)-2-nitrostyryl)-1,10-phenanthroline



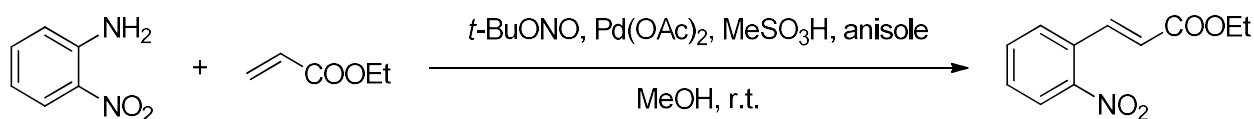
The procedure was adapted from a previous reported protocol.^[85]

In a 25 mL Schlenk flask *o*-nitrobenzaldehyde (1.43 g, 9.46 mmol) and neocuproine (593.5 mg, 2.85 mmol) were dissolved in 2 mL of acetic anhydride. After 30 min of reflux a yellow solid precipitate. It was filtered through a Buchner funnel and washed with cold hexane. 1.07 g of a yellow solid were obtained (79 % yield).

Owing to the insolubility in DMSO, it was not possible to register NMR spectra. However, the purity was confirmed by the CHN analysis.

Elemental analysis for $\text{C}_{28}\text{H}_{18}\text{N}_4\text{O}_4$. Calc.: C 70.88; H 3.82; N 11.81. Found: C 71.03; H 3.91; N 11.64.

4.12.11. Synthesis of (*E*)-ethyl 3-(2-nitrophenyl)acrylate (2-nitrocinnamate ethyl ester)



The procedure was adapted from a previous reported protocol.^[75a]

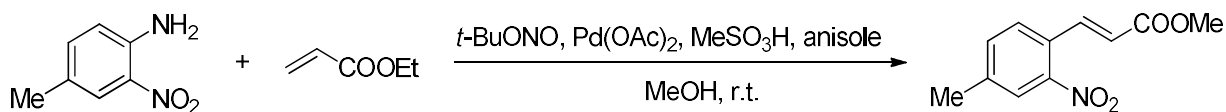
2-Nitroaniline (552.5 mg, 4 mmol) was dissolved in 20 mL of methanol. Then, *t*-BuONO (600 μ L, 5 mmol) was added. The reaction mixture was maintained under stirring for 30 minutes at 0 °C. Afterwards, a solution of ethyl acrylate (800 μ L, 8.8 mmol) and Pd(OAc)₂ (20 mg, $8.9 \cdot 10^{-2}$ mmol) in 16 mL of methanol and a solution of MeSO₃H (52 μ L, 0.8 mmol) in methanol (8 mL) were added to the previous one. During all the additions the reaction vessel was maintained at 0 °C with an ice/water bath. At the end, anisole (217 μ L, 2 mmol) was added and the reaction maintained under stirring at room temperature for 3 days. A TLC (hexane:AcOEt = 8:2) showed the disappearance of the 2-nitroaniline. The reaction mixture was poured into 30 mL of saturated solution of NaHCO₃ in water. A solid was formed. It was extracted with CH₂Cl₂ (3x60 mL). Organic layers were washed with brine, dried over Na₂SO₄, filtered and the solvent removed. A yellow oil was formed. The latter was purified through a silica filtration using hexane:AcOEt = 9:1 as the eluent. A yellow solid was obtained (760 mg, 86 % yield).

¹H NMR (400 MHz, CDCl₃) δ 7.99 (d, *J* = 15.8 Hz, 1H), 7.92 (d, *J* = 7.9 Hz, 1H), 7.68 – 7.51 (m, 2H), 7.47 (m, 1H), 6.28 (d, *J* = 15.8 Hz, 1H), 4.18 (q, *J* = 7.1 Hz, 2H), 1.25 (t, *J* = 7.1 Hz, 3H).

¹³C NMR (101 MHz, CDCl₃) δ 165.63, 148.22, 139.62, 133.53, 130.30, 129.01, 124.74, 123.15, 60.75.

Elemental analysis for C₁₁H₁₁NO₄. Calc.: C 59.73; H 5.01; N 6.33. Found: C 59.85; H 5.09; N 6.40.

Synthesis of (*E*)-methyl 3-(4-methyl-2-nitrophenyl)acrylate



The procedure was adapted from a previous reported protocol.^[75a]

4-Methyl-2-nitroaniline (604.6 mg, 4 mmol) was dissolved in 20 mL of methanol. Then, *t*-BuONO (600 μ L, 5 mmol) was added. The reaction mixture was maintained under stirring for 30 minutes at 0 °C. Afterwards, a solution of ethyl acrylate (800 μ L, 8.8 mmol) and Pd(OAc)₂ (20 mg, $8.9 \cdot 10^{-2}$ mmol) in 16 mL of methanol and a solution of MeSO₃H (52 μ L, 0.8 mmol) in methanol (8 mL) were added to the previous one. During all the additions the reaction vessel was maintained at 0 °C with an ice/water bath. At the end, anisole (217 μ L, 2 mmol) was added and the reaction maintained under stirring at room temperature for 3 days. A TLC (hexane:AcOEt = 8:2) showed the disappearance of the starting material and two spots very close to each other. In order to convert the ethyl ester into the methyl one, the reaction solvent was removed

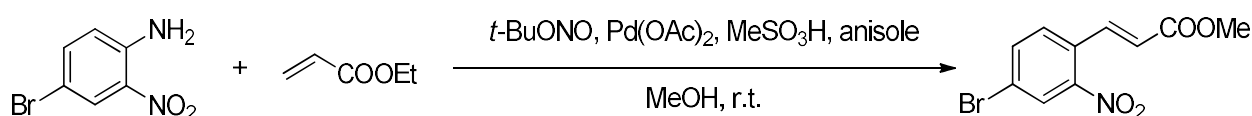
and the so obtained solid was dissolved into 20 mL of methanol. 3 drops of concentrated sulfuric acid were added and the mixture was reflux for 10 h. A TLC (hexane:AcOEt = 8:2) showed the presence of only one spot. A filtration over silica (hexane:AcOEt = 7:3 as the eluent) afforded the methyl ester as a yellowish solid (80 % yield).

^1H NMR (600 MHz, CDCl_3) δ 8.07 (d, $J = 15.8$ Hz, 1H), 7.82 (s, 1H), 7.52 (d, $J = 8.0$ Hz, 1H), 7.44 (d, $J = 7.9$ Hz, 1H), 6.33 (d, $J = 15.8$ Hz, 1H), 3.81 (s, 3H), 2.46 (s, 3H).

^{13}C NMR (151 MHz, CDCl_3) δ 166.34, 148.34, 141.38, 139.94, 134.18, 128.78, 127.57, 125.18, 122.07, 51.90, 21.07.

Elemental analysis for $\text{C}_{11}\text{H}_{11}\text{NO}_4$. Calc.: C 59.73; H 5.01; N 6.33. Found: C 59.78; H 5.23; N 6.33.

4.12.12. Synthesis of (*E*)-methyl 3-(4-bromo-2-nitrophenyl)acrylate



The procedure was adapted from a previous reported protocol.^[75a]

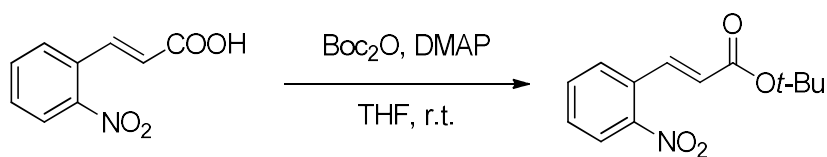
The reaction was performed under dinitrogen atmosphere. 4-Bromo-2-nitroaniline (868.1 mg, 4 mmol) was dissolved in 20 mL of methanol. Then, $t\text{-BuONO}$ (1.2 mL, 10 mmol) was added. The reaction mixture was maintained under stirring for 30 minutes at 0 °C. Afterwards, a solution of ethyl acrylate (800 μL , 8.8 mmol) and $\text{Pd}(\text{OAc})_2$ (40 mg, $1.8 \cdot 10^{-1}$ mmol) in 16 mL of methanol and a solution of MeSO_3H (52 μL , 0.8 mmol) in methanol (8 mL) were added to the previous one. During all the additions the reaction vessel was maintained at 0 °C with an ice/water bath. At the end, anisole (217 μL , 2 mmol) was added and the reaction maintained under stirring at room temperature for 10 days. A TLC (hexane:AcOEt = 8:2) showed the disappearance of the starting material. A saturated solution of Na_2CO_3 (30 mL) was added. A yellow solid precipitated that was filtered through a Buchner funnel. The solid was washed with cold methanol affording the product as a yellow solid (70 % yield). Owing to the presence of MeSO_3H and methanol as solvent, the product was obtained as methyl esters instead of ethyl one.

^1H NMR (600 MHz, CDCl_3) δ 8.18 (d, $J = 1.9$ Hz, 1H), 8.03 (d, $J = 15.8$ Hz, 1H), 7.77 (dd, $J = 8.3, 1.9$ Hz, 1H), 7.51 (d, $J = 8.4$ Hz, 1H), 6.37 (d, $J = 15.8$ Hz, 1H), 3.83 (s, 3H).

^{13}C NMR (151 MHz, CDCl_3) δ 165.92, 148.59, 138.90, 136.55, 130.24, 129.37, 127.96, 123.76, 123.45, 52.06.

Elemental analysis for $\text{C}_{10}\text{H}_8\text{BrNO}_4$. Calc.: C 41.98; H 2.82; N 4.90. Found: C 41.83; H 2.88; N 4.86.

4.12.13. Synthesis of (*E*)-*tert*-butyl 3-(2-nitrophenyl)acrylate



The procedure was adapted from a previously reported protocol.^[86]

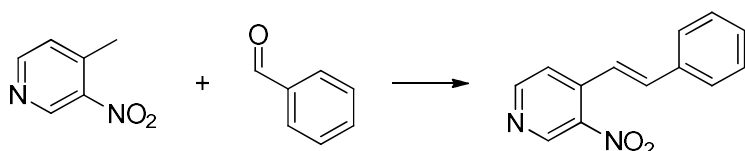
The reaction was performed under a dinitrogen atmosphere. To a solution of 2-nitrocinnamic acid (500 mg, 2.59 mmol) in dry THF (13 mL), Boc_2O (1.13 g, 5.18 mmol) and DMAP (4-dimethylaminopyridine; 95 mg, 0.78 mmol) were added. The reaction was maintained under stirring at RT for 72 h and then concentrated. The residue was purified by column chromatography (hexane:AcOEt = 8:2 as the eluent) affording a pale yellow solid (613 mg, 95 % yield).

^1H NMR (400 MHz, CDCl_3) δ 8.07 – 7.99 (m, 2H), 7.65 (d, $J = 4.2$ Hz, 2H), 7.55 (td, $J = 8.5, 4.1$ Hz, 1H), 6.32 (d, $J = 15.8$ Hz, 1H), 1.56 (s, 9H).

^{13}C NMR (75 MHz, CDCl_3) δ 165.42, 148.75, 139.05, 133.77, 131.16, 130.41, 129.48, 125.70, 125.23, 81.56, 28.52.

Elemental analysis for $\text{C}_{13}\text{H}_{15}\text{NO}_4$. Calc.: C 62.64; H 6.07; N 5.62. Found: C 62.74; H 5.59; N 5.55.

4.12.14. Synthesis of (*E*)-3-nitro-4-styrylpyridine



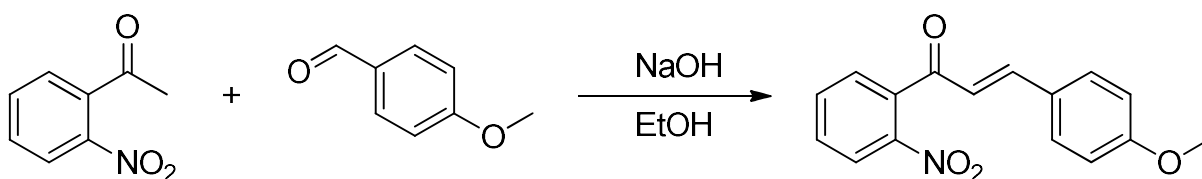
4-Methyl-2-nitropyridine (589.6 mg, 6.22 mmol), benzaldehyde (634 μL , 6.22 mmol) and piperidine (307 μL , 3.11 mmol) were added to 10 mL of methanol. After 10 h of reflux a yellow solid precipitate. This was filtered through a Büchner funnel and washed with cold methanol. 753.4 mg of solid were collected (54 % yield).

^1H NMR (300 MHz, $\text{DMSO}-d_6$) δ 9.15 (s, 1H), 8.82 (d, $J = 5.2$ Hz, 1H), 8.02 (d, $J = 5.2$ Hz, 1H), 7.72 – 7.62 (m, 3H), 7.53 (d, $J = 16.3$ Hz, 1H), 7.49 – 7.36 (m, 3H).

^{13}C NMR (75 MHz, $\text{DMSO}-d_6$) δ 154.01, 146.74, 144.65, 140.22, 138.27, 136.47, 130.41, 129.85, 128.46, 122.12, 121.34.

Elemental analysis for $\text{C}_{11}\text{H}_{10}\text{N}_2\text{O}_2$. Calc.: C 69.02; H 4.46; N 12.38. Found: C 68.76; H 4.49; N 12.34.

4.12.15. **Synthesis of (*E*)-3-(4-methoxyphenyl)-1-(2-nitrophenyl)prop-2-en-1-one**



The procedure was adapted from a previous reported protocol.^[87]

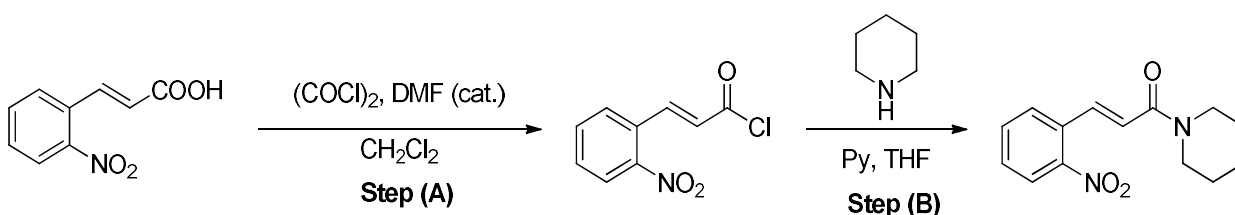
The reaction was performed under air. *o*-Nitroacetophenone (1651.5 mg, 10 mmol) and 4-methoxybenzaldehyde (1361.5 mg, 10 mmol) were mixed in water (15 mL). Then, 2 mL of a 6 % solution of NaOH in water:ethanol (2:1 by volume) were added. A gentle heating was applied (30 °C) until a brown precipitate appeared. This was filtered off and the product recrystallized from ethanol (1841 mg, 65 % yield).

¹H NMR (400 MHz, CDCl₃) δ 8.19 (d, *J* = 8.2 Hz, 1H), 7.77 (t, *J* = 7.5 Hz, 1H), 7.66 (t, *J* = 7.8 Hz, 1H), 7.52 (d, *J* = 7.4 Hz, 1H), 7.47 (d, *J* = 8.5 Hz, 2H), 7.22 (d, *J* = 16.2 Hz, 1H), 6.95 – 6.86 (m, 3H), 3.85 (s, 3H).

¹³C NMR (101 MHz, CDCl₃) δ 162.10, 146.37, 136.58, 133.93, 130.42, 128.86, 126.65, 124.53, 124.00, 114.50, 55.44. One quaternary carbon is not detected.

Elemental analysis for C₁₆H₁₃NO₄. Calc.: C 67.84; H 4.63; N 4.94. Found: C 67.80; H 4.55; N 4.90.

4.12.16. **Synthesis of (*E*)-3-(2-nitrophenyl)-1-(piperidin-1-yl)prop-2-en-1-one**



A literature procedure was followed.^[88]

Step (A). The reaction was performed under dinitrogen atmosphere. In a 25 mL Schlenk flask, 2-nitrocinnamic acid (1.162 g, 6 mmol) was suspended in 9 mL of CH₂Cl₂. Then, two drops of DMF were added. Oxalyl chloride (1.03 mL, 12 mmol) was slowly added maintaining the flask at 0 °C in a water/ice bath. After 5 minutes, the reaction mixture became clear and brown-colored. It was maintained under stirring for 5 hours. Afterwards the solvent was removed affording a brown solid. This material was directly used for the next step without further purifications.

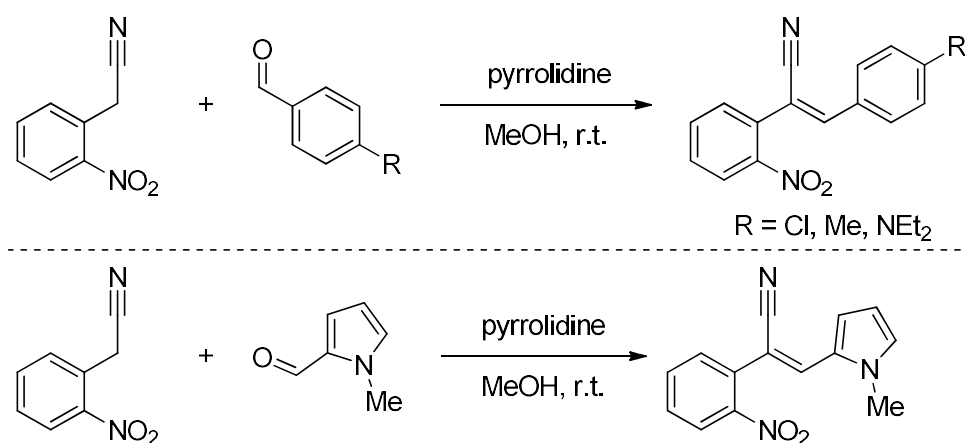
Step (B). The reaction was performed under dinitrogen atmosphere. In a 50 mL Schlenk flask a solution of pyrrolidine (592 μ L, 6 mmol) and pyridine (501 μ L, 6.2 mmol) was prepared using 10 mL of THF. To the flask containing the product prepared in Step A, 10 mL of THF were added. To this mixture, the pyridine/pyrrolidine solution was added. After 24 h, the solvent was removed and a filtration through a small pad of silica was performed using hexane:AcOEt = 8:2 as the eluant. A white solid was obtained (71 % yield).

^1H NMR (400 MHz, CDCl_3) δ 7.99 (d, J = 8.1 Hz, 1H), 7.86 (d, J = 15.5 Hz, 1H), 7.61 (d, J = 4.1 Hz, 2H), 7.56 – 7.41 (m, 1H), 6.74 (d, J = 15.5 Hz, 1H), 3.61 (d, J = 18.1 Hz, 4H), 1.74 – 1.56 (m, 6H).

^{13}C NMR (101 MHz, CDCl_3) δ 164.65, 148.22, 136.53, 133.31, 131.88, 129.47, 129.24, 124.75, 123.73, 47.17, 43.33, 26.62, 25.53, 24.49.

Elemental analysis for $\text{C}_{14}\text{H}_{16}\text{N}_2\text{O}_3$. Calc.: C 64.60; H 6.20; N 10.76. Found: C 64.80; H 6.38; N 10.63.

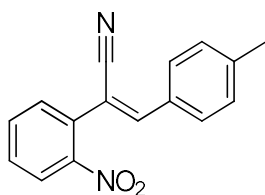
4.12.17. Synthesis of 2-(2-nitrophenyl)-3-(hetero)arylacrylonitriles



The procedure was adapted from a previously reported protocol.^[89]

2-Nitrobenzylidene nitrile (750 mg, 4.63 mmol) and the desired benzaldehyde (4.63 mmol) were dissolved into methanol (8 mL). Then, 760 μ L of pyrrolidine were added and the reaction mixture maintained under stirring at room temperature. After a few minutes (from 1 to 10 min depending from the aldehyde), the desired product precipitates and collected through filtration.

(Z)-2-(2-nitrophenyl)-3-(p-tolyl)acrylonitrile



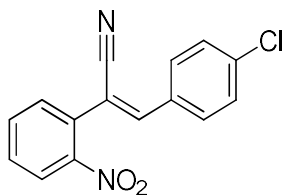
Pale white solid, 91 % yield.

^1H NMR (300 MHz, CDCl_3) δ 8.10 (d, $J = 8.1$ Hz, 1H), 7.79 (d, $J = 8.1$ Hz, 2H), 7.71 (t, $J = 7.5$ Hz, 1H), 7.58 (dd, $J = 16.3, 8.3$ Hz, 2H), 7.29 (d, $J = 8.0$ Hz, 2H), 7.14 (s, 1H), 2.42 (s, 3H).

^{13}C NMR (75 MHz, CDCl_3) δ 148.30, 146.70, 142.39, 134.12, 132.25, 131.60, 130.72, 130.53, 130.18, 129.80, 125.69, 117.10, 107.47, 22.03.

Elemental analysis for $\text{C}_{16}\text{H}_{12}\text{N}_2\text{O}_2$. Calc.: C 72.72; H 4.58; N 10.60. Found: C 72.48; H 4.68; N 10.63.

(Z)-3-(4-chlorophenyl)-2-(2-nitrophenyl)acrylonitrile



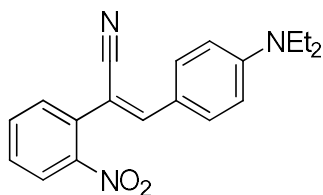
Pale white solid, 79 % yield.

^1H NMR (300 MHz, CDCl_3) δ 8.13 (d, $J = 8.0$ Hz, 1H), 7.82 (d, $J = 8.6$ Hz, 2H), 7.73 (t, $J = 7.5$ Hz, 1H), 7.62 (t, $J = 7.2$ Hz, 1H), 7.55 (d, $J = 6.6$ Hz, 1H), 7.46 (d, $J = 8.6$ Hz, 2H), 7.13 (s, 1H).

^{13}C NMR (75 MHz, CDCl_3) δ 145.07, 137.66, 134.32, 132.19, 131.81, 131.15, 130.94, 130.90, 129.79, 125.80, 116.62, 109.56. One quaternary carbon is not detected.

Elemental analysis for $\text{C}_{15}\text{H}_9\text{ClN}_2\text{O}_2$. Calc.: C 63.28; H 3.19; N 9.84. Found: C 63.06; H 3.20; N 9.85.

(Z)-3-(4-(diethylamino)phenyl)-2-(2-nitrophenyl)acrylonitrile



Red solid, 86 % yield.

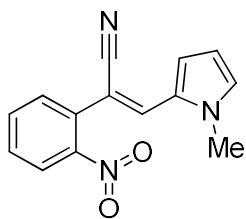
^1H NMR (300 MHz, CDCl_3) δ 7.99 (d, $J = 8.8$ Hz, 1H), 7.81 (d, $J = 9.0$ Hz, 2H), 7.64 (t, $J = 7.5$ Hz, 1H), 7.51 (m, 2H), 7.01 (s, 1H), 6.69 (d, $J = 8.6$ Hz, 2H), 3.43 (q, $J = 7.1$ Hz, 4H), 1.21 (t, $J = 7.1$ Hz, 6H).

^{13}C NMR (75 MHz, CDCl_3) δ 150.27, 148.51, 147.04, 133.66, 132.40, 132.26, 132.13, 129.53, 125.46, 120.66, 118.52, 111.52, 45.01, 12.95. One quaternary carbon is not detected.

Elemental analysis for $\text{C}_{19}\text{H}_{19}\text{N}_3\text{O}_2$. Calc.: C 71.01; H 5.96; N 13.08. Found: C 71.05; H 6.00; N 13.10.

Attention: this molecule tends to be oxidized quickly (in few days, the air exposed surface became brown). Store under dinitrogen atmosphere and in the dark.

(Z)-3-(1-methyl-1H-pyrrol-2-yl)-2-(2-nitrophenyl)acrylonitrile



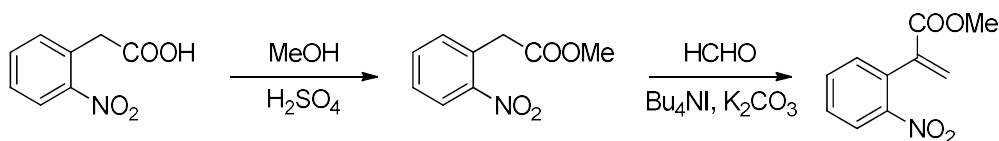
Yellow solid, 65 % yield.

^1H NMR (300 MHz, CDCl_3) δ 7.97 (d, $J = 7.7$ Hz, 1H), 7.66 (t, $J = 8.1$ Hz, 1H), 7.53 (t, $J = 6.9$ Hz, 3H), 7.02 (s, 1H), 6.84 (s, 1H), 6.32 (q, 1H), 3.68 (s, 3H).

^{13}C NMR (75 MHz, CDCl_3) δ 148.63, 133.59, 133.21, 131.91, 131.34, 129.78, 128.34, 128.17, 125.43, 117.95, 115.55, 110.84, 99.87, 34.42.

Elemental analysis for $\text{C}_{14}\text{H}_{11}\text{N}_3\text{O}_2$. Calc.: C 66.40; H 4.38; N 15.59. Found: C 66.72; H 4.18; N 15.44.

4.12.18. Synthesis of methyl 2-(2-nitrophenyl)acrylate



In a 100 mL Schlenk flask, 2-(2-Nitrophenyl)acetic acid (2.53 g, 14 mmol) were dissolved in 50 mL of methanol. 2 mL of concentrated sulfuric acid was dropwise added and the solution refluxed for 16 h. The solvent was removed and the solid residue was added with water (30 mL) and the extracted with AcOEt (3x30 mL). The organic layers were washed with a saturated solution of NaHCO_3 (3x30mL) and brine (1x30 mL). The combined organic layers were dried over Na_2SO_4 , filtered and the solvent removed affording a pale yellow oil (95 % yield).

^1H NMR (300 MHz, CDCl_3) δ 8.12 (d, $J = 7.8$ Hz, 1H), 7.57-7.63 (m, 1H), 7.44-7.51 (m, 1H), 7.36 (d, $J = 7.3$ Hz, 1H), 4.03 (s, 2H), 3.72 (s, 3H).

For the olefination step, a reported procedure was followed.^[9a]

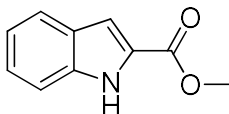
975 (5 mmol) mg of the previously obtained ester was dissolved in 5 mL of toluene. Then, paraformaldehyde (420 mg, 14 mmol), Bu_4NI (74 mg, 0.2 mmol) and potassium carbonate (2.07 g, 15 mmol) were added. The mixture was heated to 80 °C for one day. At the end of the reaction, water (10 mL) was added and the aqueous layer was extracted with toluene (3x10 mL). The combined organic layers were washed with brine (10 mL) and dried over Na_2SO_4 . The solvent was removed and the compound was isolated as a yellow oil after column chromatography (silica gel, hexane:AcOEt = 9:1 as the eluent).

^1H NMR (300 MHz, CDCl_3) δ 8.02 (d, $J = 8.1$ Hz, 1H), 7.60 (t, $J = 7.5$ Hz, 1H), 7.47 (t, $J = 7.3$ Hz, 1H), 7.35 (d, $J = 7.0$ Hz, 1H), 6.46 (s, 1H), 5.83 (s, 1H), 3.64 (s, 3H).

^{13}C NMR (75 MHz, CDCl_3) δ 165.61, 148.20, 140.15, 134.18, 133.17, 132.55, 129.82, 127.87, 124.83, 52.51.

4.13. Indoles and other heterocycles

Methyl 1*H*-indole-2-carboxylate



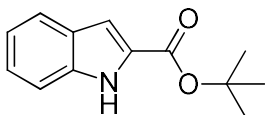
Obtained as a white solid after column chromatography (hexane:CH₂Cl₂ = 7:3 + 1 % Et₃N); 95 % yield.

¹H NMR (300 MHz, CDCl₃) δ 8.98 (br, 1H), 7.70 (d, *J* = 8.1 Hz, 1H), 7.43 (d, *J* = 8.3 Hz, 1H), 7.33 (t, *J* = 7.6 Hz, 1H), 7.25 (d, *J* = 8.2 Hz, 1H), 7.16 (t, *J* = 7.5 Hz, 1H), 3.96 (s, 3H).

¹³C NMR (75 MHz, CDCl₃) δ 162.85, 137.27, 127.90, 127.53, 125.79, 123.04, 121.24, 112.26, 109.21, 52.40.

Elemental analysis for C₁₀H₉NO₂. Calc.: C 68.56; H 5.18; N 8.00. Found: C 68.50; H 5.23; N 8.01.

t-Butyl-1*H*-indole-2-carboxylate



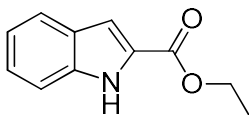
Obtained as a white solid after column chromatography (hexane:AcOEt = 1:1 + 1 % Et₃N); 87 % yield.

¹H NMR (300 MHz, CDCl₃) δ 8.95 (s, 1H), 7.68 (d, *J* = 8.9 Hz, 1H), 7.42 (d, *J* = 8.3 Hz, 1H), 7.31 (t, *J* = 7.6 Hz, 1H), 7.19 – 7.11 (m, 2H).

¹³C NMR (75 MHz, CDCl₃) δ 161.75, 137.00, 129.38, 127.97, 125.43, 122.86, 121.02, 112.16, 108.49, 82.17, 28.73.

Elemental analysis for C₁₃H₅NO₂. Calc.: C 71.87; H 6.96; N 6.45. Found: C 71.71; H 6.95; N 6.70.

Ethyl 1*H*-indole-2-carboxylate



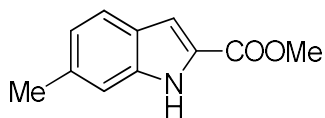
Obtained as a white solid after column chromatography (hexane:CH₂Cl₂ = 3:7 + 1 % Et₃N); 92 % yield.

¹H NMR (400 MHz, CDCl₃) δ 8.90 (br, 1H), 7.70 (dd, *J* = 8.1, 0.9 Hz, 1H), 7.43 (dd, *J* = 7.9, 1.4 Hz, 1H), 7.33 (ddd, *J* = 8.3, 7.0, 1.1 Hz, 1H), 7.24 (dd, *J* = 2.1, 1.0 Hz, 1H), 7.16 (ddd, *J* = 8.0, 7.0, 1.0 Hz, 1H), 4.42 (q, *J* = 7.1 Hz, 1H), 1.42 (t, *J* = 7.1 Hz, 1H).

¹³C NMR (101 MHz, CDCl₃) δ 161.99, 136.79, 127.52, 125.34, 122.60, 120.79, 111.82, 108.63, 61.01, 14.40.

Elemental analysis for C₁₁H₁₁NO₂. Calc.: C 69.83; H 5.86; N 7.40. Found: C 69.67; H 5.80; N 7.40.

Methyl 6-methyl-1*H*-indole-2-carboxylate



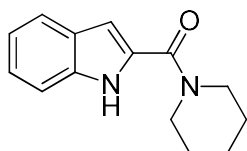
Obtained as a white solid after column chromatography (hexane:CH₂Cl₂ = 3:7 + 1 % Et₃N); 96 % yield.

¹H NMR (600 MHz, CDCl₃) δ 8.79 (br, 1H), 7.57 (d, *J* = 8.2 Hz, 1H), 7.19 (d, *J* = 11.6 Hz, 2H), 7.00 (d, *J* = 8.2 Hz, 1H), 3.94 (s, 3H), 2.47 (s, 3H).

¹³C NMR (151 MHz, CDCl₃) δ 162.48, 137.41, 135.71, 126.57, 125.42, 122.99, 122.22, 111.47, 108.82, 51.86, 21.94.

Elemental analysis for C₁₁H₁₁NO₂. Calc.: C 69.83; H 5.86; N 7.40. Found: C 69.67; H 5.80; N 7.40.

(1*H*-indol-2-yl)(piperidin-1-yl)methanone

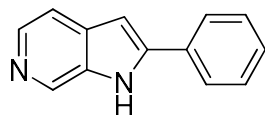


Obtained as a white solid after column chromatography (from hexane:CH₂Cl₂ = 1:1 + 1 % Et₃N to hexane:CH₂Cl₂ = 2:8 + 1 % Et₃N); 73 % yield.

¹H NMR (400 MHz, CDCl₃) δ 9.24 (s, 1H), 7.67 (d, *J* = 8.0 Hz, 1H), 7.45 (d, *J* = 8.9 Hz, 1H), 7.36 – 7.24 (m, 1H, overlapping with CHCl₃), 7.15 (t, *J* = 7.5 Hz, 1H), 6.79 (s, 1H), 3.87 (s, 4H), 1.93 – 1.57 (m, 6H).

Elemental analysis for C₁₄H₁₆N₂O. Calc.: C 73.66; H 7.06; N 12.27. Found: C 73.76; H 7.20; N 12.01.

2-Phenyl-6-azaindole



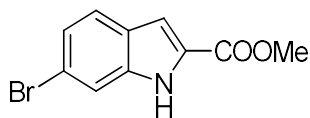
Obtained as a white solid after column chromatography (AcOEt + 2 % Et₃N + 1 % MeOH); 91 % yield.

¹H NMR (400 MHz, CDCl₃) δ 10.27 (s, 1H), 8.96 (s, 1H), 8.27 (d, *J* = 5.5 Hz, 1H), 7.82 (d, *J* = 7.3 Hz, 2H), 7.63 – 7.36 (m, 4H), 6.85 (s, 1H).

¹³C NMR (101 MHz, CDCl₃) δ 142.41, 138.83, 134.29, 134.14, 133.81, 129.17, 128.85, 126.04, 115.08, 98.91.

Elemental analysis for $C_{13}H_{10}N_2$. Calc.: C 80.39; H 5.19; N 14.42. Found: C 80.29; H 4.98; N 14.23.

Methyl 6-bromo-1*H*-indole-2-carboxylate



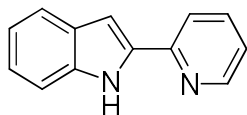
Obtained as a white solid after column chromatography (hexane:CH₂Cl₂ = 4:6 + 1 % Et₃N); 90 % yield.

Elemental analysis for $C_{10}H_8BrNO_2$. Calc.: C 47.27; H 3.17; N 5.51. Found: C 47.64; H 3.32; N 5.44

¹H NMR (600 MHz, CDCl₃) δ 8.86 (br s, 1H), 7.59 (s, 1H), 7.55 (d, *J* = 8.6 Hz, 1H), 7.27 (d *J* = 8.6 Hz, 1H), 7.18 (s, 1H), 3.95 (s, 3H).

¹³C NMR (151 MHz, CDCl₃) δ 162.01, 137.38, 127.78, 126.33, 124.50, 123.84, 119.23, 114.73, 108.79, 52.11.

2-(pyridin-2-yl)-1*H*-indole



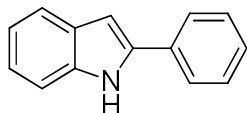
Obtained as a white solid after column chromatography (hexane:CH₂Cl₂ = 7:3 + 1 % Et₃N); 98 % yield.

¹H NMR (300 MHz, CDCl₃) δ 9.75 (br, 1H), 8.58 (d, *J* = 4.6 Hz, 1H), 7.82 (d, *J* = 8.0 Hz, 1H), 7.73 (td, *J* = 7.8, 1.7 Hz, 1H), 7.66 (d, *J* = 7.9 Hz, 1H), 7.42 (d, *J* = 8.2 Hz, 1H), 7.26-7.16 (m, 2H, overlapping with CDCl₃), 7.12 (t, *J* = 7.5 Hz, 1H), 7.04 (d, *J* = 1.1 Hz, 1H).

¹³C NMR (75 MHz, CDCl₃) δ 150.53, 149.04, 137.36, 137.07, 136.61, 129.43, 123.77, 122.39, 121.34, 120.62, 120.41, 111.88, 101.38.

Elemental analysis for $C_{13}H_{10}N$. Calc.: C 80.39; H 5.19; N 14.42. Found: C 80.19; H 5.23; N 14.35.

2-phenyl-1*H*-indole



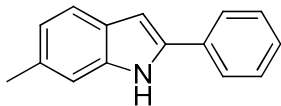
Obtained as a white solid after column chromatography (hexane:CH₂Cl₂ = 7:3 + 1 % Et₃N); 90 % yield.

Elemental analysis for $C_{14}H_{11}N$. Calc.: C 87.01; H 5.74; N 7.25. Found: C 86.85; H 5.80; N 7.30.

¹H NMR (300 MHz, CDCl₃) δ 8.33 (br, 1H), 7.73 – 7.64 (m, 3H), 7.53 – 7.40 (m, 4H), 7.36 (t, *J* = 7.3 Hz, 1H), 7.25 (dd, *J* = 13.4, 5.3 Hz, 1H), 7.18 (t, *J* = 7.4 Hz, 1H), 6.87 (s, 1H).

^{13}C NMR (75 MHz, CDCl_3) δ 138.31, 137.26, 132.80, 129.71, 129.44, 128.14, 125.59, 122.79, 121.10, 120.71, 111.33, 100.43.

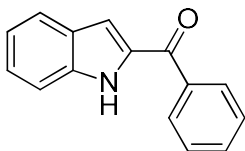
6-methyl-2-phenyl-1H-indole



Obtained as a white solid after column chromatography (hexane:AcOEt = 85:15 + 1 % Et_3N); 79 % yield.

^1H NMR (300 MHz, CDCl_3) δ 8.19 (s, 1H), 7.65 (d, $J = 7.3$ Hz, 2H), 7.51 (d, $J = 8.1$ Hz, 1H), 7.44 (t, $J = 7.6$ Hz, 2H), 7.31 (t, $J = 7.4$ Hz, 1H), 7.20 (s, 1H), 6.96 (d, $J = 8.0$ Hz, 1H), 6.78 (s, 1H), 2.48 (s, 3H).

(1H-indol-2-yl)(phenyl)methanone



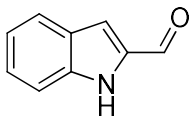
Obtained as a white solid after column chromatography (hexane:AcOEt = 7:3 + 1 % Et_3N); 79 % yield.

^1H NMR (300 MHz, CDCl_3) δ 9.40 (s, 1H), 8.01 (d, $J = 7.0$ Hz, 2H), 7.73 (d, $J = 8.1$ Hz, 1H), 7.63 (t, $J = 7.3$ Hz, 1H), 7.59 – 7.45 (m, 3H), 7.39 (t, $J = 7.6$ Hz, 1H), 7.22 – 7.13 (m, 2H).

^{13}C NMR (75 MHz, CDCl_3) δ 187.56, 138.41, 137.92, 134.76, 132.74, 129.61, 128.87, 128.17, 126.93, 123.64, 121.45, 113.15, 112.56.

Elemental analysis for $\text{C}_{15}\text{H}_{11}\text{NO}$. Calc.: C 81.43; H 5.01; N 6.33. Found: C 81.60; H 5.11; N 6.30.

1H-indole-2-carbaldehyde



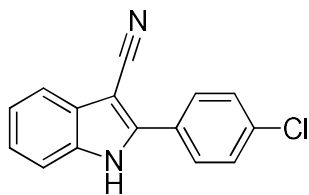
Obtained as a white solid after column chromatography (hexane: CH_2Cl_2 = 4:6 + 1 % Et_3N); 50 % yield.

Elemental analysis for $\text{C}_9\text{H}_7\text{NO}$. Calc.: C 74.47; H 4.86; N 9.65. Found: C 74.30; H 4.55; N 9.60.

^1H NMR (400 MHz, CDCl_3) δ 9.87 (s, 1H), 9.75 (s, 1H), 7.76 (d, $J = 8.1$ Hz, 1H), 7.51 (d, $J = 8.4$ Hz, 1H), 7.40 (dd, $J = 13.7, 5.6$ Hz, 1H), 7.30 (s, 1H), 7.19 (t, $J = 7.5$ Hz, 1H).

^{13}C NMR (101 MHz, CDCl_3) δ 182.41, 138.37, 135.99, 127.39, 127.33, 123.42, 121.25, 115.24, 112.70.

2-(4-chlorophenyl)-1H-indole-3-carbonitrile



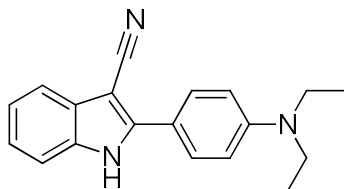
Obtained as a white solid after column chromatography (hexane:CH₂Cl₂ = 7:3 + 1 % Et₃N); 94 % yield.

Elemental analysis for C₁₅H₉ClN₂. Calc.: C 71.29; H 3.59; N 11.09. Found: C 71.29; H 3.62; N 10.97.

¹H NMR (600 MHz, DMSO-*d*⁶) δ 12.65 (s, 1H), 8.00 (d, *J* = 8.6 Hz, 2H), 7.72 (d, *J* = 8.6 Hz, 2H), 7.66 (d, *J* = 7.9 Hz, 1H), 7.57 (d, *J* = 8.1 Hz, 1H), 7.34 (t, *J* = 8.1 Hz, 1H), 7.28 (t, *J* = 7.4 Hz, 1H).

¹³C NMR (151 MHz, DMSO-*d*⁶) δ 143.83, 136.07, 135.11, 129.90, 129.16, 128.69, 124.62, 122.64, 118.92, 117.21, 113.18, 82.28.

2-(4-(diethylamino)phenyl)-1H-indole-3-carbonitrile



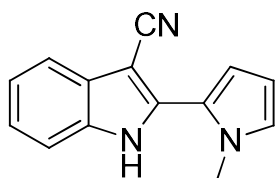
Obtained as a white solid after column chromatography (hexane:CH₂Cl₂ = 8:2 + 1 % Et₃N); 95 % yield.

Elemental analysis for C₁₅H₉ClN₂. Calc.: C 78.86; H 6.62; N 14.52. Found: C 78.87; H 6.60; N 14.50.

¹H NMR (400 MHz, DMSO-*d*⁶) δ 7.84 (d, *J* = 9.0 Hz, 2H), 7.54 (d, *J* = 7.0 Hz, 1H), 7.47 (d, *J* = 7.4 Hz, 1H), 7.28 – 7.15 (m, 2H), 6.85 (d, *J* = 9.1 Hz, 2H), 3.43 (q, *J* = 7.0 Hz, 4H), 1.14 (t, *J* = 7.0 Hz, 6H).

¹³C NMR (101 MHz, DMSO-*d*⁶) δ 148.94, 146.56, 135.74, 129.16, 128.51, 123.40, 121.99, 118.22, 118.10, 115.74, 112.47, 111.80, 78.78, 44.15, 12.89.

2-(1-methyl-1H-pyrrol-2-yl)-1H-indole-3-carbonitrile



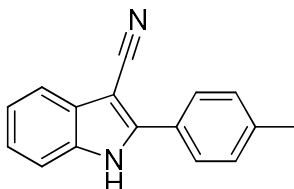
Obtained as a white solid after column chromatography (hexane:CH₂Cl₂ = 4:6 + 1 % Et₃N); 51 % yield.

¹H NMR (400 MHz, CDCl₃) δ 8.53 (s, 1H), 7.79 – 7.72 (m, 1H), 7.46 – 7.41 (m, 1H), 7.36 – 7.27 (m, 2H), 6.90 – 6.84 (m, 1H), 6.58 (dd, *J* = 3.8, 1.7 Hz, 1H), 6.31 – 6.24 (m, 1H), 3.86 (s, 3H).

^{13}C NMR (101 MHz, CDCl_3) δ 137.95, 134.67, 128.45, 126.63, 124.22, 122.82, 122.42, 119.39, 116.68, 112.45, 111.49, 109.21, 85.26, 35.65.

Elemental analysis for $\text{C}_{14}\text{H}_{11}\text{N}_3$. Calc.: C 76.00; H 5.01; N 18.99. Found: C 76.25; H 5.5.13; N 18.70.

2-(*p*-tolyl)-1*H*-indole-3-carbonitrile



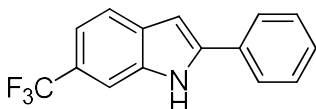
Obtained as a white solid after column chromatography (hexane: CH_2Cl_2 = 7:3 + 1 % Et_3N); 95 % yield.

Elemental analysis for $\text{C}_{16}\text{H}_{12}\text{N}_2$. Calc.: C 82.73; H 5.21; N 12.06. Found: C 82.38; H 5.23; N 11.72.

^1H NMR (400 MHz, $\text{DMSO}-d^6$) δ 12.52 (br, 1H), 7.89 (d, J = 8.1 Hz, 2H), 7.63 (d, J = 7.6 Hz, 1H), 7.55 (d, J = 8.0 Hz, 1H), 7.44 (d, J = 8.0 Hz, 2H), 7.28 (dt, J = 22.4, 7.1 Hz, 2H), 2.41 (s, 3H).

^{13}C NMR (101 MHz, $\text{DMSO}-d^6$) δ 145.38, 140.34, 135.92, 130.32, 128.79, 127.29, 127.04, 124.23, 122.42, 118.71, 117.56, 113.02, 81.37, 21.41.

2-phenyl-6-(trifluoromethyl)-1*H*-indole



Obtained as a white solid after column chromatography (hexane: CH_2Cl_2 = 8:2 + 1 % Et_3N); 98 % yield.

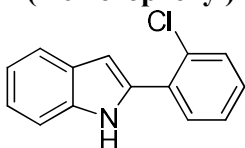
Elemental analysis for $\text{C}_{15}\text{H}_{10}\text{F}_3\text{N}$. Calc.: C 68.96; H 3.86; N 5.36. Found: C 68.70; H 3.66; N 5.15.

^1H NMR (600 MHz, CDCl_3) δ 8.55 (brs, 1H), 7.71-7.68 (m, 4H), 7.48 (t, J = 7.7 Hz, 2H), 7.40-7.36 (m, 2H), 6.88 (d, J = 1.7 Hz, 1H).

^{13}C NMR (151 MHz, CDCl_3) δ 140.57, 135.58, 131.60, 129.22, 128.50, 125.44, 125.22, 120.92, 117.03, 108.39, 100.06.

^{19}F NMR (282 MHz, CDCl_3) δ -60.96 (s).

2-(2-chlorophenyl)-1*H*-indole



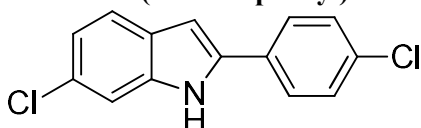
Obtained as a white solid after column chromatography (hexane: CH_2Cl_2 = 7:3 + 1 % Et_3N); 69 % yield.

Elemental analysis for C₁₄H₁₀ClN. Calc.: C 73.85; H 4.43; N 6.15. Found: C 73.50; H 4.66; N 6.01.

¹H NMR (300 MHz, CDCl₃) δ 7.78 – 7.66 (m, 1H), 7.56 – 7.51 (m, 1H), 7.46 (d, *J* = 8.1 Hz, 1H), 7.39 (dd, *J* = 7.5, 1.4 Hz, 1H), 7.34 (dd, *J* = 5.3, 1.7 Hz, 1H), 7.32 – 7.27 (m, 1H), 7.24 – 7.15 (m, 1H), 6.92 (d, *J* = 1.3 Hz, 1H).

¹³C NMR (75 MHz, CDCl₃) δ 136.82, 135.51, 131.77, 131.62, 131.24, 131.13, 129.23, 128.60, 127.67, 123.10, 121.22, 120.63, 111.48, 104.00.

6-chloro-2-(4-chlorophenyl)-1*H*-indole



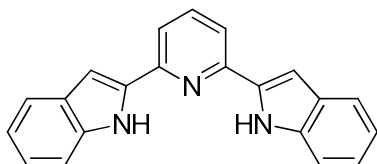
Obtained as a white solid after column chromatography (hexane:CH₂Cl₂ = 7:3 + 1 % Et₃N); 92 % yield.

Elemental analysis for C₁₄H₁₀ClN. Calc.: C 64.15; H 3.46; N 5.34. Found: C 64.50; H 3.66; N 5.15.

¹H NMR (400 MHz, CDCl₃) δ 8.28 (br, 1H), 7.63 – 7.52 (m, 3H), 7.48 – 7.36 (m, 3H), 7.12 (d, *J* = 8.4 Hz, 1H), 6.79 (s, 1H).

¹³C NMR (101 MHz, CDCl₃) δ 137.43, 137.19, 133.78, 130.42, 129.31, 128.37, 127.73, 126.31, 121.56, 121.25, 110.88, 100.42.

2,6-di(1*H*-indol-2-yl)pyridine



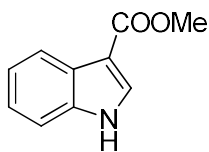
Obtained as a white solid after column chromatography (hexane:CH₂Cl₂ = 7:3 + 1 % Et₃N); 78 % yield.

Elemental analysis for C₂₁H₁₅N₃. Calc.: C 81.55; H 4.89; N 13.58. Found: C 81.75; H 4.83; N 13.34.

¹H NMR (300 MHz, DMSO-*d*⁶) δ 11.71 (s, 1H), 7.88 (t, 2H), 7.61 (dd, *J* = 17.9, 8.0 Hz, 4H), 7.28 (d, *J* = 1.2 Hz, 2H), 7.25 – 7.18 (m, 2H), 7.07 (t, *J* = 7.1 Hz, 2H).

¹³C NMR (75 MHz, DMSO-*d*⁶) δ 150.31, 138.68, 137.87, 137.62, 129.53, 123.61, 121.77, 120.48, 118.70, 112.42, 101.67.

Methyl 1*H*-indole-3-carboxylate



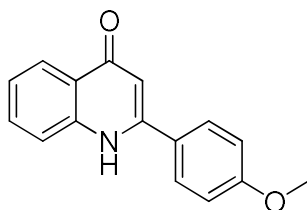
Obtained as a white solid after column chromatography (hexane:CH₂Cl₂ =8:2 + 1 % Et₃N); 45 % yield.

Elemental analysis for C₂₁H₁₅N₃. Calc.: C 68.56; H 5.18; N 8.00. Found: C 68.75; H 5.03; N 8.24.

¹H NMR (400 MHz, CDCl₃) δ 8.69 (s, 1H), 8.26 – 8.10 (m, 1H), 7.92 (d, *J* = 3.0 Hz, 1H), 7.46 – 7.36 (m, 1H), 7.35 – 7.21 (m, 2H), 3.93 (s, 3H).

¹³C NMR (101 MHz, CDCl₃) δ 165.64, 136.06, 130.97, 125.78, 123.23, 122.06, 121.53, 111.47, 108.85, 51.07.

2-(4-methoxyphenyl)quinolin-4(1*H*)-one



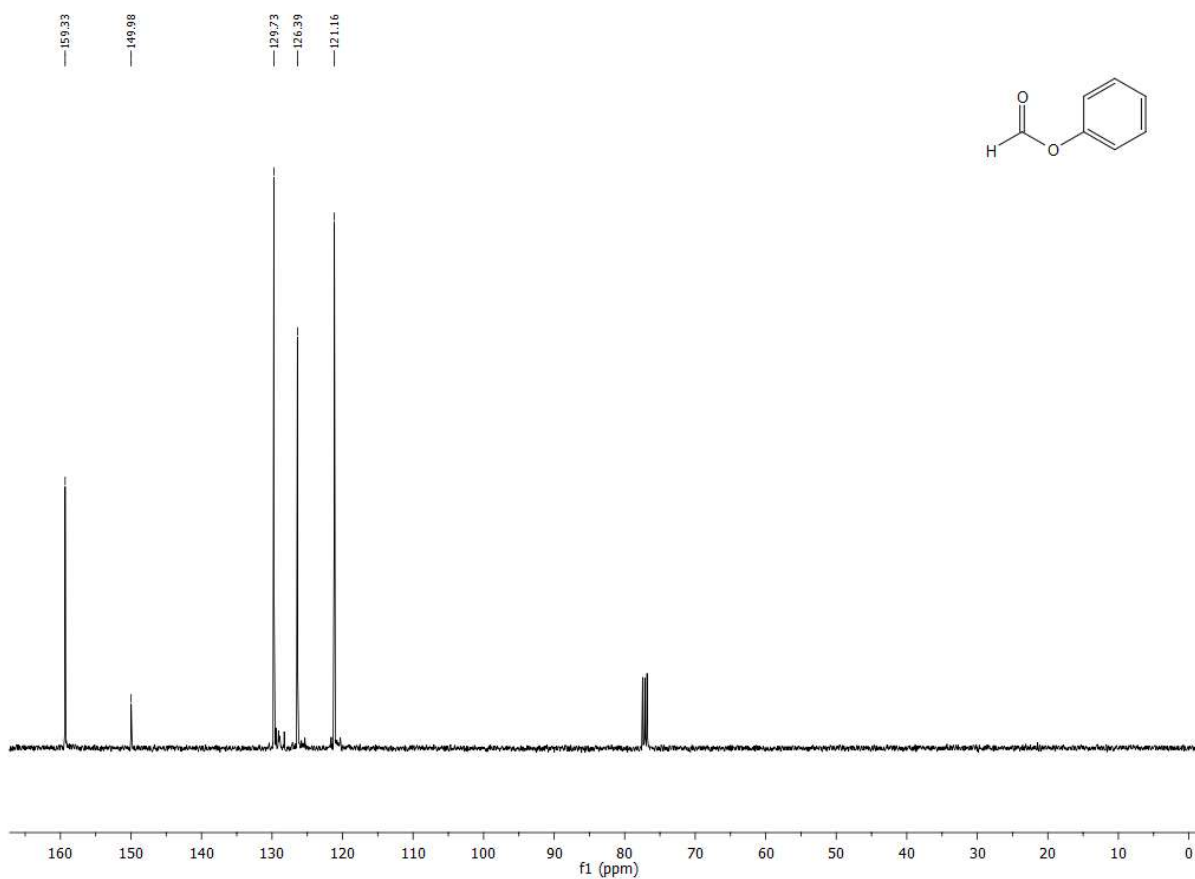
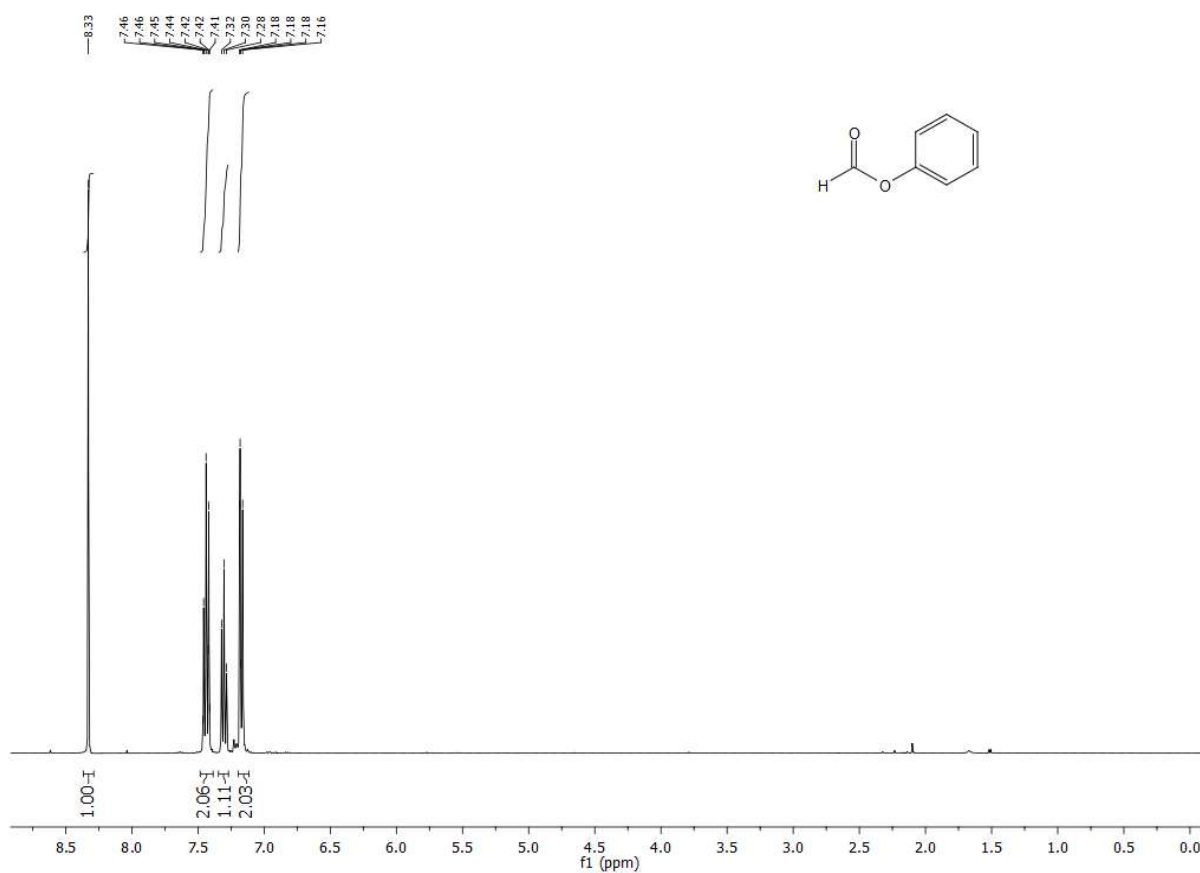
After the catalytic reaction, a white solid precipitate from the mixture. It was filtered through Büchner funnel, washed with cold acetonitrile and dried under vacuum. 67 % yield.

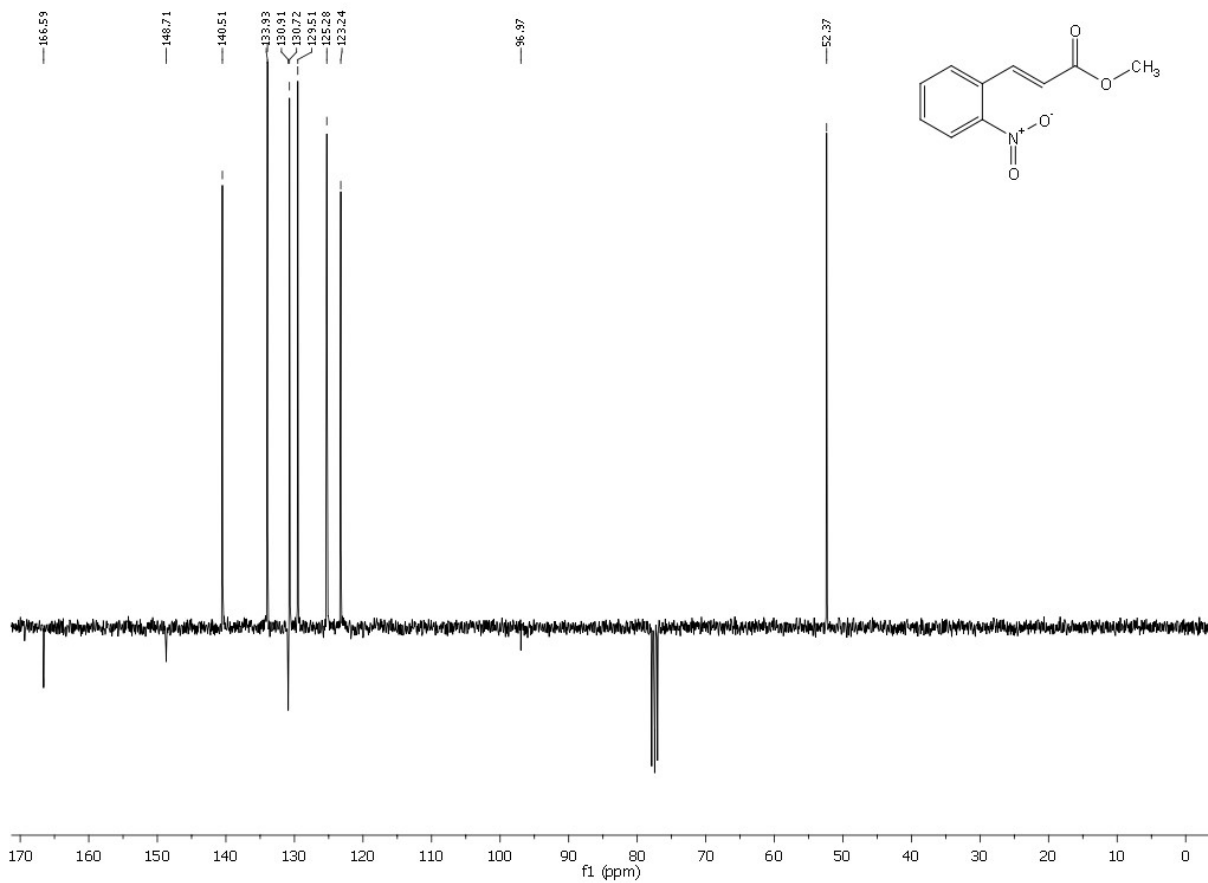
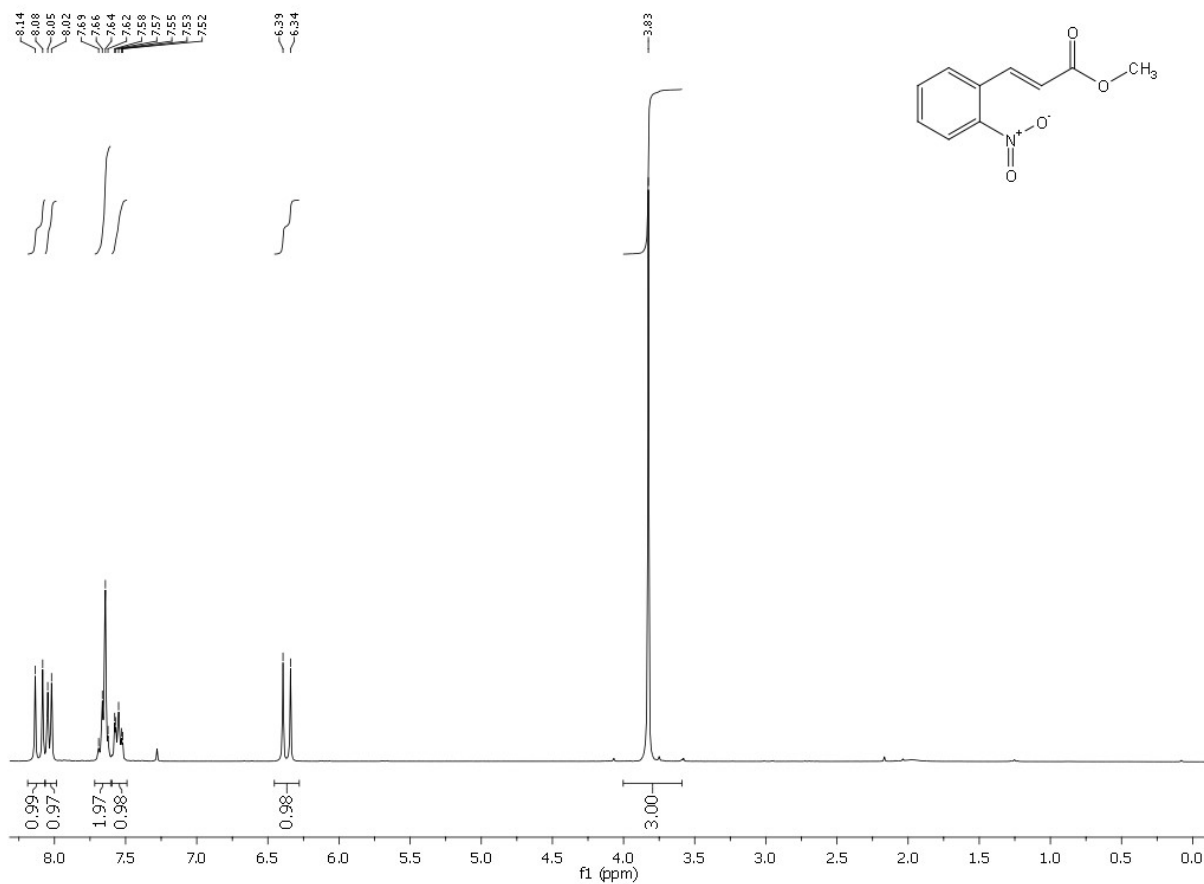
Elemental analysis for C₁₆H₁₃NO₂. Calc.: C 76.48; H 5.21; N 5.57. Found: C 76.28; H 4.96; N 5.51.

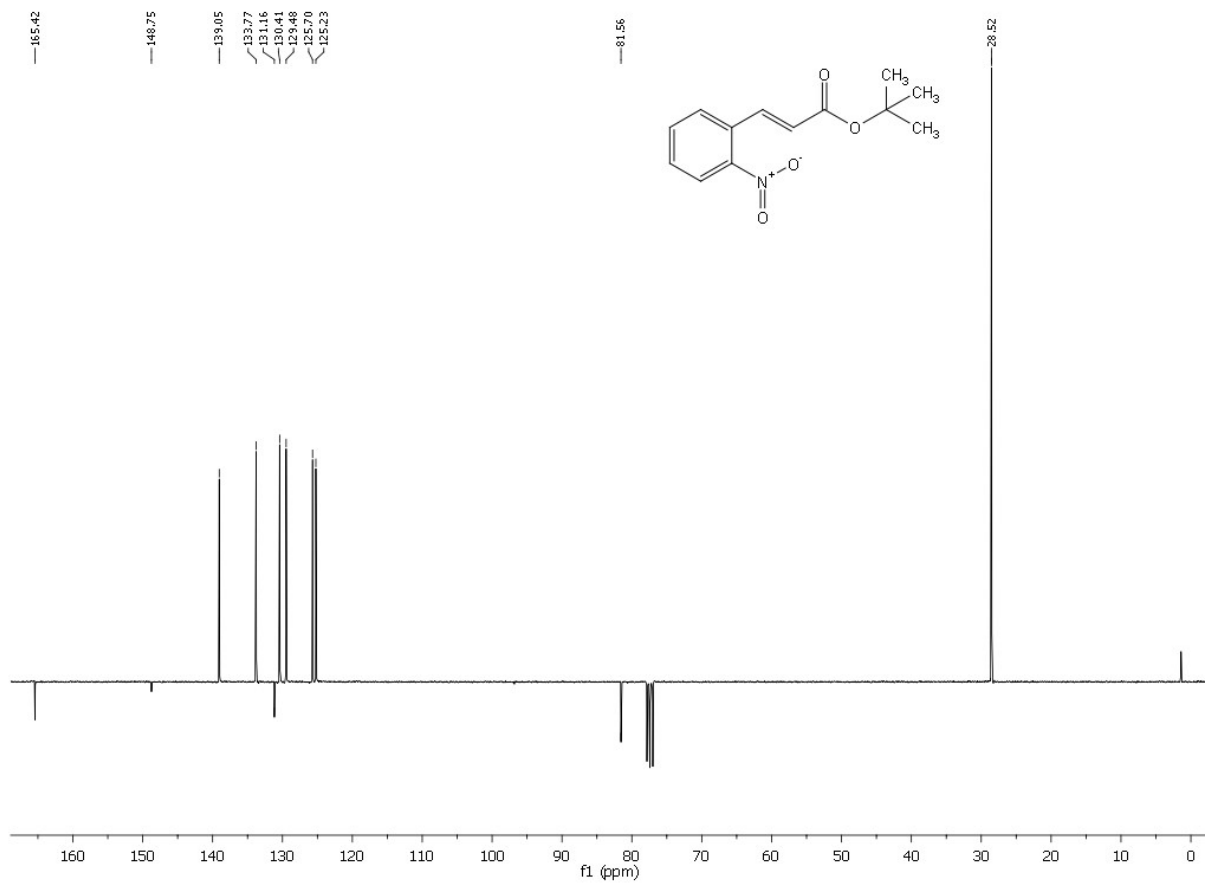
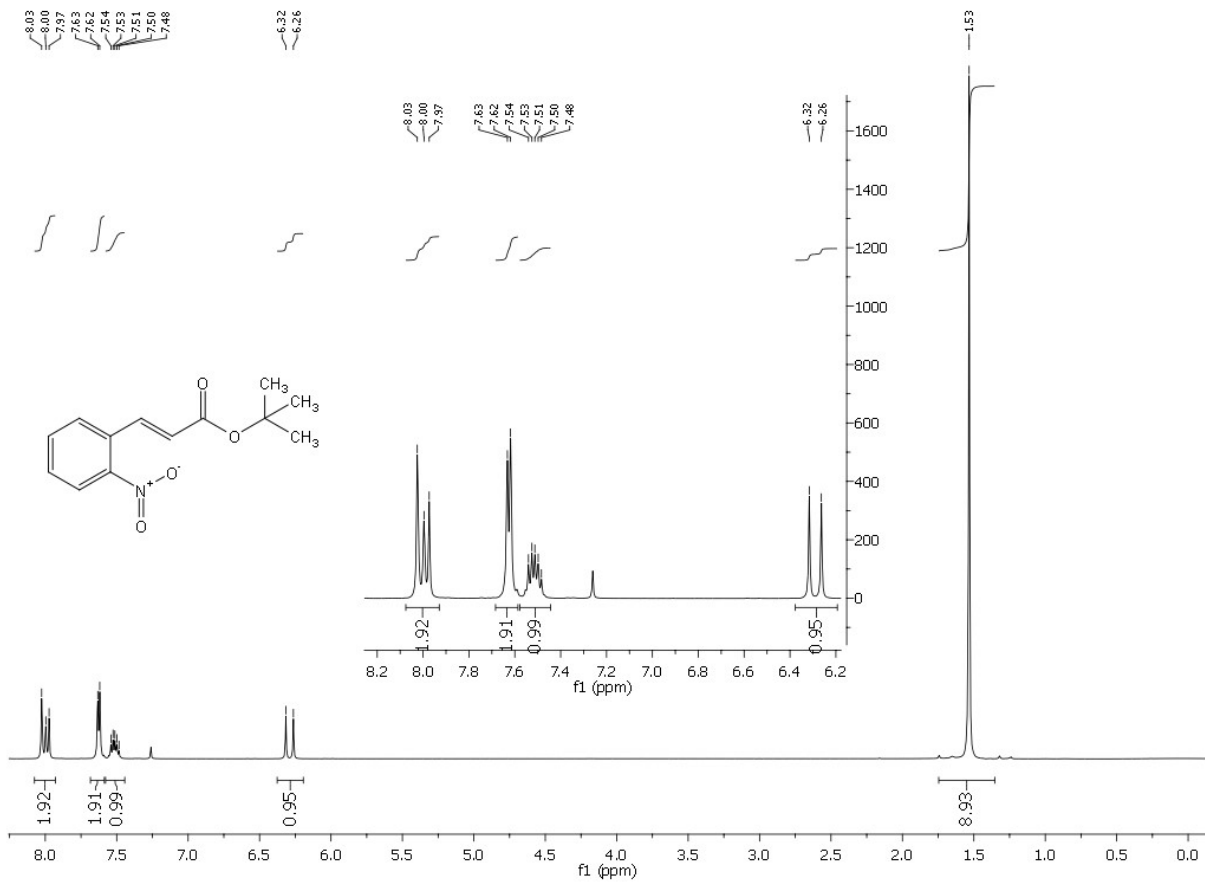
¹H NMR (600 MHz, DMSO-*d*⁶) δ 11.57 (s, 1H), 8.09 (d, *J* = 8.0 Hz, 1H), 7.81 (d, *J* = 8.7 Hz, 2H), 7.77 (d, *J* = 8.3 Hz, 1H), 7.66 (t, *J* = 7.3 Hz, 1H), 7.32 (t, *J* = 7.5 Hz, 1H), 7.15 (d, *J* = 8.7 Hz, 2H), 6.31 (s, 1H), 3.86 (s, 3H).

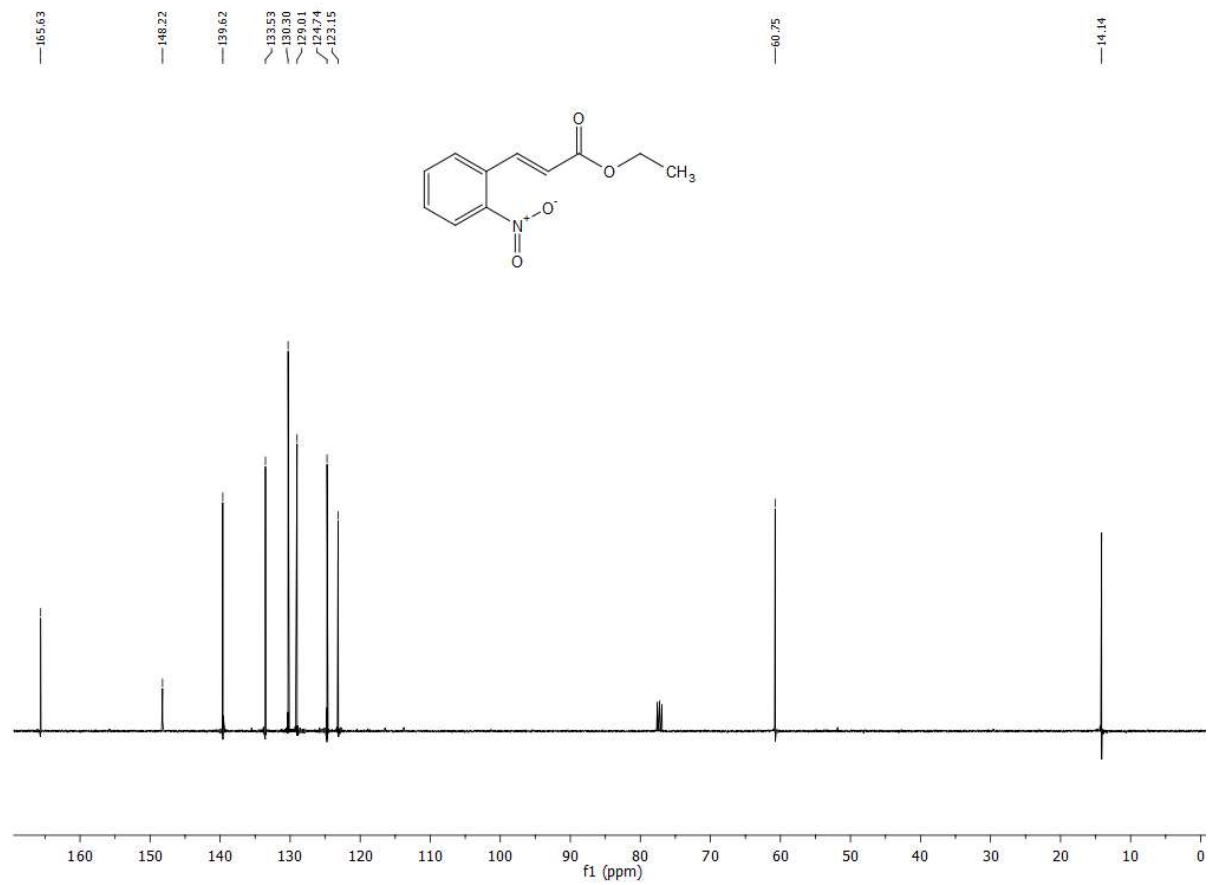
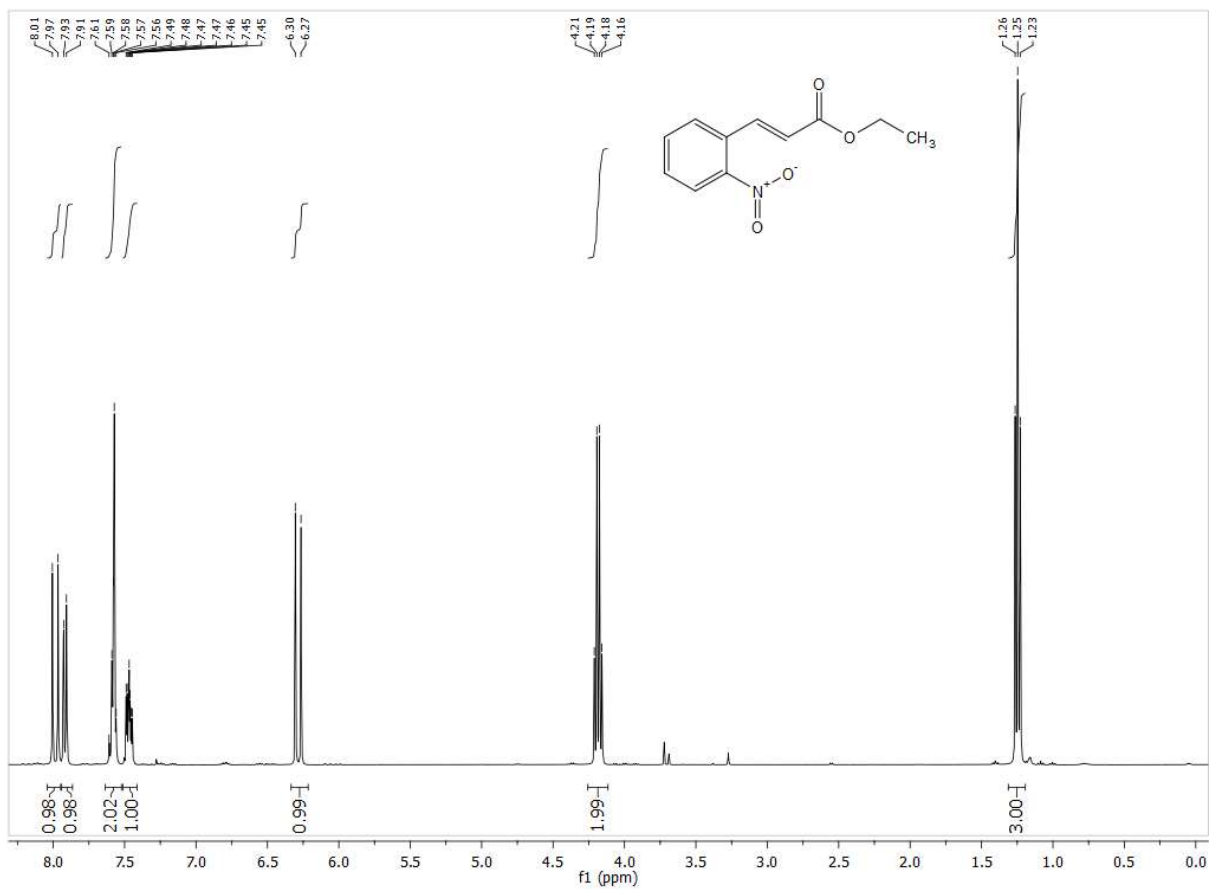
¹³C NMR (151 MHz, DMSO-*d*⁶) δ 177.32, 161.55, 150.12, 140.98, 132.10, 129.31, 126.75, 125.30, 125.16, 123.53, 119.07, 114.88, 106.99, 55.93.

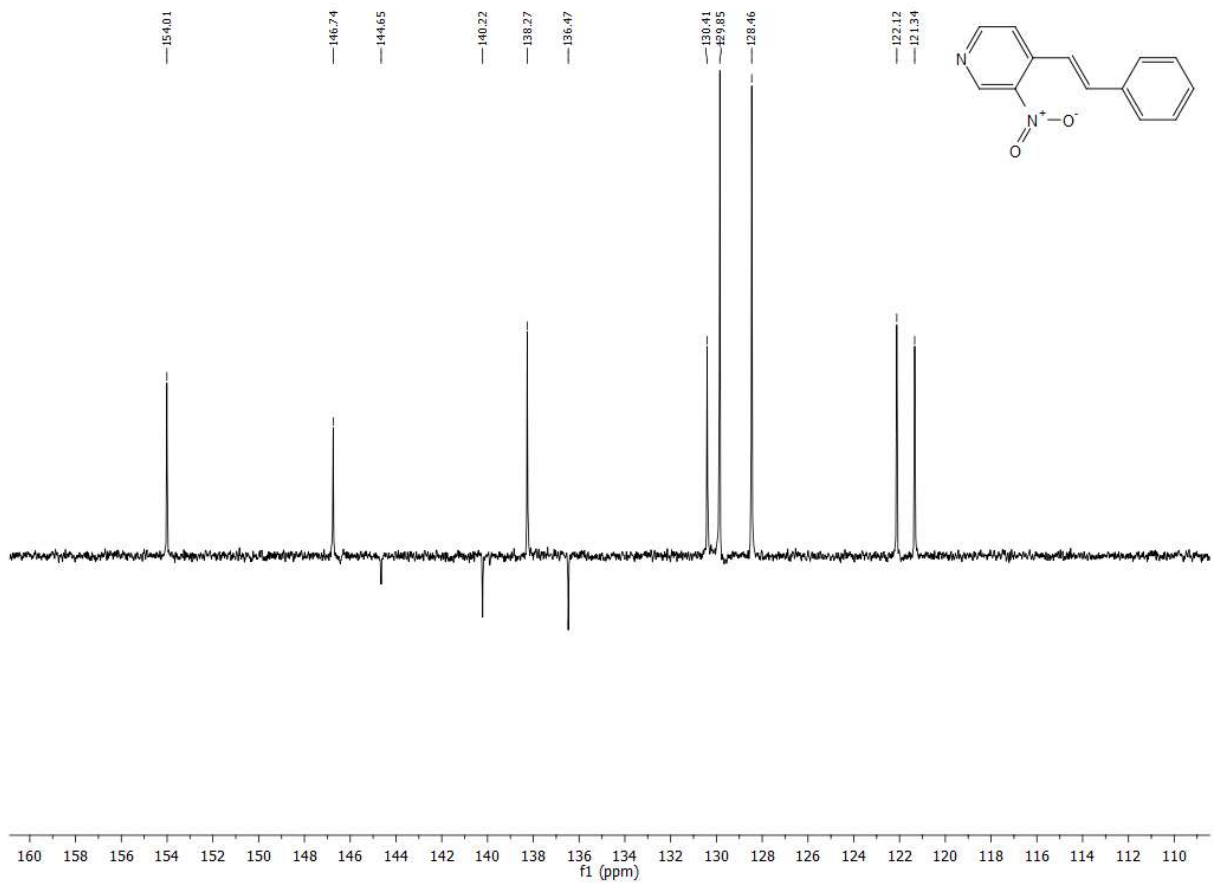
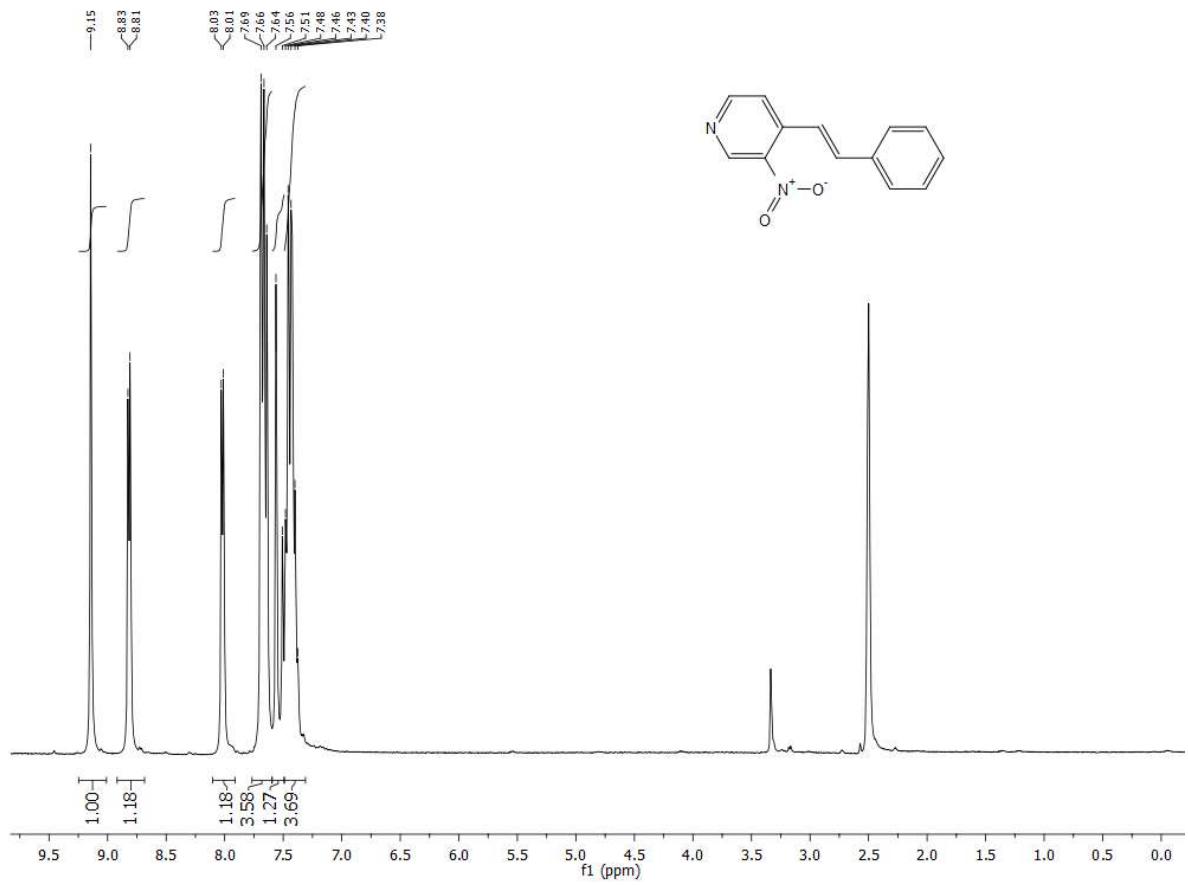
4.14. NMR Spectra

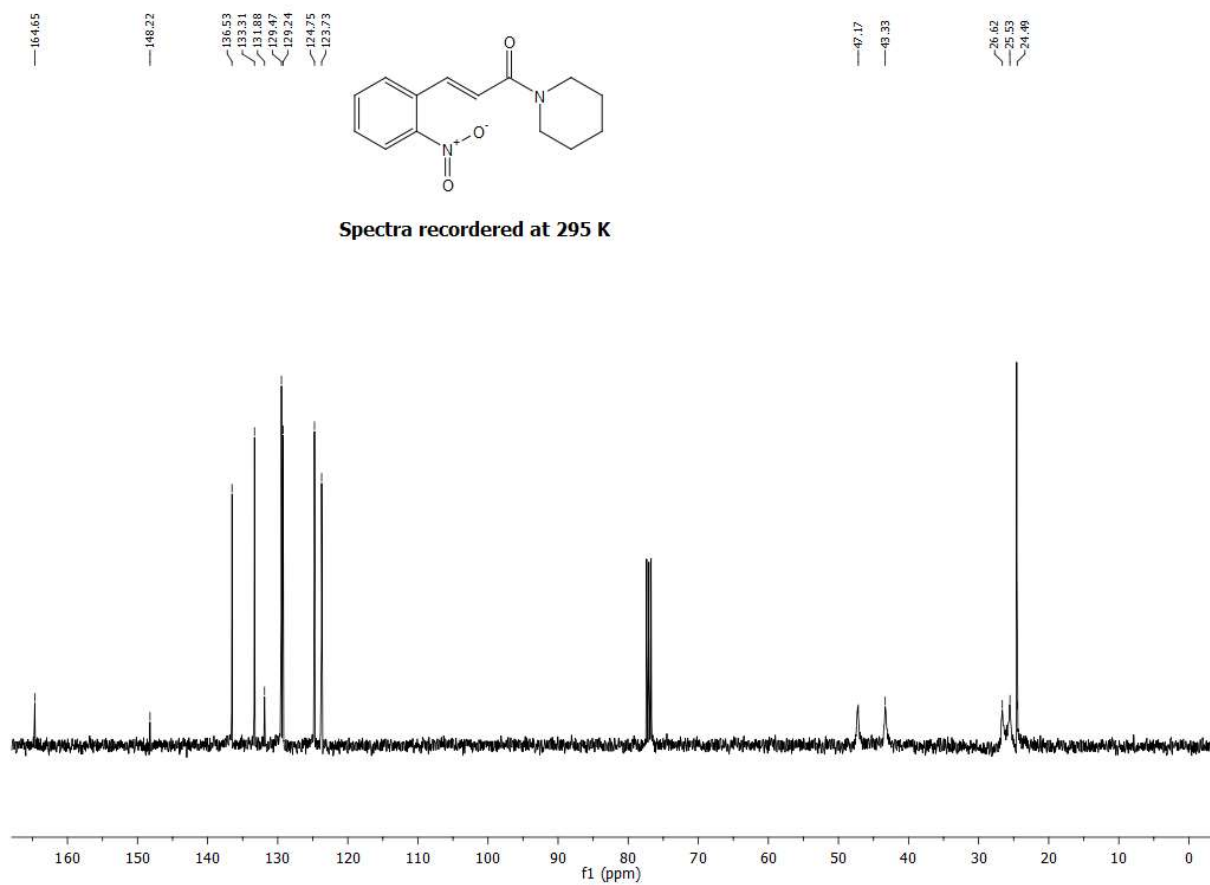
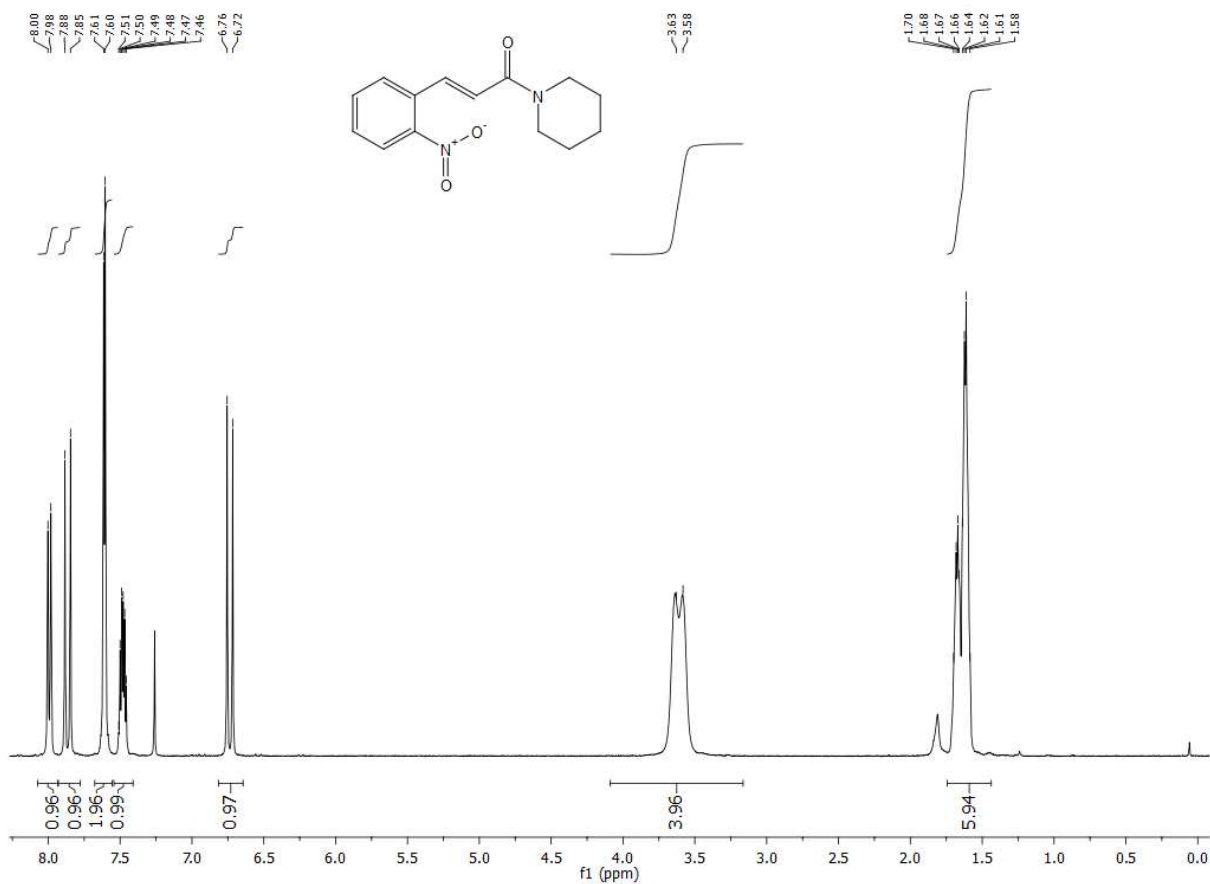




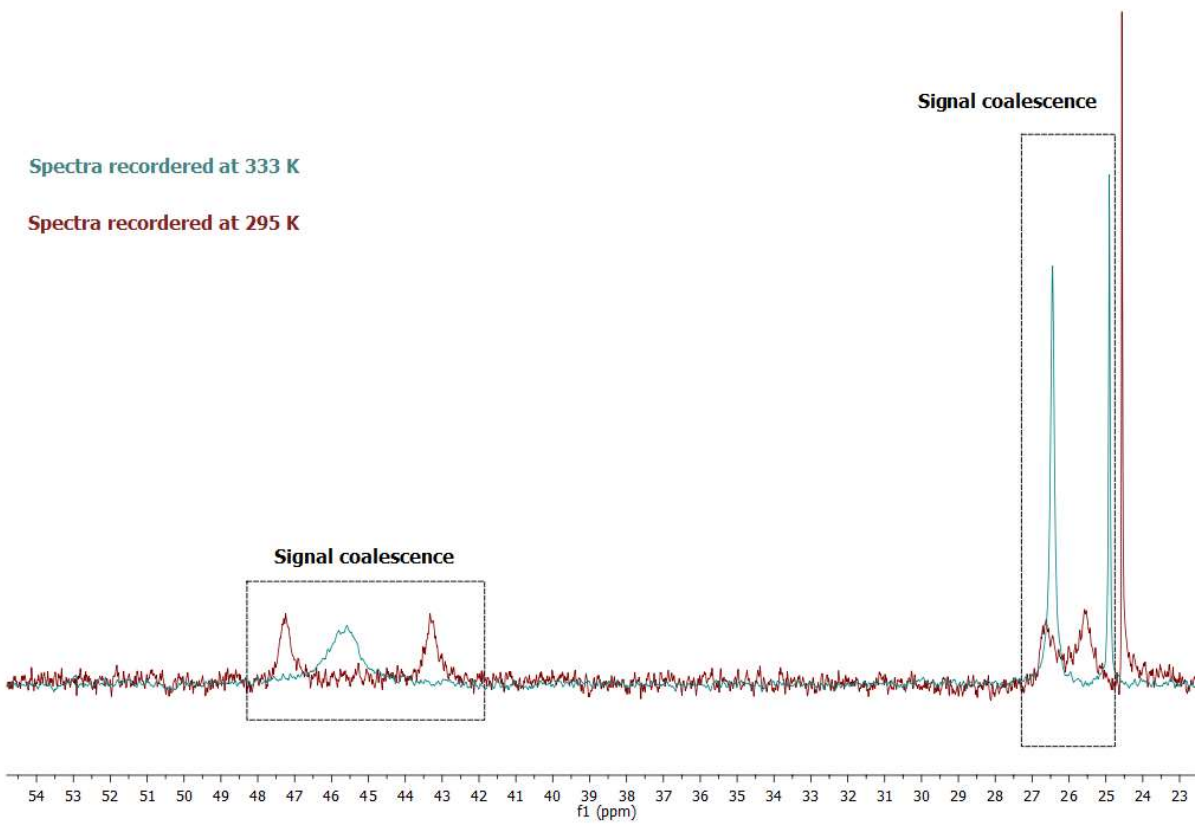
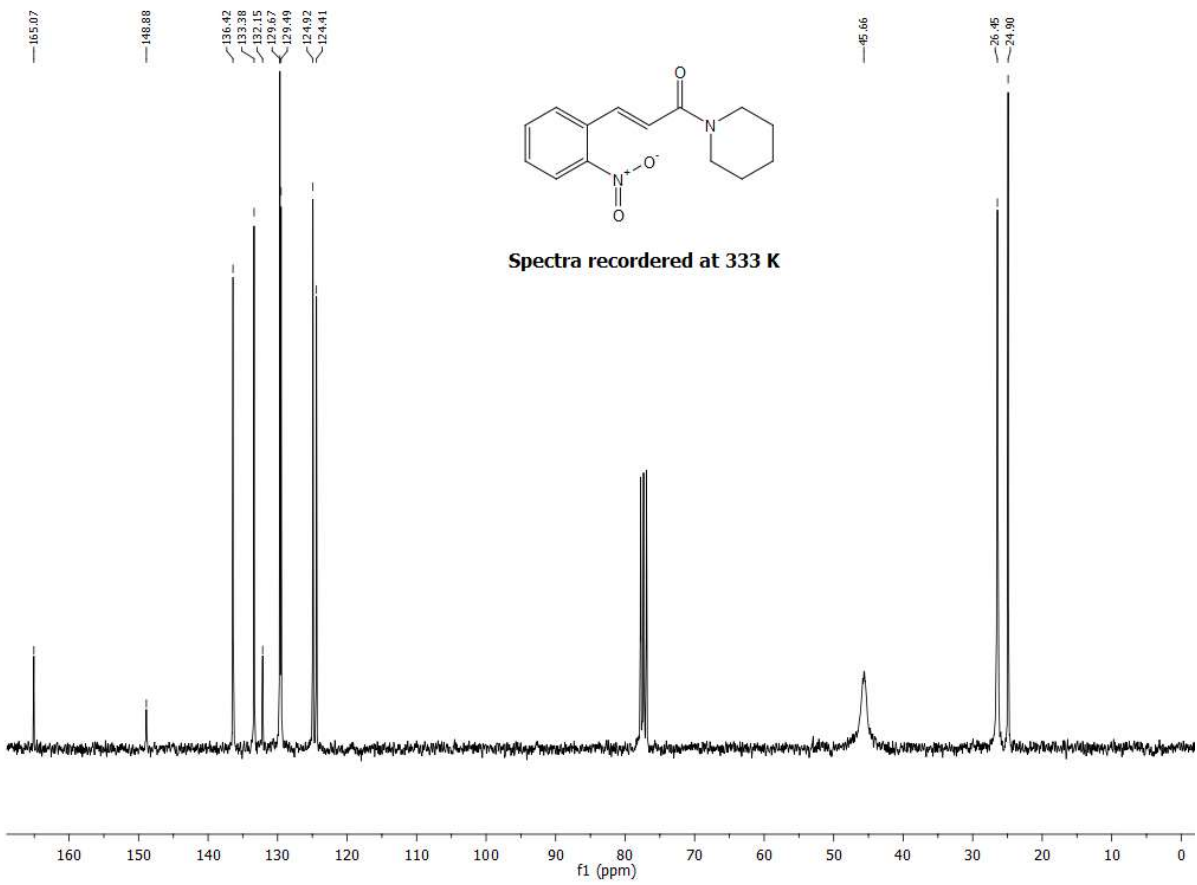


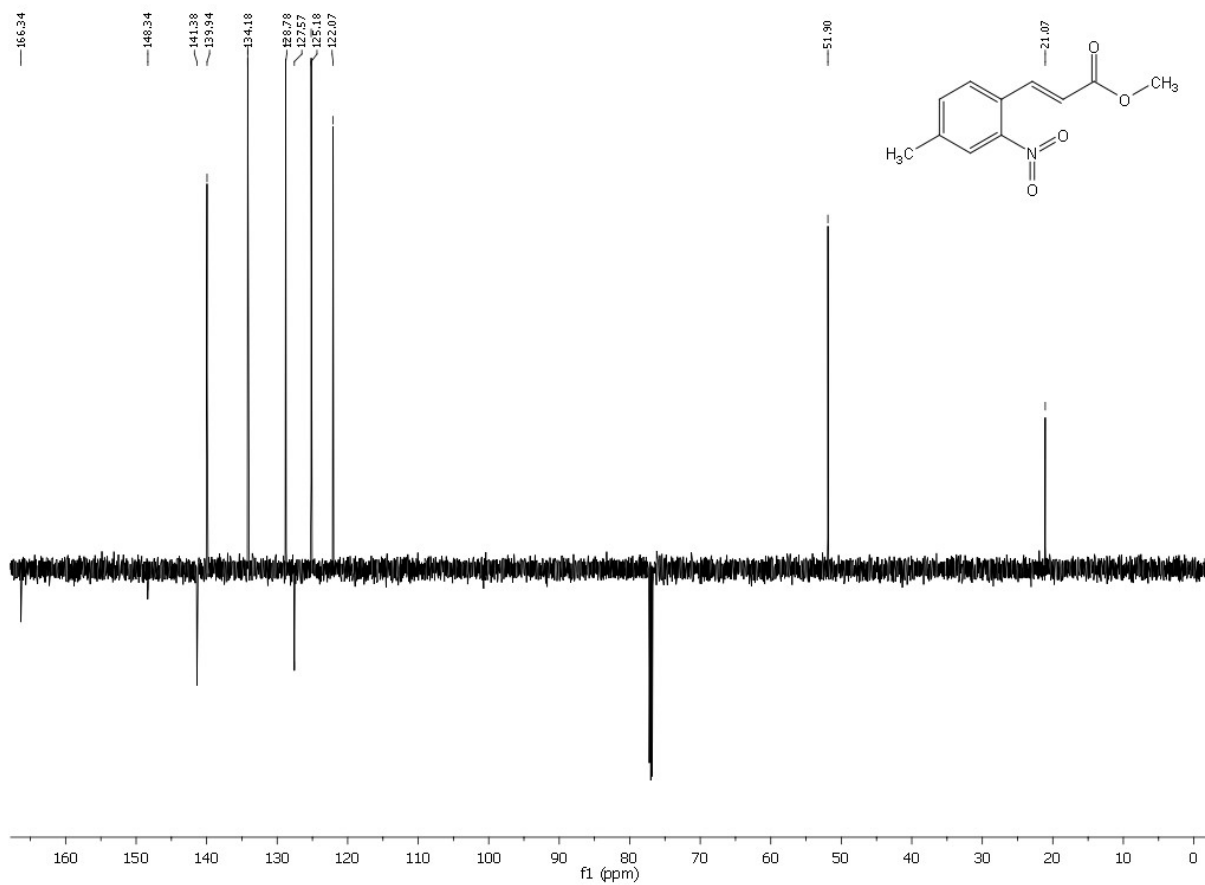
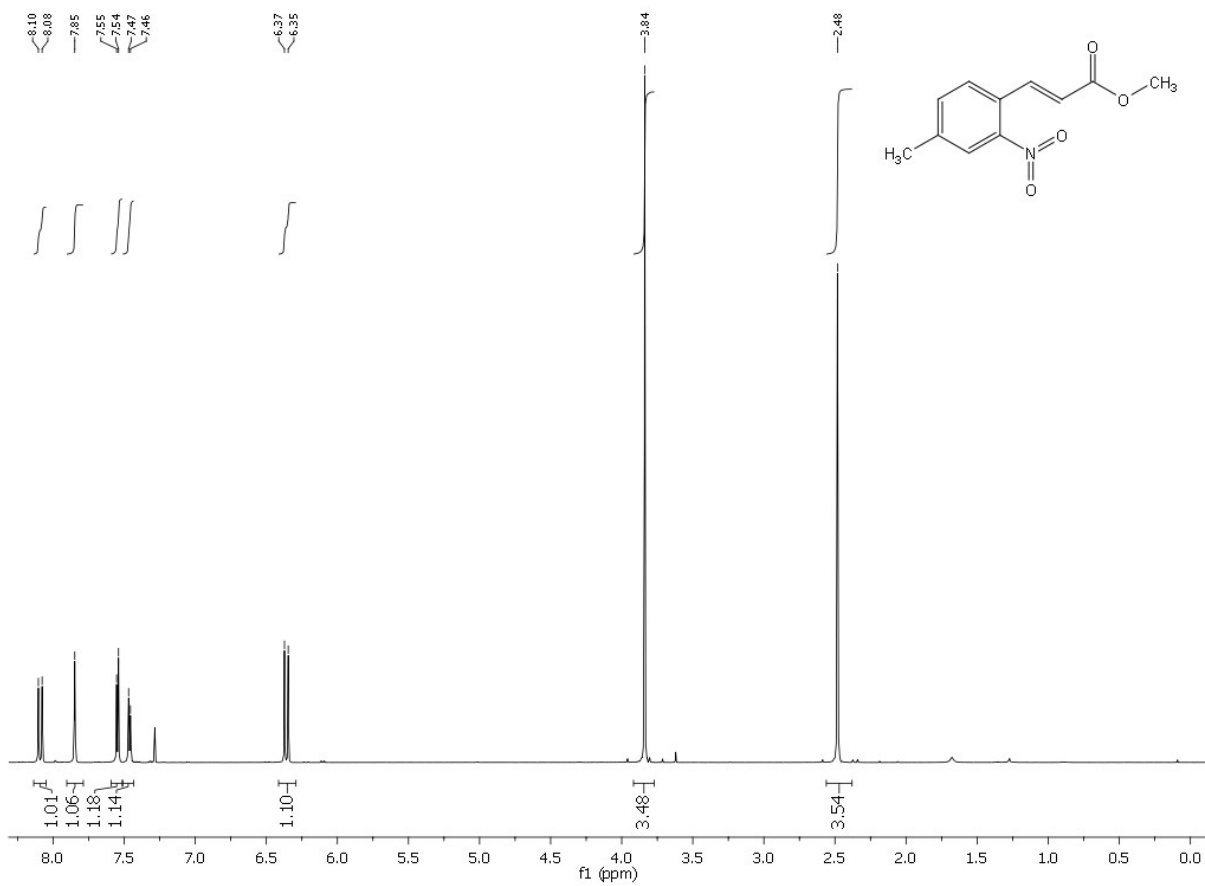


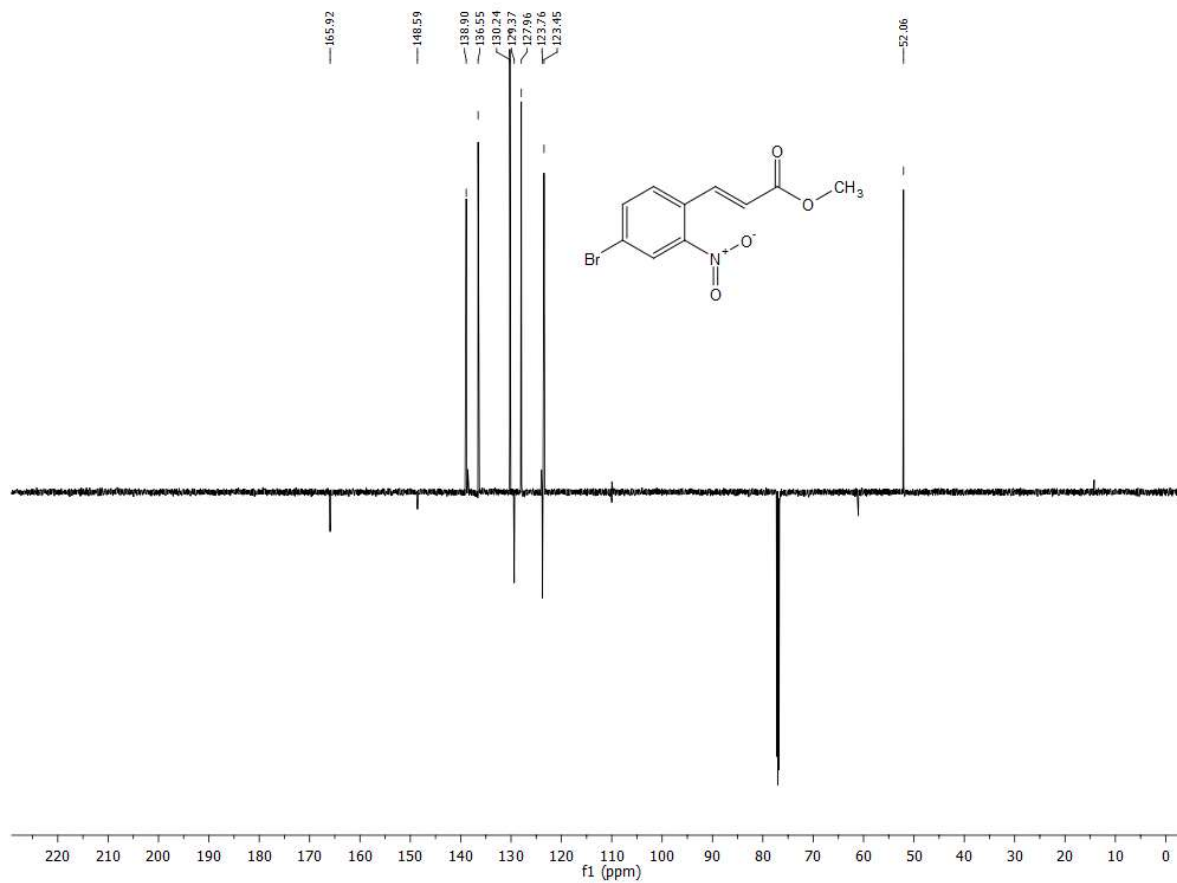
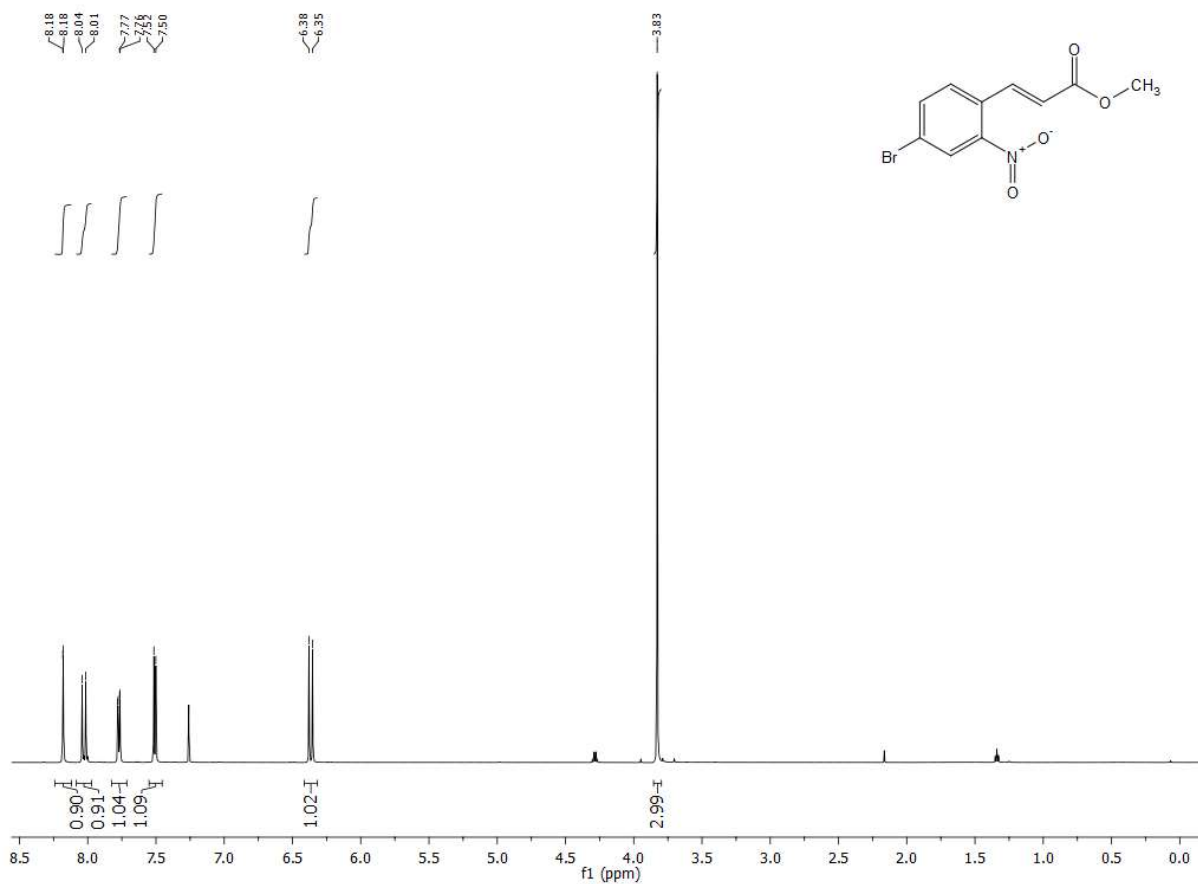


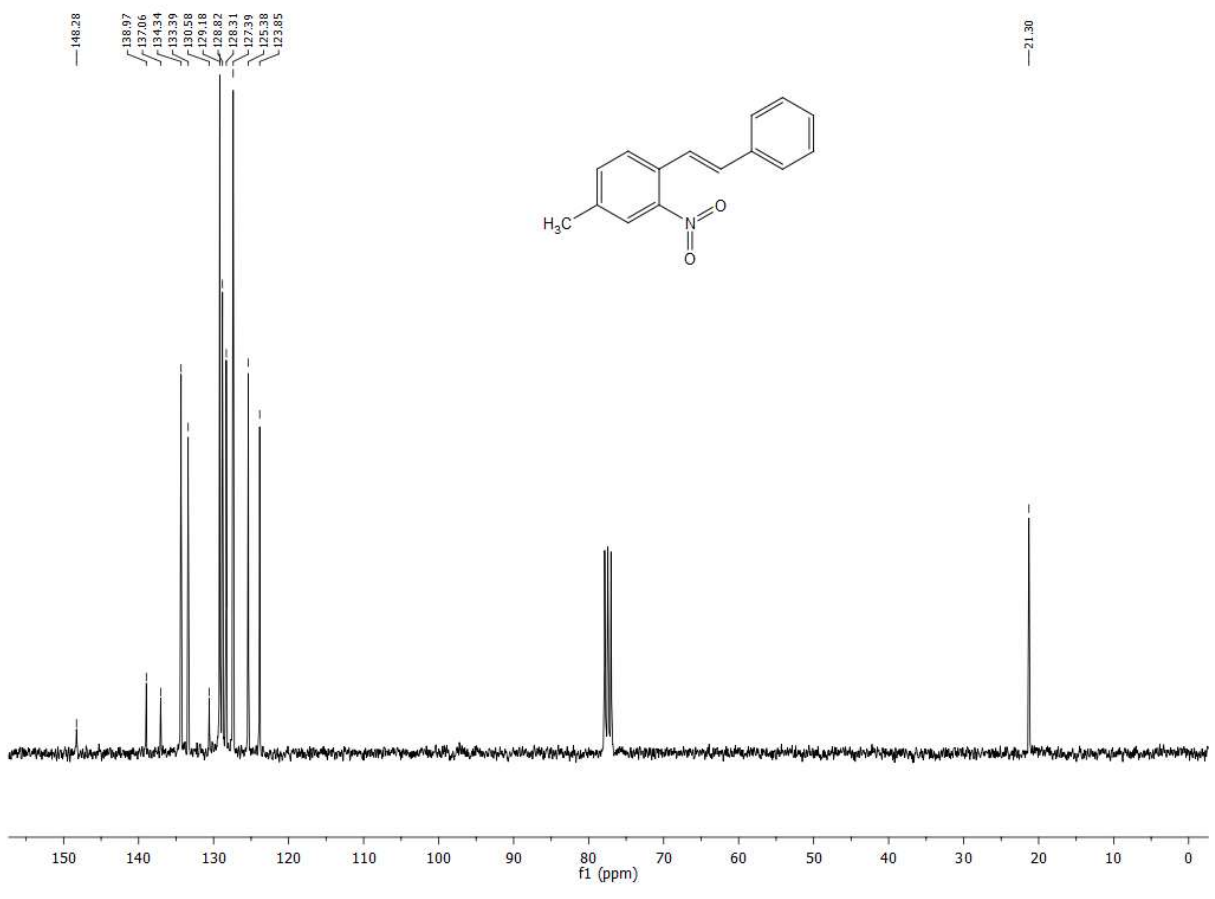
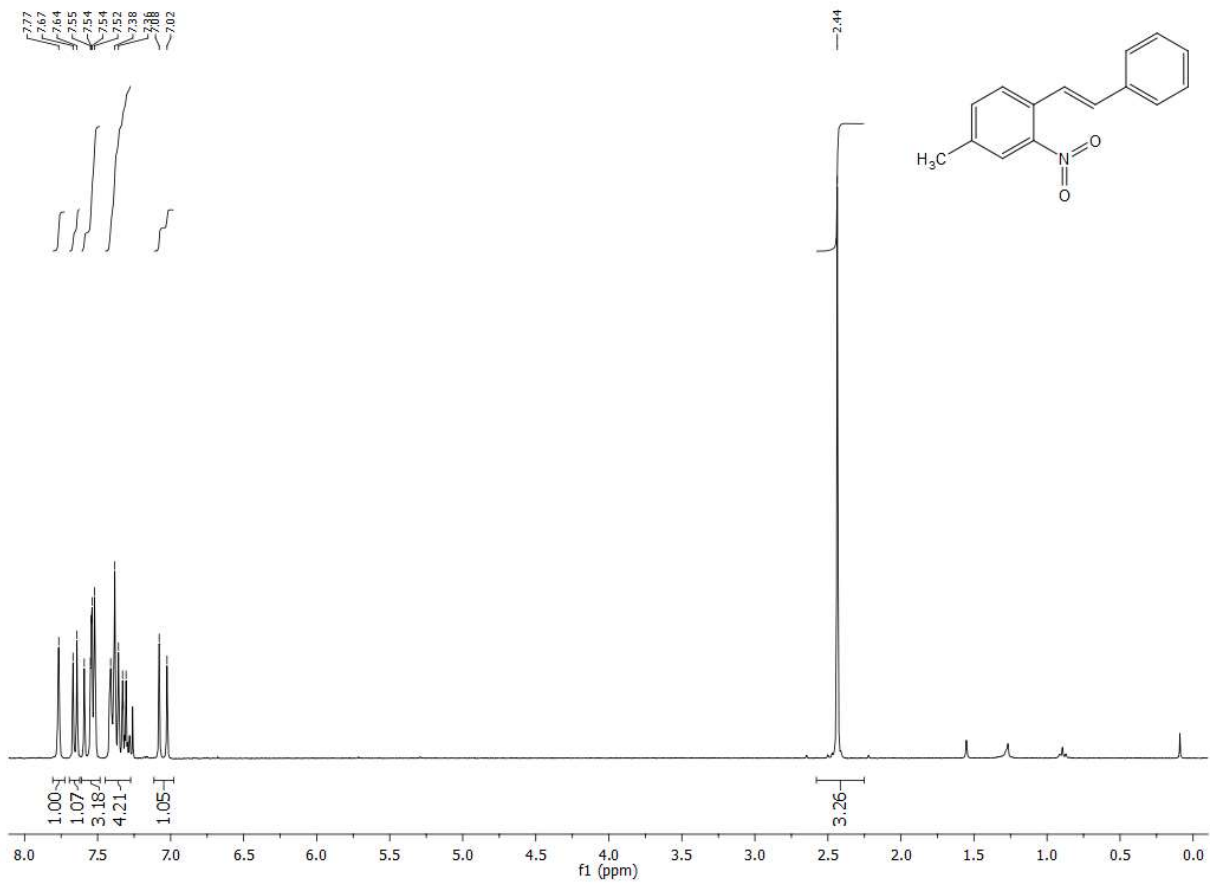


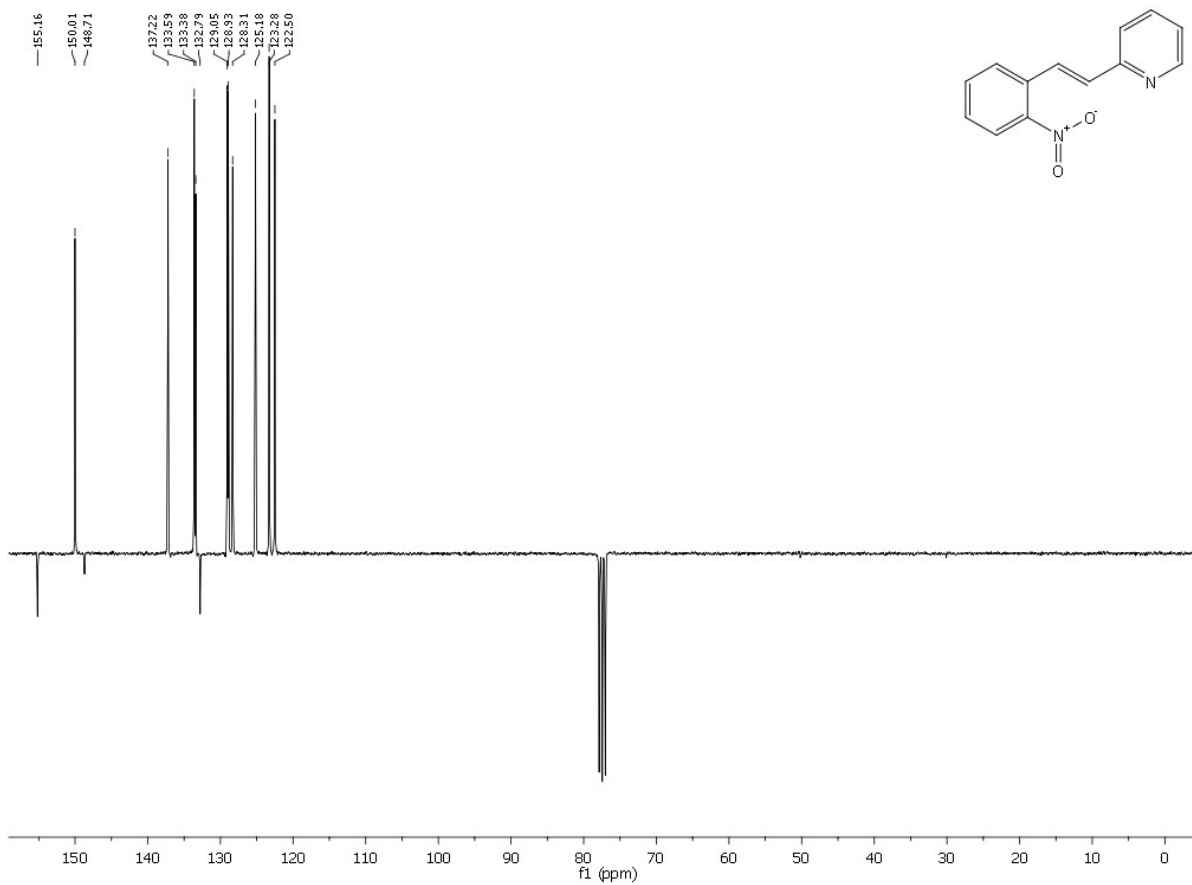
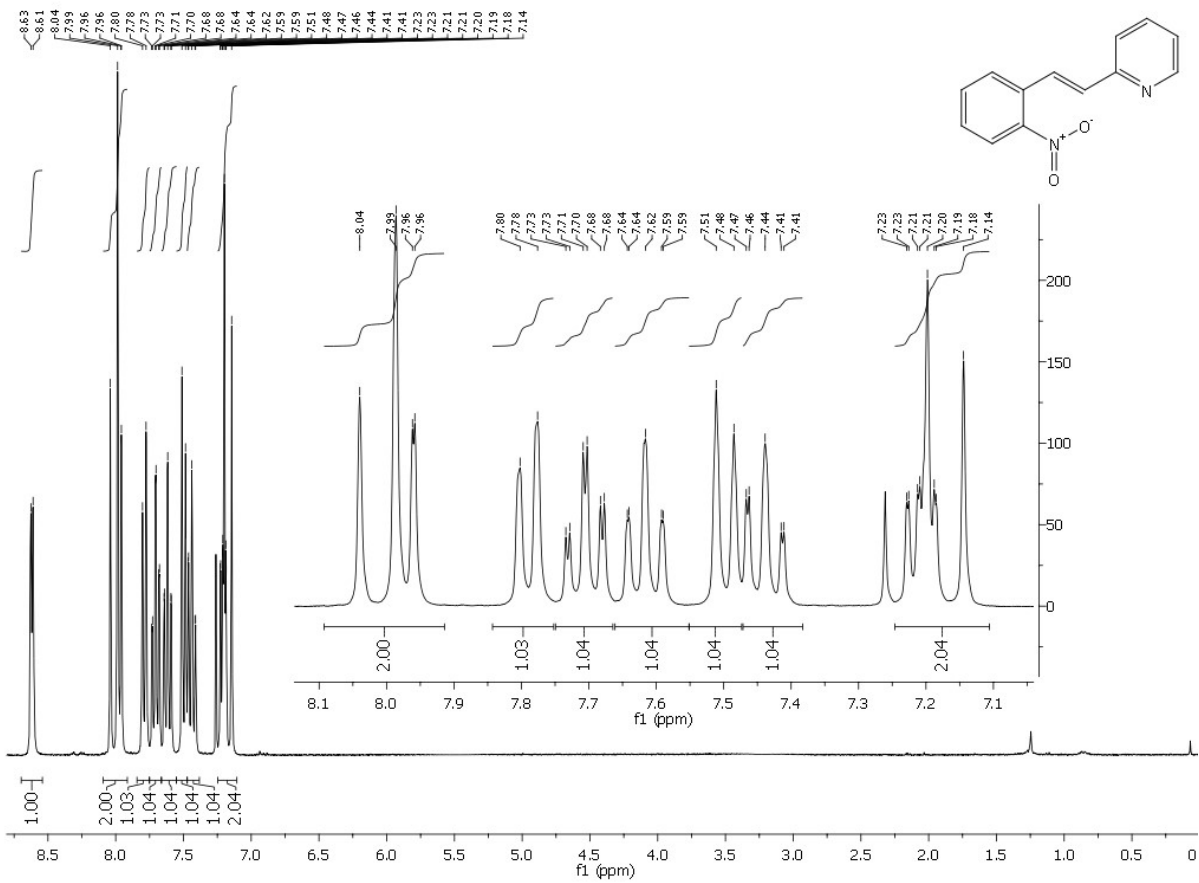
Spectra recorded at 295 K

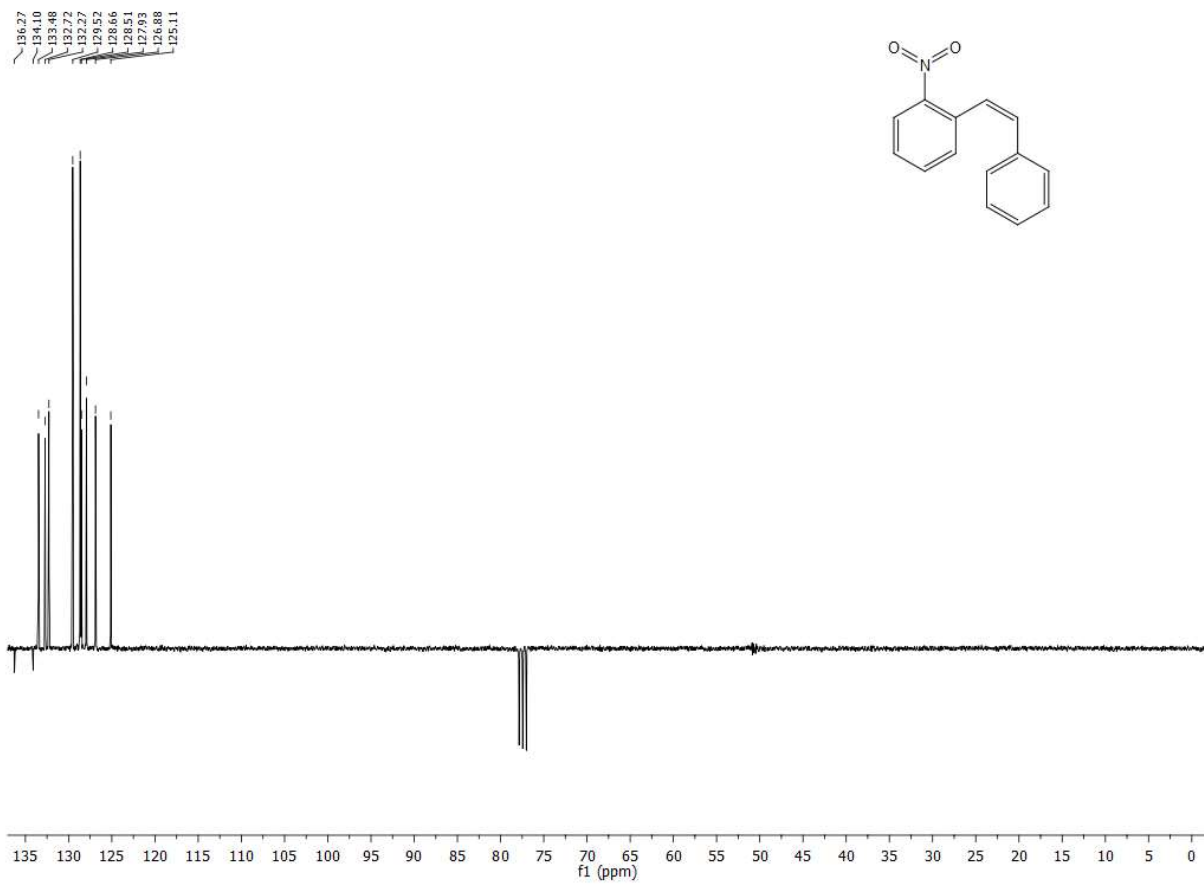
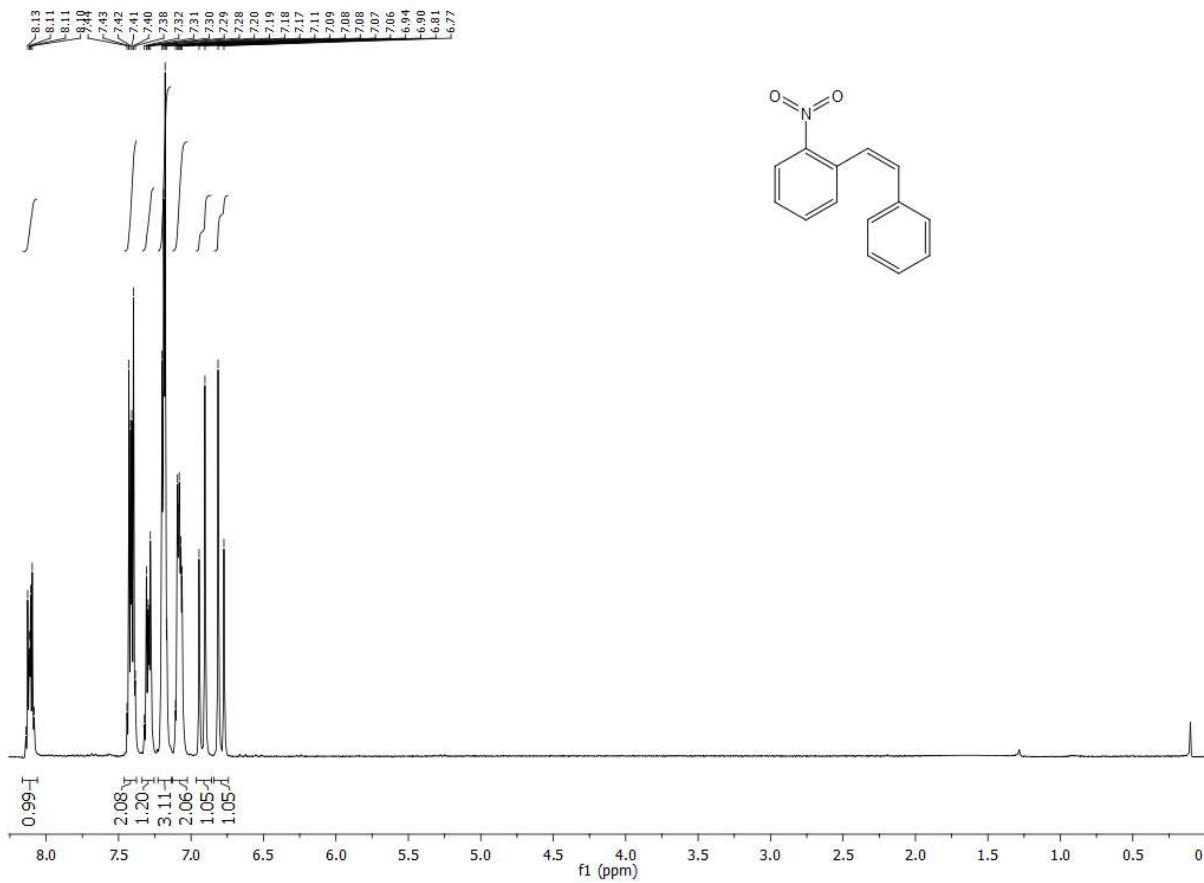


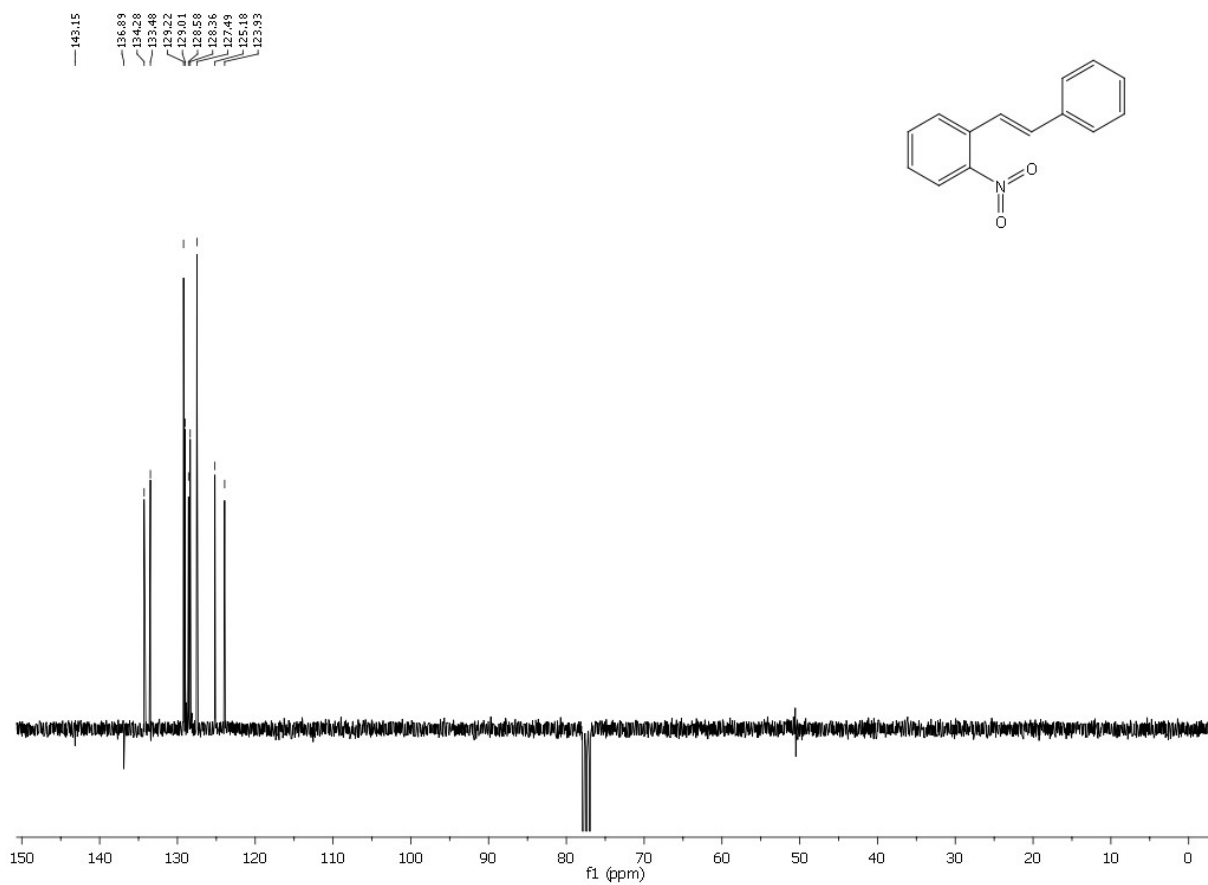
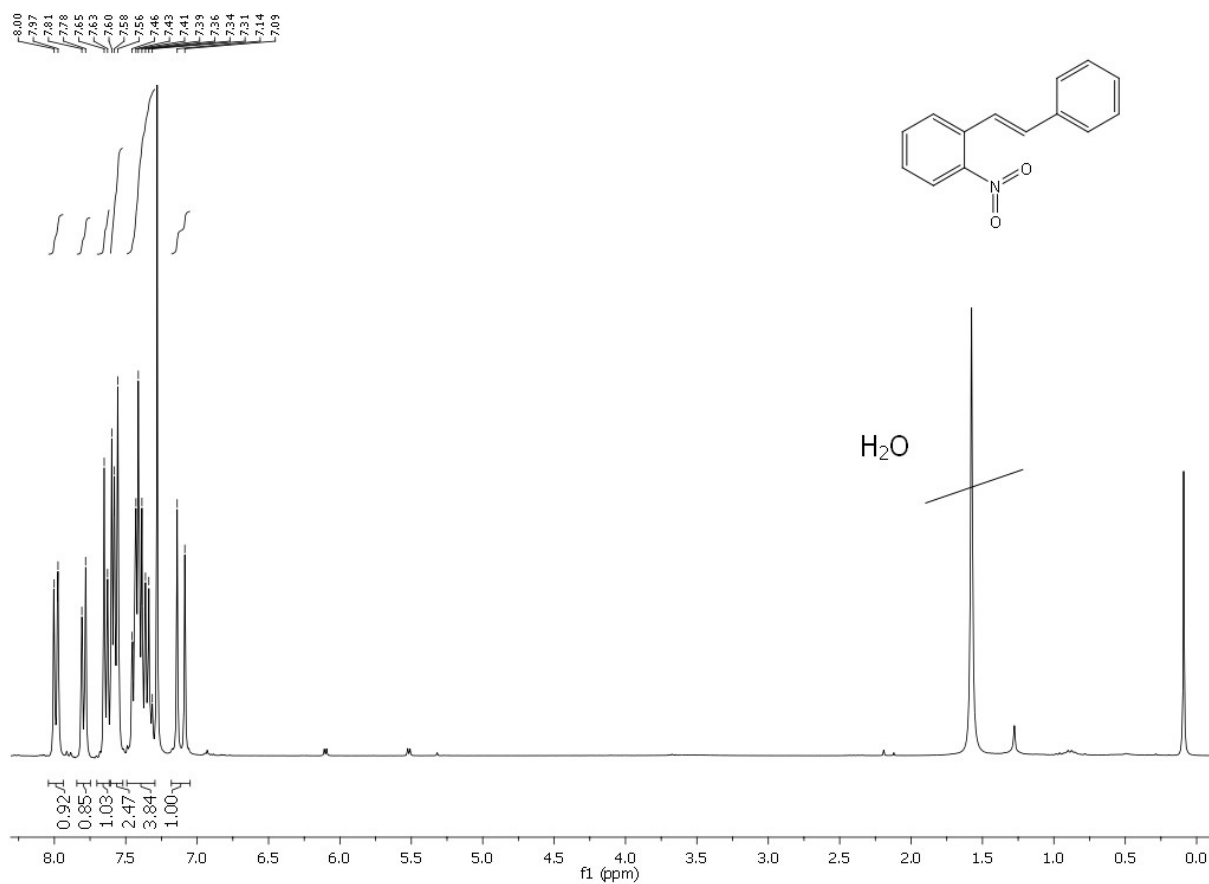


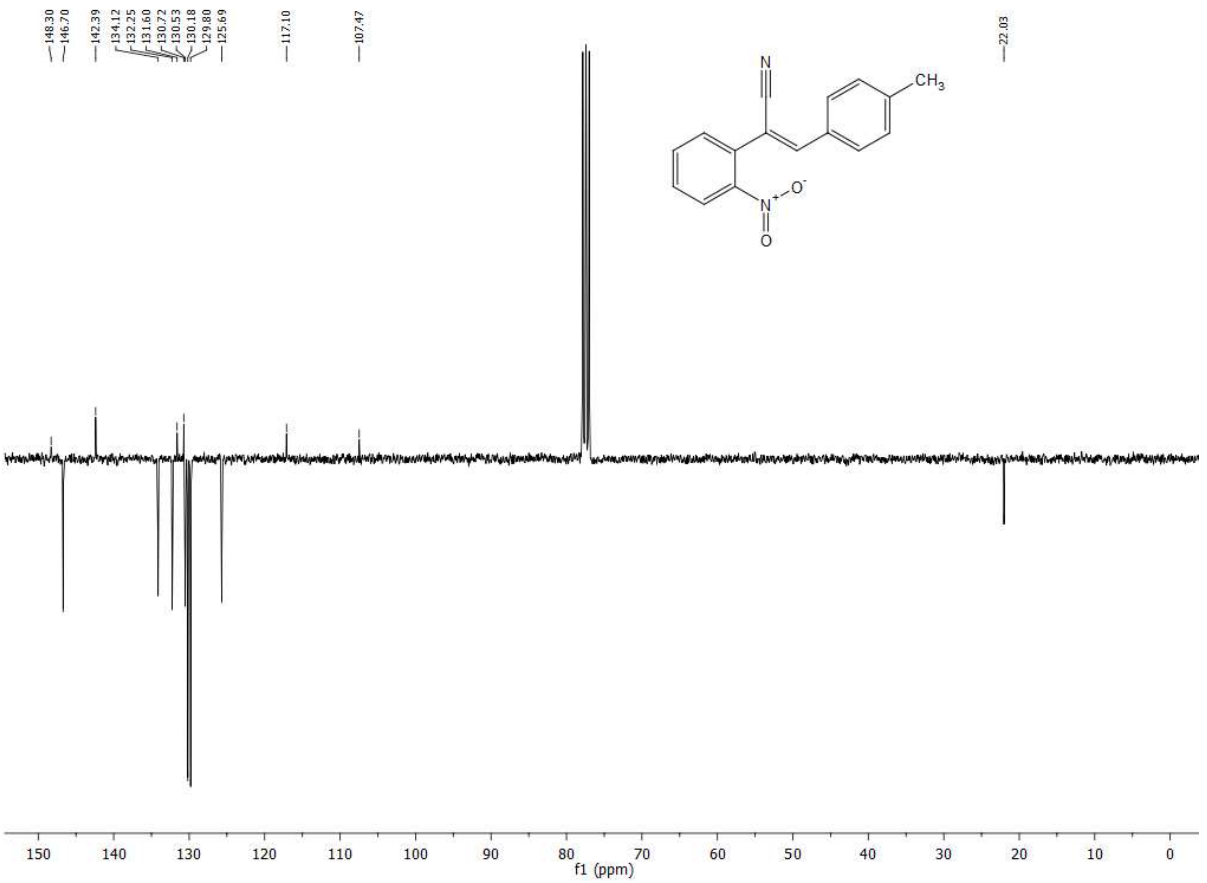
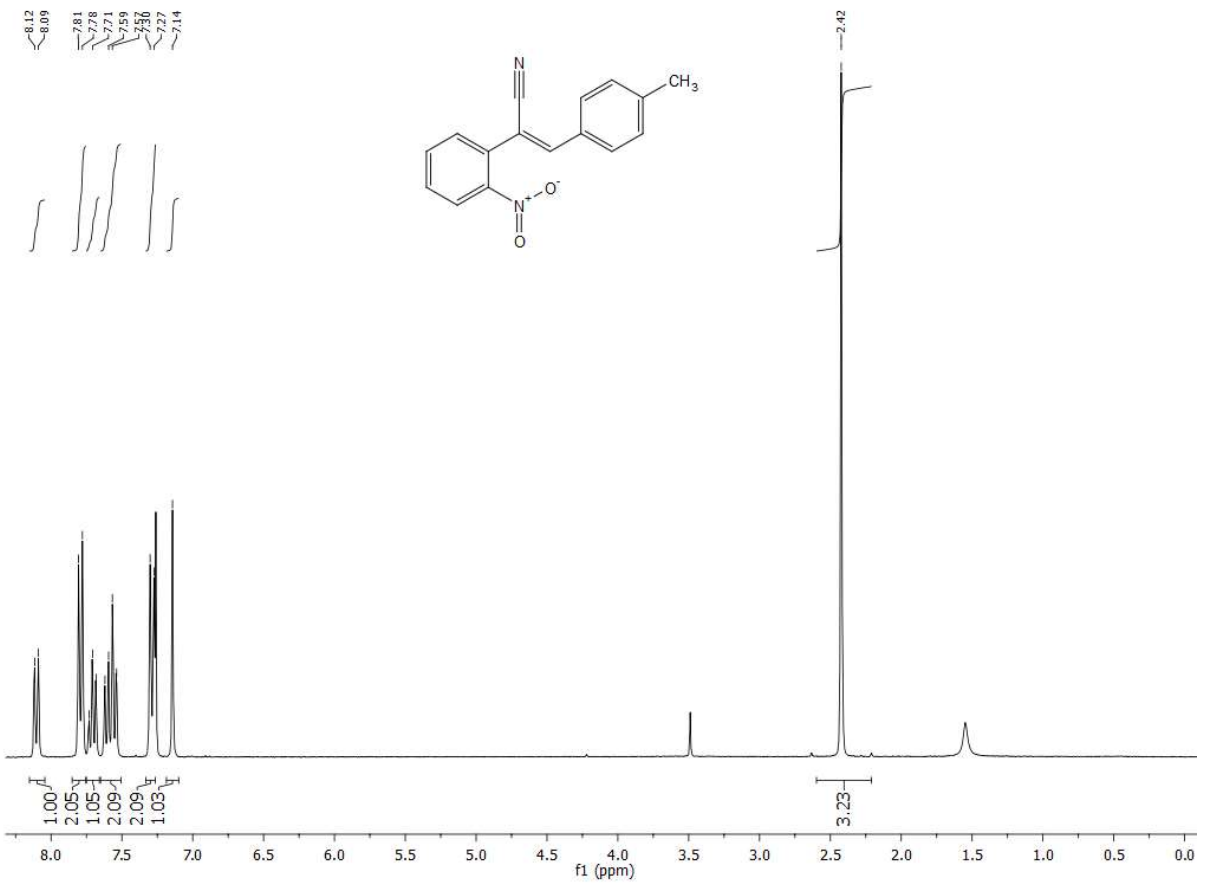


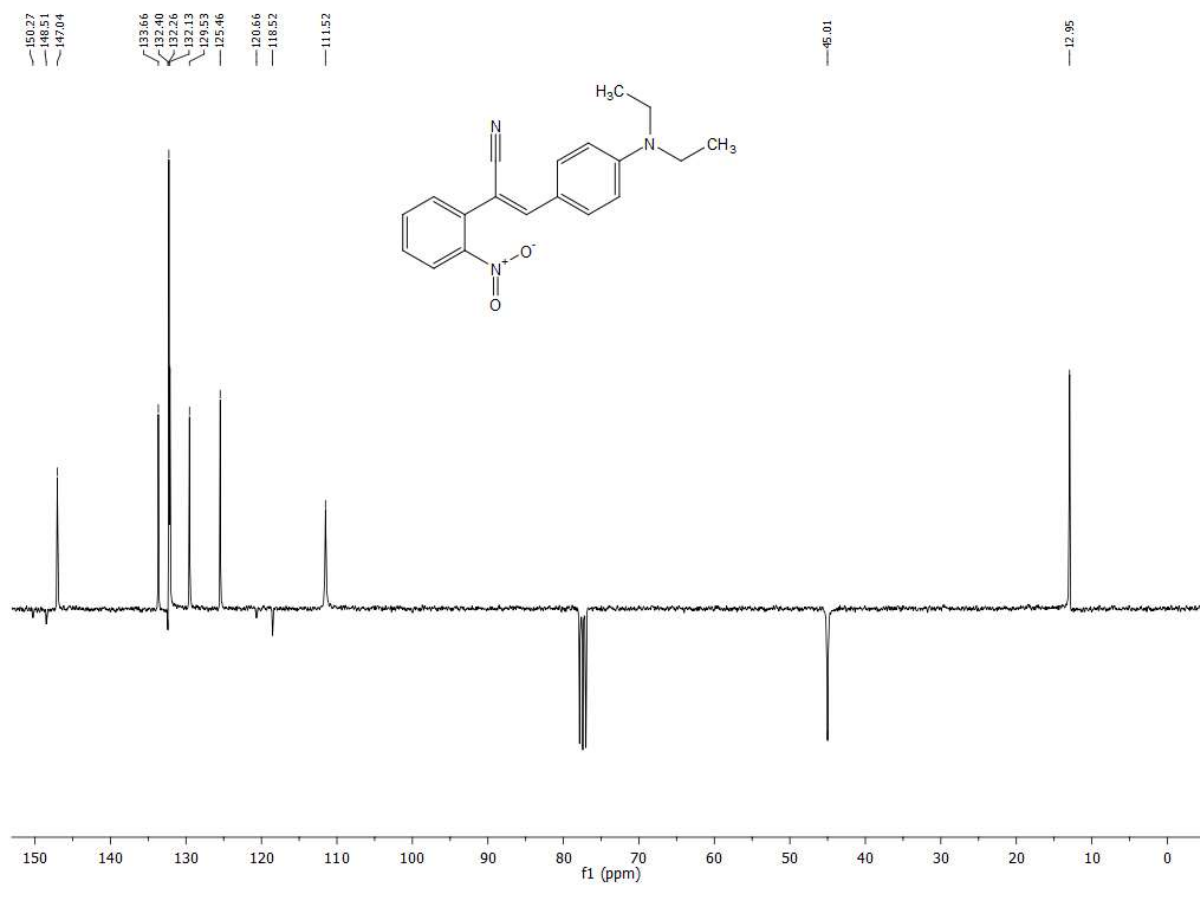
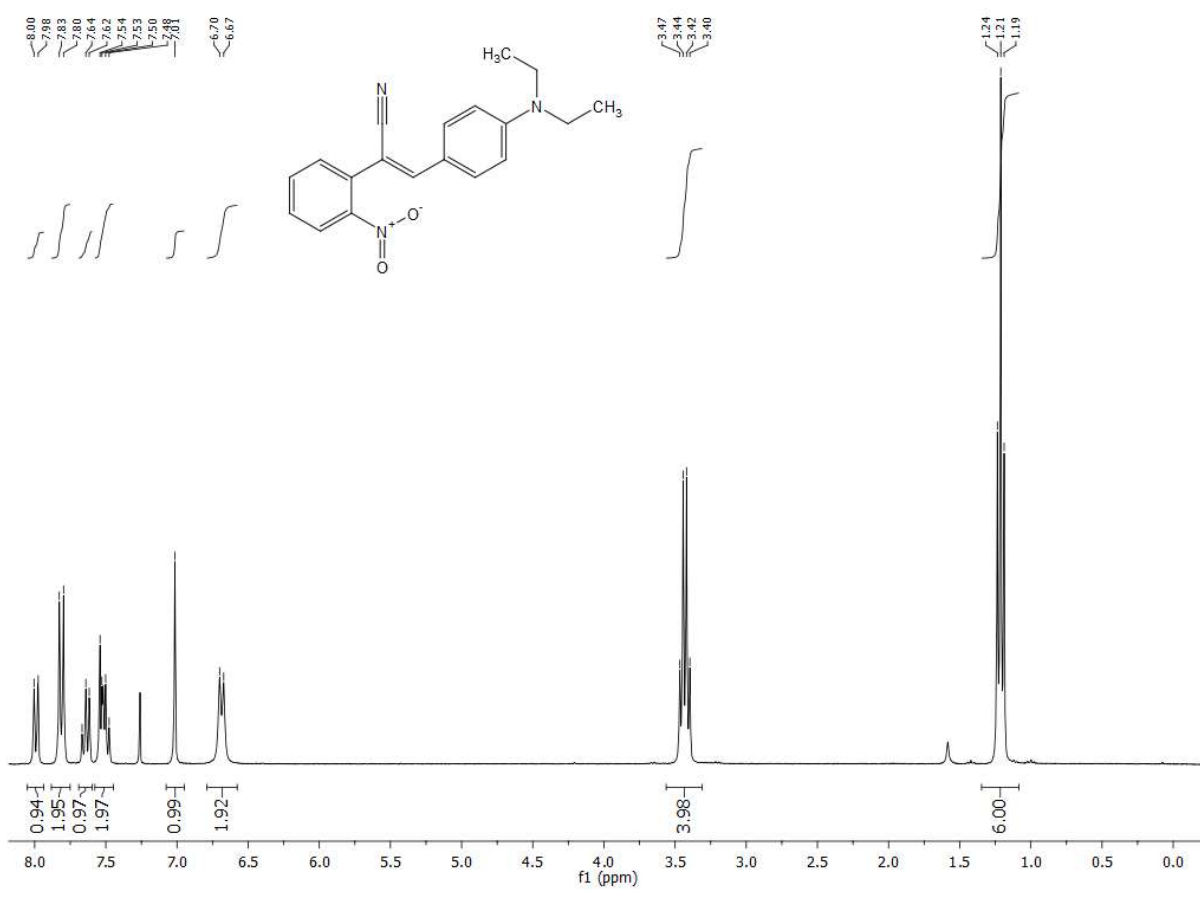


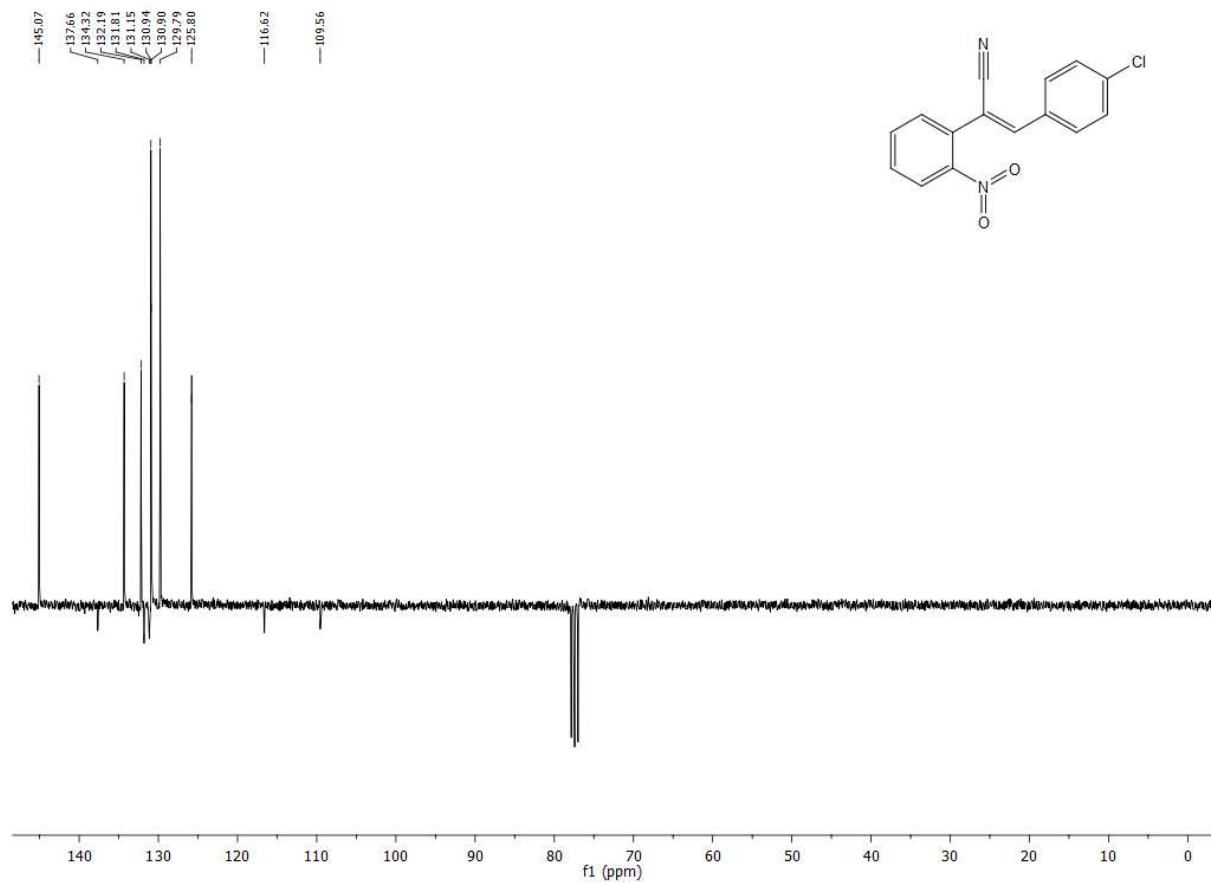
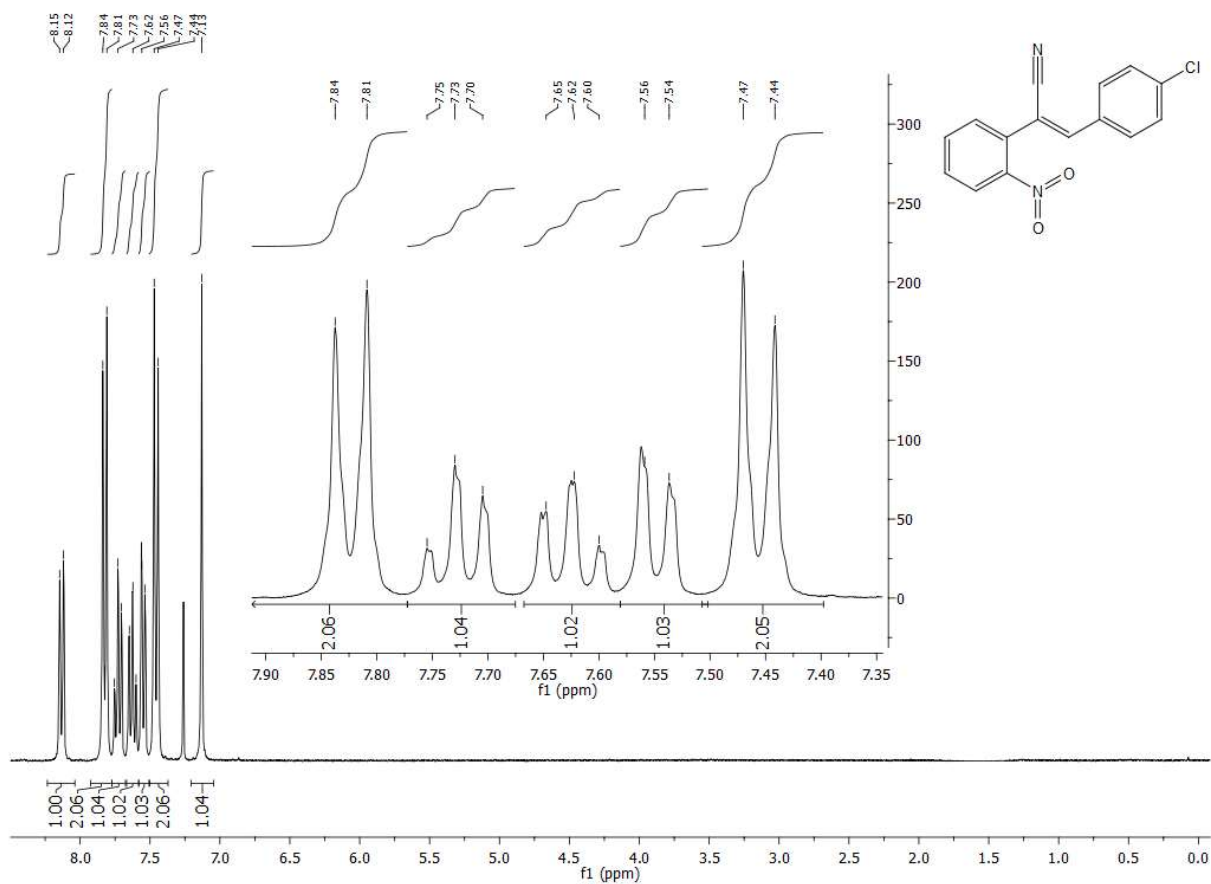


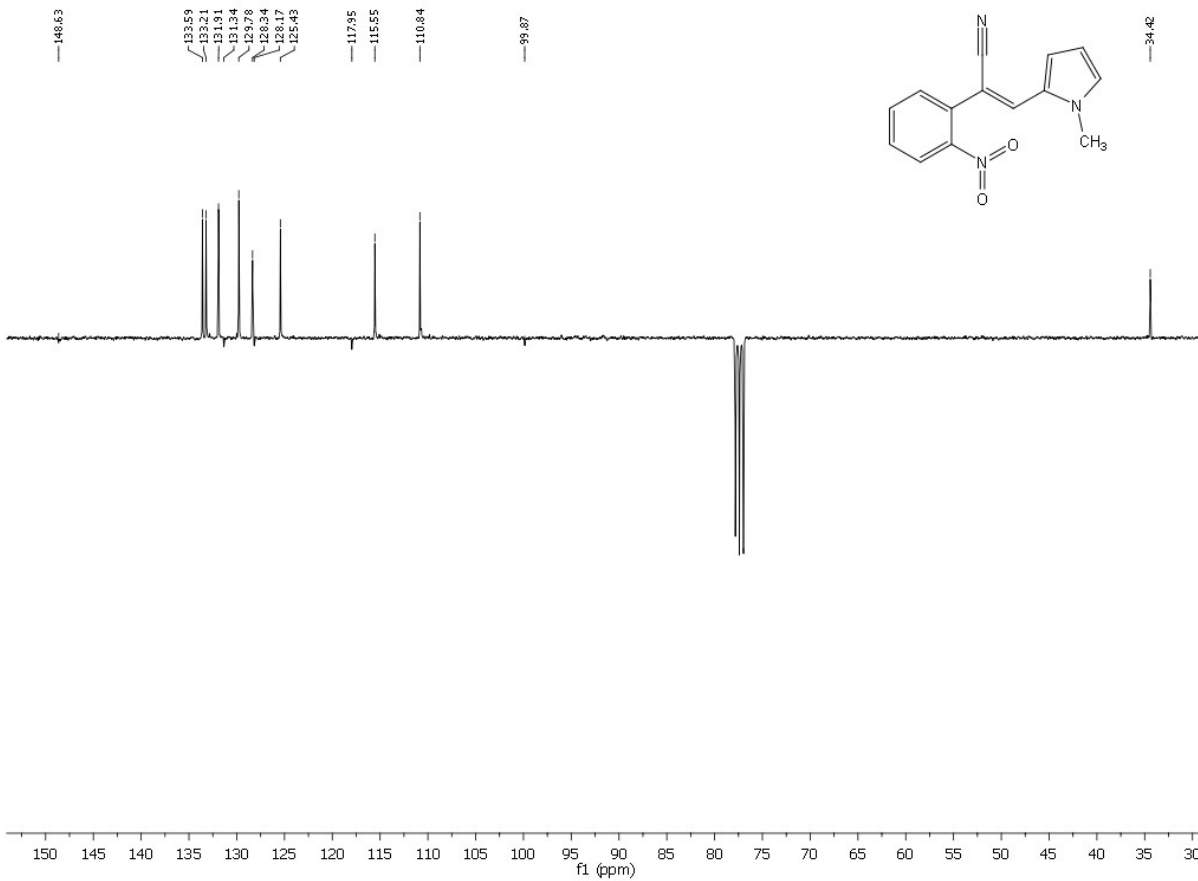
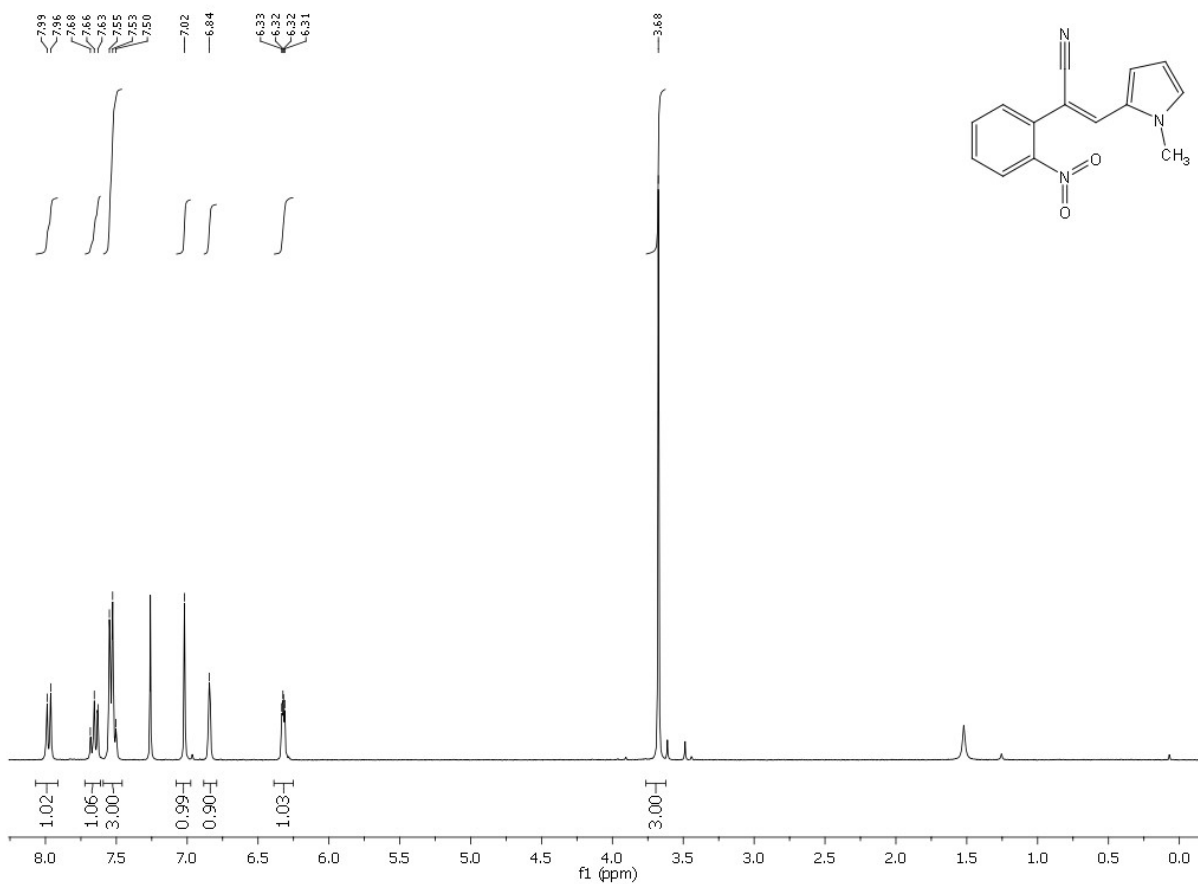


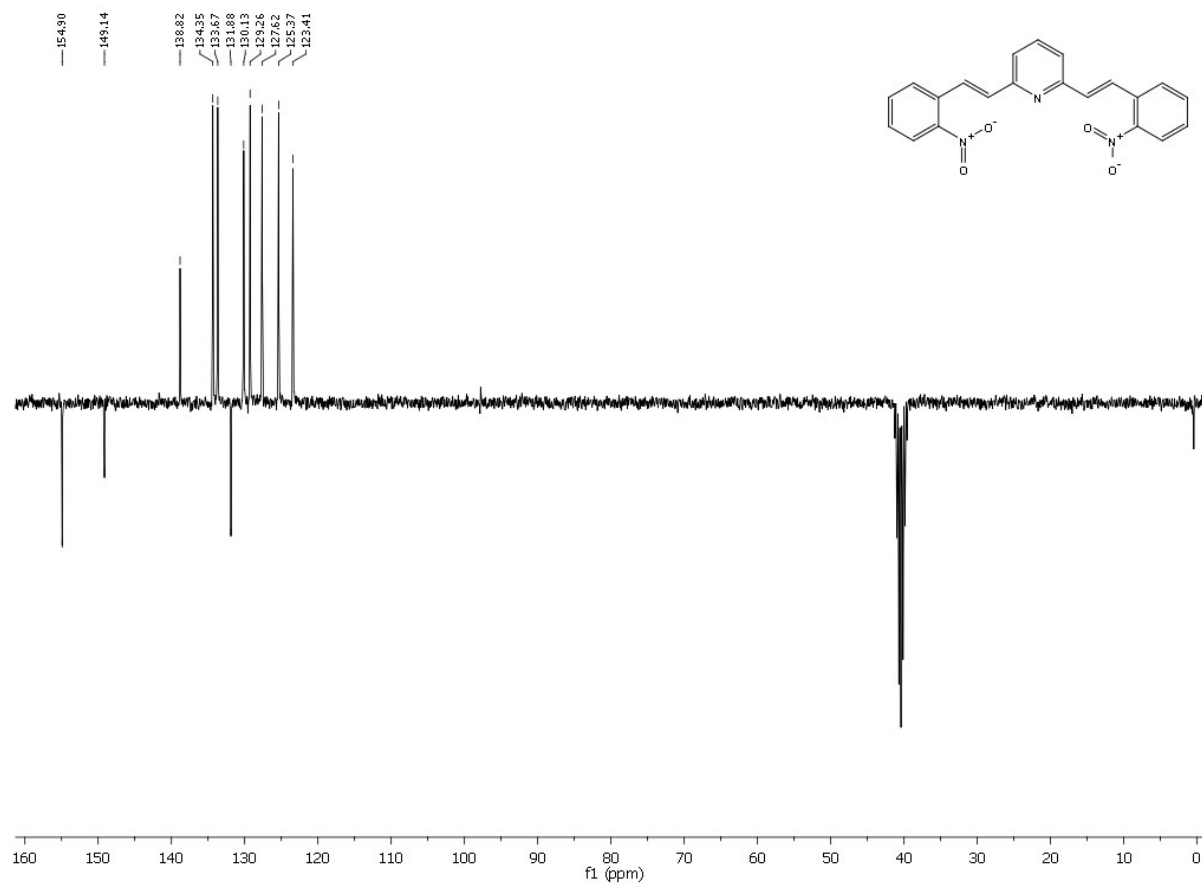
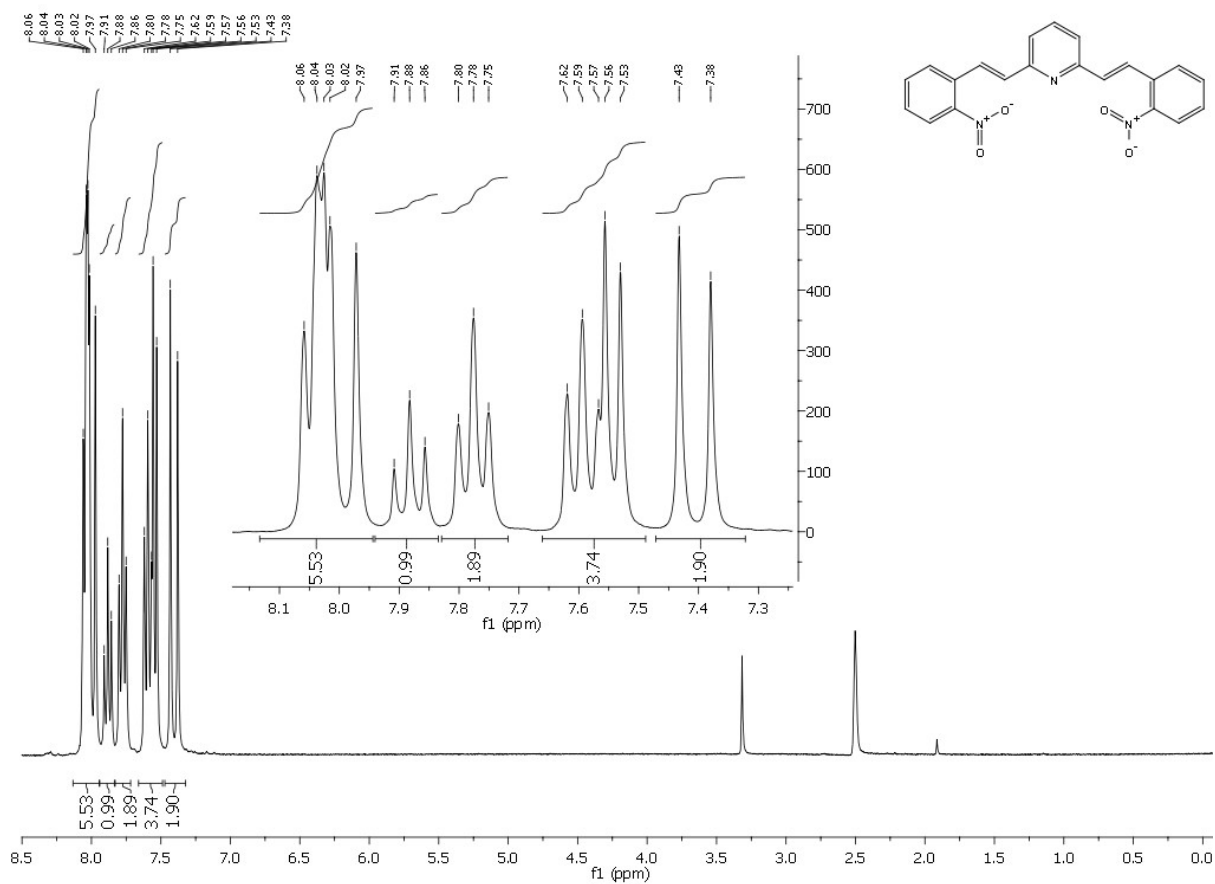


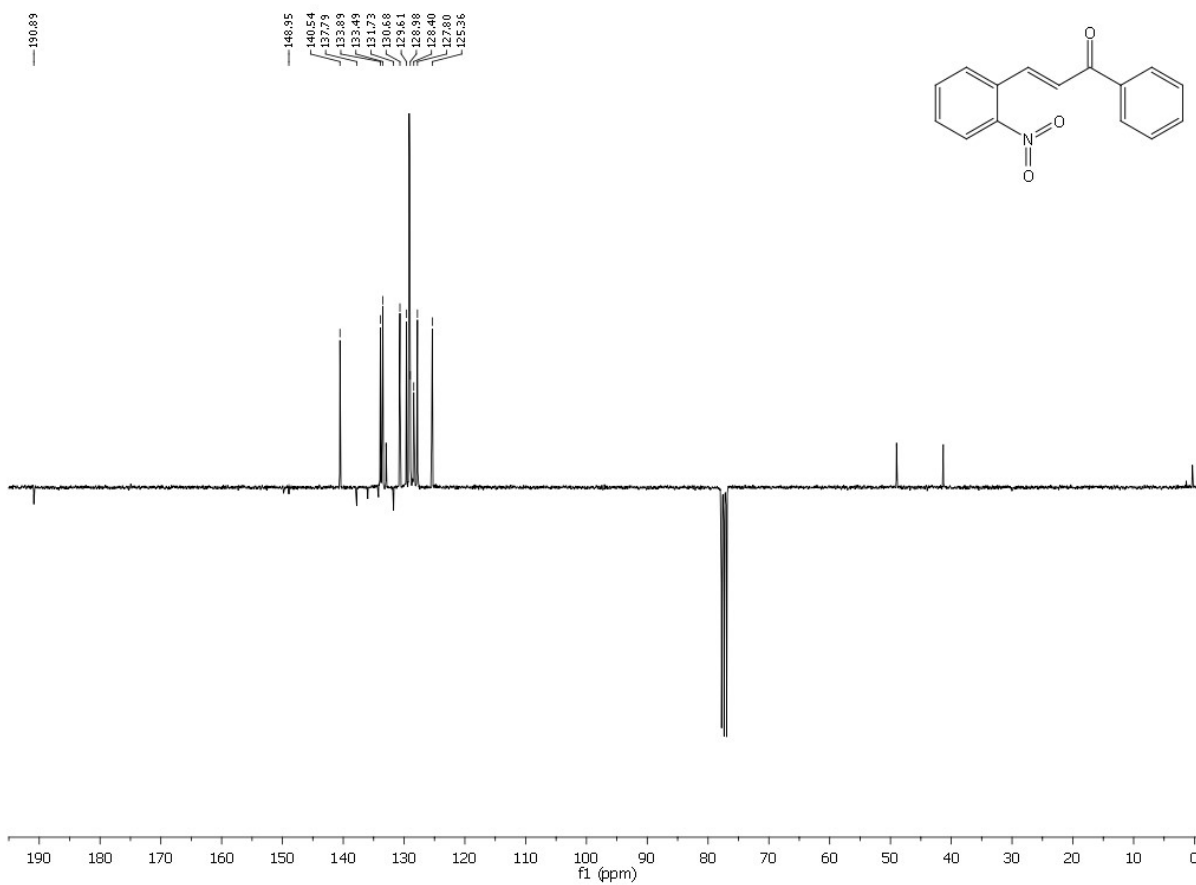
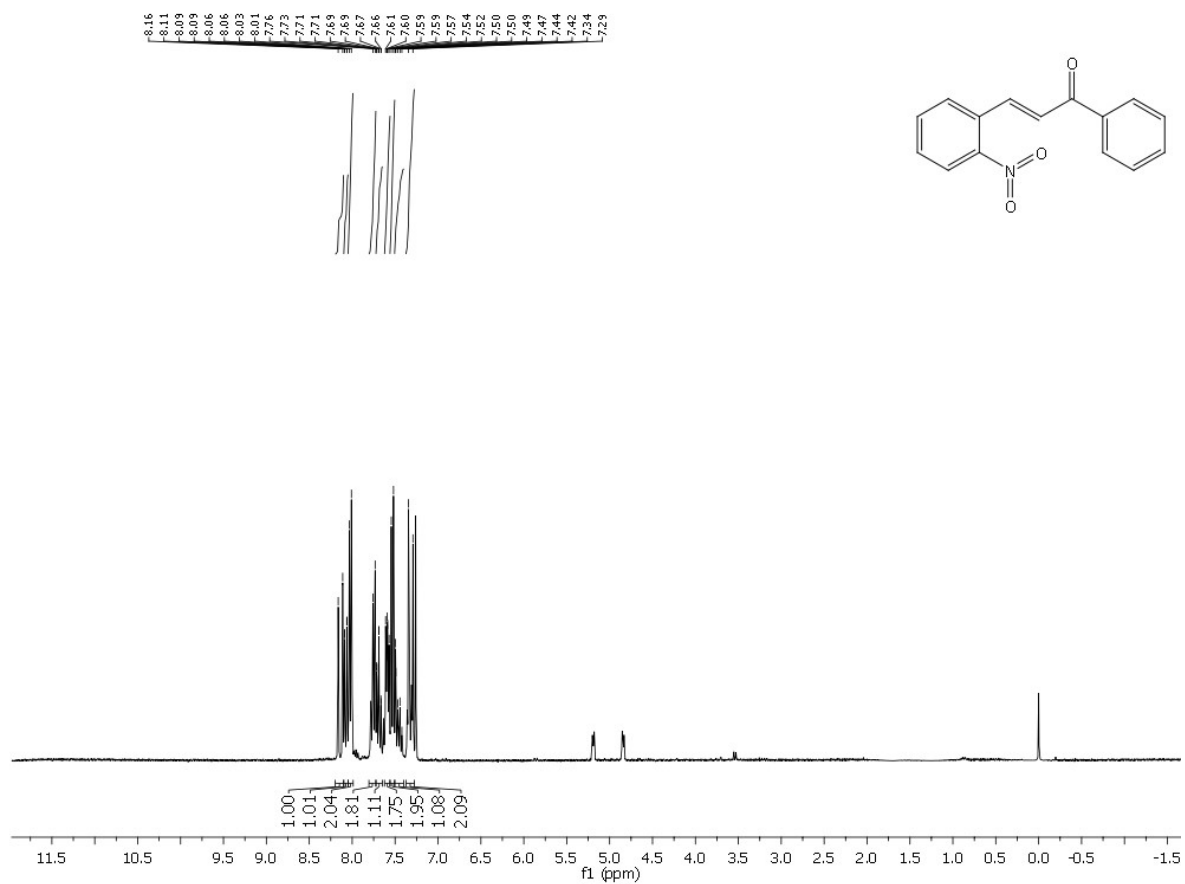


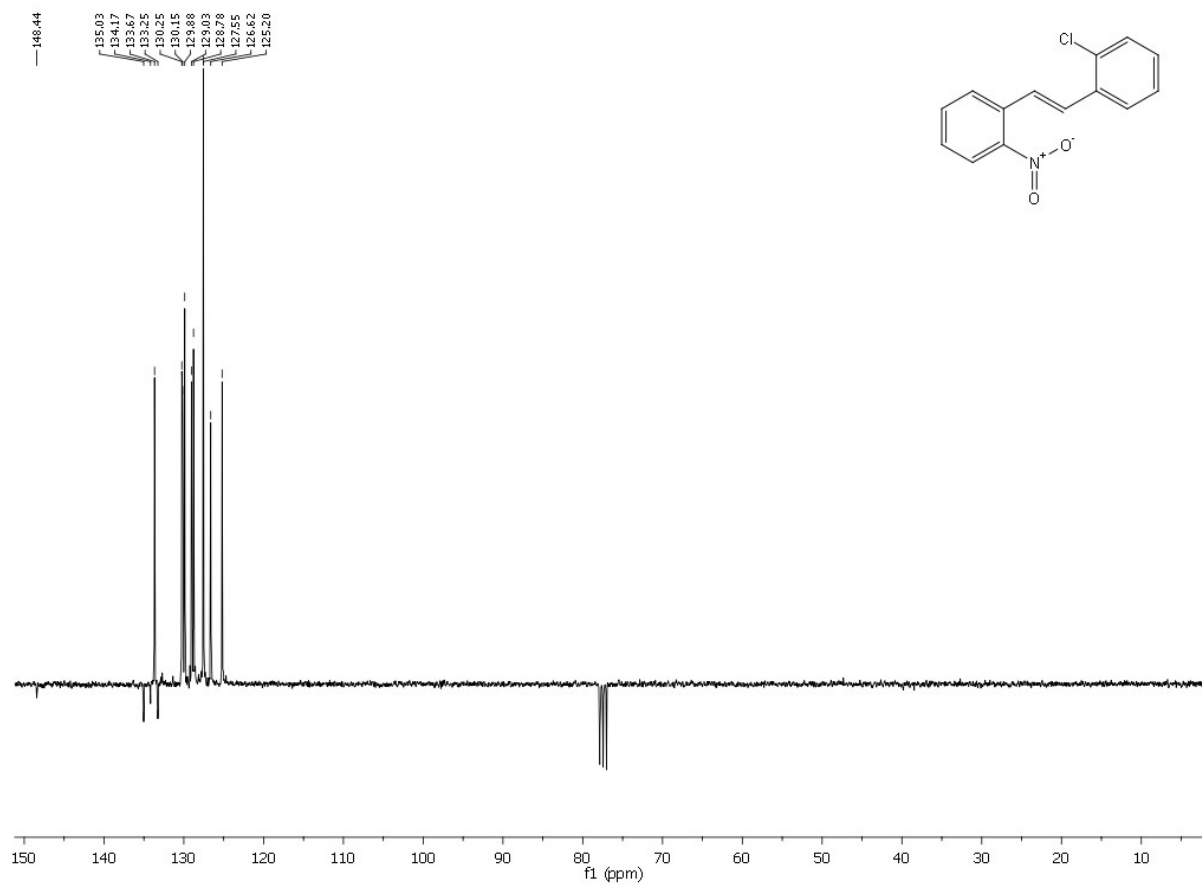
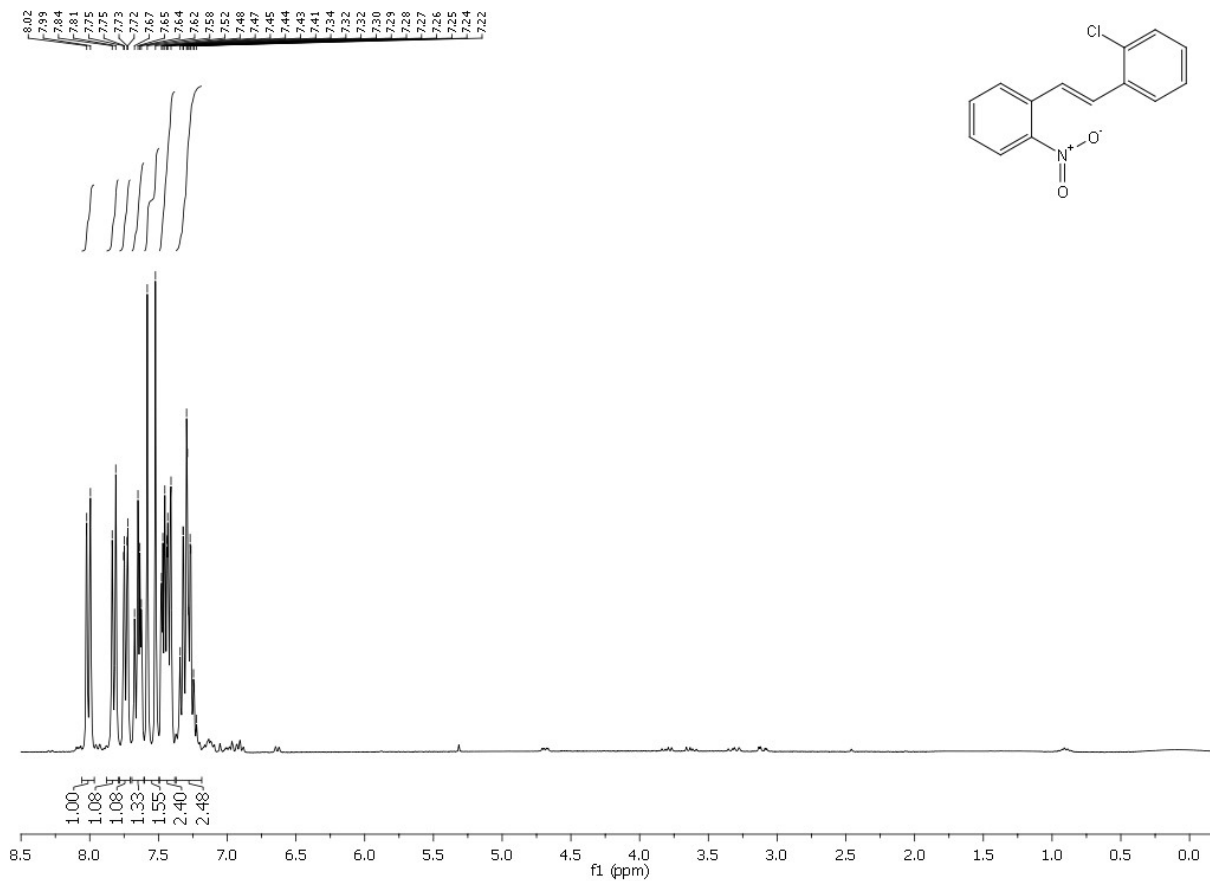


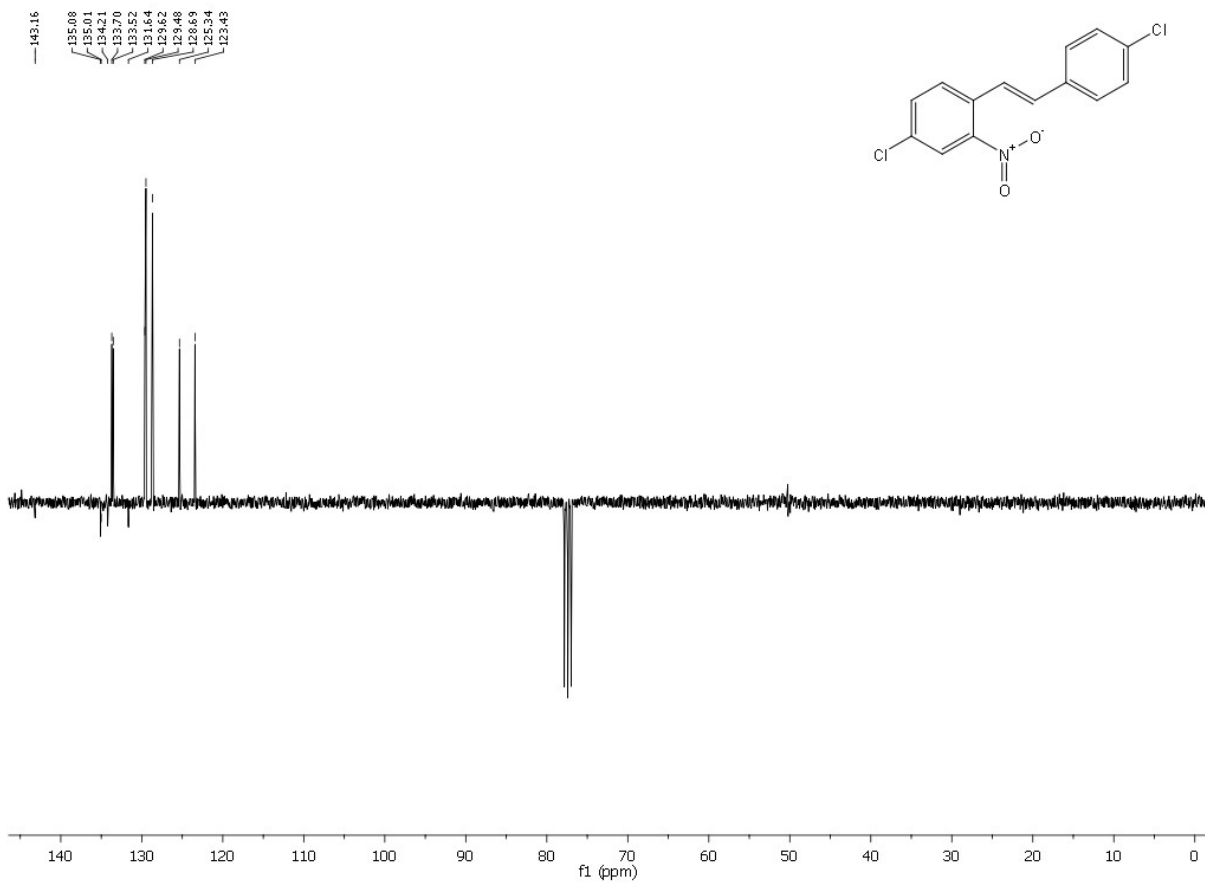
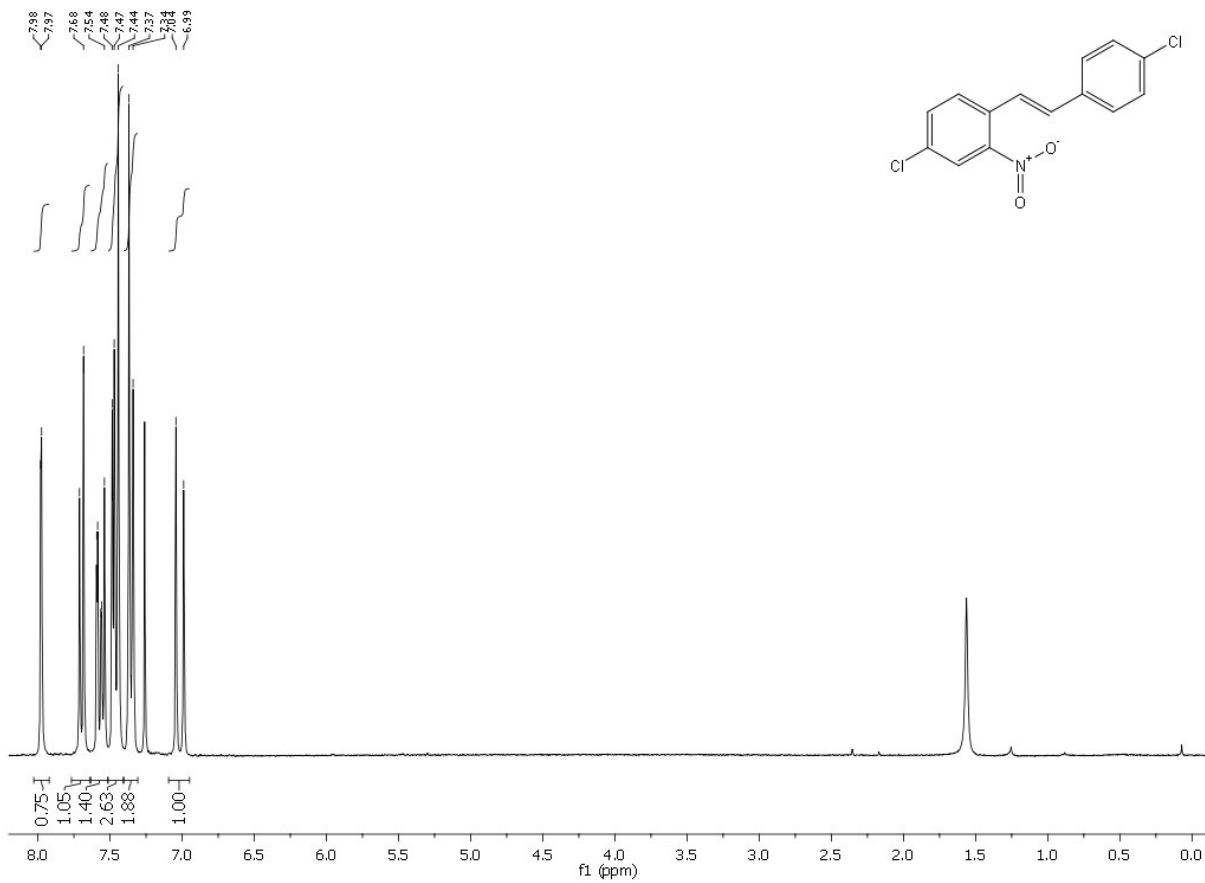


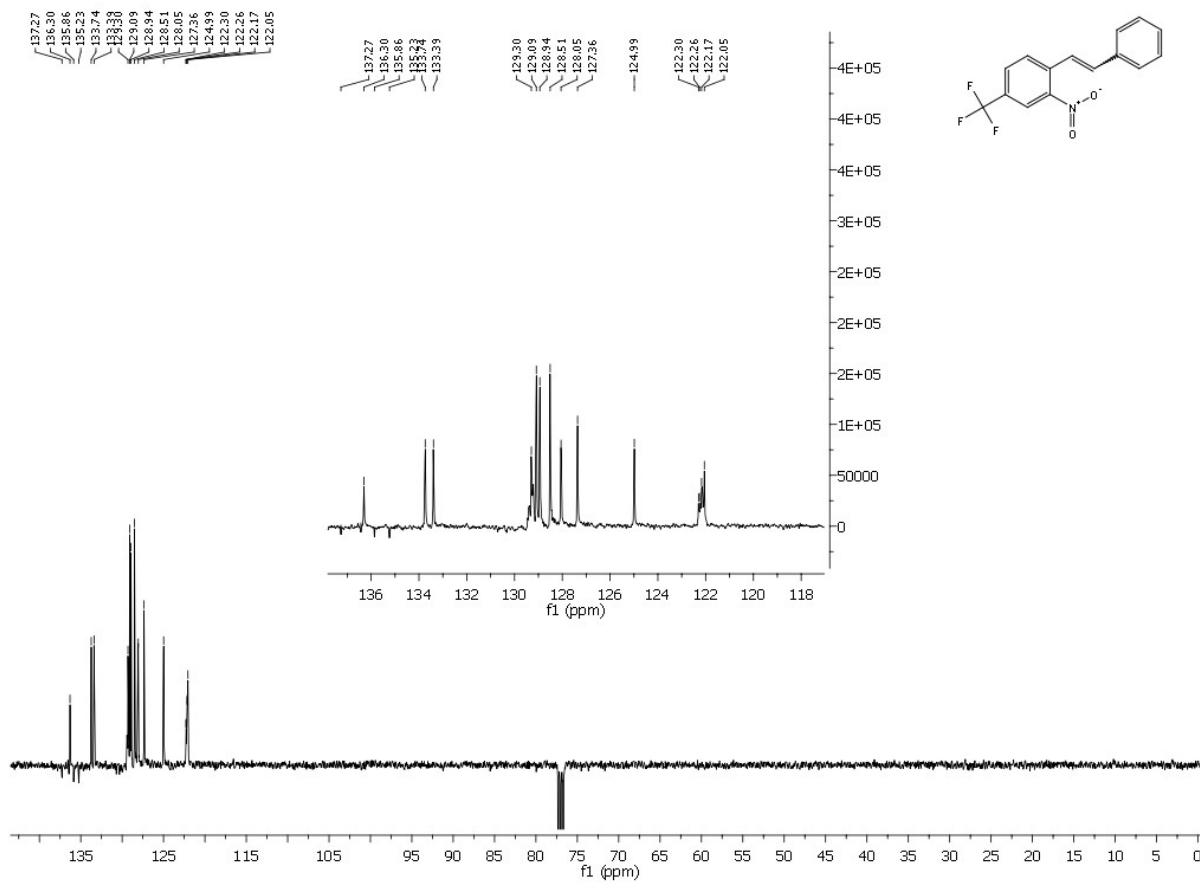
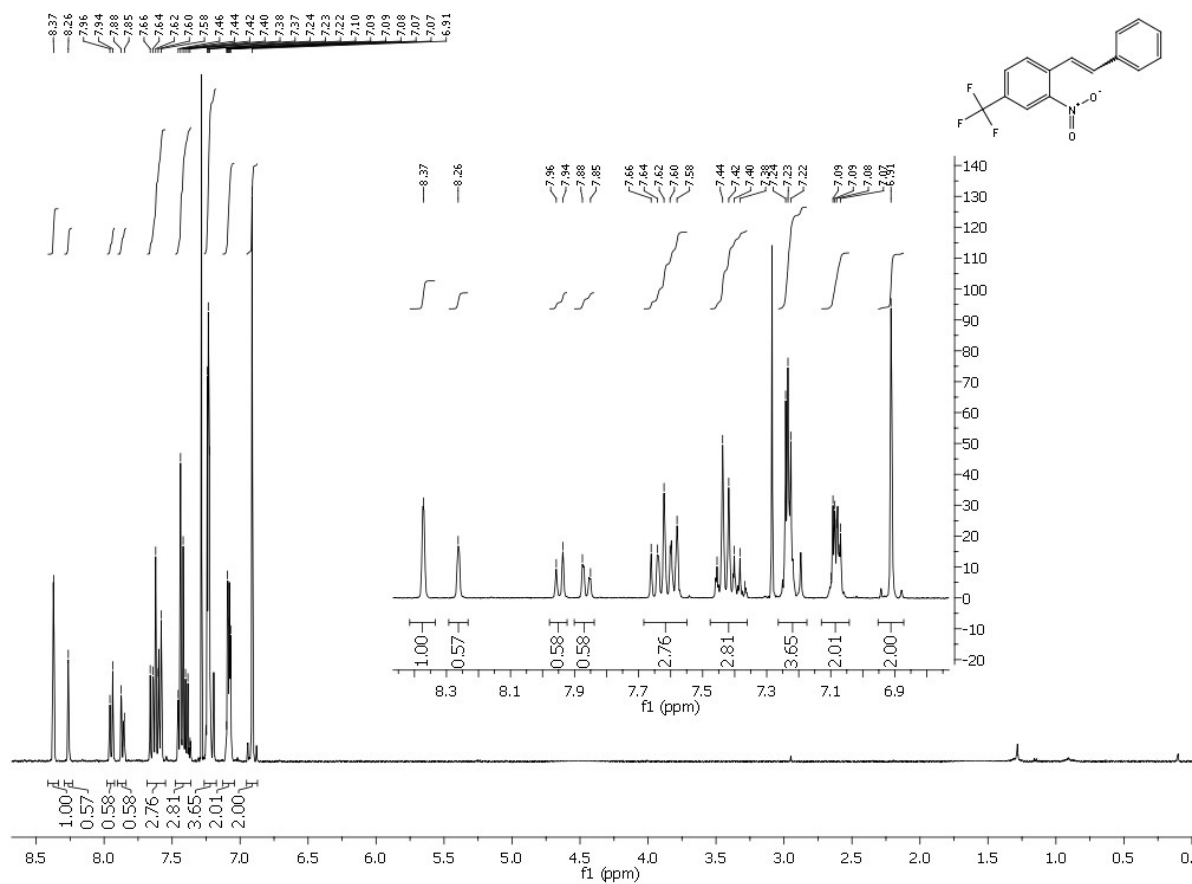


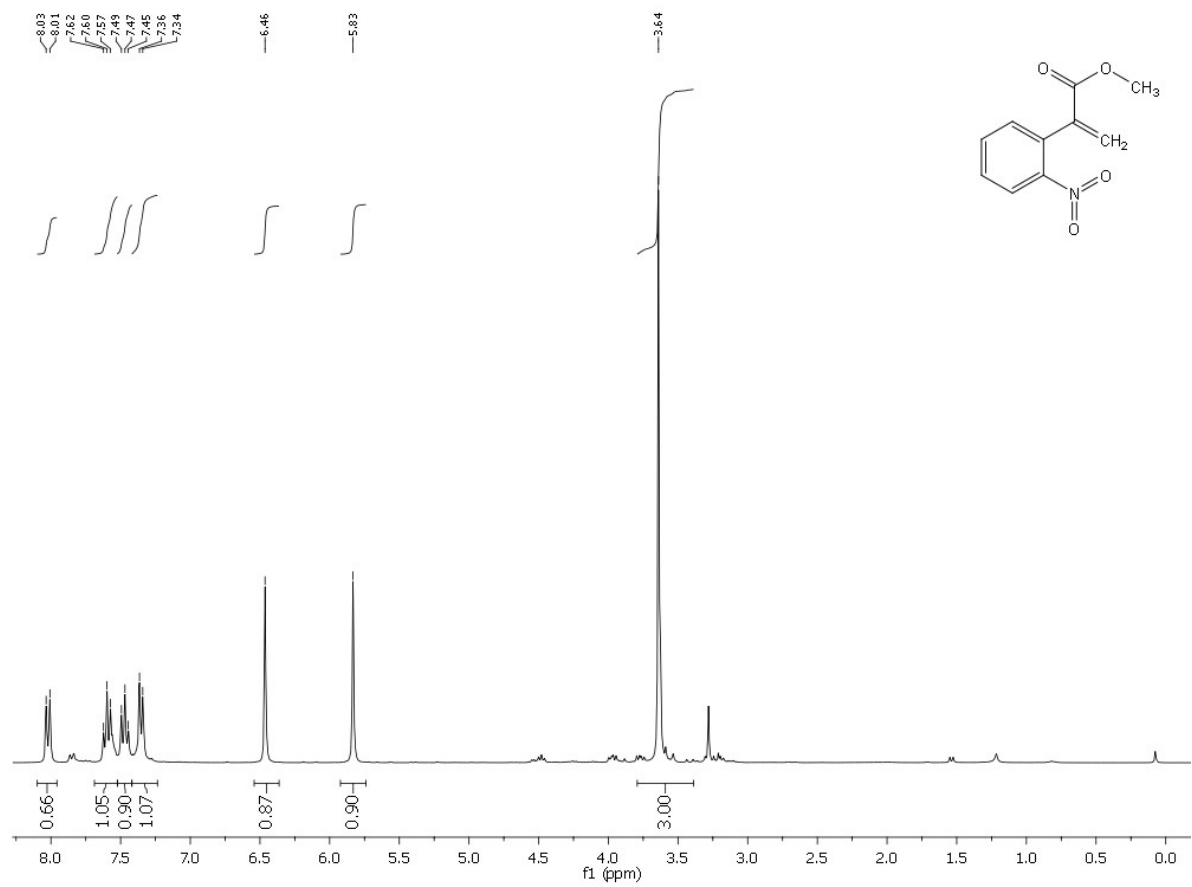
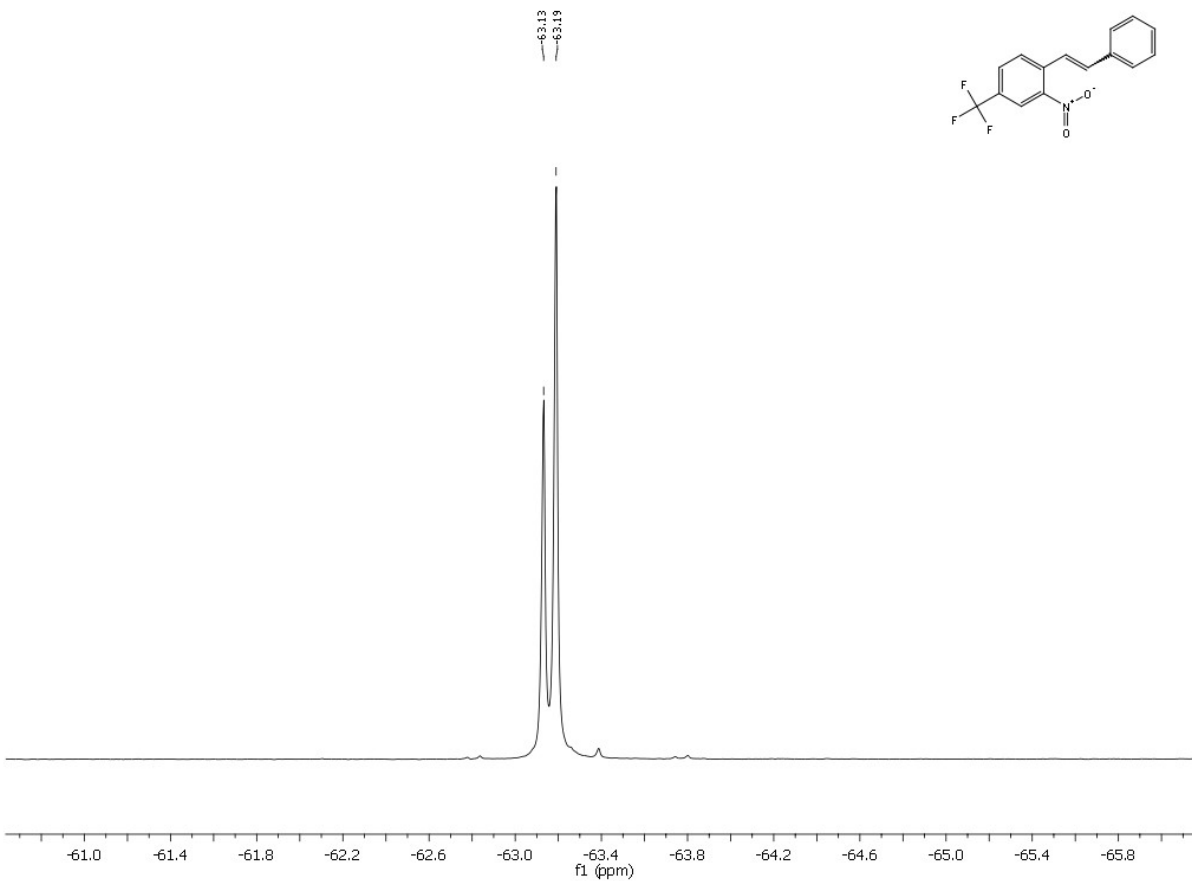


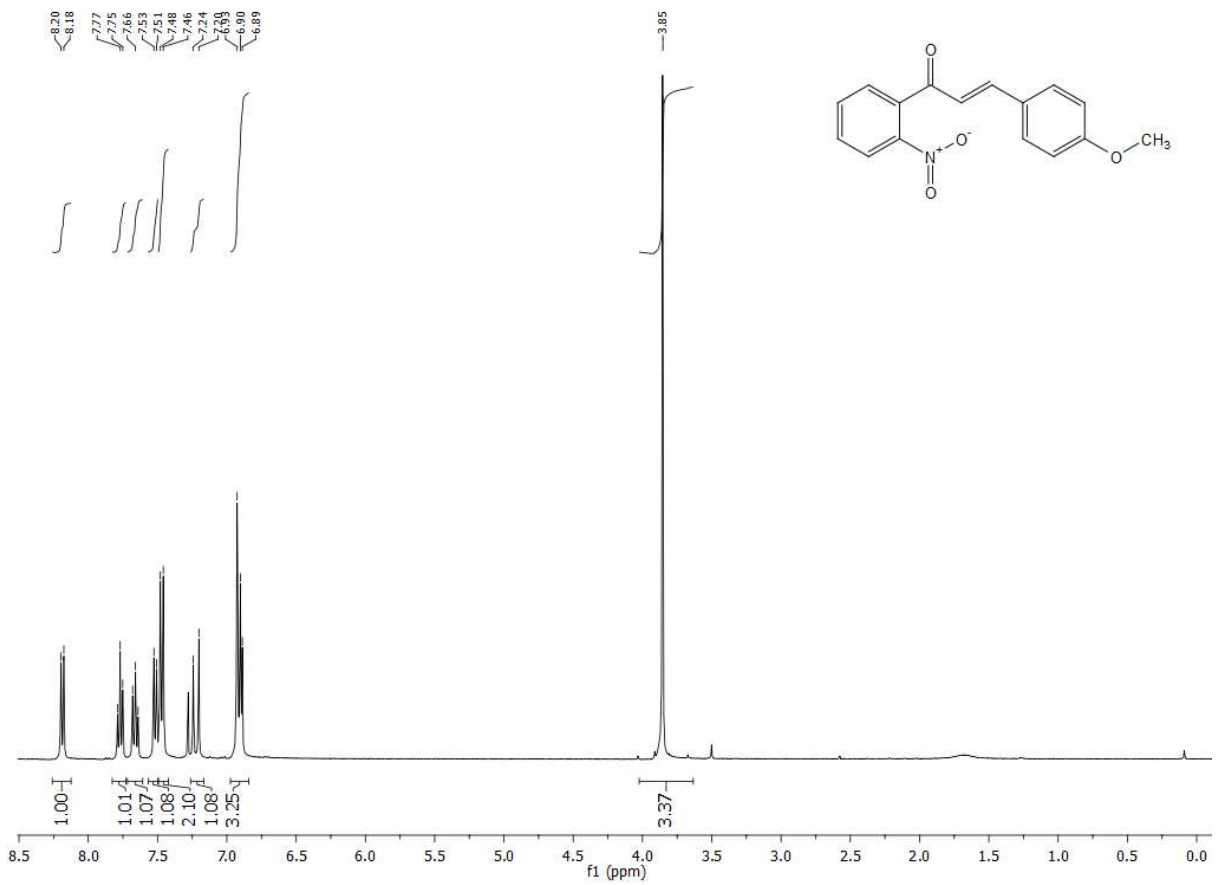
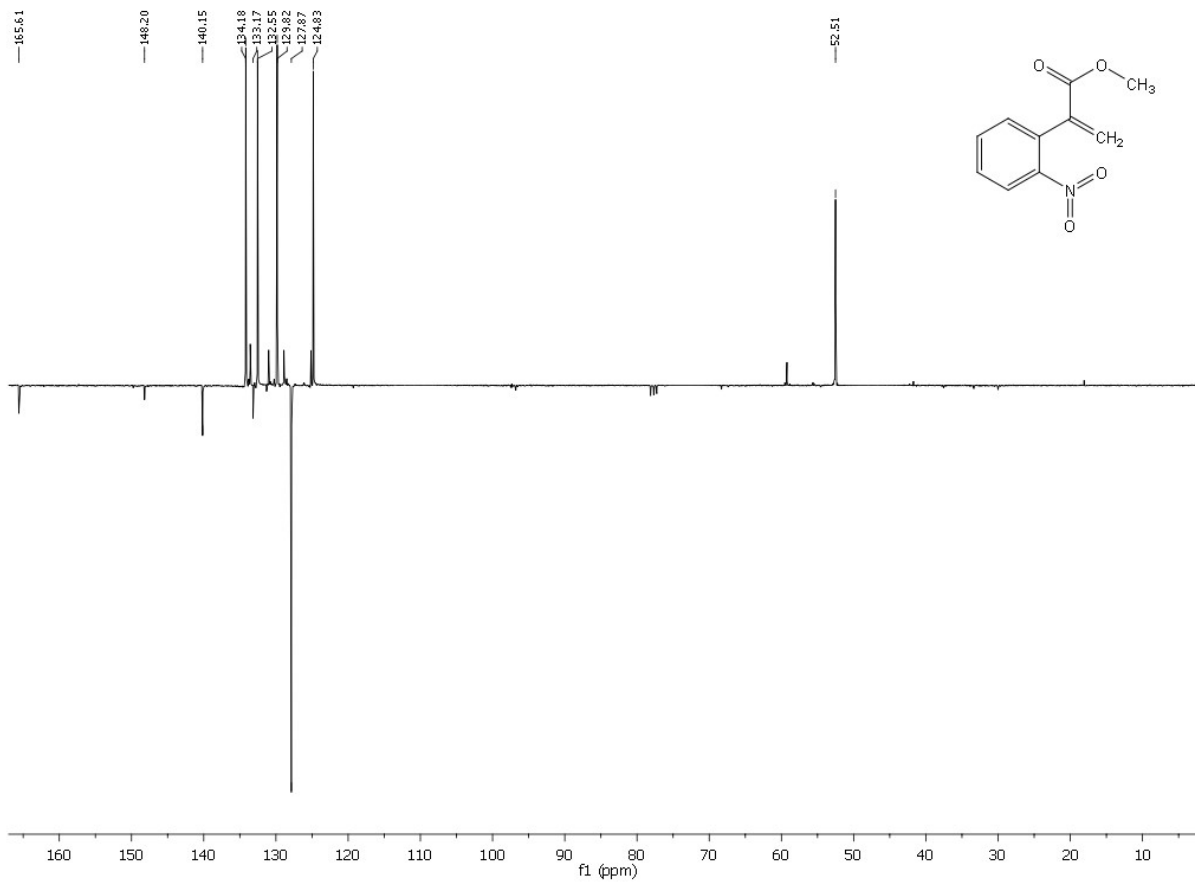


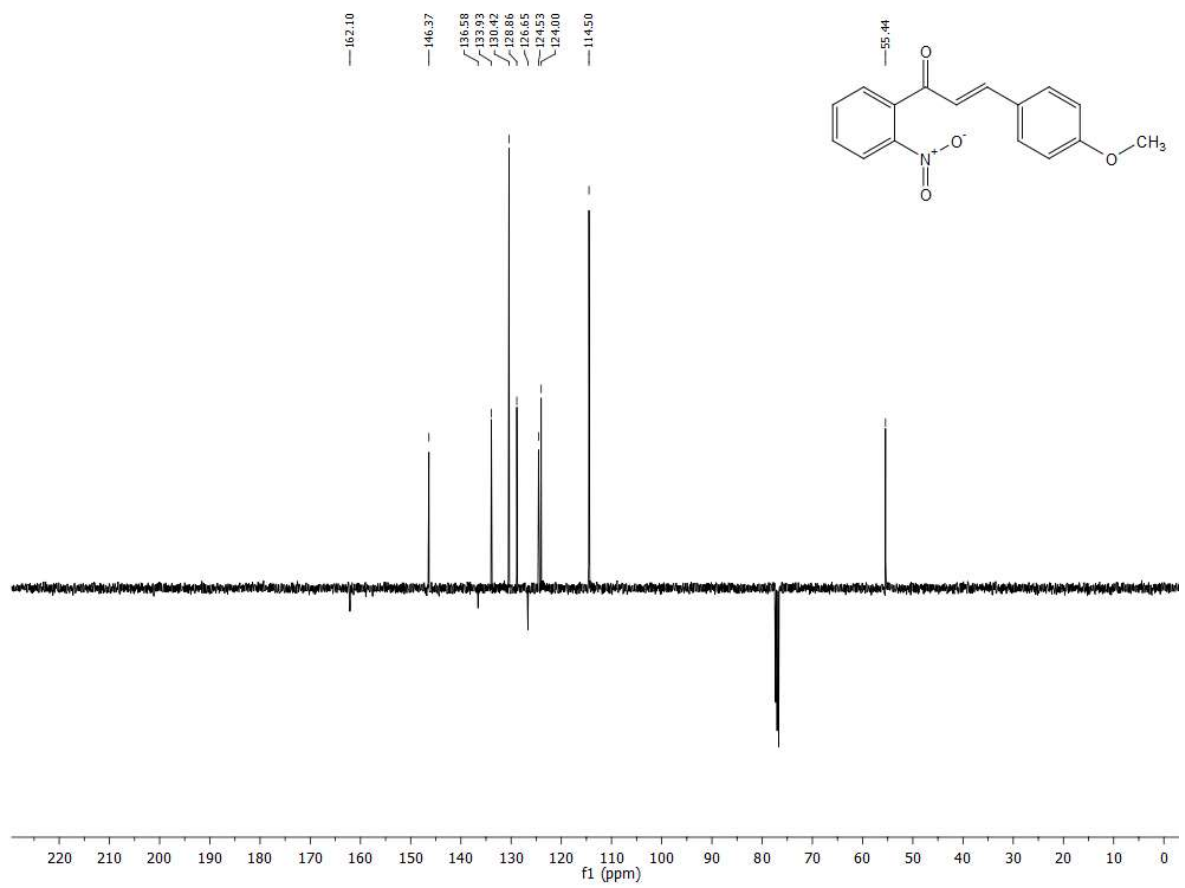


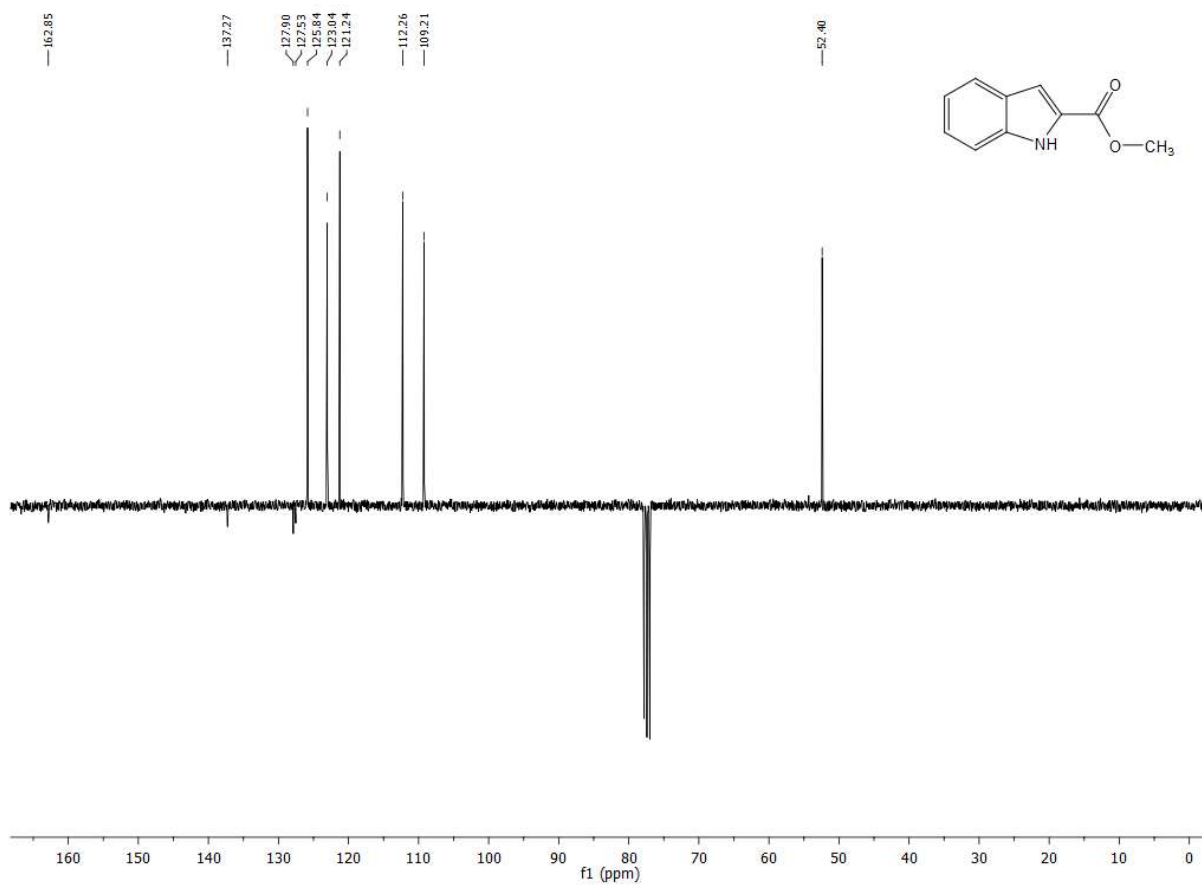
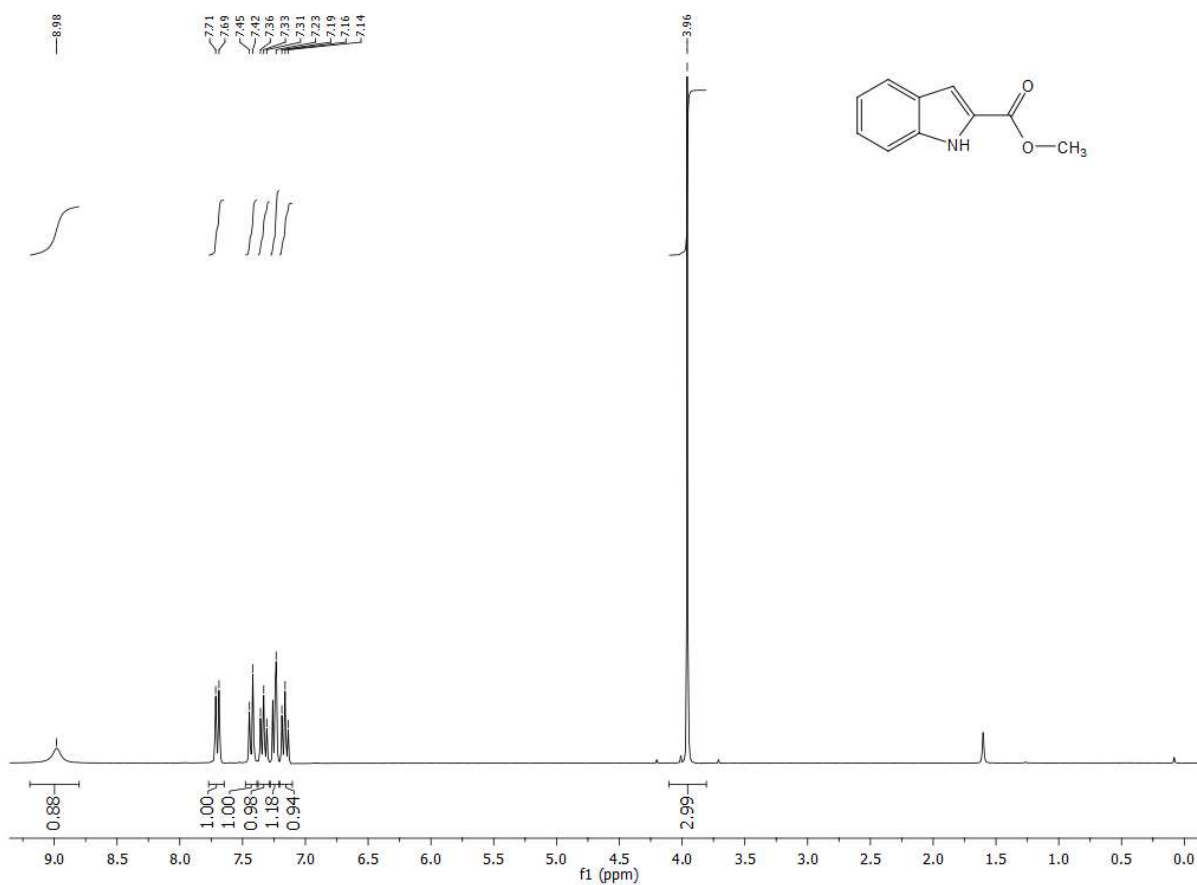


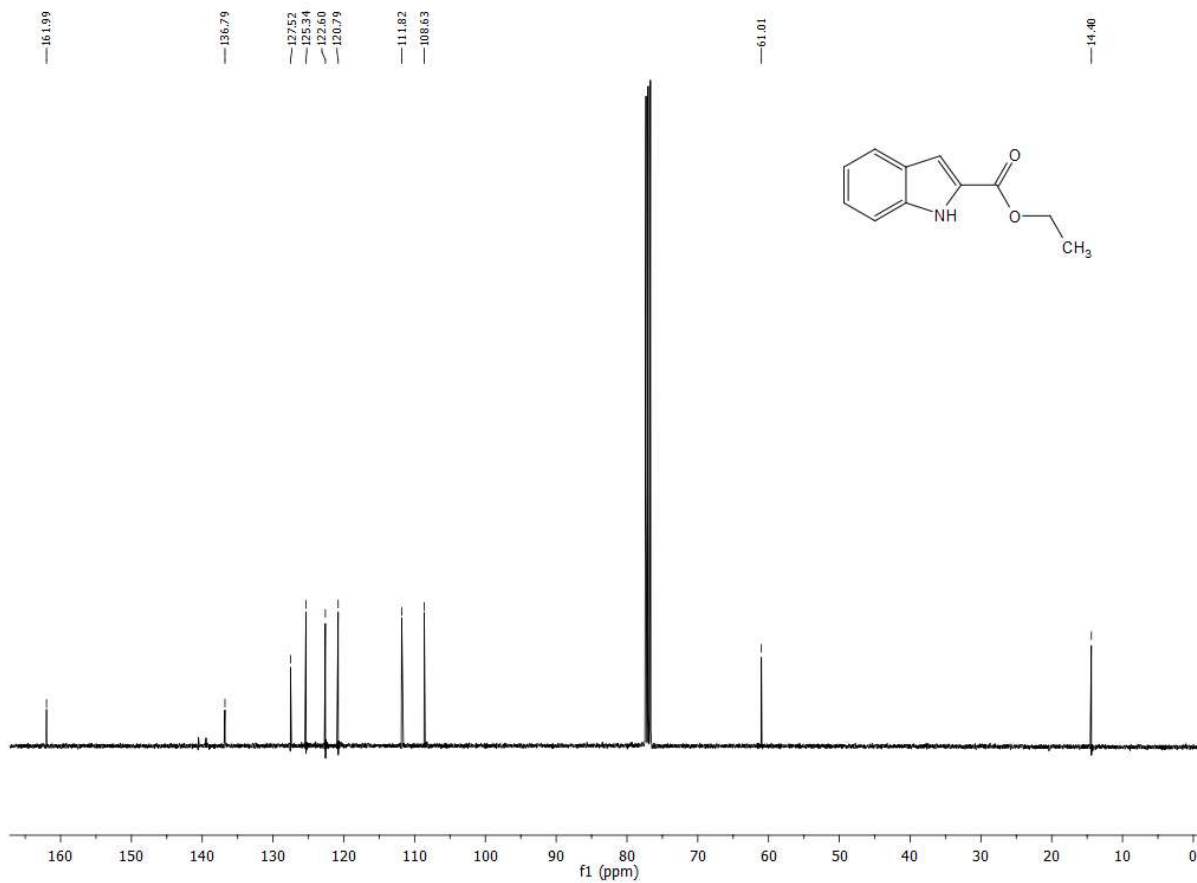
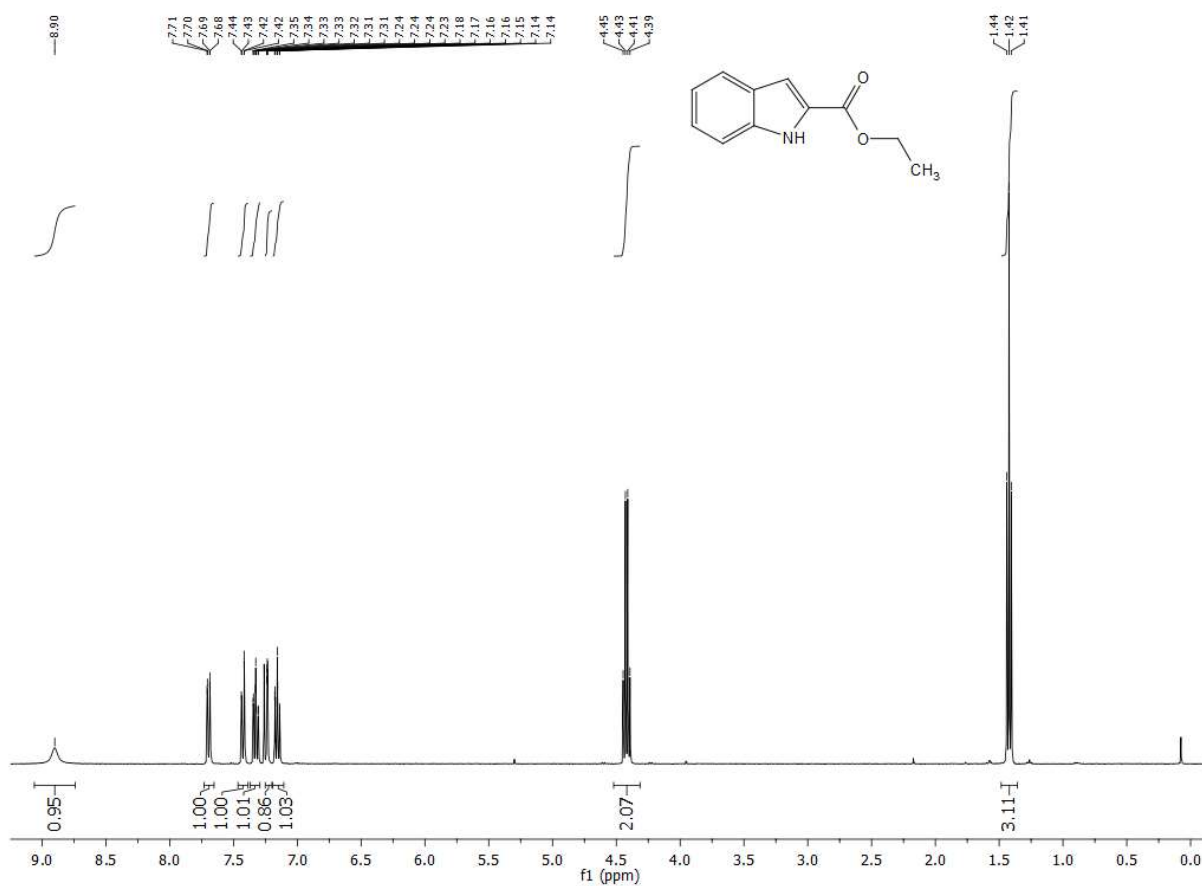


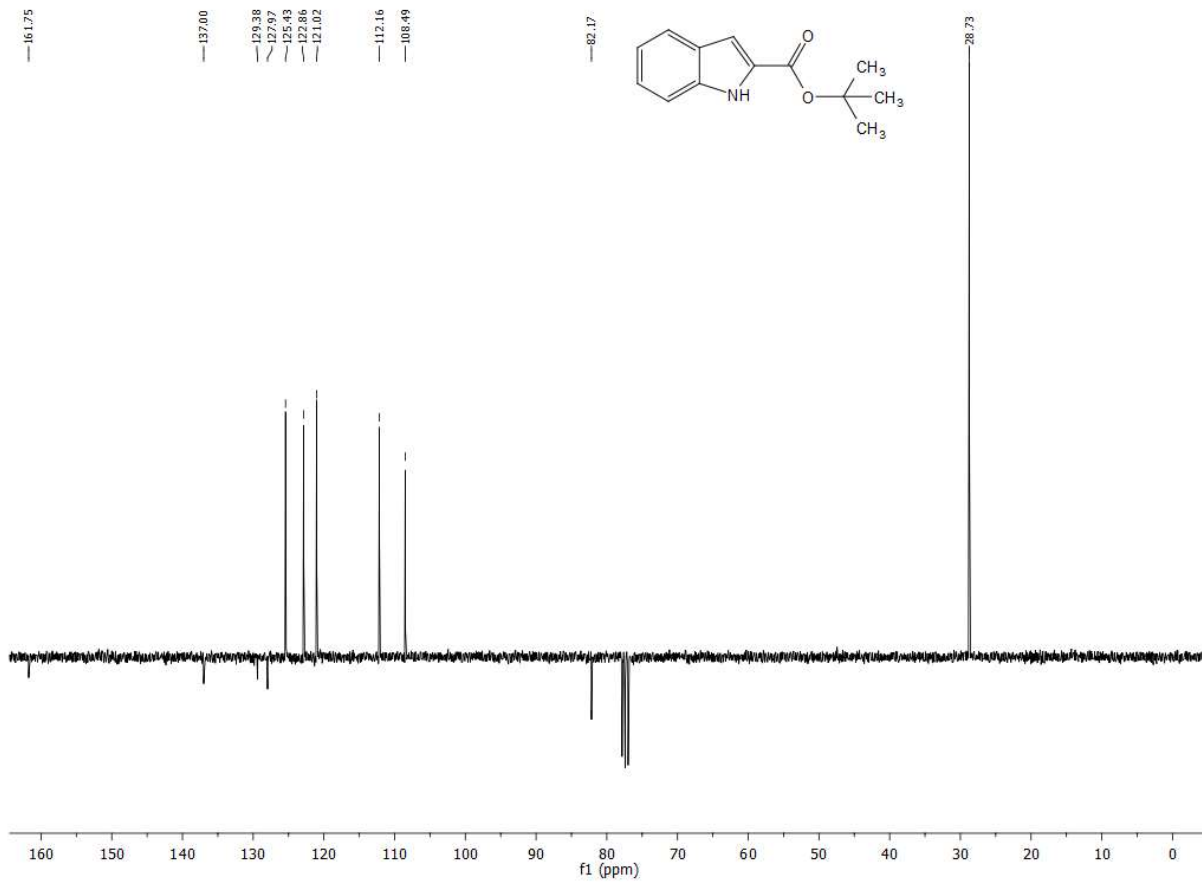
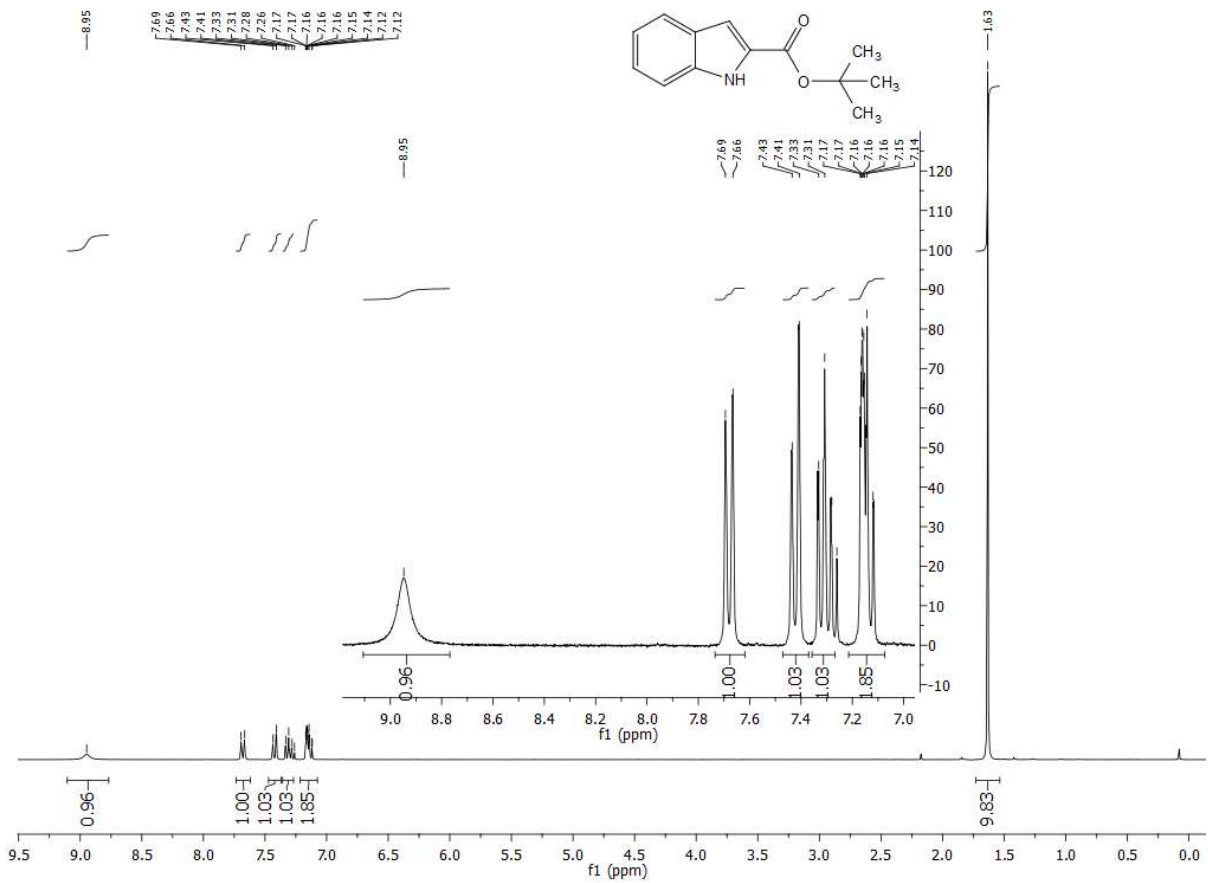


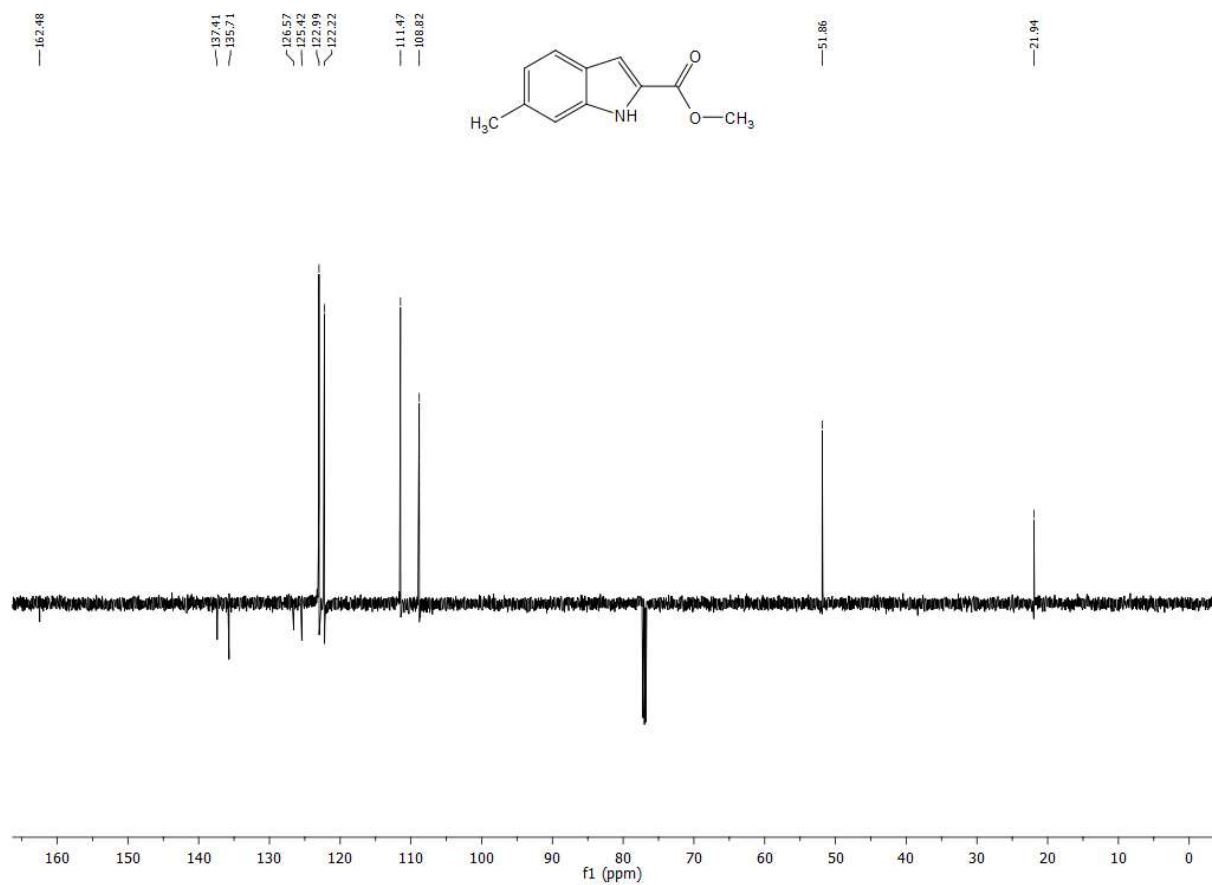
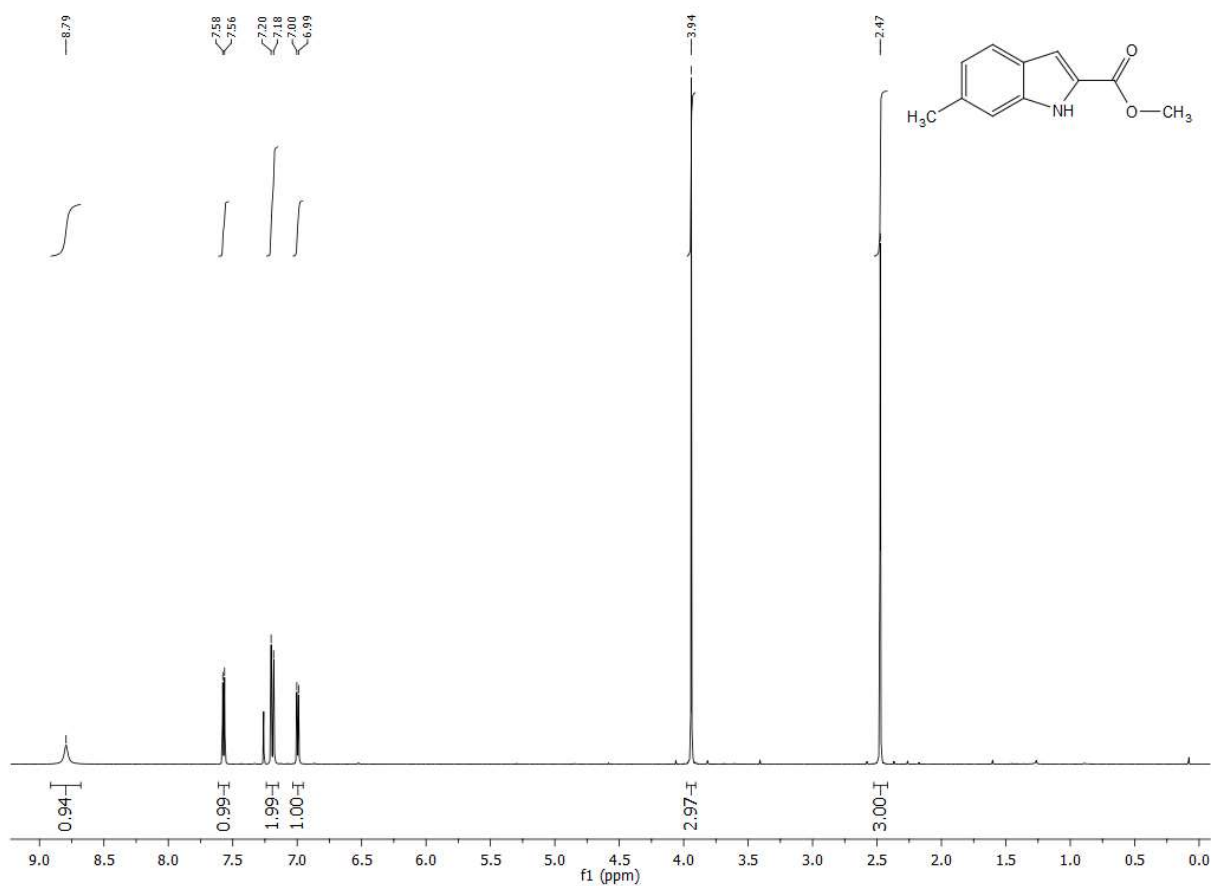


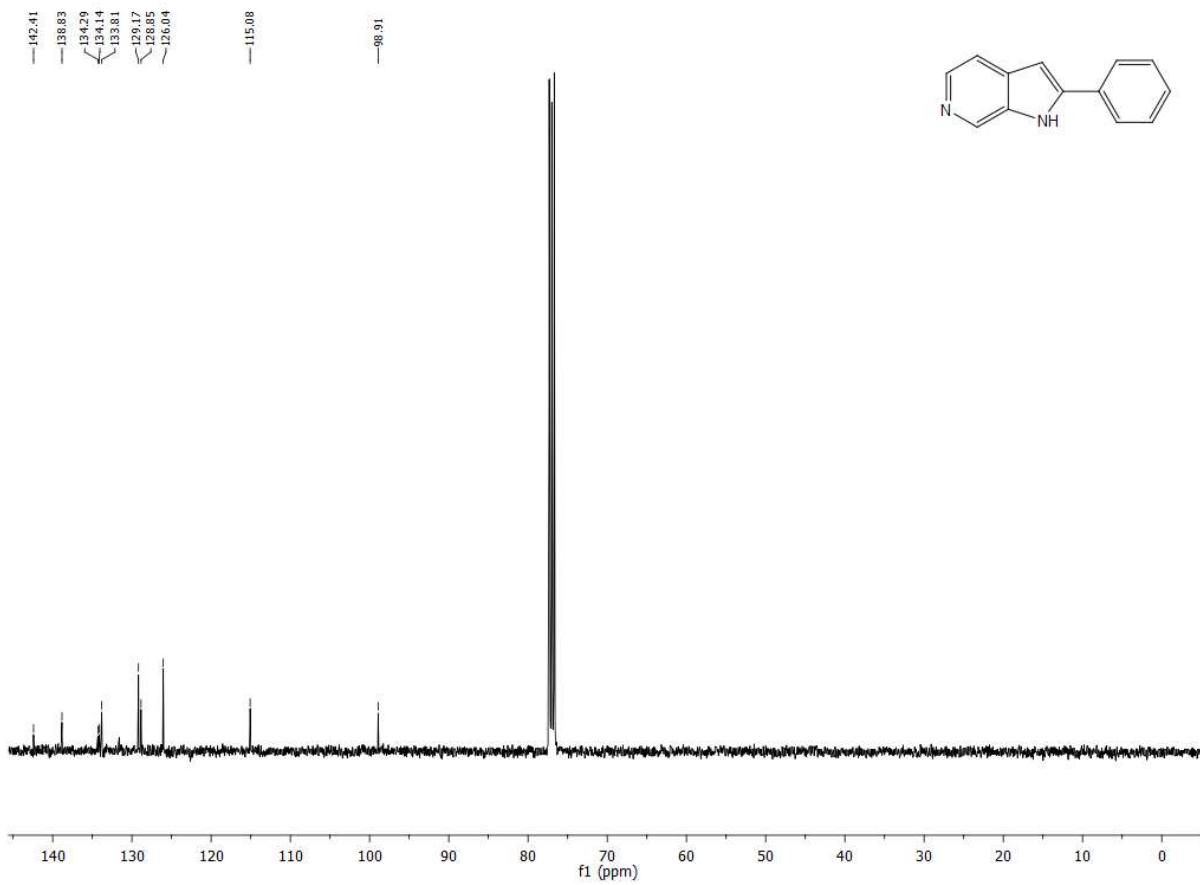
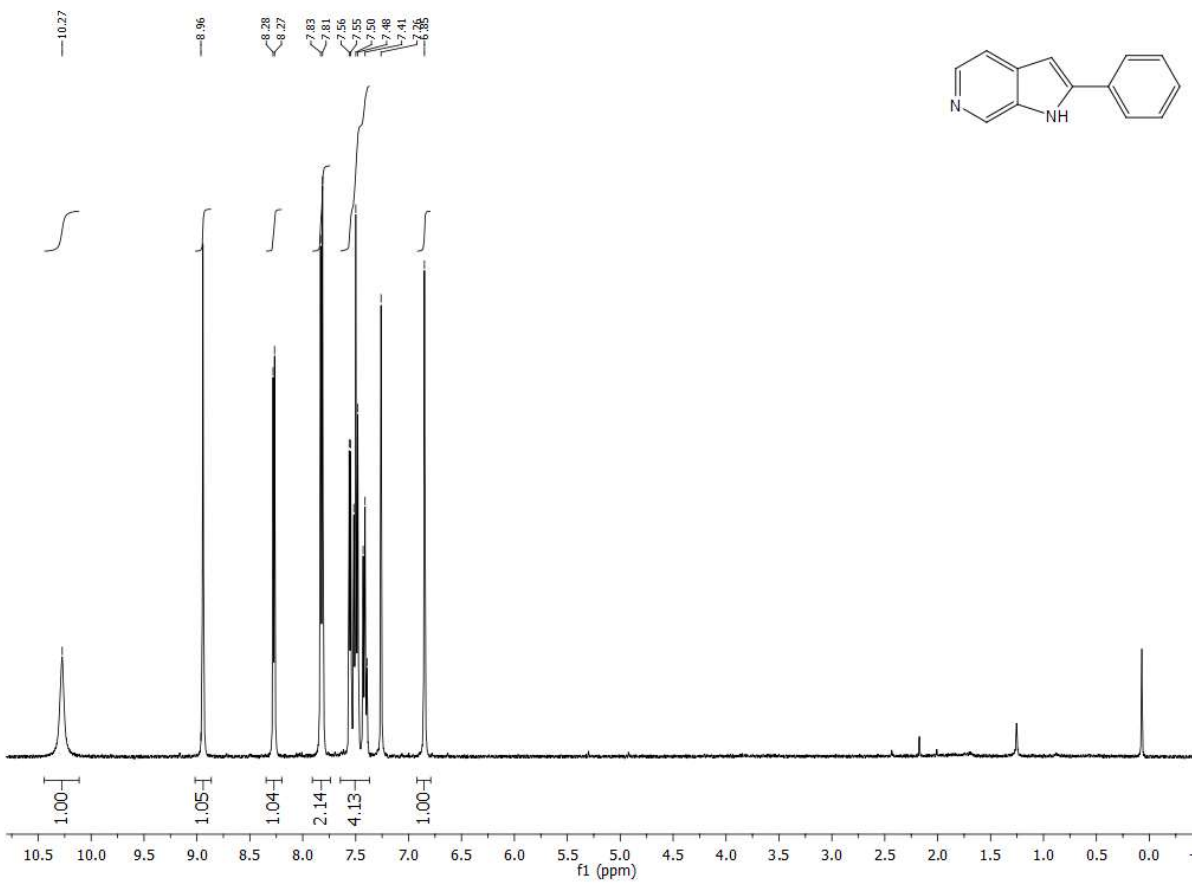


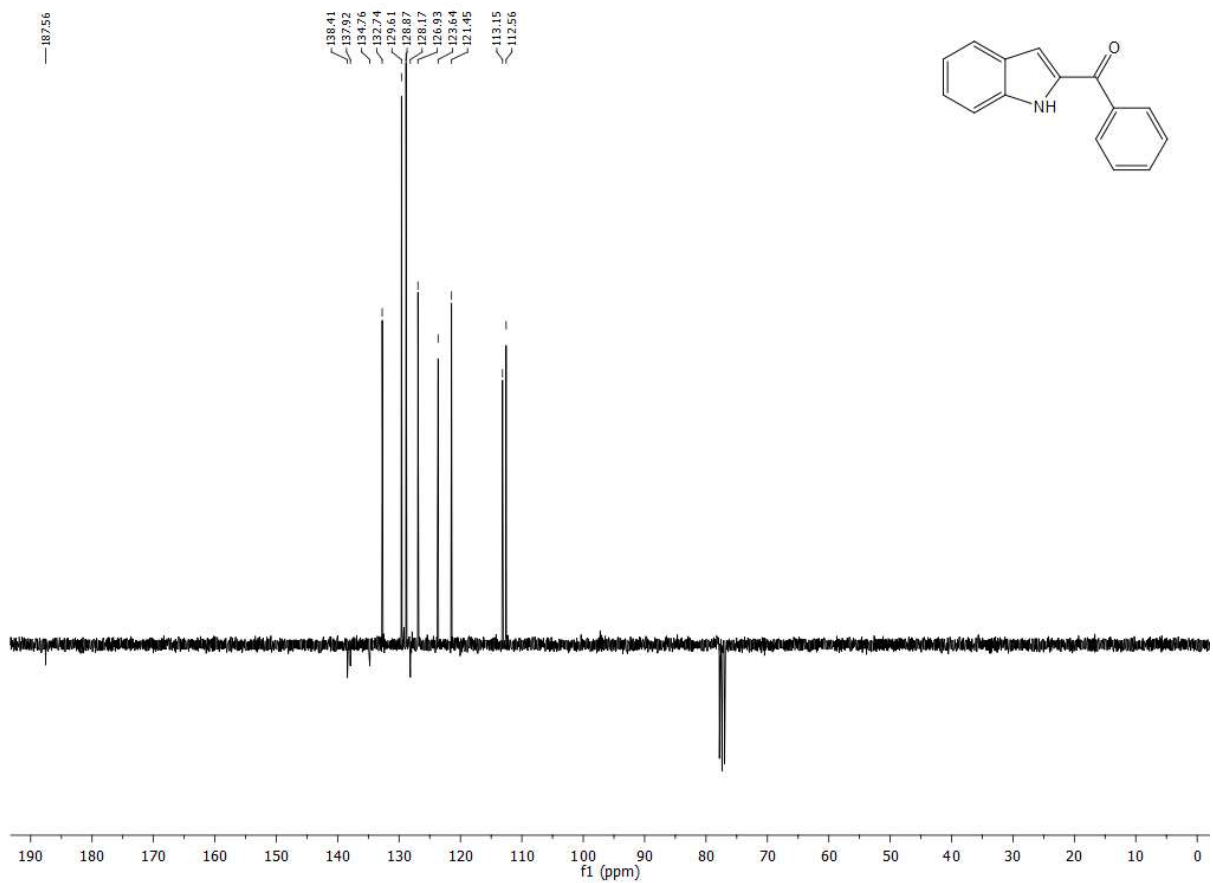
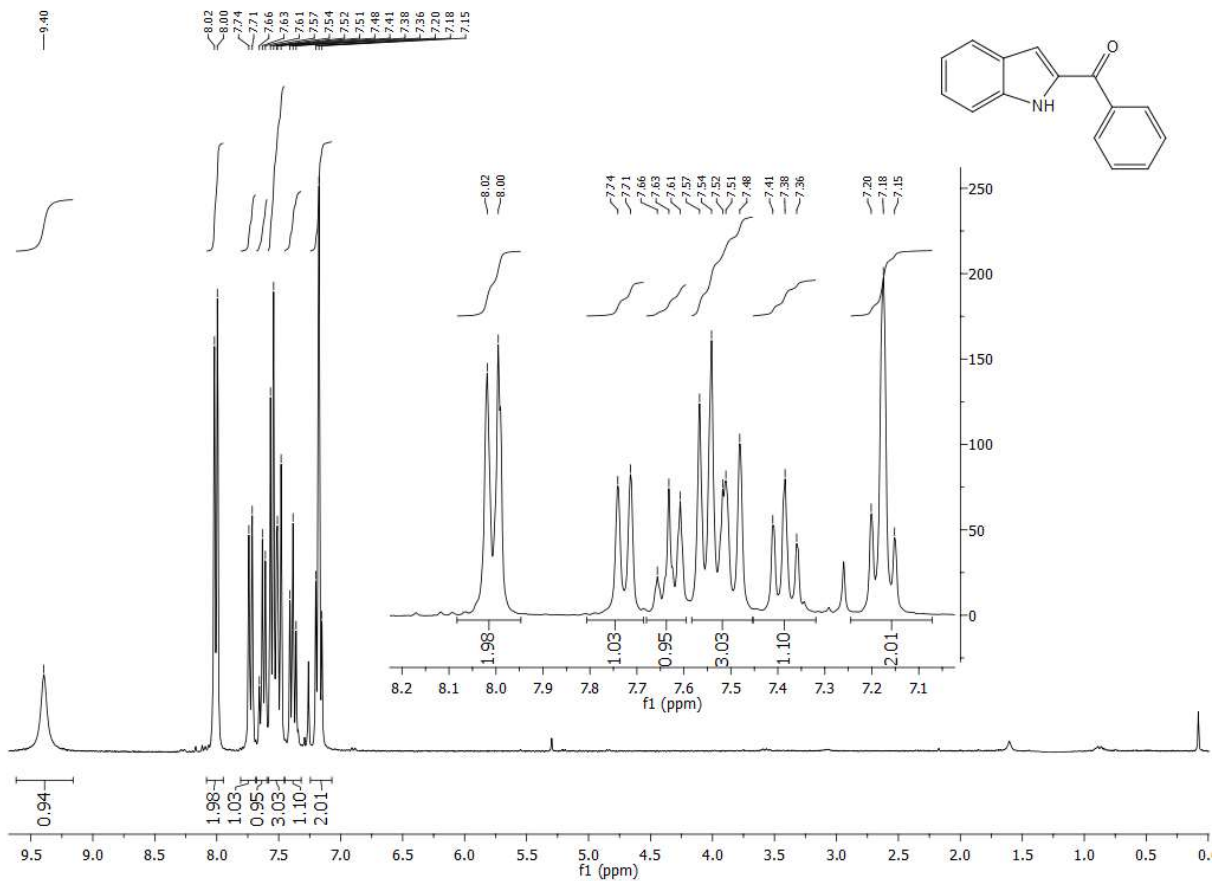


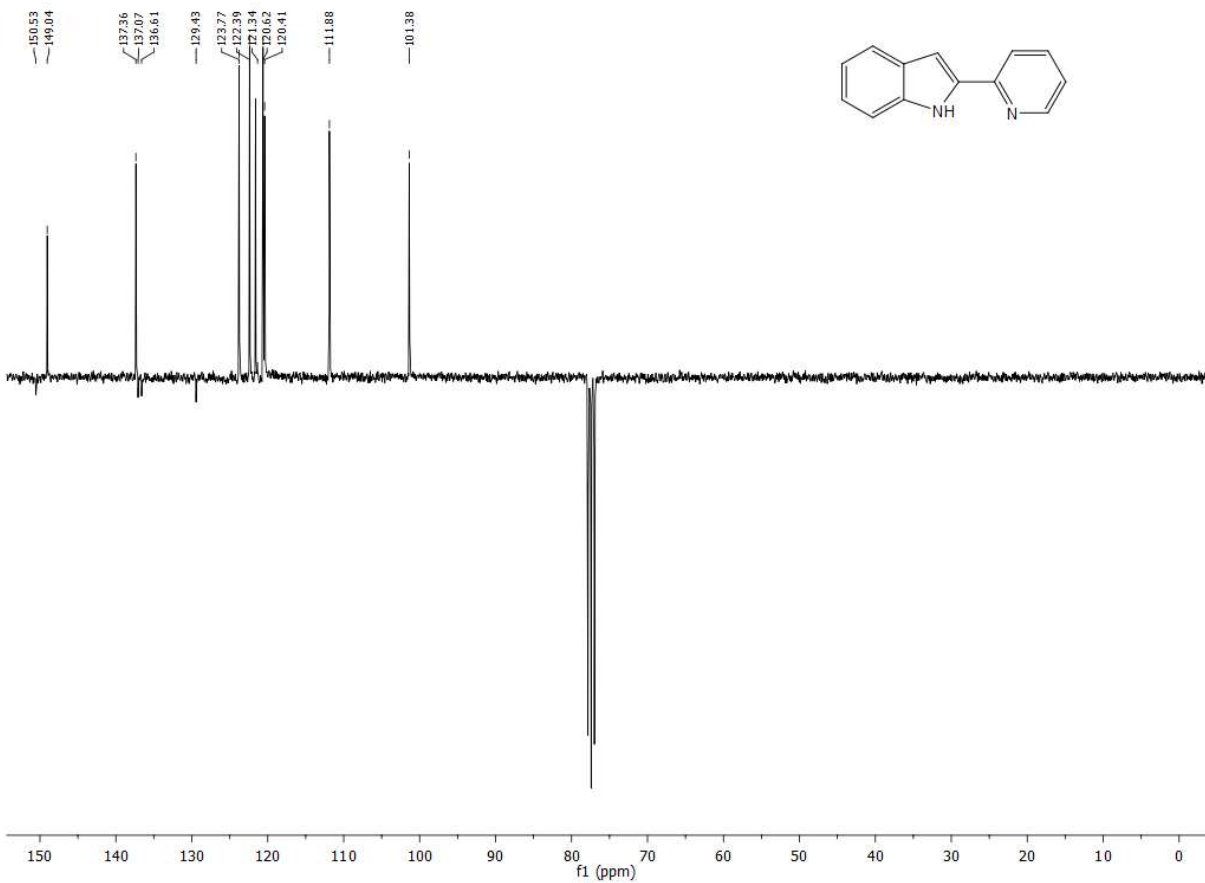
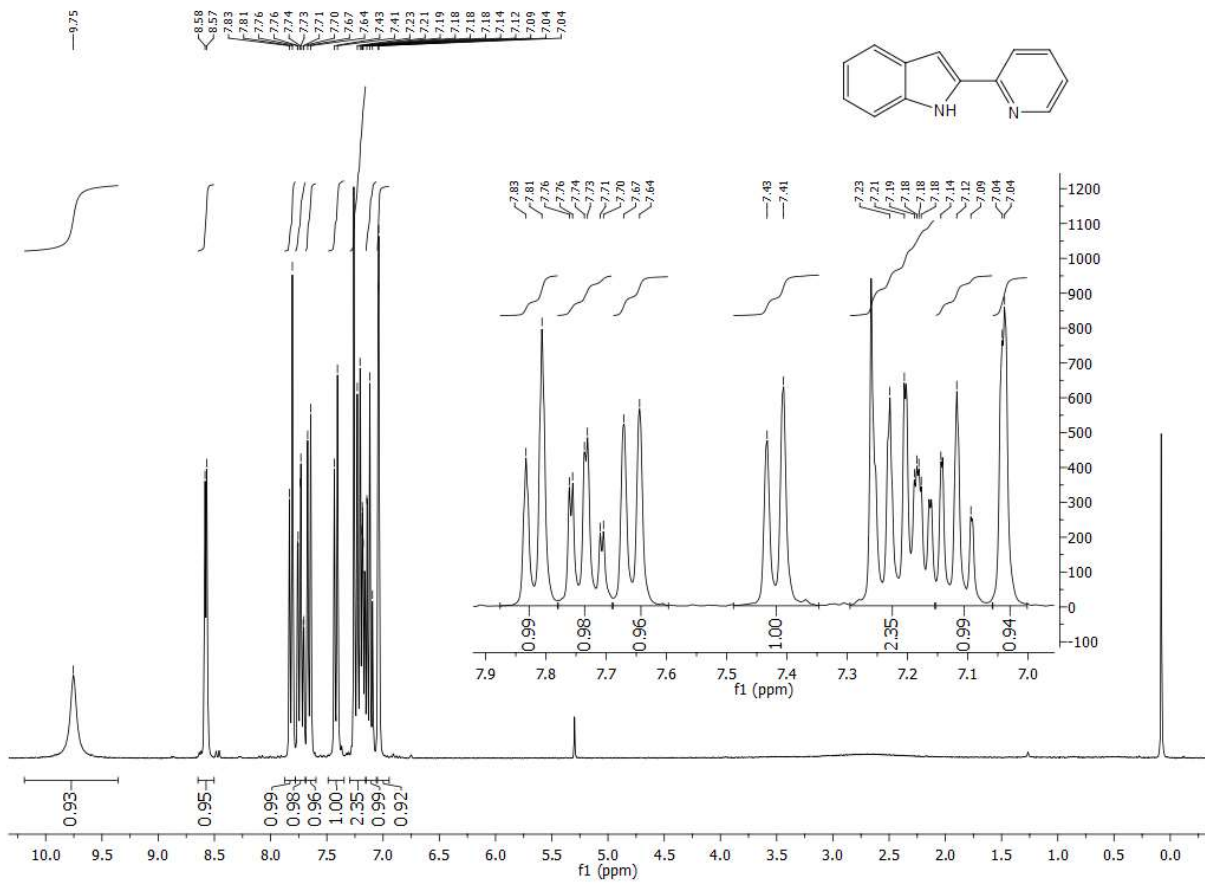


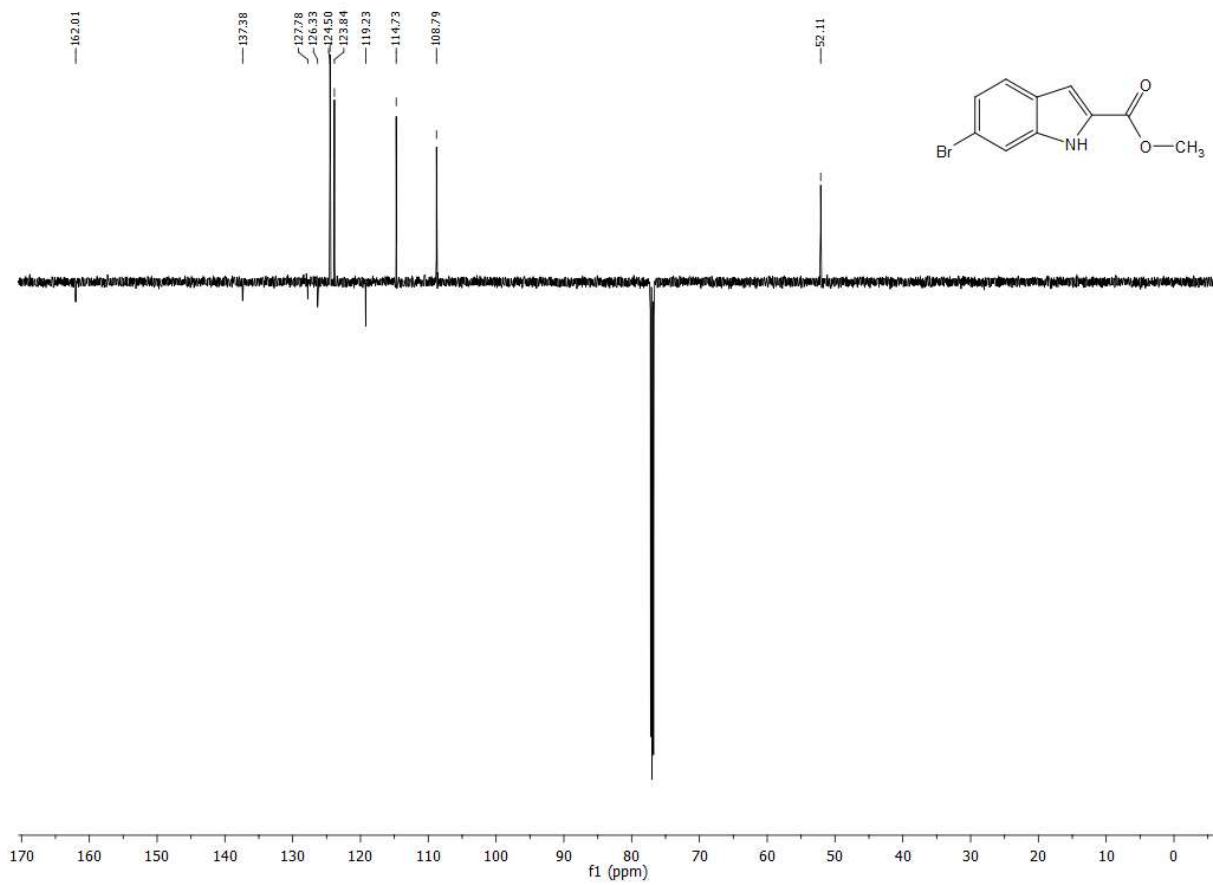
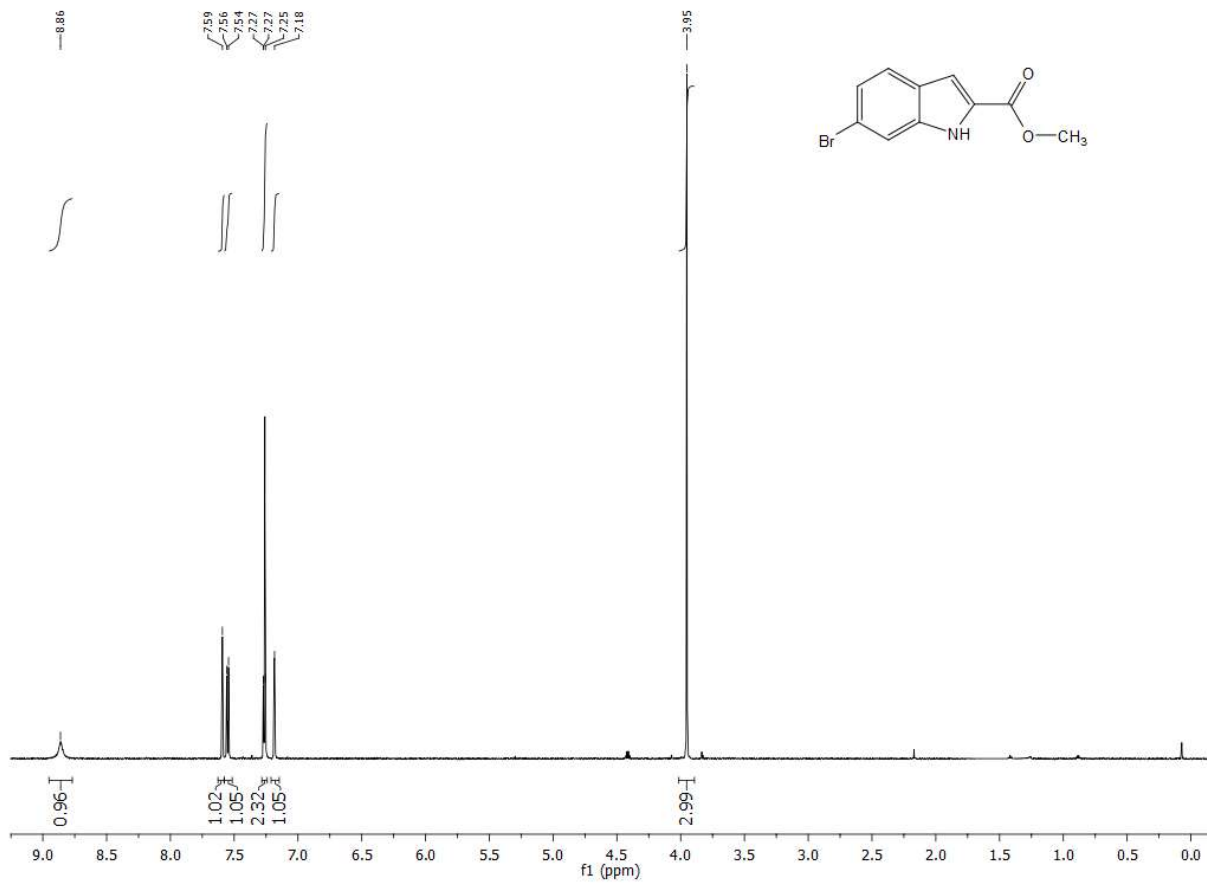


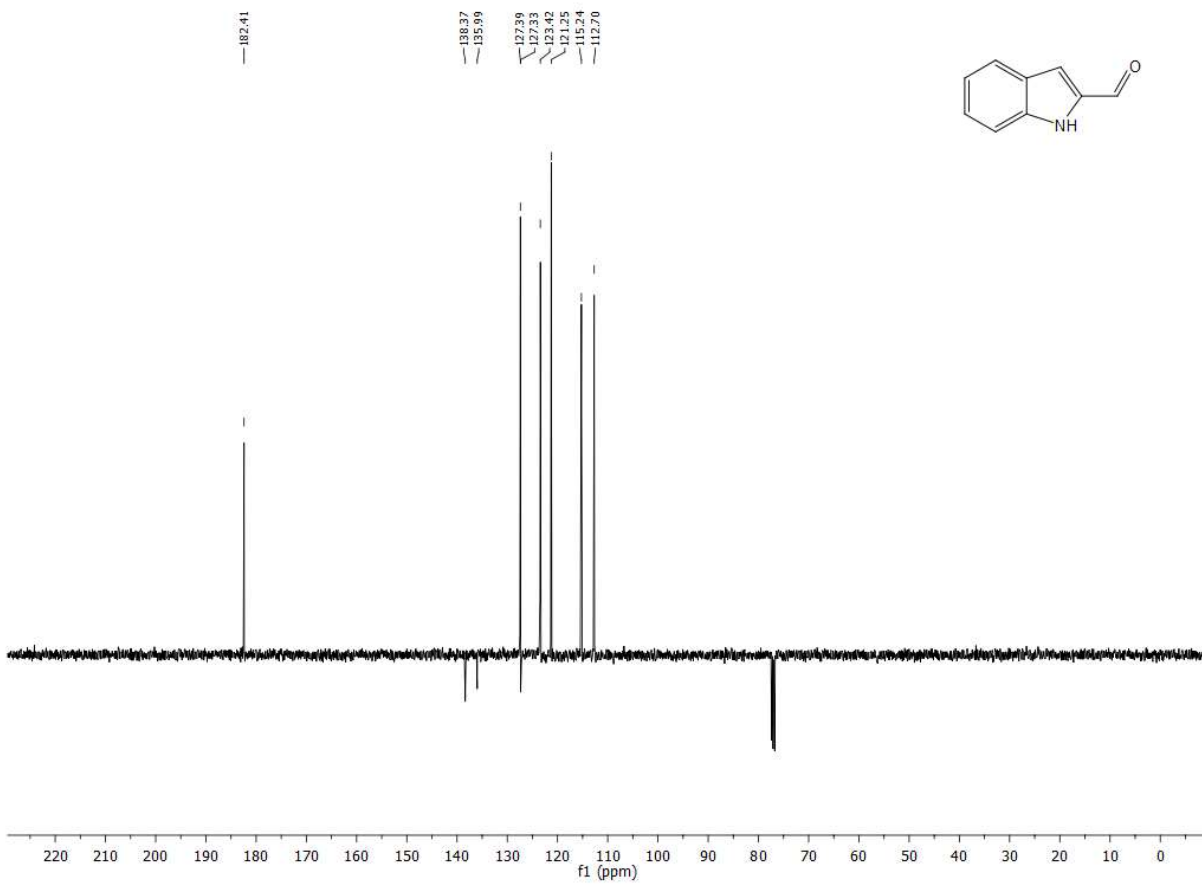
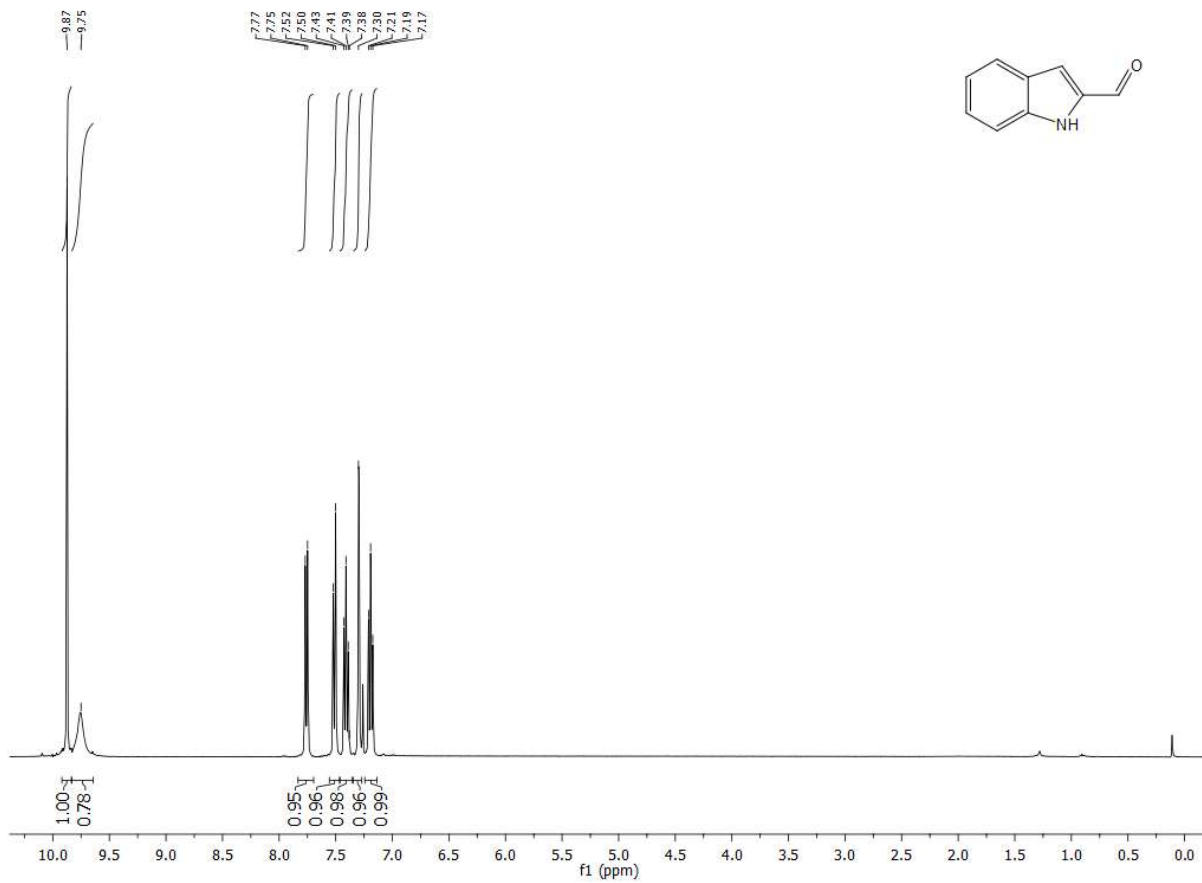


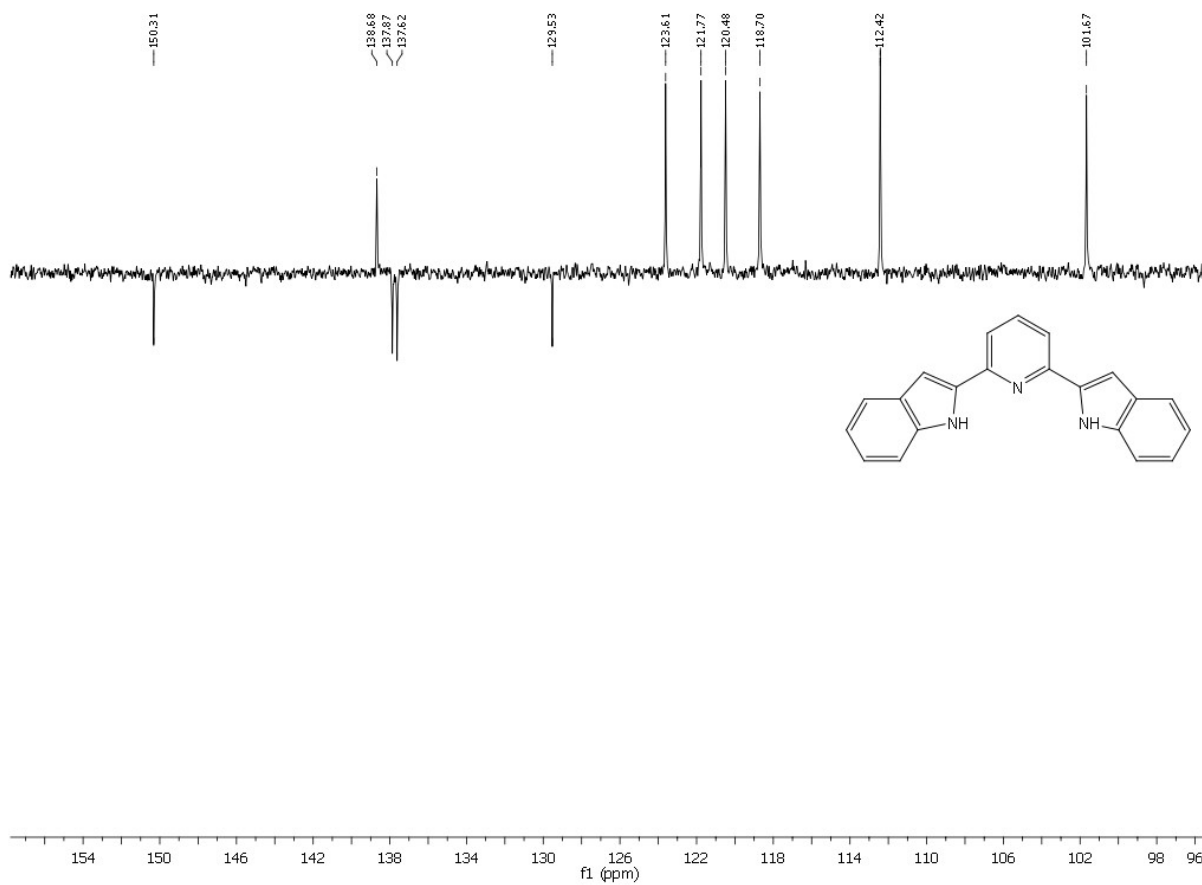
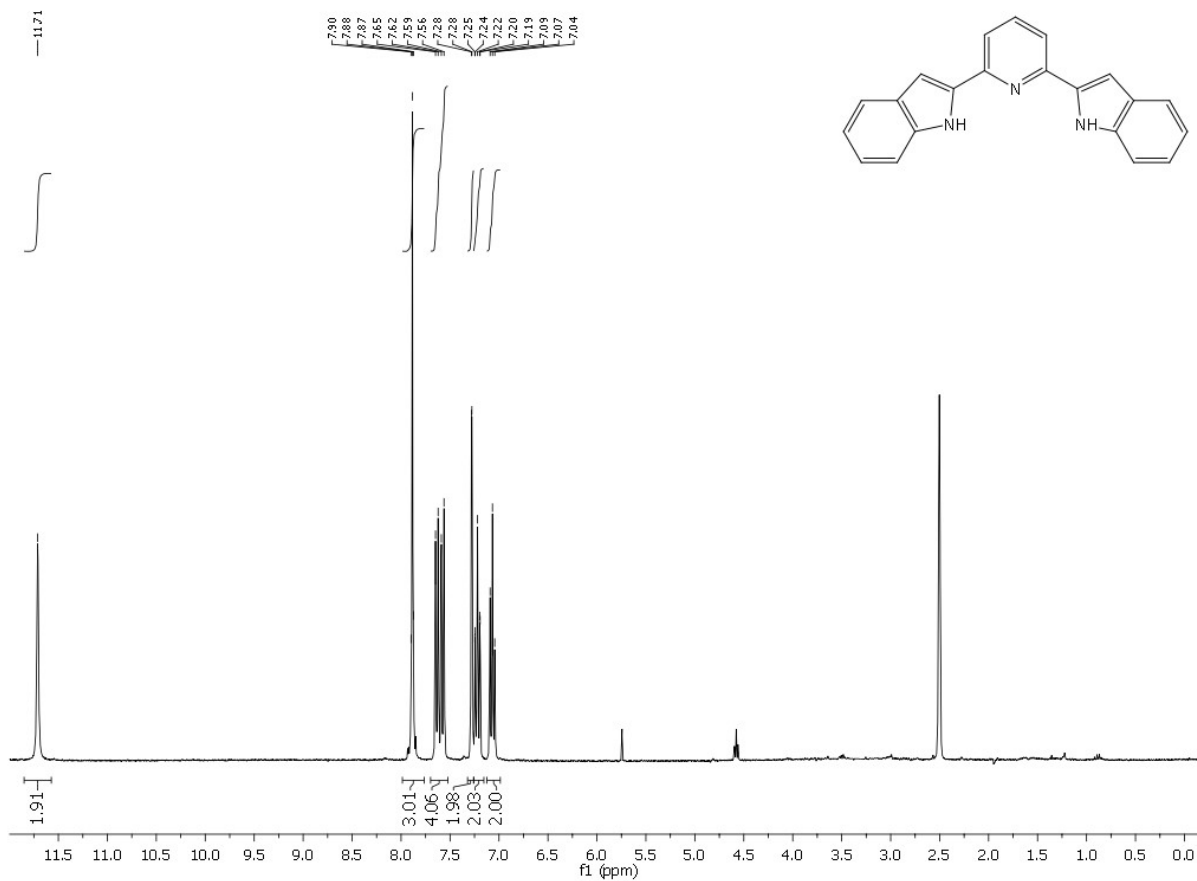


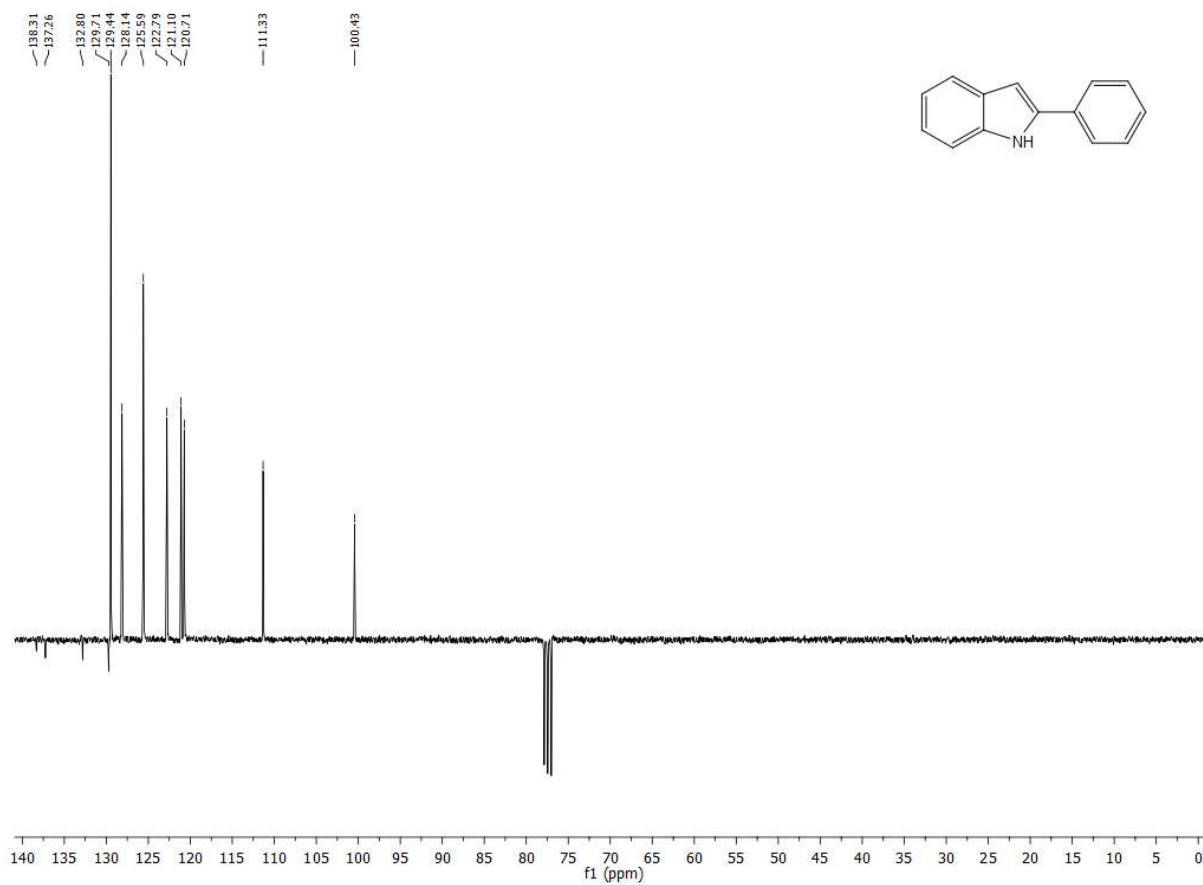
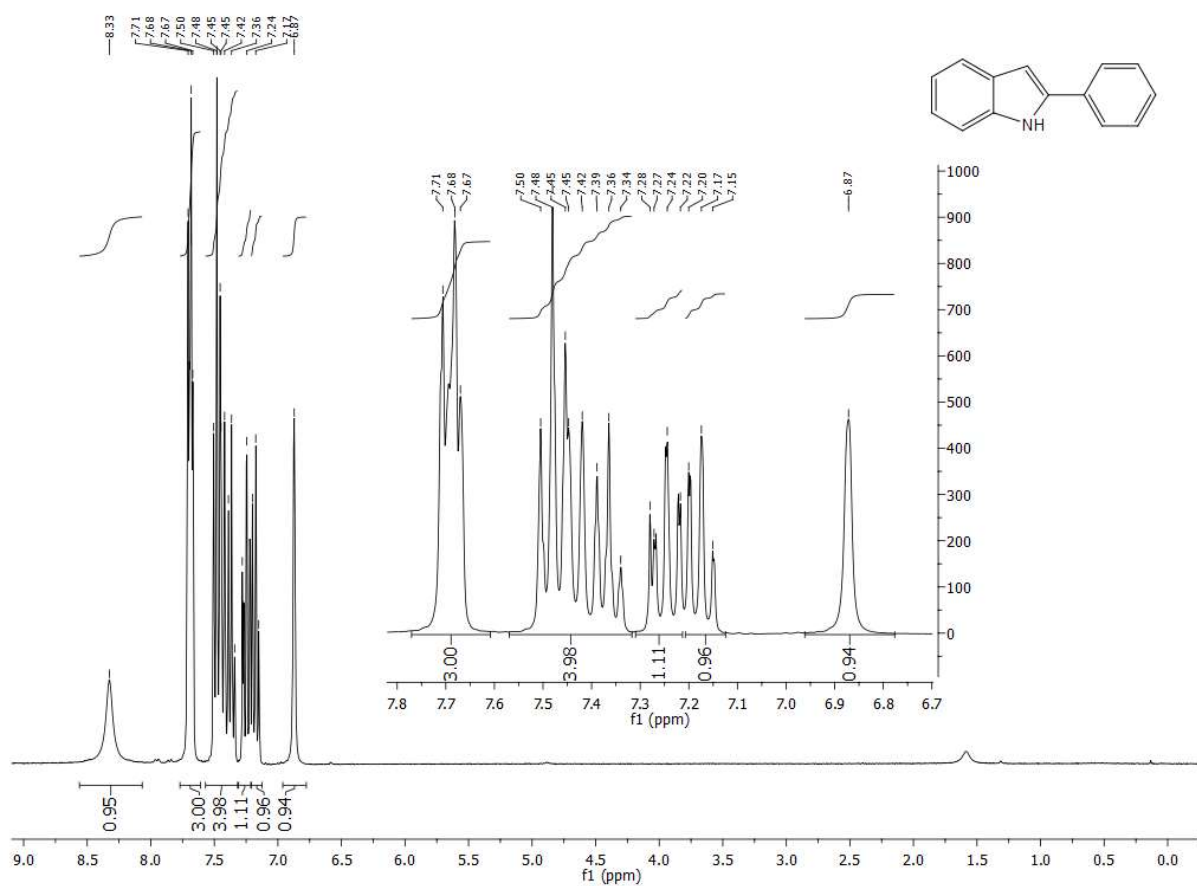


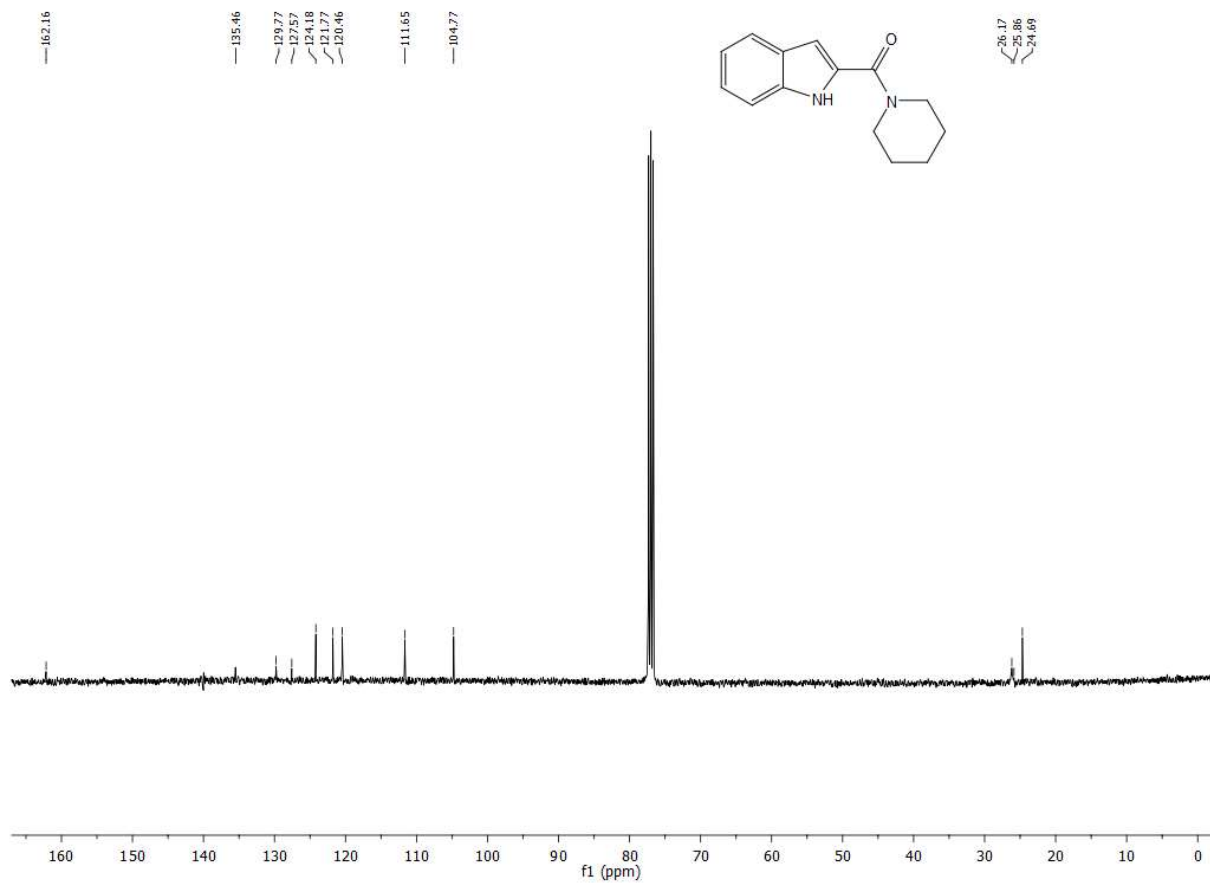
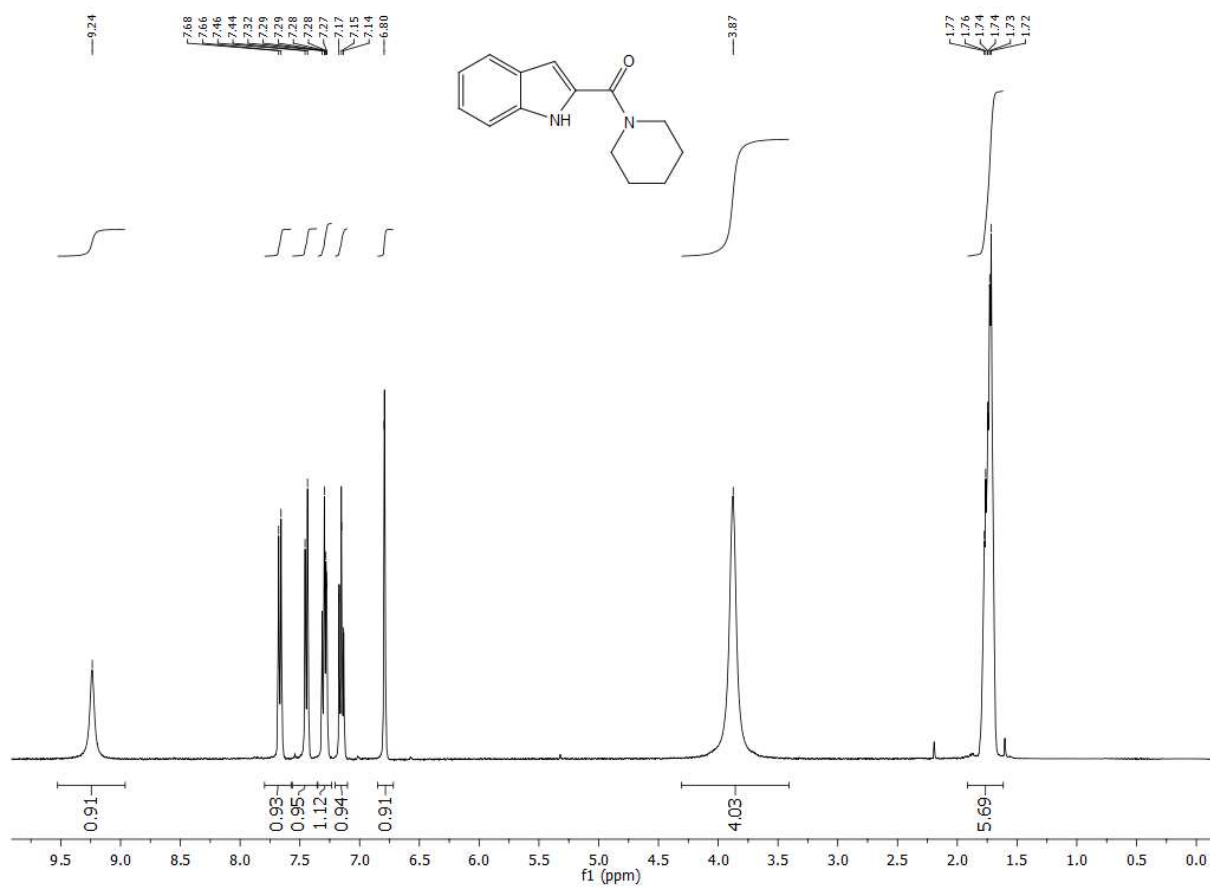


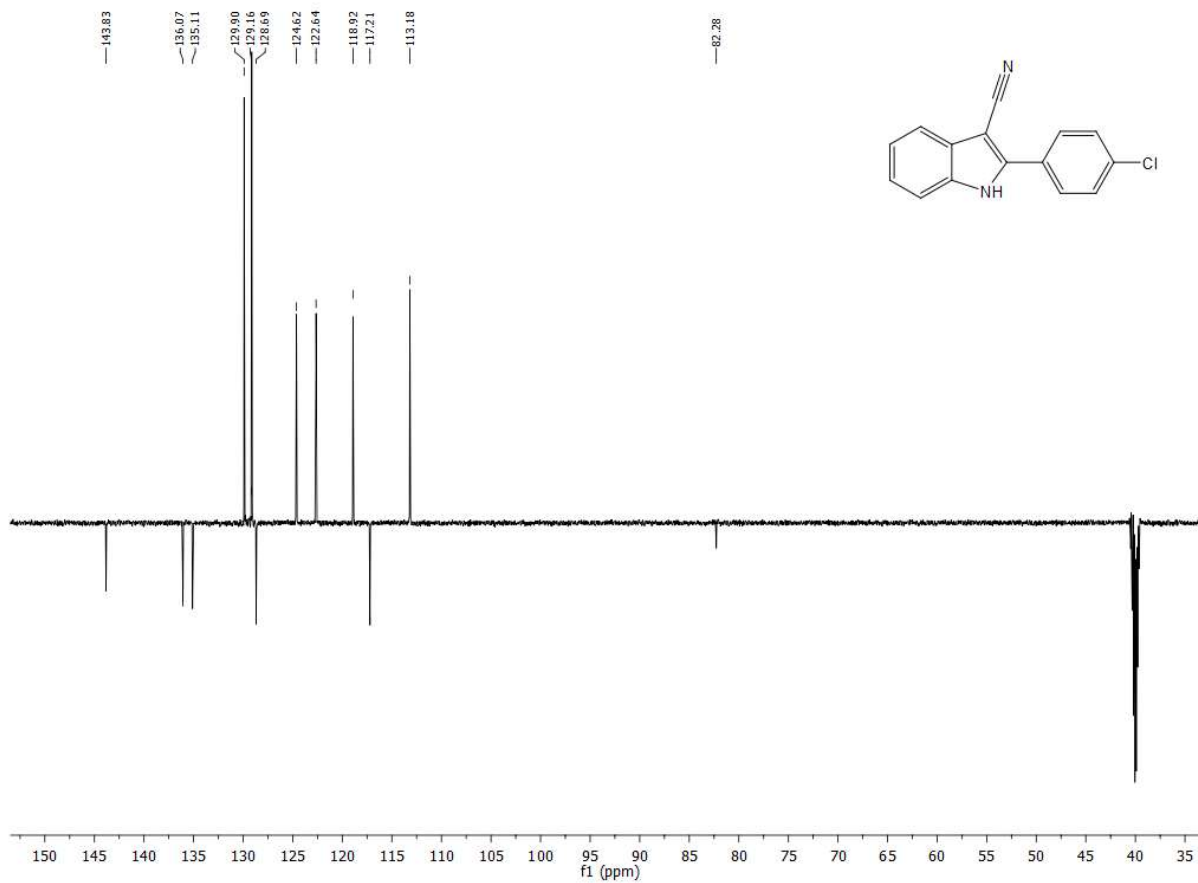
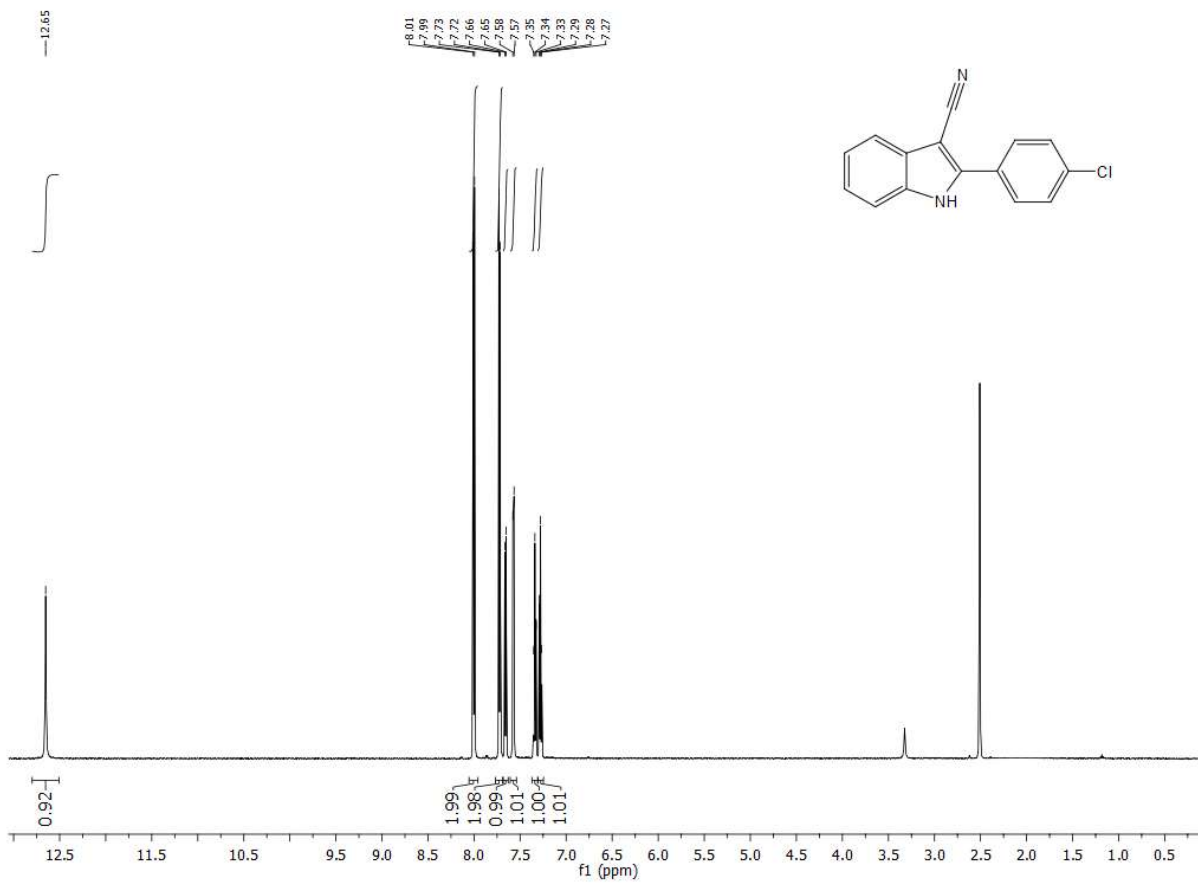


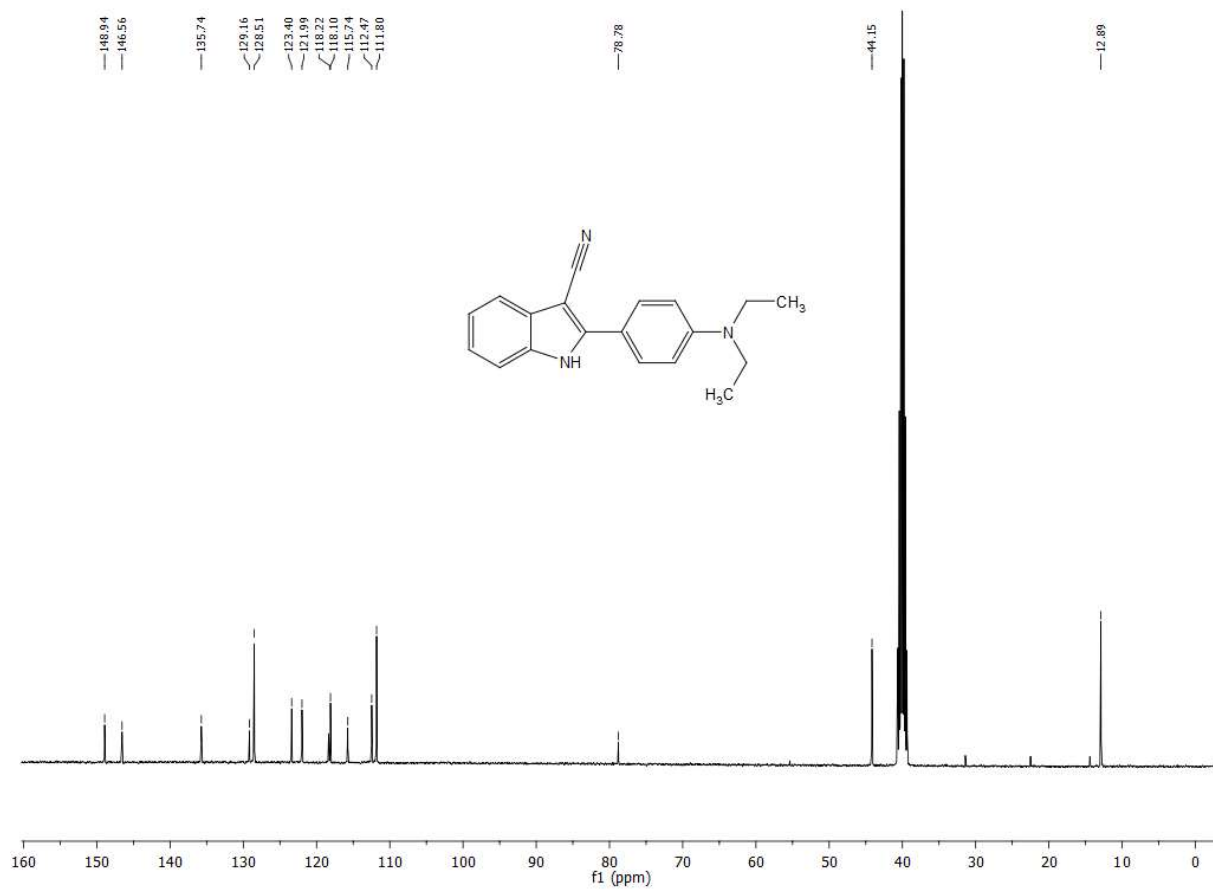
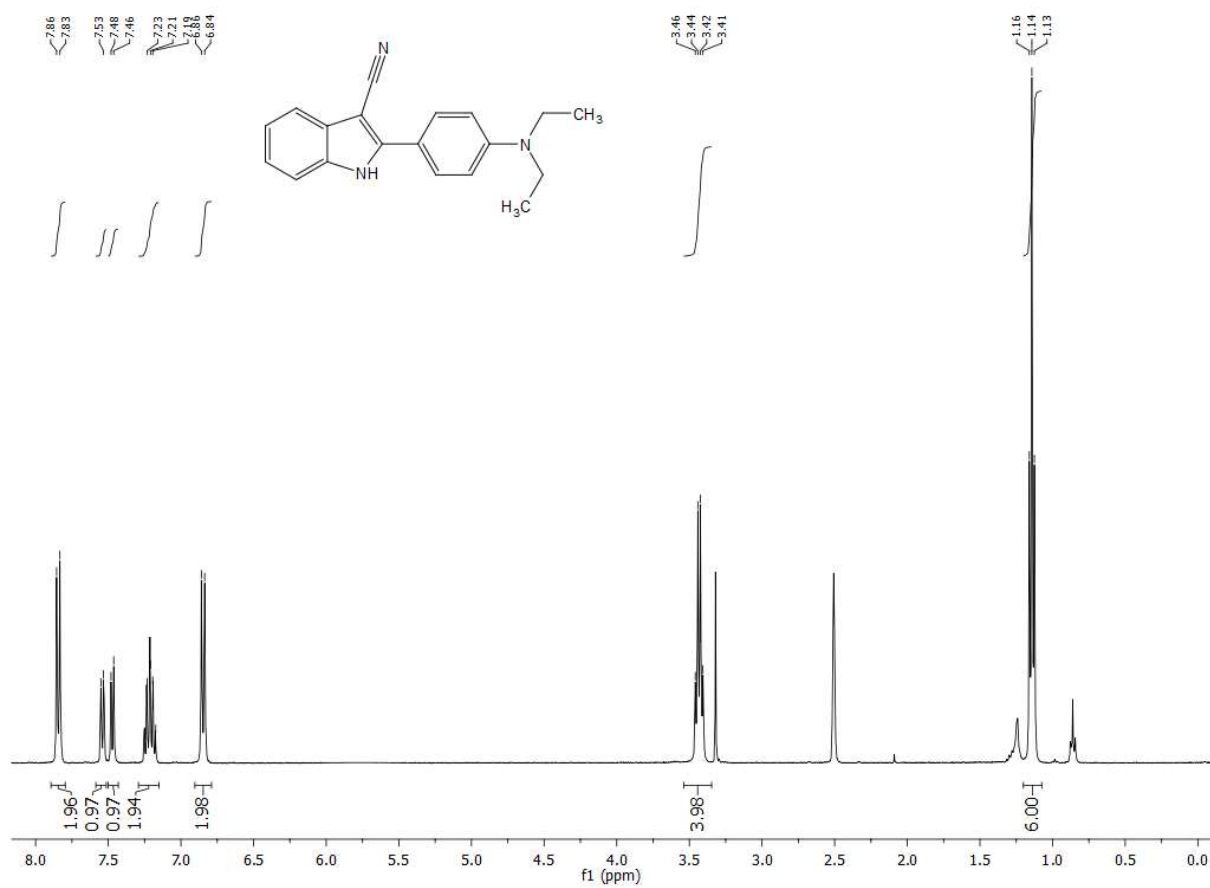


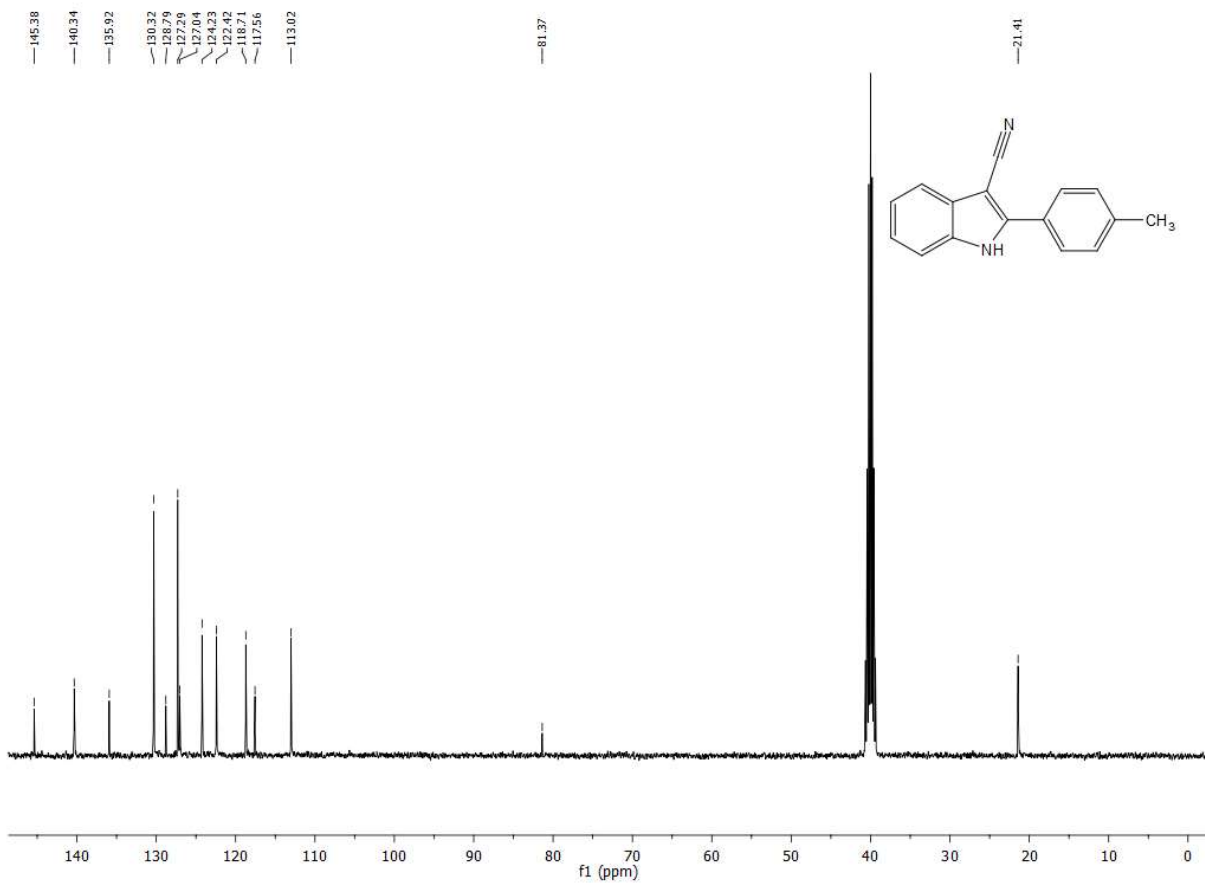
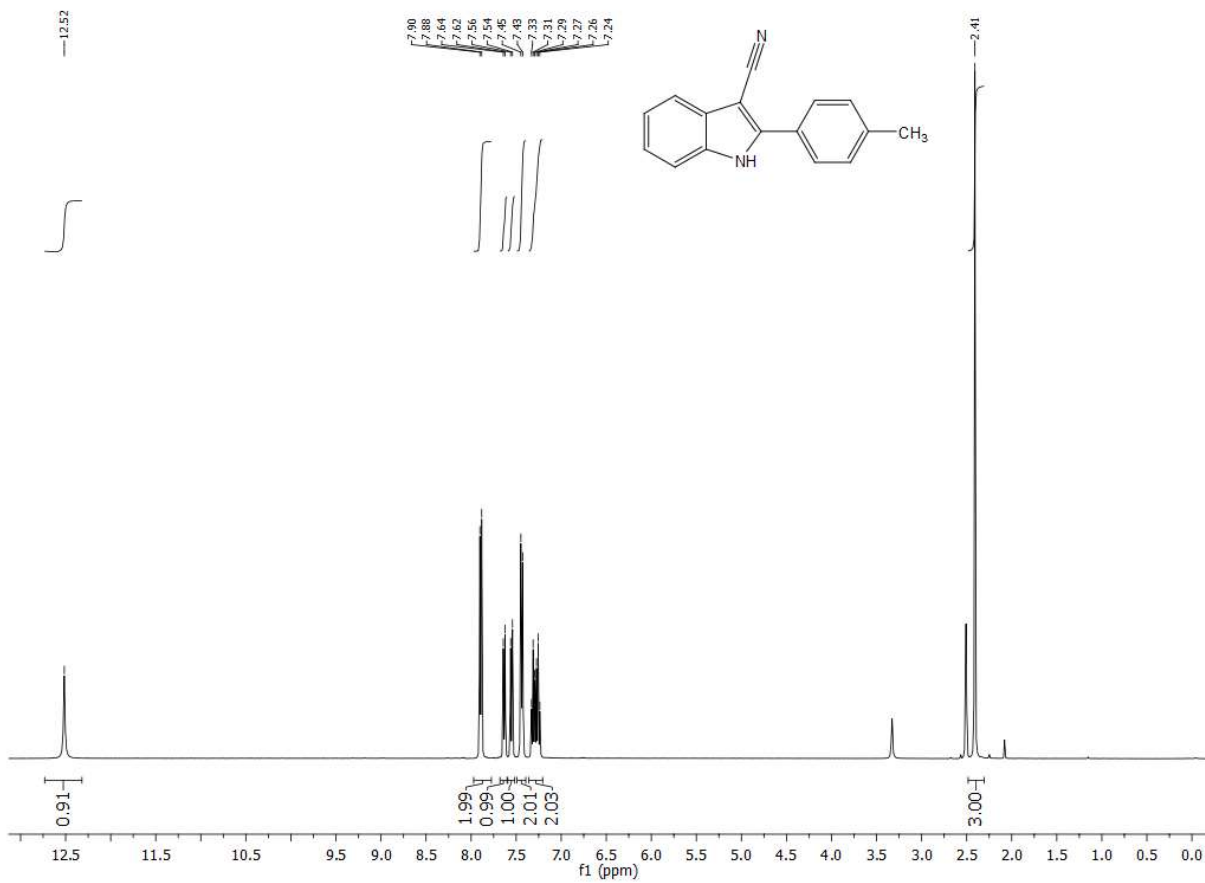


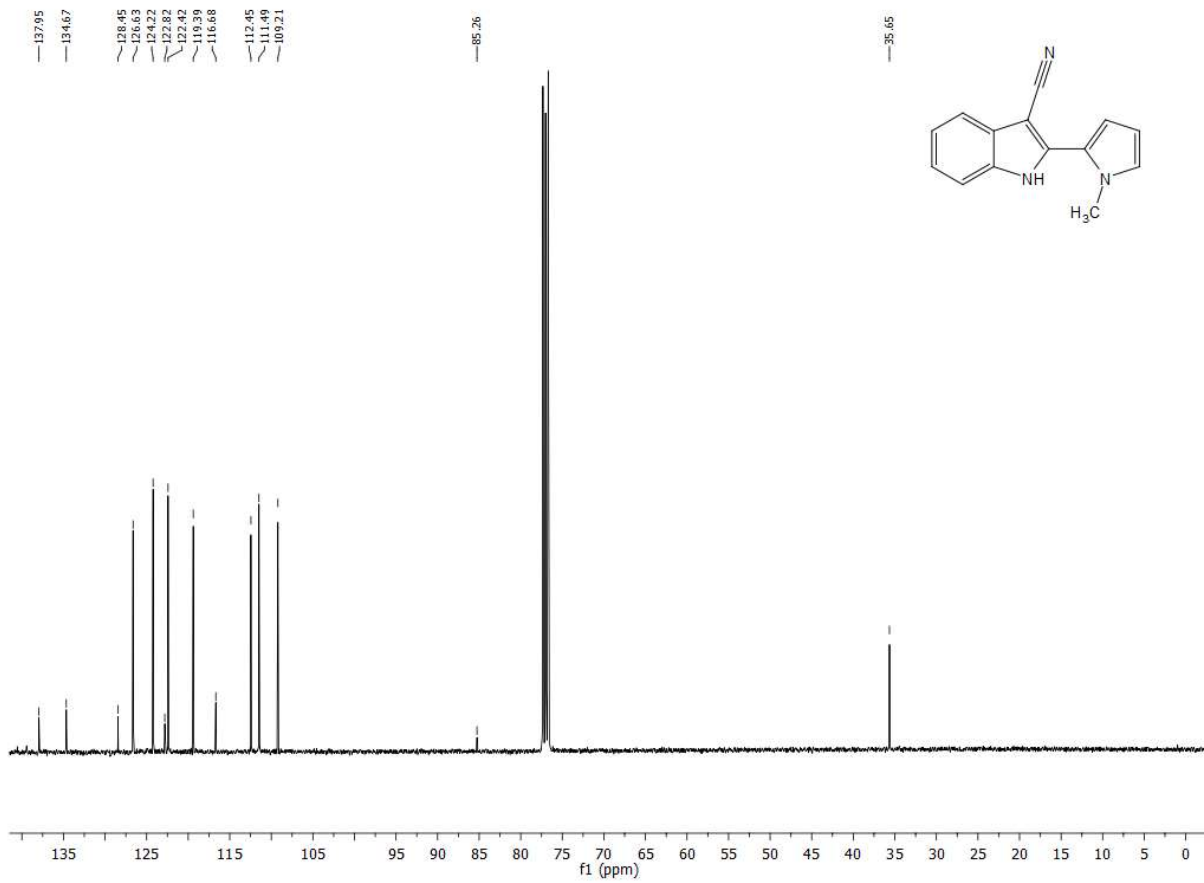
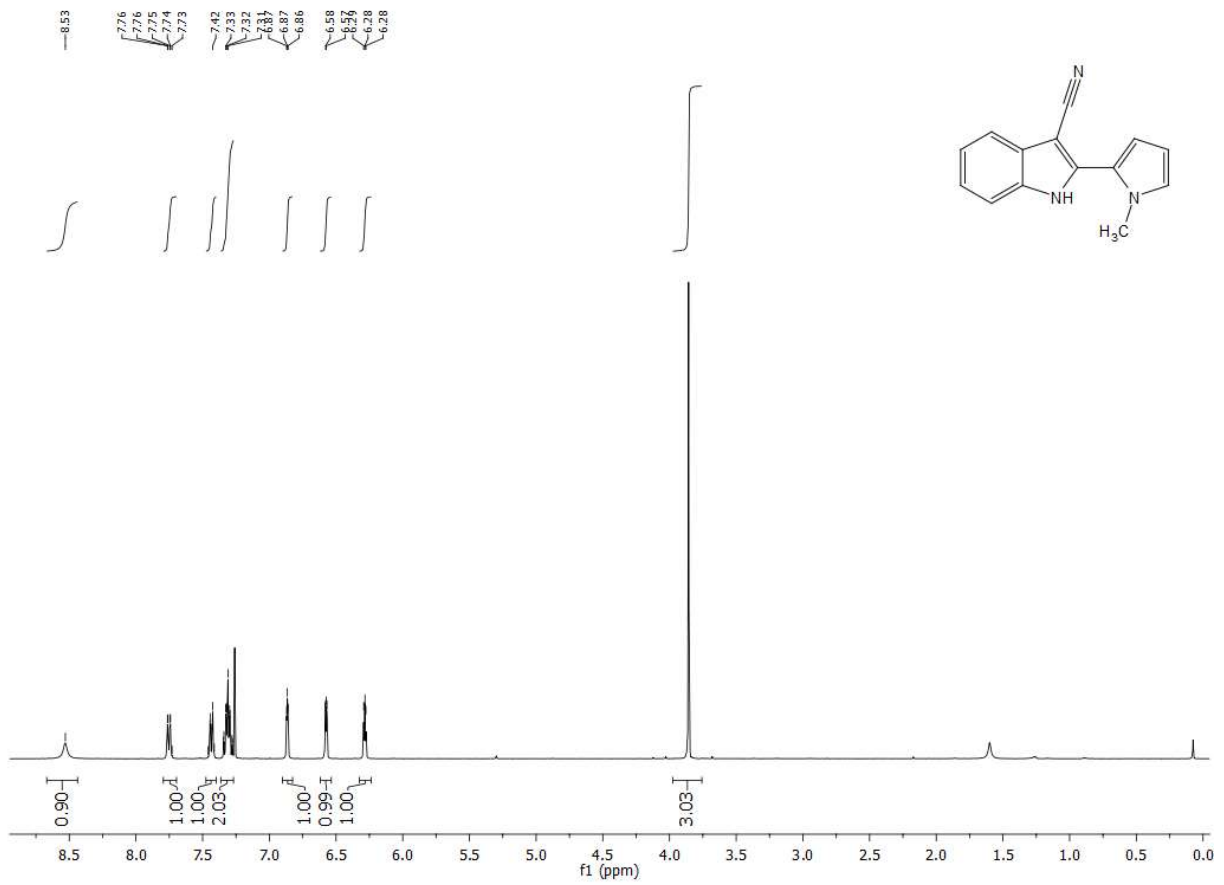


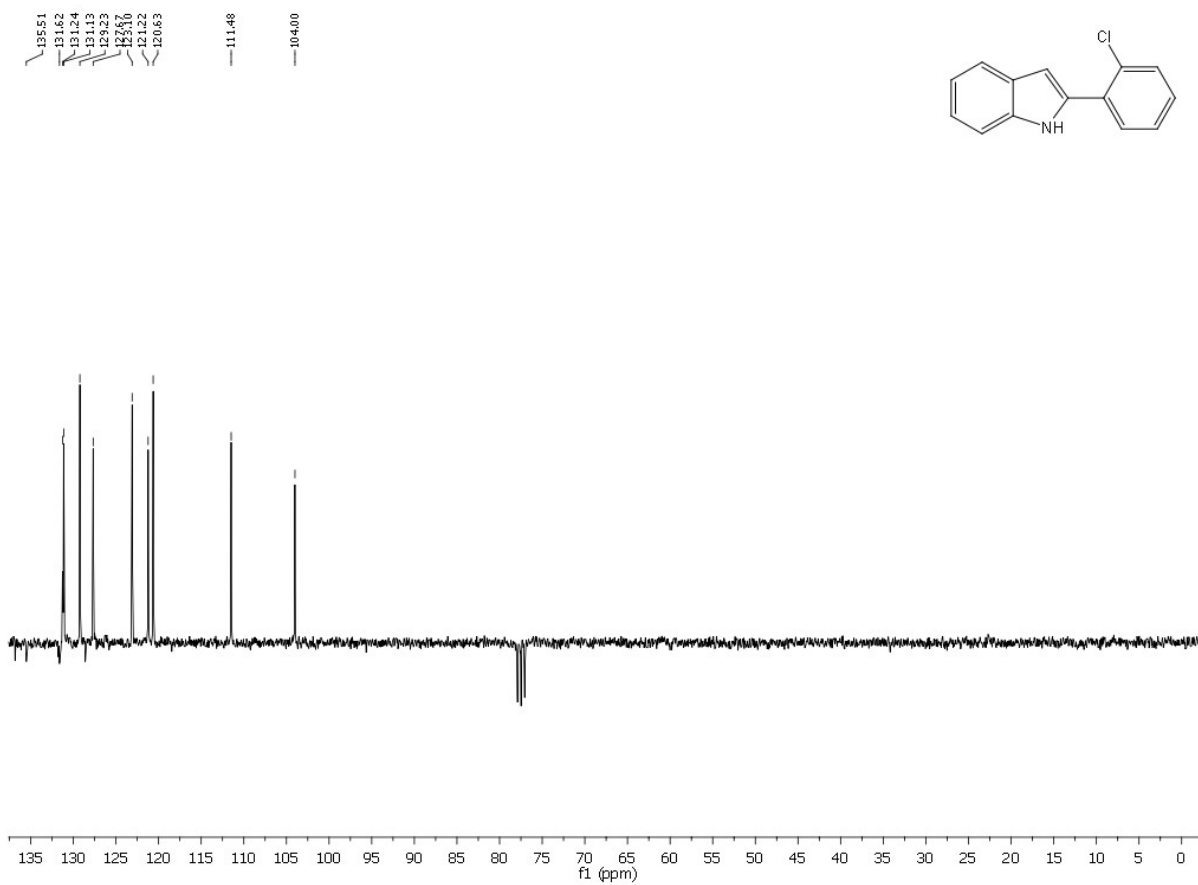
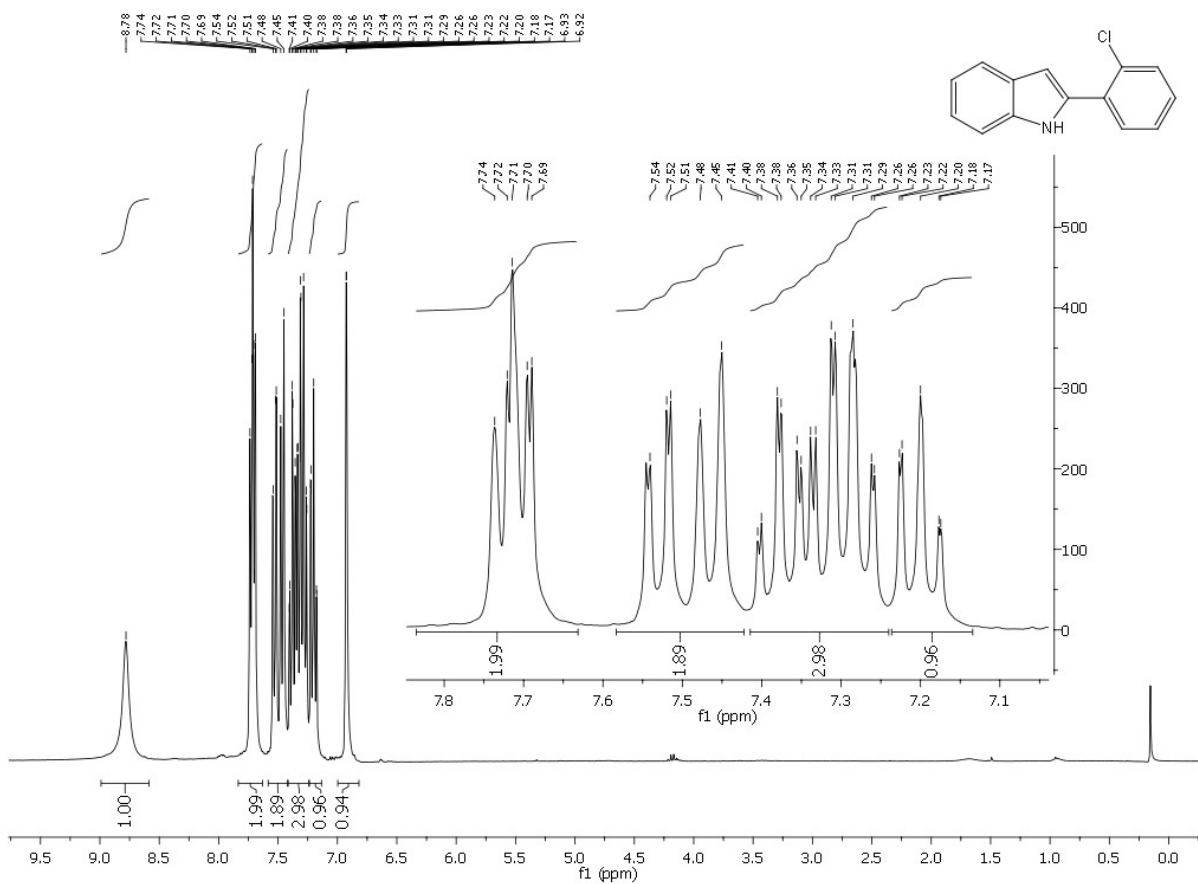


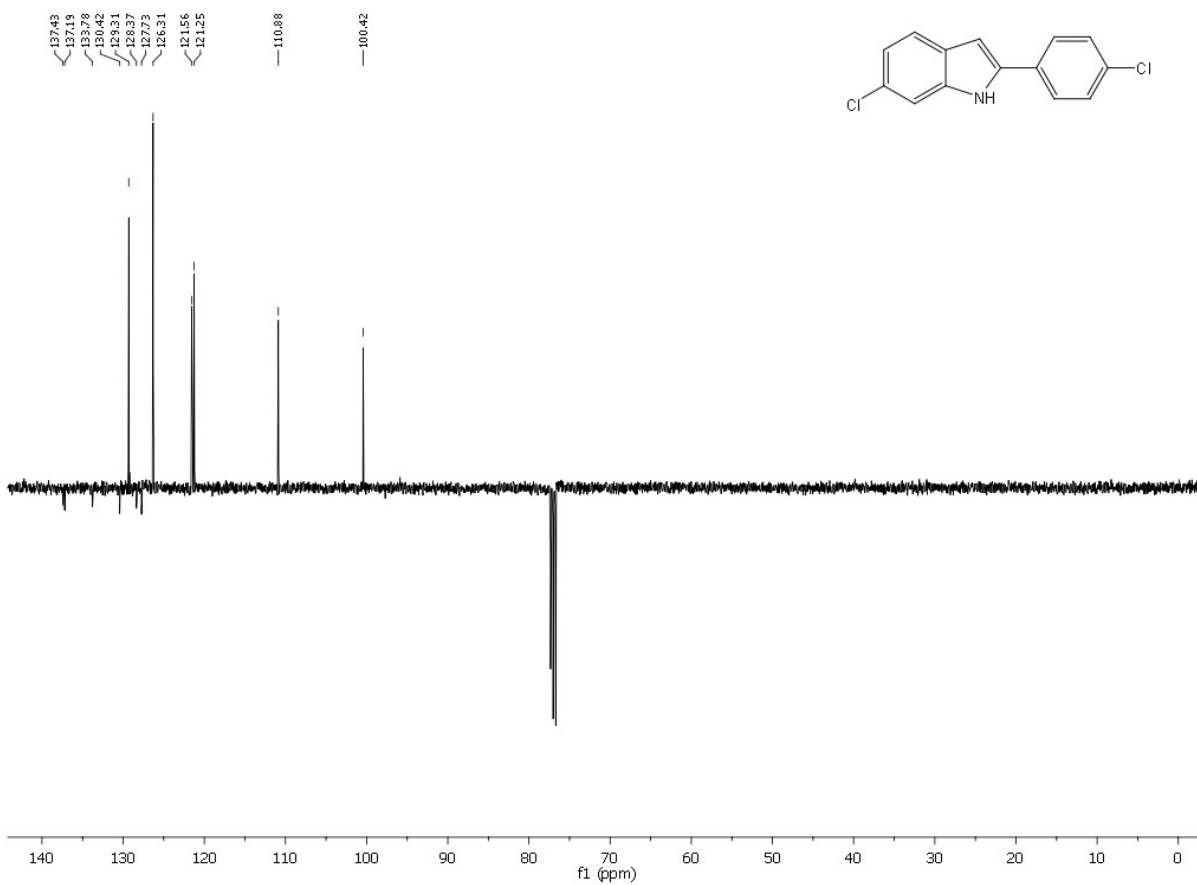
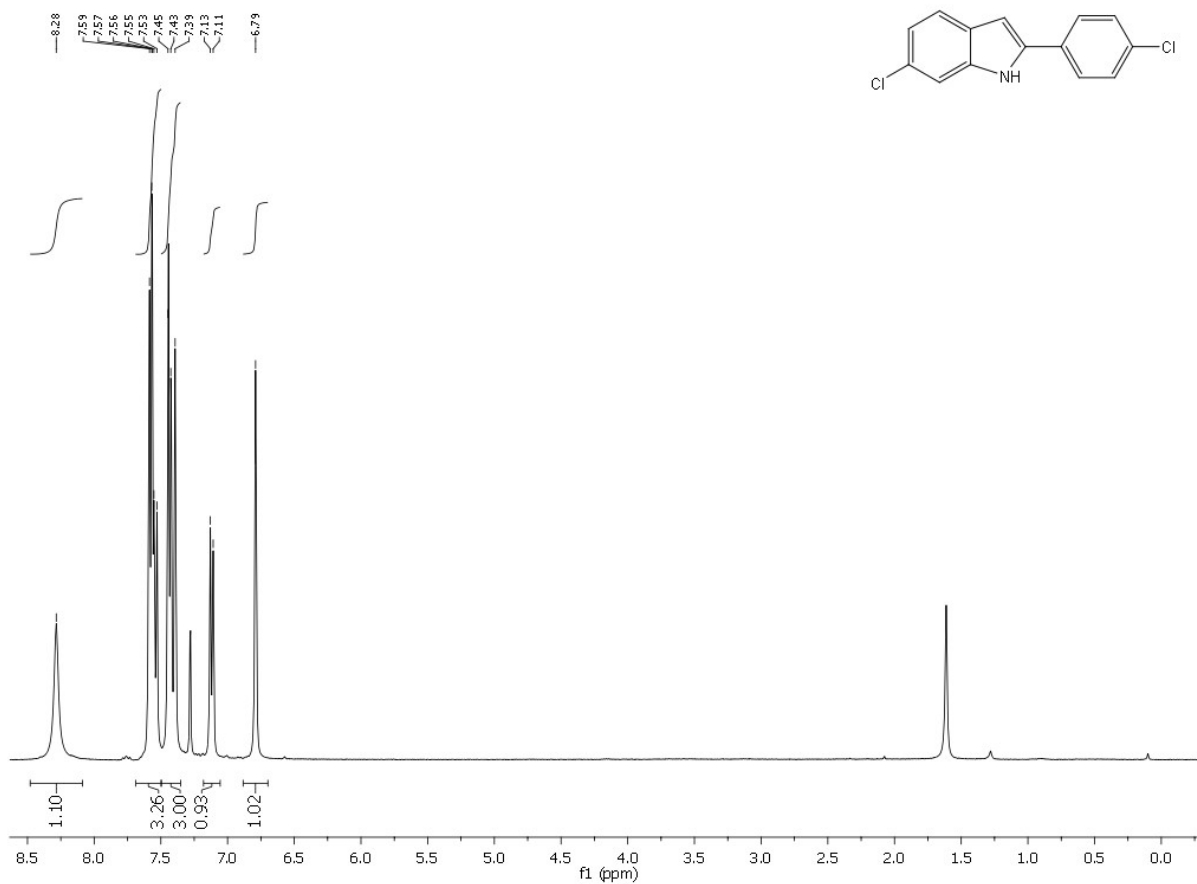


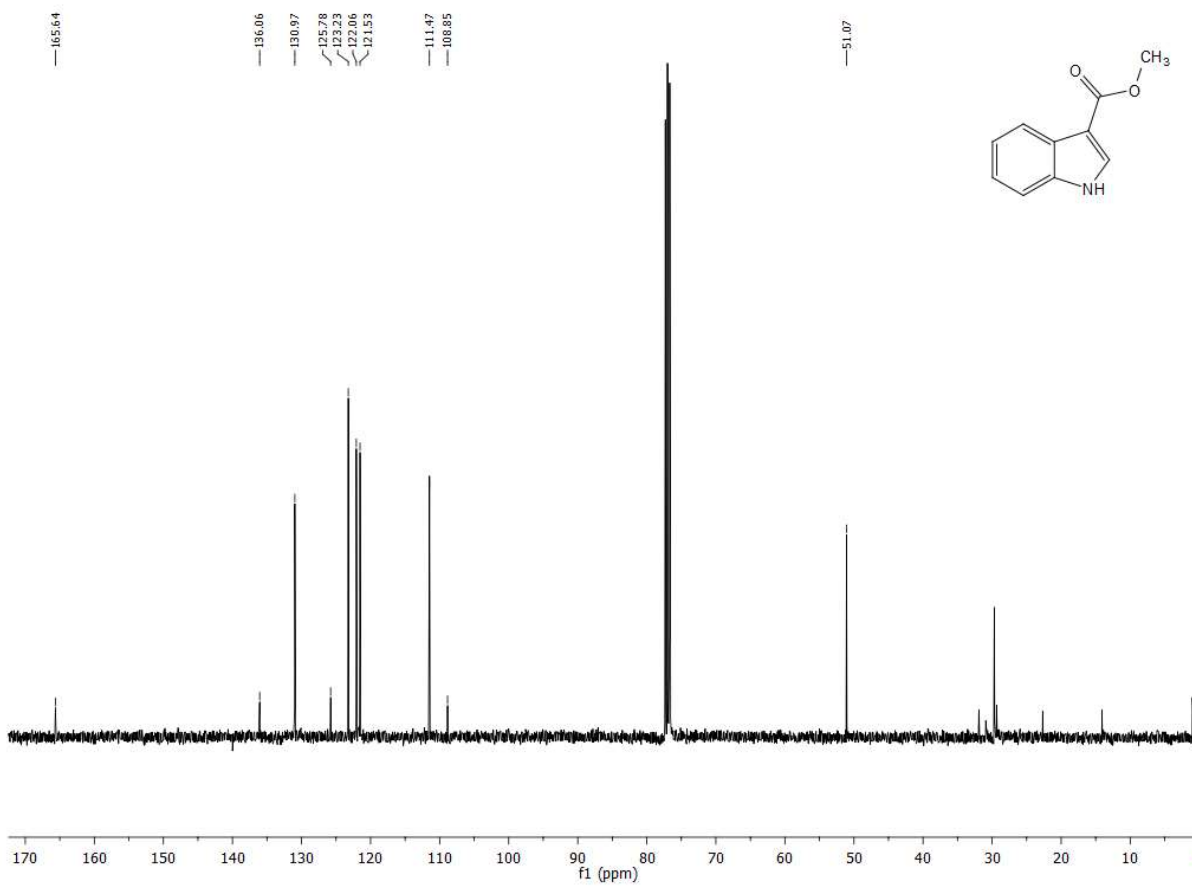
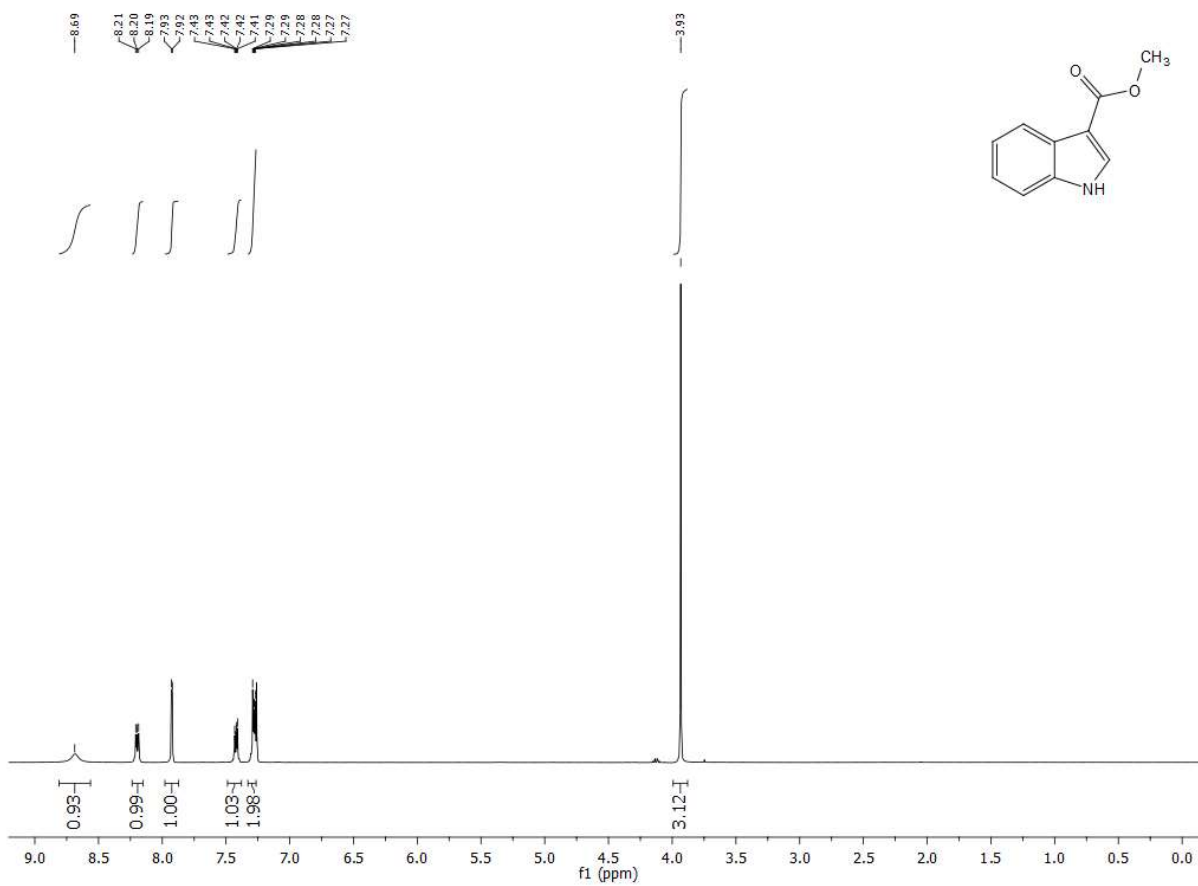


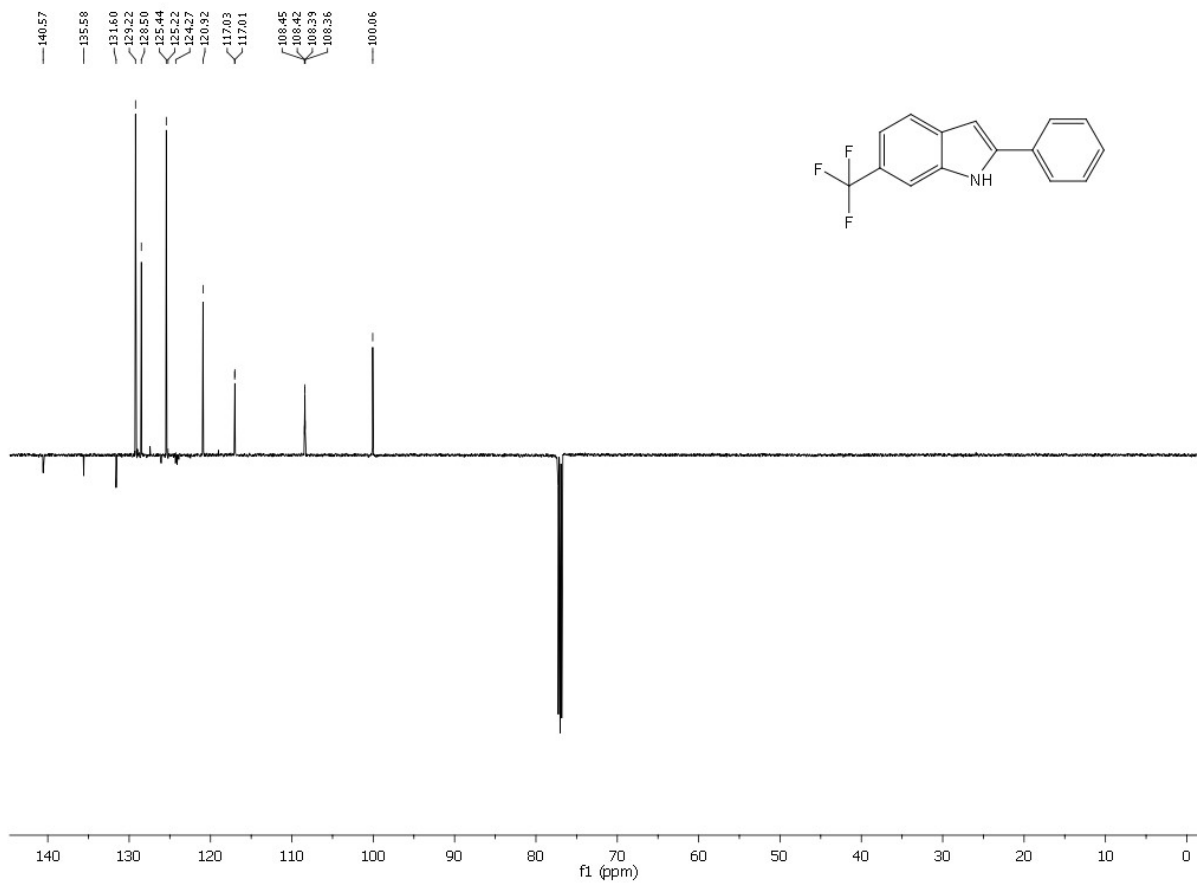
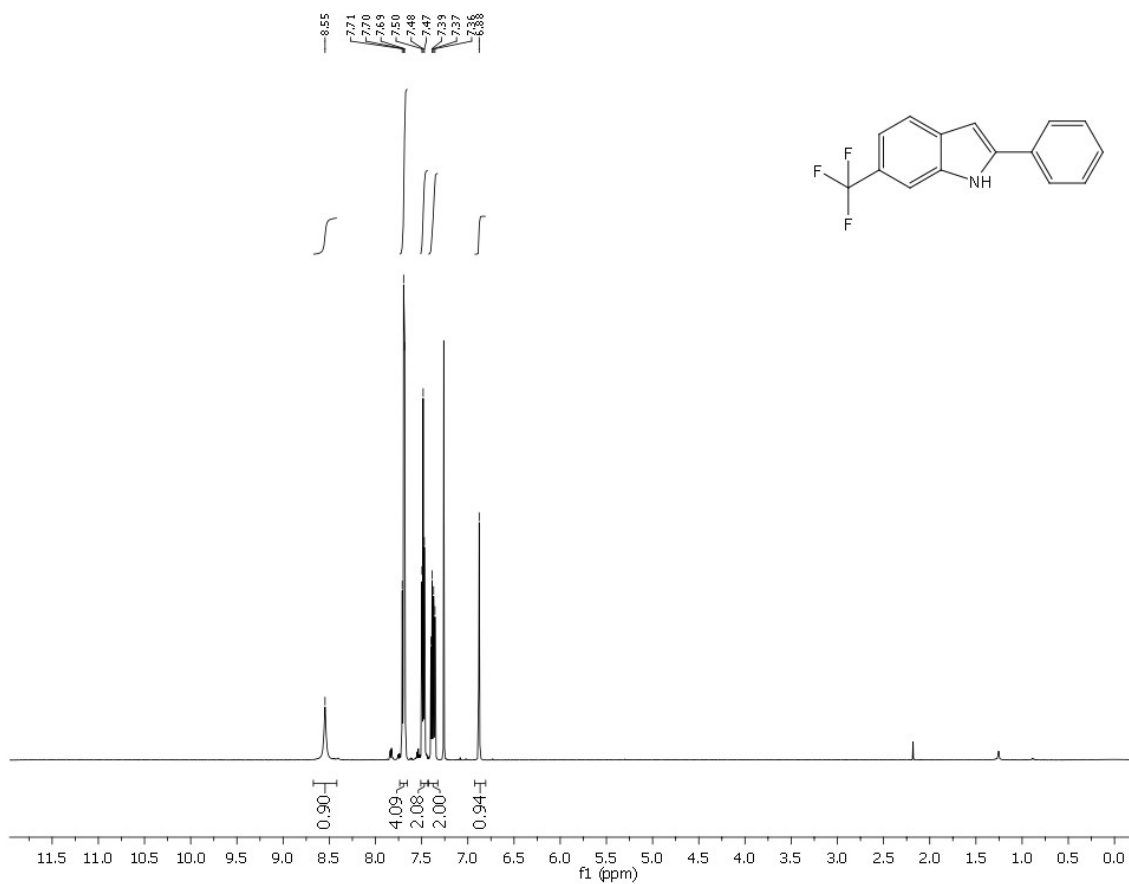


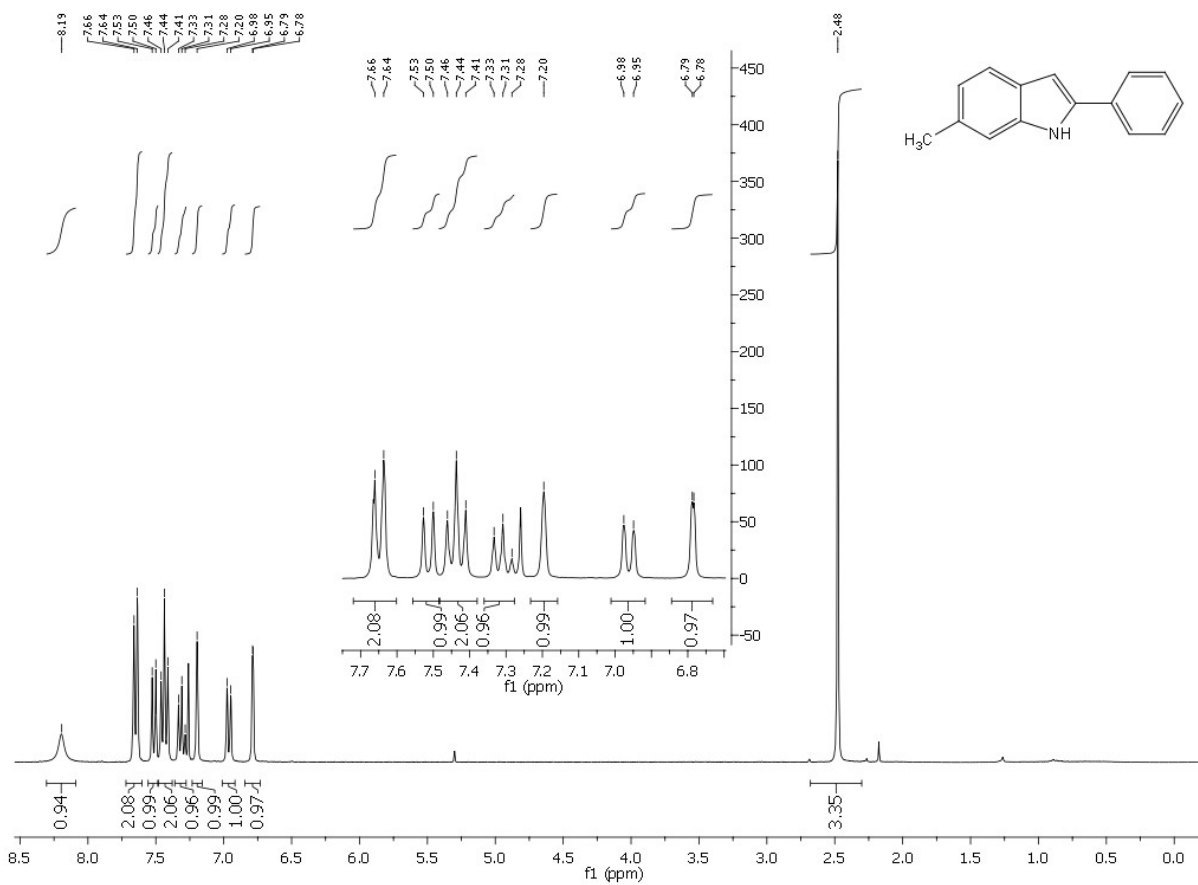
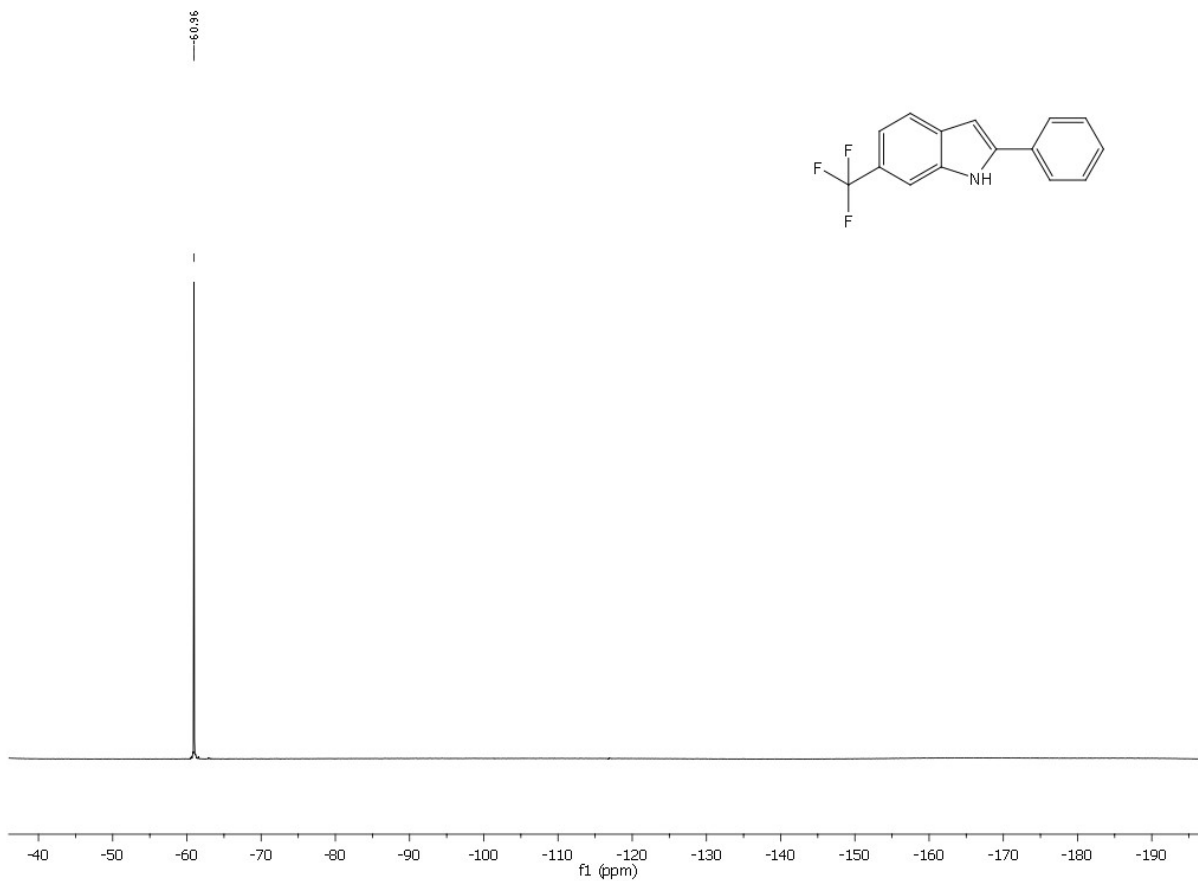


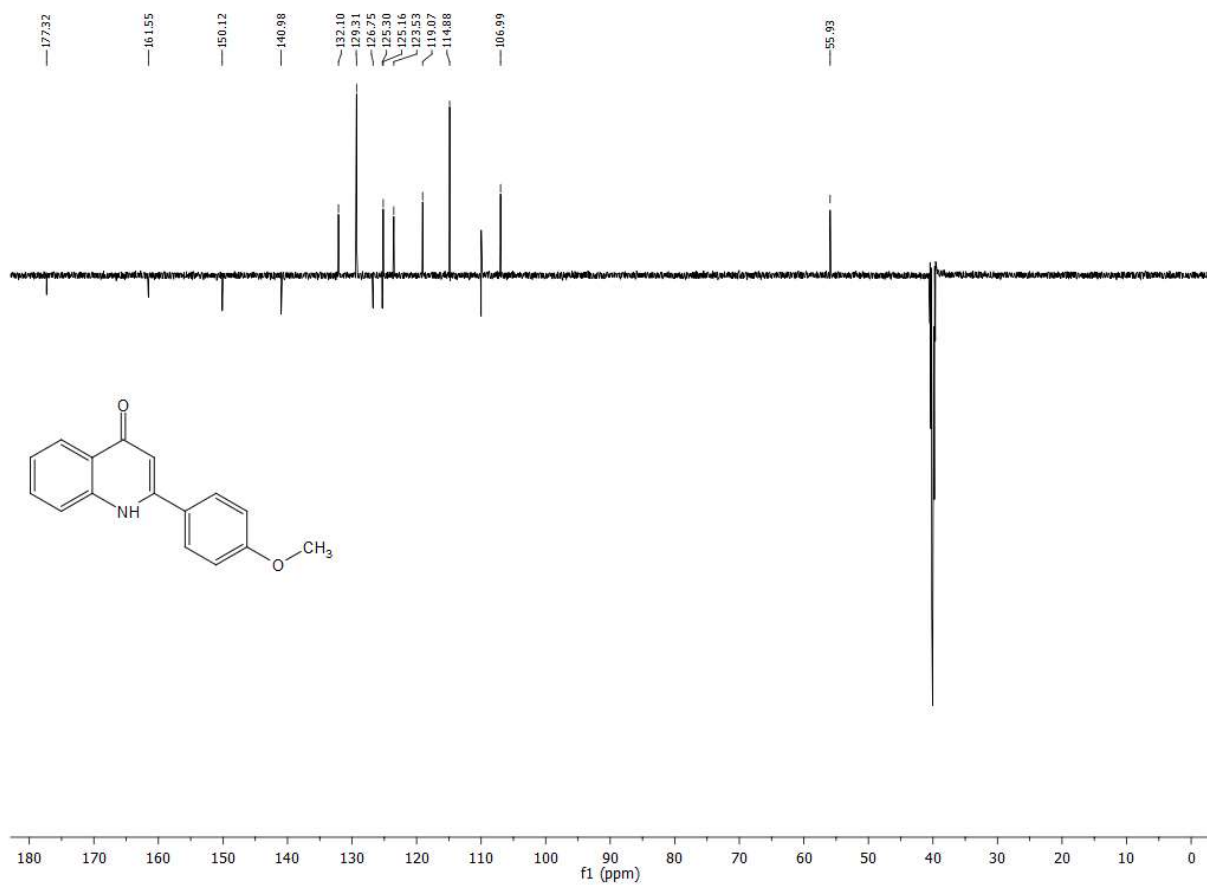
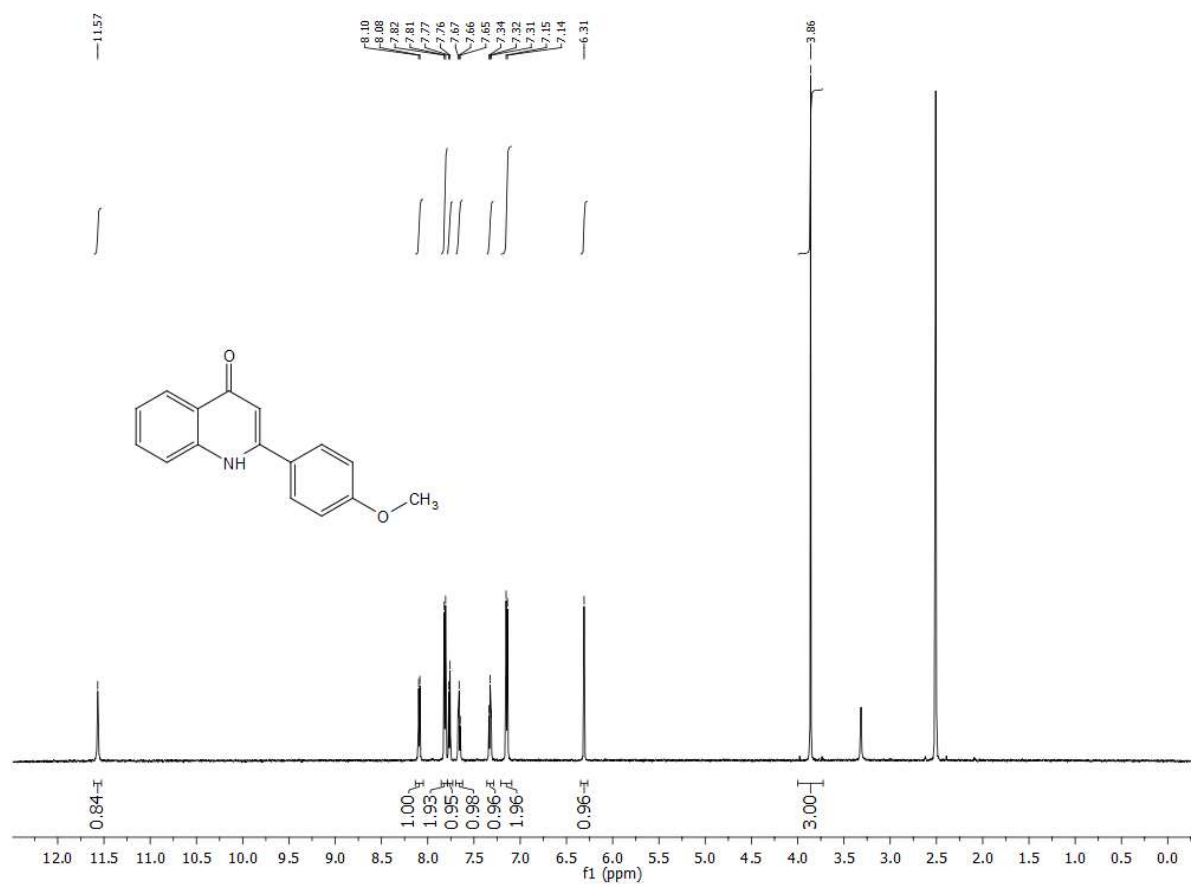












- [1] A. M. Tafesh, J. Weiguny, *Chem. Rev.* **1996**, *96*, 2035-2052.
- [2] (a) N. Vemula, A. C. Stevens, T. B. Schon, B. L. Pagenkopf, *Chem. Commun.* **2014**, *50*, 1668-1670; (b) I. Chatterjee, R. Fröhlich, A. Studer, *Angew. Chem. Int. Ed.* **2011**, *50*, 11257-11260; (c) S. Chakrabarty, I. Chatterjee, L. Tebben, A. Studer, *Angew. Chem. Int. Ed.* **2013**, *52*, 2968-2971; (d) R. Han, J. Qi, J. Gu, D. Ma, X. Xie, X. She, *ACS Catal.* **2013**, *3*, 2705-2709; (e) Y. Li, S. Chakrabarty, A. Studer, *Angew. Chem. Int. Ed.* **2015**, *54*, 3587-3591; (f) W. Adam, O. Krebs, *Chem. Rev.* **2003**, *103*, 4131-4146; (g) T. L. Gilchrist, *Chem. Soc. Rev.* **1983**, *12*, 53-73.
- [3] (a) T. B. Nguyen, K. Pasturaud, L. Ermolenko, A. Al-Mourabit, *Org. Lett.* **2015**, *17*, 2562-2565; (b) T. Guntreddi, R. Vanjari, K. N. Singh, *Org. Lett.* **2015**, *17*, 976-978.
- [4] (a) R. Umeda, T. Mashino, Y. Nishiyama, *Tetrahedron* **2014**, *70*, 4395-4399; (b) X. Wu, Z. Yu, *Tetrahedron Lett.* **2010**, *51*, 1500-1503.
- [5] D. Sawant, R. Kumar, P. R. Maulik, B. Kundu, *Org. Lett.* **2006**, *8*, 1525-1528.
- [6] F. Sun, X. Feng, X. Zhao, Z.-B. Huang, D.-Q. Shi, *Tetrahedron* **2012**, *68*, 3851-3855.
- [7] (a) P. J. Bunyan, J. I. G. Cadogan, *Journal of the Chemical Society (Resumed)* **1963**, 42-49; (b) N. E. Genung, L. Wei, G. E. Aspnes, *Org. Lett.* **2014**, *16*, 3114-3117; (c) J. Duchek, A. Vasella, *Helv. Chim. Acta* **2011**, *94*, 977-986; (d) A. W. Freeman, M. Urvoy, M. E. Criswell, *J. Org. Chem.* **2005**, *70*, 5014-5019; (e) B. Li, J. D. Williams, N. P. Peet, *Tetrahedron Lett.* **2013**, *54*, 3124-3126.
- [8] P. Du, J. L. Brosmer, D. G. Peters, *Org. Lett.* **2011**, *13*, 4072-4075.
- [9] (a) S. Tong, Z. Xu, M. Mamboury, Q. Wang, J. Zhu, *Angew. Chem. Int. Ed.* **2015**, *54*, 11809-11812; (b) K. Yang, F. Zhou, Z. Kuang, G. Gao, T. G. Driver, Q. Song, *Org. Lett.* **2016**, *18*, 4088-4091.
- [10] For reviews in the field see: (a) F. Ragaini, S. Cenini, E. Gallo, A. Caselli, S. Fantauzzi, *Curr. Org. Chem.* **2006**, *10*, 1479-1510; (b) F. Ragaini, S. Cenini, in *Catalytic Reductive Carbonylation of Organic Nitro Compounds* (Eds.: D. Cole-Hamilton, P. v. Leeuwen), Kluwer Academic Publisher, **1997**, pp. 177-243; (c) B. J. Stokes, T. G. Driver, *Eur. J. Org. Chem.* **2011**, *2011*, 4071-4088; (d) J. Jiao, K. Murakami, K. Itami, *ACS Catal.* **2016**, *6*, 610-633; (e) G. Palmisano, A. Penoni, M. Sisti, F. Tibiletti, S. Tollari, K. M. Nicholas, *Curr. Org. Chem.* **2010**, *14*, 2409-2441; (f) F. Ferretti, D. Formenti, F. Ragaini, *Rendiconti Lincei* **2016**, accepted manuscript.
- [11] For reviews in the field see: (a) T. Morimoto, K. Kakiuchi, *Angew. Chem. Int. Ed.* **2004**, *43*, 5580-5588; (b) L. R. Odell, F. Russo, M. Larhed, *Synlett* **2012**, *23*, 685-698; (c) H. Konishi, K. Manabe, *Synlett* **2014**, *25*, 1971-1986; (d) L. Wu, Q. Liu, R. Jackstell, M. Beller, *Angew. Chem. Int. Ed.* **2014**, *53*, 6310-6320; (e) P. Gautam, B. M. Bhanage, *Catal. Sci. Technol.* **2015**, *5*, 4663-4702; (f) W. Li, X.-F. Wu, *Adv. Synth. Catal.* **2015**, *357*, 3393-3418; (g) S. D. Friis, A. T. Lindhardt, T. Skrydstrup, *Acc. Chem. Res.* **2016**, *49*, 594-605.
- [12] Two-chamber system (commercially available from Sigma Aldrich as COWare) is a sealable, two-chamber reactor composed by two vessels linked each other by a bridge thus allowing gas transfer. Typically, in the first chamber the decarbonylation reactor occur whereas in the second one the carbonylation reaction takes place.
- [13] R. Alberto, K. Ortner, N. Wheatley, R. Schibli, A. P. Schubiger, *J. Am. Chem. Soc.* **2001**, *123*, 3135-3136.
- [14] (a) S. N. Gockel, K. L. Hull, *Org. Lett.* **2015**, *17*, 3236-3239; (b) V. V. Grushin, H. Alper, *Organometallics* **1993**, *12*, 3846-3850; (c) Z. Li, L. Wang, *Adv. Synth. Catal.* **2015**, *357*, 3469-3473.
- [15] (a) J. Muzart, *Tetrahedron* **2009**, *65*, 8313-8323; (b) S. Ding, N. Jiao, *Angew. Chem. Int. Ed.* **2012**, *51*, 9226-9237.
- [16] H. W. Gibson, *Chem. Rev.* **1969**, *69*, 673-692.
- [17] G. Jenner, E. M. Nahmed, H. Leismann, *Tetrahedron Lett.* **1989**, *30*, 6501-6502.
- [18] T. Kondo, S. Tantayanon, Y. Tsuji, Y. Watanabe, *Tetrahedron Lett.* **1989**, *30*, 4137-4140.
- [19] (a) H. A. Zahalka, H. Alper, Y. Sasson, *Organometallics* **1986**, *5*, 2497-2499; (b) H. A. Zahalka, H. Alper, *Tetrahedron Lett.* **1987**, *28*, 2215-2216.
- [20] M. R. Sandner, D. J. Trecker, *J. Org. Chem.* **1973**, *38*, 3954-3956.
- [21] J. S. Matthews, D. C. Ketter, R. F. Hall, *J. Org. Chem.* **1970**, *35*, 1694-1695.
- [22] (a) E. M. Nahmed, G. Jenner, *J. Mol. Catal.* **1990**, *59*, L15-L19; (b) S. Fabre, P. Kalck, G. Lavigne, *Angew. Chem. Int. Ed. Engl.* **1997**, *36*, 1092-1095; (c) S. Ko, Y. Na, S. Chang, *J. Am. Chem. Soc.* **2002**, *124*, 750-751; (d) I. Fleischer, R. Jennerjahn, D. Cozzula, R. Jackstell, R. Franke, M. Beller, *ChemSusChem* **2013**, *6*, 417-420; (e) I. Profir, M. Beller, I. Fleischer, *Organic & Biomolecular Chemistry* **2014**, *12*, 6972-6976.

- [23] (a) T. Schareina, A. Zapf, A. Cotté, M. Gotta, M. Beller, *Adv. Synth. Catal.* **2010**, *352*, 1205-1209; (b) S. Pellegrini, Y. Castanet, A. Mortreux, *J. Mol. Catal. A: Chem.* **1999**, *138*, 103-106; (c) I. Pri-Bar, O. Buchman, *J. Org. Chem.* **1988**, *53*, 624-626.
- [24] G. Jenner, *Applied Catalysis* **1991**, *75*, 289-298.
- [25] (a) K. H. Park, I. G. Jung, S. Y. Kim, Y. K. Chung, *Org. Lett.* **2003**, *5*, 4967-4970; (b) H. W. Lee, A. S. C. Chan, F. Y. Kwong, *Chem. Commun.* **2007**, 2633-2635.
- [26] A. B. Taleb, G. Jenner, *J. Organomet. Chem.* **1993**, *456*, 263-269.
- [27] I. J. B. Lin, H. Alper, *J. Chem. Soc., Chem. Commun.* **1989**, 248-249.
- [28] X.-G. Yang, J.-Q. Zhang, Z.-T. Liu, *Appl. Catal., A* **1998**, *173*, 11-17.
- [29] Y. Katafuchi, T. Fujihara, T. Iwai, J. Terao, Y. Tsuji, *Adv. Synth. Catal.* **2011**, *353*, 475-482.
- [30] H. Li, H. Neumann, M. Beller, X.-F. Wu, *Angew. Chem. Int. Ed.* **2014**, *53*, 3183-3186.
- [31] (a) Y. Wang, W. Ren, J. Li, H. Wang, Y. Shi, *Org. Lett.* **2014**, *16*, 5960-5963; (b) J. Li, W. Chang, W. Ren, W. Liu, H. Wang, Y. Shi, *Org. Biomol. Chem.* **2015**, *13*, 10341-10347; (c) W. Ren, W. Chang, Y. Wang, J. Li, Y. Shi, *Org. Lett.* **2015**, *17*, 3544-3547.
- [32] T. Fujihara, T. Hosoki, Y. Katafuchi, T. Iwai, J. Terao, Y. Tsuji, *Chem. Commun.* **2012**, *48*, 8012-8014.
- [33] (a) T. Ueda, H. Konishi, K. Manabe, *Org. Lett.* **2012**, *14*, 3100-3103; (b) T. Ueda, H. Konishi, K. Manabe, *Tetrahedron Lett.* **2012**, *53*, 5171-5175; (c) H. Konishi, T. Ueda, T. Muto, K. Manabe, *Org. Lett.* **2012**, *14*, 4722-4725; (d) H. Konishi, H. Nagase, K. Manabe, *Chem. Commun.* **2015**, *51*, 1854-1857.
- [34] T. Ueda, H. Konishi, K. Manabe, *Org. Lett.* **2012**, *14*, 5370-5373.
- [35] (a) C. Brancour, T. Fukuyama, Y. Mukai, T. Skrydstrup, I. Ryu, *Org. Lett.* **2013**, *15*, 2794-2797; (b) P. Losch, A.-S. Felten, P. Pale, *Adv. Synth. Catal.* **2015**, *357*, 2931-2938.
- [36] (a) Y. Wan, M. Alterman, M. Larhed, A. Hallberg, *J. Org. Chem.* **2002**, *67*, 6232-6235; (b) Y. Wan, M. Alterman, M. Larhed, A. Hallberg, *J. Comb. Chem.* **2003**, *5*, 82-84; (c) K. Hosoi, K. Nozaki, T. Hiyama, *Org. Lett.* **2002**, *4*, 2849-2851; (d) D. N. Sawant, Y. S. Wagh, K. D. Bhatte, B. M. Bhanage, *J. Org. Chem.* **2011**, *76*, 5489-5494.
- [37] (a) N. Jana, F. Zhou, T. G. Driver, *J. Am. Chem. Soc.* **2015**, *137*, 6738-6741; (b) F. Zhou, D.-S. Wang, T. G. Driver, *Adv. Synth. Catal.* **2015**, *357*, 3463-3468.
- [38] (a) V. Sharma, P. Kumar, D. Pathak, *J. Heterocycl. Chem.* **2010**, *47*, 491-502; (b) T. Barden, in *Heterocyclic Scaffolds II*; Vol. 26 (Ed.: G. W. Gribble), Springer Berlin Heidelberg, **2011**, pp. 31-46.
- [39] (a) H. Johansson, T. B. Jorgensen, D. E. Gloriam, H. Brauner-Osborne, D. S. Pedersen, *RSC Adv.* **2013**, *3*, 945-960; (b) F. R. d. S. Alves, E. J. Barreiro, C. A. M. Fraga, *Mini-Rev. Med. Chem.* **2009**, *9*, 782-793.
- [40] (a) G. Nie, Z. Bai, J. Chen, W. Yu, *ACS Macro Letters* **2012**, *1*, 1304-1307; (b) M. S. Park, D. H. Choi, B. S. Lee, J. Y. Lee, *J. Mater. Chem.* **2012**, *22*, 3099-3104; (c) K. Rakstys, A. Abate, M. I. Dar, P. Gao, V. Jankauskas, G. Jacopin, E. Kamarauskas, S. Kazim, S. Ahmad, M. Grätzel, M. K. Nazeeruddin, *J. Am. Chem. Soc.* **2015**, *137*, 16172-16178.
- [41] (a) R. Vicente, *Org. Biomol. Chem.* **2011**, *9*, 6469-6480; (b) D. F. Taber, P. K. Tirunahari, *Tetrahedron* **2011**, *67*, 7195-7210; (c) S. Cacchi, G. Fabrizi, *Chem. Rev.* **2011**, *111*, PR215-PR283; (d) G. R. Humphrey, J. T. Kuethe, *Chem. Rev.* **2006**, *106*, 2875-2911.
- [42] (a) S. Cacchi, G. Fabrizi, A. Goggiamani, in *Organic Reactions*, John Wiley & Sons, Inc., **2004**; (b) G. Battistuzzi, S. Cacchi, G. Fabrizi, *Eur. J. Org. Chem.* **2002**, *2002*, 2671-2681; (c) M. Platon, R. Amardeil, L. Djakovitch, J.-C. Hierso, *Chem. Soc. Rev.* **2012**, *41*, 3929-3968; (d) X.-F. Wu, H. Neumann, M. Beller, *Chem. Rev.* **2012**.
- [43] M. Bandini, A. Eichholzer, *Angew. Chem. Int. Ed.* **2009**, *48*, 9608-9644.
- [44] J. J. Brunet, *Chem. Rev.* **1990**, *90*, 1041-1059.
- [45] K. Cann, T. Cole, W. Slegeir, R. Pettit, *J. Am. Chem. Soc.* **1978**, *100*, 3969-3971.
- [46] (a) S. Cenini, E. Bettetini, M. Fedele, S. Tollari, *J. Mol. Catal. A: Chem.* **1996**, *111*, 37-41; (b) M. Pizzotti, S. Cenini, S. Quici, S. Tollari, *J. Chem. Soc., Perkin Trans. 2* **1994**, 913-917; (c) C. Crotti, S. Cenini, R. Todeschini, S. Tollari, *J. Chem. Soc., Faraday Trans.* **1991**, *87*, 2811-2820.
- [47] F. Ferretti, M. A. El-Atawy, S. Muto, M. Hagar, E. Gallo, F. Ragaini, *Eur. J. Org. Chem.* **2015**, *2015*, 5712-5715.

- [48] (a) R. S. Mane, B. M. Bhanage, *J. Org. Chem.* **2016**, *81*, 4974-4980; (b) A. M. Trzeciak, J. J. Ziółkowski, *Organometallics* **2002**, *21*, 132-137; (c) K. Ouyang, W. Hao, W.-X. Zhang, Z. Xi, *Chem. Rev.* **2015**, *115*, 12045-12090.
- [49] V. I. Timokhin, S. S. Stahl, *J. Am. Chem. Soc.* **2005**, *127*, 17888-17893.
- [50] F. Ragaini, S. Cenini, M. Gasperini, *J. Mol. Catal. A: Chem.* **2001**, *174*, 51-57.
- [51] Z. V. Todres, G. V. Gridunova, K. I. Dyusengaliev, Y. T. Struchkov, *Zh. Org. Khim.* **1987**, *23*, 1805-1807.
- [52] O. H. Wheeler, *Can. J. Chem.* **1963**, *41*, 192-194.
- [53] C. J. Finder, M. G. Newton, N. L. Allinger, *Acta Cryst. Sect. B* **1974**, *30*, 411-415.
- [54] M. Traetteberg, E. B. Frantsen, *J. Mol. Struct.* **1975**, *26*, 69-76.
- [55] G. Jenner, *Appl. Catal., A* **1995**, *121*, 25-44.
- [56] (a) J.-Y. Mérour, F. Buron, K. Plé, P. Bonnet, S. Routier, *Molecules* **2014**, *19*, 19935; (b) J. J. Song, J. T. Reeves, F. Gallou, Z. Tan, N. K. Yee, C. H. Senanayake, *Chem. Soc. Rev.* **2007**, *36*, 1120-1132.
- [57] (a) W.-L. Jia, Q.-D. Liu, R. Wang, S. Wang, *Organometallics* **2003**, *22*, 4070-4078; (b) Q. Liu, L. Thorne, I. Kozin, D. Song, C. Seward, M. D'Iorio, Y. Tao, S. Wang, *J. Chem. Soc., Dalton Trans.* **2002**, 3234-3240.
- [58] P. Rhoennstad, E. Kallin, T. Apelqvist, M. Wennerstaal, A. Cheng, Karo Bio AB, Swed. . **2009**, p. 122pp.
- [59] K. Okuro, J. Gurnham, H. Alper, *J. Org. Chem.* **2011**, *76*, 4715-4720.
- [60] C. Crotti, S. Cenini, B. Rindone, S. Tollari, F. Demartin, *J. Chem. Soc., Chem. Commun.* **1986**, *0*, 784-786.
- [61] S. P. Gorugantula, G. M. Carrero-Martínez, S. W. Dantale, B. C. G. Söderberg, *Tetrahedron* **2010**, *66*, 1800-1805.
- [62] B. C. Söderberg, J. A. Shriver, *J. Org. Chem.* **1997**, *62*, 5838-5845.
- [63] M. S. Yalfani, G. Lolli, A. Wolf, L. Mleczko, T. E. Muller, W. Leitner, *Green Chem.* **2013**, *15*, 1146-1149.
- [64] F. Ragaini, *Dalton Trans.* **2009**, *0*, 6251-6266.
- [65] R. S. Berman, J. K. Kochi, *Inorg. Chem.* **1980**, *19*, 248-254.
- [66] A. J. Kunin, M. D. Noirot, W. L. Gladfelter, *J. Am. Chem. Soc.* **1989**, *111*, 2739-2741.
- [67] F. Ragaini, J.-S. Song, D. L. Ramage, G. L. Geoffroy, G. A. P. Yap, A. L. Rheingold, *Organometallics* **1995**, *14*, 387-400.
- [68] F. Ragaini, S. Cenini, F. Demartin, *J. Chem. Soc., Chem. Commun.* **1992**, 1467-1468.
- [69] (a) E. Gallo, F. Ragaini, S. Cenini, F. Demartin, *J. Organomet. Chem.* **1999**, *586*, 190-195; (b) N. C. Tomson, L. A. Labios, T. Weyhermüller, J. S. Figueroa, K. Wieghardt, *Inorg. Chem.* **2011**, *50*, 5763-5776.
- [70] (a) I. W. Davies, V. A. Guner, K. N. Houk, *Org. Lett.* **2004**, *6*, 743-746; (b) A. G. Leach, K. N. Houk, I. W. Davies, *Synthesis* **2005**, *2005*, 3463-3467.
- [71] (a) L. M. Kogan, *Russ. Chem. Rev.* **1986**, *55*, 1164; (b) N. F. Hepfinger, C. E. Griffin, *Tetrahedron Lett.* **1963**, *4*, 1361-1364.
- [72] D. Kuzmich, C. Mulrooney, *Synthesis* **2003**, *2003*, 1671-1678.
- [73] I. W. Davies, J. H. Smitrovich, R. Sidler, C. Qu, V. Gresham, C. Bazaral, *Tetrahedron* **2005**, *61*, 6425-6437.
- [74] K. Kikukawa, K. Maemura, Y. Kiseki, F. Wada, T. Matsuda, C. S. Giam, *J. Org. Chem.* **1981**, *46*, 4885-4888.
- [75] (a) F. L. Callonnet, E. Fouquet, F.-X. Felpin, *Org. Lett.* **2011**, *13*, 2646-2649; (b) N. Susperregui, K. Miqueu, J.-M. Sotiropoulos, F. Le Callonnet, E. Fouquet, F.-X. Felpin, *Chem. Eur. J.* **2012**, *18*, 7210-7218.
- [76] M. Rimoldi, F. Ragaini, E. Gallo, F. Ferretti, P. Macchi, N. Casati, *Dalton Trans.* **2012**, *41*, 3648-3658.
- [77] A. Bontempi, E. Alessio, G. Chanos, G. Mestroni, *J. Mol. Catal.* **1987**, *42*, 67-80.
- [78] M. F. Rettig, P. M. Maitlis, F. A. Cotton, T. R. Webb, in *Inorg. Synth.*, John Wiley & Sons, Inc., **2007**, pp. 134-137.
- [79] V. I. Bakhmutov, J. F. Berry, F. A. Cotton, S. Ibragimov, C. A. Murillo, *Dalton Trans.* **2005**, 1989-1992.
- [80] C. R. Eady, P. F. Jackson, B. F. G. Johnson, J. Lewis, M. C. Malatesta, M. McPartlin, W. J. H. Nelson, *J. Chem. Soc., Dalton Trans.* **1980**, 383-392.

- [81] M. Chalal, D. Vervandier-Fasseur, P. Meunier, H. Cattey, J.-C. Hierso, *Tetrahedron* **2012**, *68*, 3899-3907.
- [82] R. Siles, J. F. Ackley, M. B. Hadimani, J. J. Hall, B. E. Mugabe, R. Guddneppanavar, K. A. Monk, J.-C. Chapuis, G. R. Pettit, D. J. Chaplin, K. Edvardsen, M. L. Trawick, C. M. Garner, K. G. Pinney, *J. Nat. Prod.* **2008**, *71*, 313-320.
- [83] F. Nepveu, S. Kim, J. Boyer, O. Chatriant, H. Ibrahim, K. Reybier, M.-C. Monje, S. Chevalley, P. Perio, B. H. Lajoie, J. Bouajila, E. Deharo, M. Sauvain, R. Tahar, L. Basco, A. Pantaleo, F. Turini, P. Arese, A. Valentin, E. Thompson, L. Vivas, S. Petit, J.-P. Nallet, *J. Med. Chem.* **2010**, *53*, 699-714.
- [84] R.-G. Xing, Y.-N. Li, Q. Liu, Y.-F. Han, X. Wei, J. Li, B. Zhou, *Synthesis* **2011**, *2011*, 2066-2072.
- [85] D. H. Leung, J. W. Ziller, Z. Guan, *J. Am. Chem. Soc.* **2008**, *130*, 7538-7539.
- [86] J.-F. Paquin, C. R. J. Stephenson, C. Defieber, E. M. Carreira, *Org. Lett.* **2005**, *7*, 3821-3824.
- [87] R. P. Barnes, J. H. Graham, M. A. S. Qureshi, *J. Org. Chem.* **1963**, *28*, 2890-2893.
- [88] B. Burja, M. Kočevár, S. Polanc, *Tetrahedron* **2009**, *65*, 8690-8696.
- [89] S. Lieber, F. Scheer, W. Meissner, S. Naruhn, T. Adhikary, S. Müller-Brüsselbach, W. E. Diederich, R. Müller, *J. Med. Chem.* **2012**, *55*, 2858-2868.

Chapter III

Co and Fe Doped-Carbon-Based Heterogeneous Catalysts for the Selective Hydrogenation of Nitroaromatics

1. Background

As previously mentioned in Chapter I, the reduction of nitrobenzene to aniline is an industrially-relevant transformation. In 2004, the production capacity worldwide for aniline reached $3.4 \cdot 10^6$ t \cdot y $^{-1}$ and market analysis estimates a production of $5.6 \cdot 10^6$ t in 2017. Aniline is one of the most important organic chemicals. It is directly used for the synthesis of cyclohexylamine, benzoquinone, acetanilide and secondary or tertiary anilines that in turn constitute platforms for a large variety of other functionalized molecules (Figure 1).

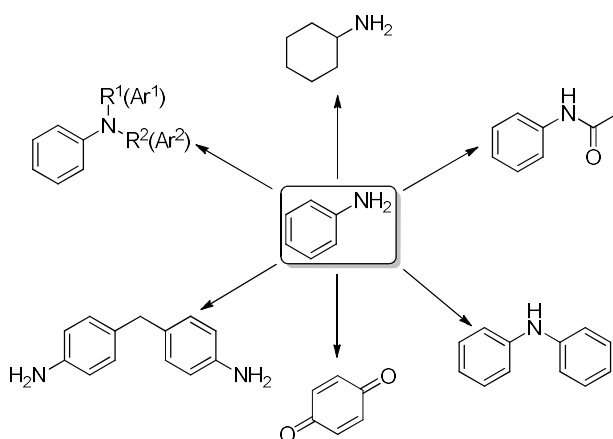
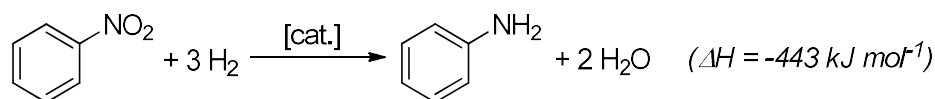


Figure 1. Chemical compounds directly produced from aniline.

Despite other manufacturing methods were developed during the years (for example starting from chlorobenzene or phenol), hydrogenation of nitrobenzene is the most employed route.



One of the oldest industrial manufacturing procedures for aniline is represented by the stoichiometric reduction of nitrobenzene with metallic iron in aqueous hydrochloric acid. This process has survived for decades since the obtained iron oxides as by products are valuable materials for the pigment industry. Nevertheless, when the increasing demand for aniline has surpassed the market of the pigments, the industrial production shifted from stoichiometric to catalytic processes. However, it is noteworthy that Bayer AG still employs this process for the industrial production of aniline in two plants. During the last century several heterogeneous catalytic systems have been developed by many chemical industries for the hydrogenation of nitrobenzene.^[1] They differ not only from the active metal, but also from the reaction conditions under which it is employed (gas or liquid phase reactions) and the reactor configuration. Unfortunately, each of these catalytic system is covered by industrial trade secret that generally do not allow for an exhaustive description of it. Examples are summarized in Table 1.

Table 1. Industrial hydrogenation of nitrobenzene.^[1a]

Catalyst	Company	Reaction conditions	Aniline selectivity
Ni sulphides	Bayer, Allied	300-475 °C	> 99 %
Cu, Mn, Fe	ICI	300.475 °C	> 99 %
Pd/Al ₂ O ₃	Bayer	250.350 °C 7 bar	> 99 %
Cu/SiO ₂ (Cr, Ba and Zn as promoters)	BASF, Cynamide, Lonza	270-290 °C 5 bar	> 99 %
Pd-Pt/C (Fe as modifier)	DuPont (Dow Chemicals)	90-200 °C 6 bar	> 99 %

These catalysts offer a good combination of activity and reusability (although in some cases reactivation is required). Concerning selectivity, hydrogenation of nitrobenzene (or simply substituted nitro compounds) does not pose significant problems since no other side reactions can occur (hydrodeamination and saturation of the aryl ring only occur in the presence of special catalysts – *e.g.* Ru NPs – and/or under harsh conditions). However, the situation is much more different for aromatic nitro compounds carrying reducible, labile or poisoning-capable functional groups such as halogens, carbonyl compounds, carboxylic acid derivatives, unsaturated hydrocarbons or heterocycles. Unfortunately, the majority of the catalysts reported in Table 1 (and even others such as Ni-Raney®, PtO₂ and Pd or Pt on various carbonaceous supports) do not have acceptable selectivities towards functionalized nitro derivatives especially if the nitro moiety is present in molecules with a high degree of functionalization (pharmaceuticals or natural-derived molecules). In Figure

2 selected industrial real cases in which the hydrogenation of nitro group represented a selectivity issue are depicted.

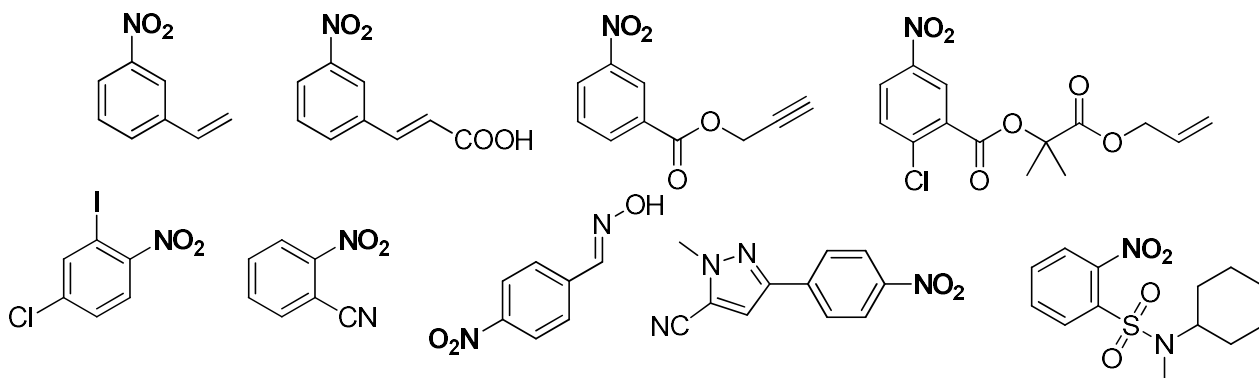


Figure 2

In order to produce selective catalysts for nitroaromatics hydrogenation, various solutions were developed. One of the most employed includes the production of modified heterogeneous catalysts. For example, in order to avoid hydrodehalogenation, Pt/C-based materials were modified with metallic salts (based on Pb, Bi, Sn, Ge, Zn, Al or Ag) or *in-situ* modified with acids (e.g. inorganic phosphorus ones) or bases (morpholine). Furthermore, Lindlar (Pd/CaCO₃ poisoned with Pb(OAc)₂ and quinoline) and Lindlar-like catalysts were found to be selective catalysts for the hydrogenation of nitro compounds carrying reducible functional moieties such as multiple carbon-carbon bonds, carbonyl and cyano groups.^[2] Nevertheless, apart from the high cost and toxicity of both the main metal and the promoters, efficient separation and reutilization of these kind of catalytic system is often complicated. A breakthrough in the field was made by Corma^[3] and Qui^[4] when they demonstrated for the first time that supported Au and Ag nanoparticles are competitive catalyst for the chemoselective hydrogenation of nitro compounds, respectively.

Unfortunately, although activity can be generally correlated with surface area and metal site accessibility, selectivity does not depend on a single and discrete factor. In fact, as outstandingly reviewed by H.-U. Blaser,^[2a, 5] selectivity in the hydrogenation of nitro compounds depends on a plethora of parameters such as nature and distribution of the active metal, support, kind of metal-support interactions, support dopants, additives, reaction medium and reaction conditions. Furthermore, since heat and transfer phenomena are crucial issues in industrial-scale reactions, reactor configuration can affect selectivity for a given transformation. Nonetheless, it is not possible to assign a hierarchical order among them, thus each case is in principle different from another.

Most of the industrially relevant catalytic processes are nowadays based on expensive and rare late transition metals such as Pd, Pt, Rh, Ir and Ru. The scarcity of these elements strongly dictates for the development of efficient alternative metal-based catalysts. In this perspective, the design of catalytic systems based of abundant and biocompatible metals is a mandatory goal. Among the various metals, Fe, Co, Cu, Mn, Ni and Bi are ideal candidates that fully fit those requirements (Table 2).^[6] Although their abundance

and relatively low price, the catalytic chemistry of Mn^[6g] and Bi^[6h] is still in an emerging phase. However, as pointed out by influent scientists in the field, they could become valuable alternatives to noble metals along with Fe, Co, Ni and Cu.

Table 2. Price, extraction amount and extraction country of the most important transition metals employed in catalysis.

Metal	Main countries of extraction	Price [€·kg⁻¹]	Average amount extracted
Re	Chile, USA, Poland	9000	53 t·y ⁻¹
Ru	South Africa, Russia	2400	12 t·y ⁻¹
Ir	South Africa, Russia, Canada	17100	10 t·y ⁻¹
Pd	South Africa, USA, Canada, Russia	21133	208 t·y ⁻¹
Pt	South Africa, Colombia	34500	178 t·y ⁻¹
Rh	South Africa, USA, Russia	18600	30 t·y ⁻¹
Co	Zambia, Finland, other African countries	28	55·10 ³ t·y ⁻¹
Bi	China, Vietnam, Mexico	23	1.4·10 ⁴ t·y ⁻¹
Ni	Russia, Australia, Canada, France	16	2.3·10 ⁶ t·y ⁻¹
Cu	Chile, Peru, USA	10	1.9·10 ⁷ t·y ⁻¹
Mn	South Africa, Australia, China, Brazil	1.53	1.8·10 ⁷ t·y ⁻¹
Fe	China, Australia, Brazil, India	0.16	2.3·10 ⁹ t·y ⁻¹

As a matter of fact, these elements are among the most abundant metals in the Earth's upper crust, thus being readily accessible.^[7] Consequently, it is clear how the disclosure of active, selective and cheap catalytic materials is still a challenging goal in synthetic chemistry.

2. Transition-metal based heteroatom-doped carbon catalysts: general overview and introduction to the presented work

Carbon-based materials are a widespread class of supports for many metals that play a central role in heterogeneous catalysis. Their unique features such as microporose structure, chemical resistance, electrical conductivity and presence of surface chemical groups make it a perfect material that can host metals, both in forms of single atoms, nanoparticles or small clusters. Despite the aforementioned properties, suitable structural modifications can lead to the generation of new kind of materials with altered chemical behavior. Within this framework, by substituting some carbon atoms with other elements, it is possible to modify the reactivity of the active metal center.

Heteroatom-doped carbonaceous composites are an emerging class of materials that attract interest in the field of metal supported heterogeneous catalysts for both chemical synthesis^[8] and energy-relevant transformations.^[9, 12e] Indeed, doping graphene with heteroatoms such as N, B, P or S leads to radical modification of both the support and the supported metal.^[10] Therefore, it is possible to modify the activity and adjust the selectivity of the final catalytic material towards the desired transformation. Among the various dopant, nitrogen attracted most interest.^[11] When nitrogen atoms are incorporated into graphene, diverse bonding configurations can arise: the most frequent ones involve the presence of quaternary (or graphitic) N, pyridinic N, pyrrolic N and pyridinic oxide N (Figure 3) in various relative proportions.

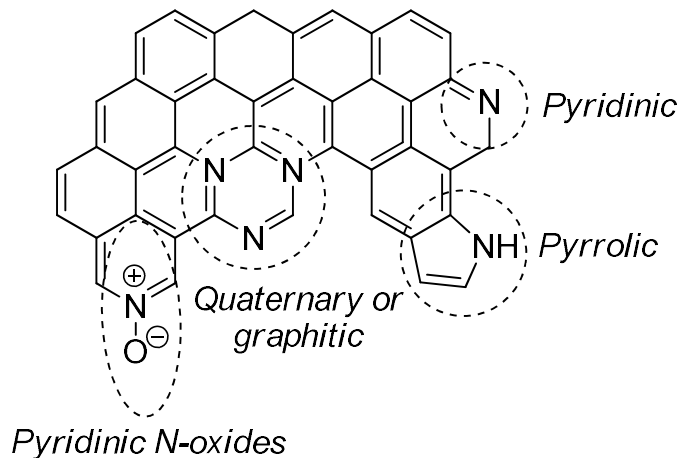
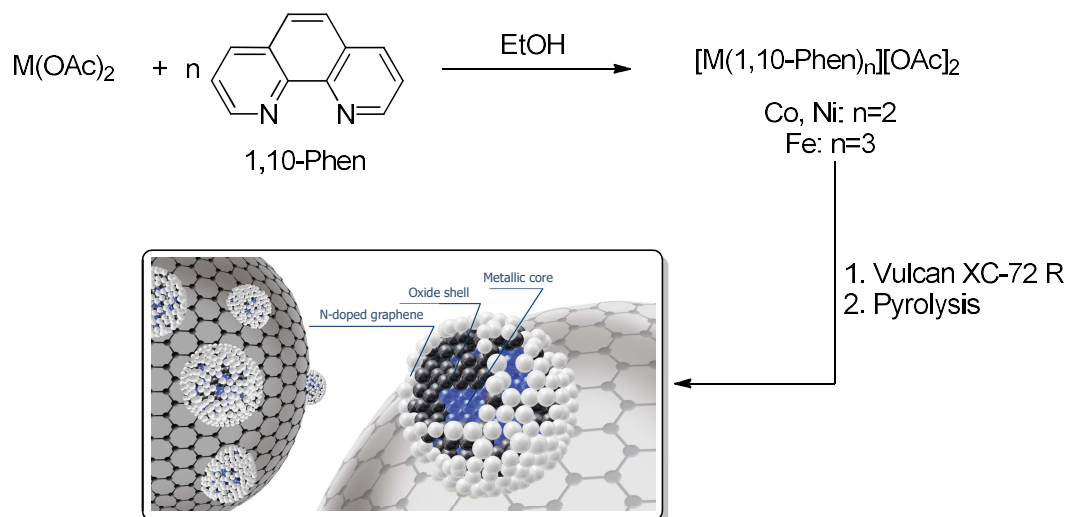


Figure 3. Bonding configurations for N atoms in NGr.

Each of these configurations produce different local electronic behavior in the NGr with respect to the pristine one. For example, spin density and charge distributions of the adjacent carbon atoms are deeply influenced by the dopant thus creating active sites for the nucleation and growth of metal nanoparticles. Intriguingly, small clusters (nanoclusters) or even single atoms can be effectively anchored on the doped carbonaceous material. To some extent, it was possible to create metal complexes in which the metal is embedded in the doped-carbon matrix. In addition, N doping is able to open the band gap between the conduction and the valence band allowing for promising applications in semiconductors. Currently, there are numerous methods appeared in the literature for the production of NGr: examples are chemical vapor

deposition (CVD), solvothermal synthesis, arc discharge, thermal or plasma treatments. Each of the latter methods presents advantages or disadvantages over the other. In addition, by using specific preparation conditions, it is possible to tune the doping level (N %) and/or the doping structure providing specific N configurations. Among the various methods, thermal treatment (pyrolysis) of N-containing molecules have attracted the attention owing to their easy preparation. Moreover, if one properly combines NGr with transition metals it is possible to paves the way for a huge number of applications such as in fuel cells, transistors and semiconductors, batteries and especially catalysis. One of the simple approach to produce such materials involves the pyrolysis (or in general the thermal treatment) of metal complexes using appropriate N-ligands or metal complexes adsorbed on N-enriched molecules. Examples of these are hexamethylenediamine, polypyrrole, melamine, ammonia, porphyrins, cyanamide, carbon nitride, common nitrogen ligands, triazine, urea and so on. Recently, metal-organic frameworks (MOFs) have emerged as sacrificial templates in which the structure of the final material strictly depends on the initial construction of the employed MOFs. Thus, by using different MOFs is possible to produce different N-doped carbon materials. Applications of transition metals/N-doped graphene-based catalytic systems (TM/NGr) ranges from oxygen reduction reactions (ORR), hydrogen evolving reactions (HER), photocatalysis, oxidation and reduction reactions of organic substrates, C-C bond formation to many others.^[9a, 12]

In 2013 and 2016, Beller and co-workers developed a series of carbon-based heterogeneous catalysts based on Fe,^[13] Co^[14] and Ni.^[15] The catalytic materials were prepared by pyrolysis under inert atmosphere of molecular defined metal complexes between Co, Fe and Ni acetates and 1,10-phenanthroline (Phen) using Vulcan® XC 72R as carbon support (Scheme 2).



Scheme 2. Preparation of the catalytic materials.

Structural elucidations (XRD, XPS, TEM, EPR, BET) demonstrated that the obtained materials are formed by nanocomposites exhibiting a core-shell structure that constitutes the structural prerequisite for catalytic activity. In the case of Co and Ni-base catalysts (named Co-Co₃O₄/NGr@C and Ni-NiO/NGr@C, respectively) an inner metallic core is surrounded by an oxidic layer (Co₃O₄ and NiO), whereas in the Fe

congener (named $\text{Fe}_2\text{O}_3/\text{NGr}@C$) almost only an oxidic phase composed of Fe_2O_3 is present. In both the cases, the oxidic shell is decorated with layers (“flakes”) of nitrogen-doped graphene (NGr) derived from the thermal decomposition of the ligated phen. Notably, the three catalysts exhibit a complete stability under air preserving their activity for months. In Figure 4, STEM images of two catalysts are depicted and the NGr layers highlighted by arrows. Control experiments (in all the three cases) demonstrated that the materials prepared without any N-ligand do not show any catalytic activity. As the consequence, the presence of nitrogen atoms in the carbon matrix is crucial for exert the catalytic activity.

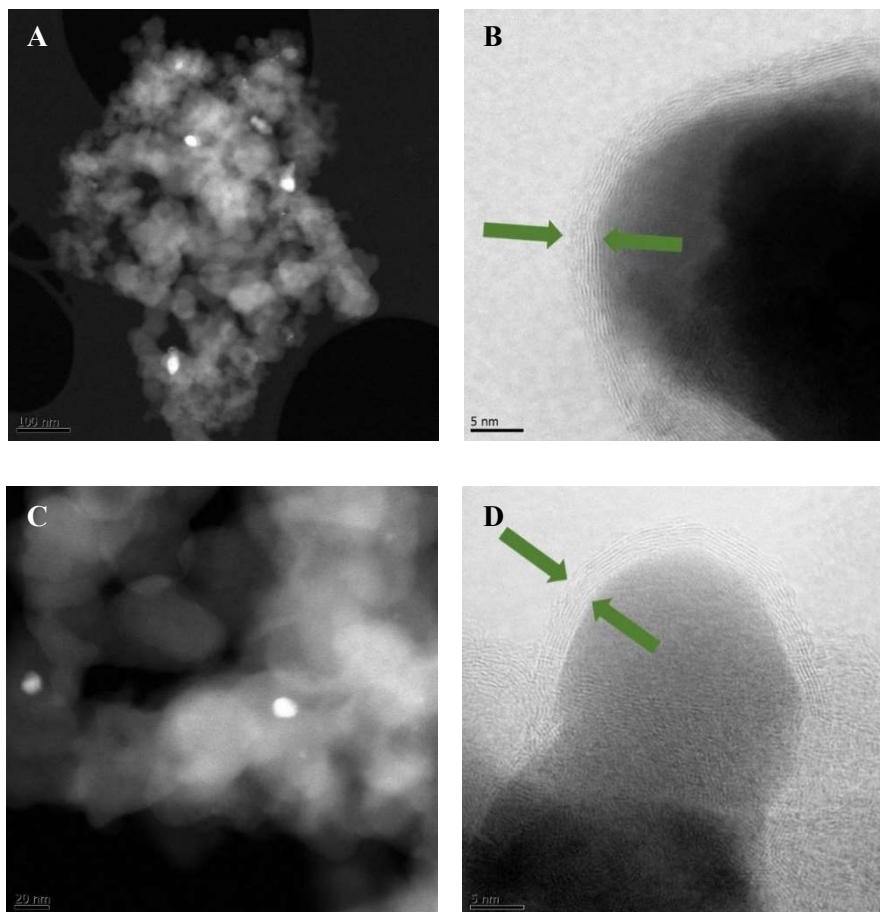


Figure 4. STEM images (HAADF and BF) of $\text{Co}_3\text{O}_4/\text{NGr}@C$ (A and B) and $\text{Fe}_2\text{O}_3/\text{NGr}@C$ (C and D). Enclose in the arrows, the NGr layers are highlighted.

The three catalysts were firstly employed in the hydrogenation of aromatic nitro compounds. Excellent chemoselectivities were achieved in the case of nitroaromatics substituted with reducible functional groups such as multiple carbon-carbon bonds, nitriles, ketones, esters and halogens. Concerning the relative activity in the same kind of reaction, $\text{Co-Co}_3\text{O}_4/\text{NGr}@C$ was found to be the most active one followed by $\text{Ni-NiO}/\text{NGr}@C$ and $\text{Fe}_2\text{O}_3/\text{NGr}@C$. Furthermore, these catalysts were further successfully employed in other catalytic transformations such as oxidations,^[16] transfer hydrogenations,^[17] synthesis of amines by reductive aminations^[18] and others.^[19]

However, in the case of nitro compounds hydrogenation, the reaction conditions were quite severe ($T > 110\text{ }^\circ\text{C}$ and up to 50 bar of H_2 pressure). In the first part of Project 2, we focused our efforts towards

decreasing temperature and pressure in order to conduct hydrogenations using non-noble-metal catalysts under mild conditions. In particular, polar solvents and base addition were found to be the key-points that allowed us to achieve our goal. In the second part of the Project 2, we demonstrated that Phen is not the sole N-ligand able to generate active catalysts belonging to this family. In fact, by using Ar-BIANs and related α -diimine complexes we prepared an array of Co-based catalysts active in the desired transformation. In addition, aided by kinetic experiments, we discovered for the first time a correlation between the catalytic activity and the N content/configuration in the final material.

3. Fe₂O₃/NGr@C- and Co-Co₃O₄/NGr@C-catalysed hydrogenation of nitroarenes under mild conditions

3.1. Introduction

As previously mentioned, in the case of Fe₂O₃/NGr@C and Co-Co₃O₄/NGr@C catalysts, the original reaction conditions involved high temperatures and pressures (Table 3).

Table 3. Original reaction conditions for the hydrogenation of nitrobenzene to aniline.

Catalyst	Temperature [°C]	H ₂ pressure [bar]	Catalyst loading [mol %]
Fe ₂ O ₃ /NGr@C ^[13]	120	50	4.5
Co-Co ₃ O ₄ /NGr@C ^[14]	110	50	1

With the aim of decreasing the values of these two parameters, two different approaches were employed. Concerning Co-Co₃O₄/NGr@C, we investigated the reaction outcome starting from target mild conditions (*upward approach*): 0.5 mol % Co (5 mg), 70 °C, 20 bar H₂, 13 h. While in the case of Fe₂O₃/NGr@C, we proceeded by employing the previously reported reaction conditions with a shortened reaction time (*downward approach*): 4.5 mol % Fe (42 mg), 120 °C, 50 bar H₂, 4 h.

3.2. Results and discussion

We commenced our study with testing various solvents employing the hydrogenation of nitrobenzene to aniline as the benchmark reaction. As shown in Figure 5, the use of polar solvent mixtures results in an increase of the conversion compared to apolar or low-polar ones. In particular, alcoholic solvents such as ethanol or methanol give higher conversions.

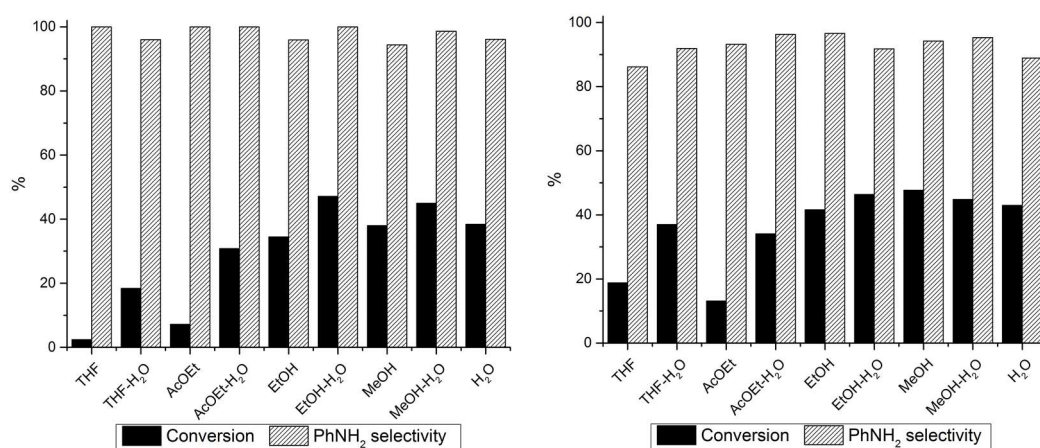


Figure 5. Influence of the solvent on conversion and selectivity for Co-Co₃O₄/NGr@C (left) and Fe₂O₃/NGr@C (right). Reaction conditions are reported in the text (if stated, main solvent: H₂O = 20:1 by volume).

Furthermore, addition of water leads to improvement in almost every cases. Merely, with MeOH as solvent, addition of water does not affect conversion or selectivity (Figure 5, right). Thus, EtOH-H₂O and MeOH

were chosen as solvents, which are in accordance with guidelines as green and sustainable choice for chemical transformations.^[20] As shown in Tables S1 and S2, the catalysts prepared without Phen ($\text{Co}_x\text{O}_y@\text{C}$ and $\text{Fe}_x\text{O}_y@\text{C}$) do not exhibit any catalytic activity. Thus, the basicity provided by the NGr is crucial for the activity. This evidence is in agreement with a heterolytic activation of the dihydrogen molecule in which the N present in the graphitic matrix can act as proton acceptor. As a consequence, an additional base present in the liquid phase should enhance the catalytic activity. In order to confirm this assumption, we tested the model reaction in the presence of a variety of inorganic and organic bases (1 equiv. with respect to PhNO_2). For both the catalysts, although high conversions were achieved, poor aniline selectivities were observed when inorganic bases (except for aq. NH_3) were added to the reaction mixture. In this case, azobenzene and azoxybenzene were identified as the major side products.

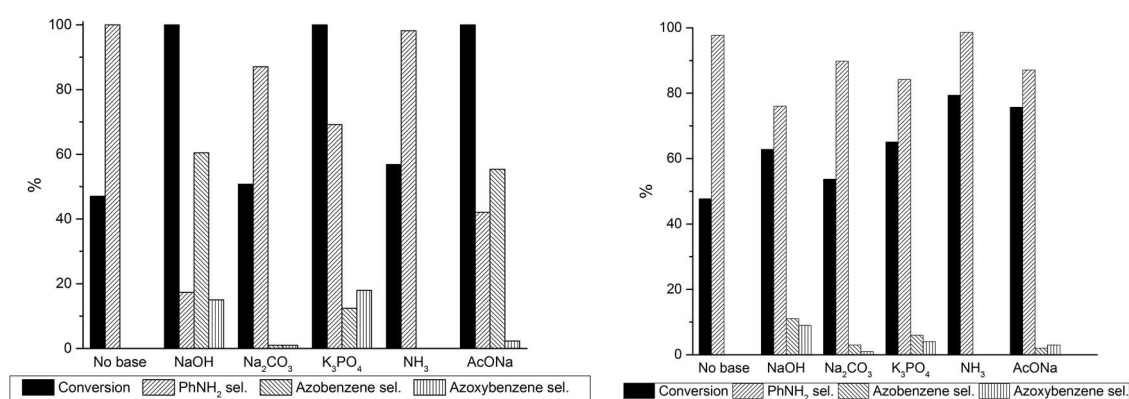


Figure 6. Influence of added inorganic bases on conversion and selectivity for $\text{Co-Co}_3\text{O}_4/\text{NGr}@C$ (left) and $\text{Fe}_2\text{O}_3/\text{NGr}@C$ (right). Reaction conditions are stated in the text.

In fact, it is known that alcohols in combination with strong inorganic bases can act as reducing agent towards nitro compounds, giving rise to undesired coupling products.^[21] On the contrary, when the catalytic transformation was conducted in the presence of an organic base, higher conversions were achieved compared to the reactions that was carried out without additives. Noteworthy, unwanted by-products did not form and the selectivity towards aniline remained very good ($> 95\%$) (see Figure 7).

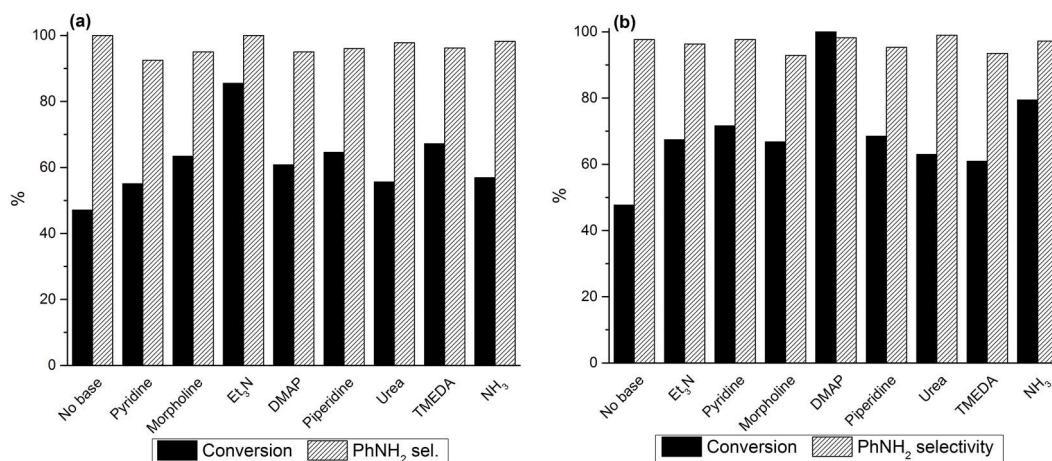


Figure 7. Influence of added organic base on conversion and selectivity for $\text{Co-Co}_3\text{O}_4/\text{NGr}@C$ (a) and $\text{Fe}_2\text{O}_3/\text{NGr}@C$ (b). Reaction conditions are stated in the text.

Among the tested bases, triethylamine (Et_3N) and 4-dimethylaminopyridine (DMAP) were found to be the best additives for $\text{Co-Co}_3\text{O}_4/\text{NGr}@C$ and $\text{Fe}_2\text{O}_3/\text{NGr}@C$, respectively. However, DMAP is a toxic and corrosive solid,^[22] which makes the use of chromatographic separation methods for its removal from the reaction mixture indispensable. Therefore, aqueous ammonia was chosen instead of DMAP since it is less toxic and possesses a negligible environmental impact.^[22] Advantageously, ammonia is gaseous and thus readily removed from the reaction mixture. Since bases and alcoholic solvents are known to act as transfer hydrogenation agents, control experiments were carried out in order to rule out this reaction pathway (Tables S1 and S2). As expected, no substrate conversion was detected in each case. Following our initial hypothesis, acidic additives were also examined (Figure 8).

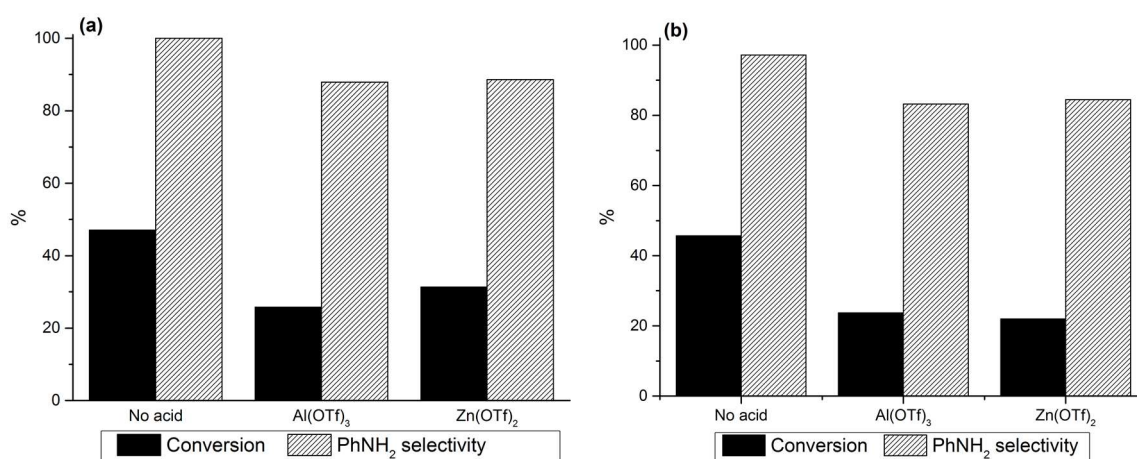


Figure 8. Influence of added Lewis acids on conversion and selectivity for $\text{Co-Co}_3\text{O}_4/\text{NGr}@C$ (a) and $\text{Fe}_2\text{O}_3/\text{NGr}@C$ (b). Reaction conditions are stated in the text.

The results clearly indicate that addition of Lewis acids has a detrimental effect for the reaction outcomes. For both the homogeneous materials the addition of metal triflates led to a marked decrease of catalyst performances. This behavior can be attributed to the interaction of acidic additives with the basic N-sites in the NGr that inhibit the catalytic activity. Next, we proceed to evaluate the optimum amount of base. We conducted the reaction applying different equivalents of Et_3N and NH_3 for $\text{Co-Co}_3\text{O}_4/\text{NGr}@C$ and $\text{Fe}_2\text{O}_3/\text{NGr}@C$, respectively. The results are summarized in Figure 9.

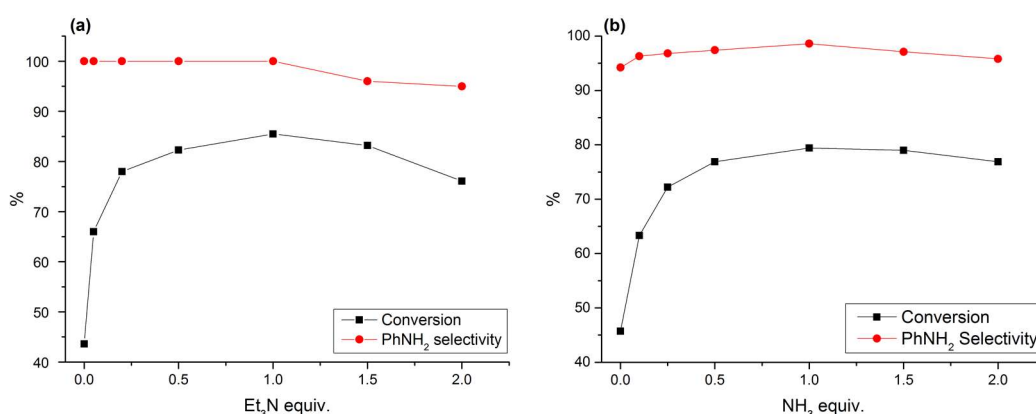


Figure 9. Et_3N and NH_3 optimization for $\text{Co-Co}_3\text{O}_4/\text{NGr}@C$ (a) and $\text{Fe}_2\text{O}_3/\text{NGr}@C$ (b).

Even small amounts of base (0.05 and 0.1 equiv. of Et₃N and NH₃ for Co-Co₃O₄/NGr@C and Fe₂O₃/NGr@C, respectively) is able to significantly accelerate the reaction. However, best conversions were achieved with 1 equiv. of base with respect to the substrate. Using amounts of bases higher than 1 equiv. (for Co-Co₃O₄/NGr@C) or 1.5 equiv. (for Fe₂O₃/NGr@C), resulted in a slight decreasing of both conversion and selectivity. In the presence of an optimal base amount, catalytic hydrogenations were conducted under mild conditions (Table 4).

Table 4. Hydrogenation of nitrobenzene to aniline: reaching mild conditions.^a

Entry	Catalyst	Temp. [°C]	H ₂ pressure [bar]	Time [h]	Conversion [%] ^b	Selectivity [%] ^b
1	Co-Co ₃ O ₄ /NGr@C	70	20	13	85	>99
2	Co-Co ₃ O ₄ /NGr@C	70	20	18	95	>99
3	Co-Co₃O₄/NGr@C	70	20	20	>99	>99
4	Fe ₂ O ₃ /NGr@C	120	50	4	79	99
5	Fe ₂ O ₃ /NGr@C	90	30	20	65	>99
6	Fe ₂ O ₃ /NGr@C	90	30	24	86	>99
7	Fe₂O₃/NGr@C	90	30	28	>99	>99

^a Reaction conditions for Co-Co₃O₄/NGr@C: 0.5 mmol PhNO₂, 0.5 mol % [Co] (5 mg), 2 mL EtOH + 100 μL H₂O, 1 equiv. of Et₃N; reaction conditions for [Fe]: 0.5 mmol PhNO₂, 4.5 mol % Fe₂O₃/NGr@C (42 mg), 3 mL MeOH, 1 equiv. of NH₃; ^b Conversions and selectivities were determined by GC using *n*-hexadecane as internal standard.

In the case of Co-Co₃O₄/NGr@C, a prolonged reaction time allowed for complete conversion at 70 °C and 20 bar (Table 4, entry 3), whereas with Fe₂O₃/NGr@C 90 °C and 30 bar of hydrogen pressure were required. Nevertheless, to the best of our knowledge this latter example represents the first Fe-catalysed hydrogenation of nitroarenes at such low temperature and pressure values.

The recyclability of the employed catalysts was then explored (Figure 10). In the case of the Co catalyst, a slight decreasing of the conversion was detected in the third run whereas for Fe after an initial decreasing after the first run, the activity stayed almost constant.

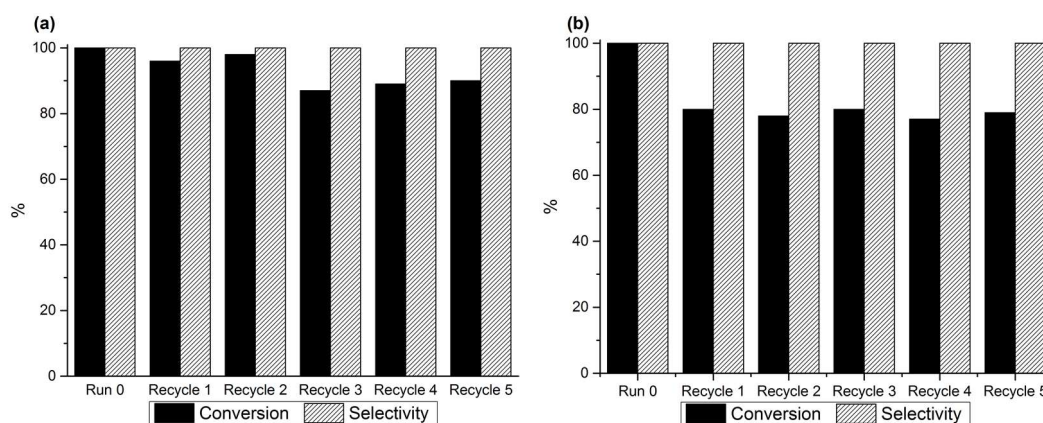
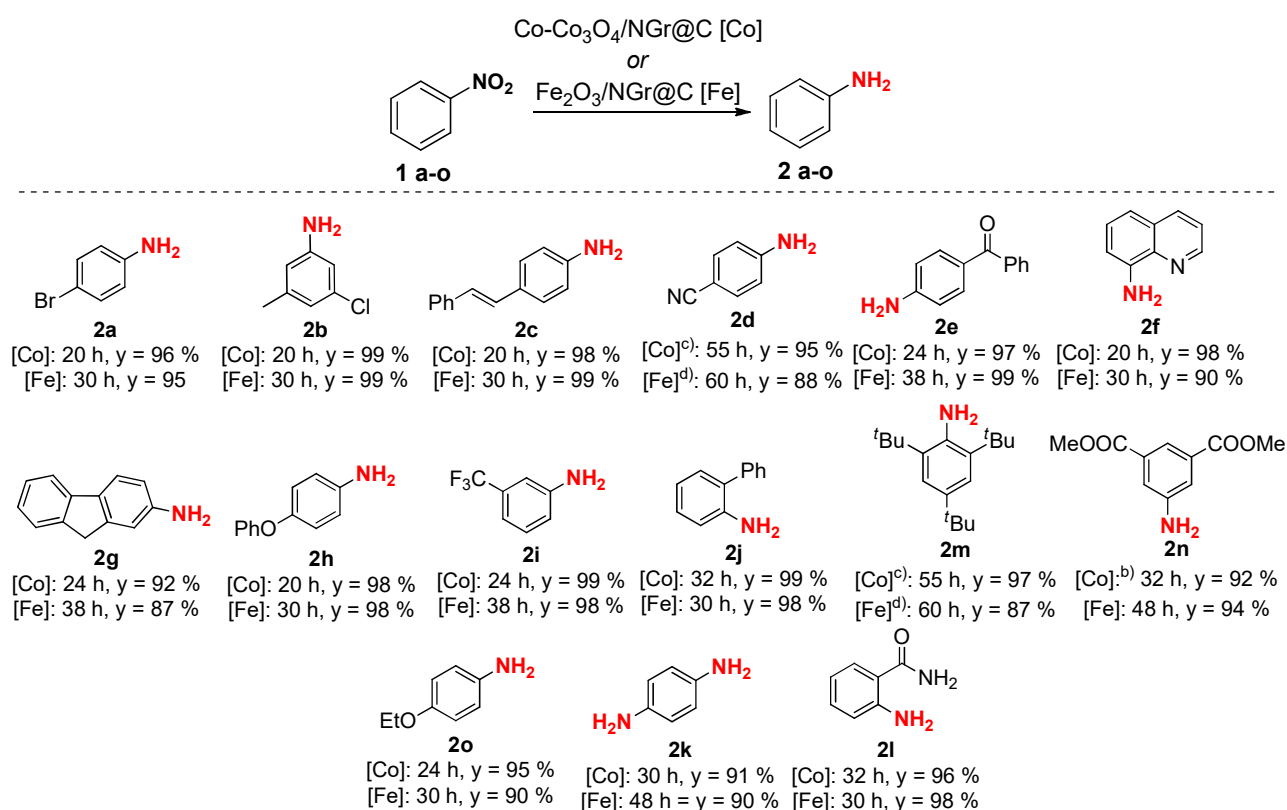


Figure 10. Recycling experiments for Co-Co₃O₄/NGr@C (a) and Fe₂O₃/NGr@C (b). Reaction conditions are reported in Table 4, entries 3 and 7.

ICP analysis of the liquid phase after each run reveals no metal leaching for both the catalysts (detection limit <0.5 ppm). In addition, CHN analysis of the catalysts after the last recycle did not evidence significant perturbation in the composition of both the materials (compare Table S5 and S6 with Table S7). Furthermore, Maitlis' hot filtration test ruled out any catalytic activity provided by soluble Co or Fe metal species (see Table S8). The latter findings clearly demonstrated that the two employed catalysts are inherently heterogeneous.

To evaluate the scope of the new catalytic protocol, we tested various substituted aromatic nitro compounds bearing reducing-labile functional groups (Scheme 3).



Scheme 3. Co-Co₃O₄/NGr@C- and Fe₂O₃/NGr@C-catalysed hydrogenation of substituted nitro compounds: reaction scope. Reaction conditions for [Co]: 0.5 mol % Co (5 mg), 0.5 mmol ArNO₂, 70 °C, 20 bar H₂, 1 equiv. Et₃N, 2 mL EtOH + 100 μL H₂O. Reaction conditions for [Fe]: 4.5 mol % Fe (42 mg), 0.5 mmol ArNO₂, 90 °C, 30 bar H₂, 1 equiv. aqueous NH₃, 3 mL MeOH. Yields were calculated by GC analysis (calibration curve, *n*-hexadecane as internal standard) using commercially available anilines. In all cases, complete conversions were observed. b) Reaction carried out without Et₃N. c) 1 mol % Co was used. d) 6 mol % Fe was used.

Substrates carrying halogen atoms are smoothly converted to the corresponding anilines (**2a** and **2b**) without any dehalogenation. Furthermore, both the catalysts tolerate C=C double bonds (**2c**), nitriles (**2d**), carbonyl (**2e**), esters (**2n**) and amides (**2i**). In the case of **2n**, a reaction carried out with the addition of Et₃N produces mono- and di-ethyl esters from the methyl congener by base-mediate transesterification after 20 h (conv. > 99 %) (Figures S9 and S10). The ratio between the two compounds was around 2:1 in favor of the diethylated product. In order to avoid this side-reaction, Co-catalysed hydrogenation of **2n** was run in the absence of any base. As expected, no transesterification product was detected and thus an excellent yield of the desired aniline derivative was achieved. Sterically demanding substrates such as 2-nitrophenyl (**1j**) and

2,4,6-tri-*t*-butylnitrobenzene (**1m**) were hydrogenated upon applying a prolonged reaction time without affecting the selectivity and hence the corresponding yield.

Based on the presented results we conclude that:

- 1) a correlation between higher solvent polarity and higher conversion is present;
- 2) basic additives are able to increase the catalytic activity;
- 3) acid additives are detrimental for the conversion.

On the basis of these outcomes it is clear that the reaction needs a basic and polar environment. These observations support our working hypothesis that the dihydrogen molecule is activated by heterolytic cleavage. This assumption is in agreement with observations made by Sánchez-Delgado and co-workers for Ru and Rh NPs supported on MgO.^[23] In this process the dihydrogen molecule is formally cleaved into a hydride and a proton.^[24] The hydride atom is bound to the metal-based NP whereas the proton is attached to the basic N atoms in close proximity to the NP or by the basic additive present in the liquid phase. In order to further understand this heterolytic activation mechanism, we decided to hydrogenate non-polar 1-decene. In principle, this terminal olefin is less prone to heterolytic hydrogenation compared to nitrobenzene. Accordingly, Co-based catalysts prepared with and without Phen, do not show any difference in the hydrogenation of 1-decene (Table 5, entries 1 and 2). Moreover, addition of basic promoters does not affect the rate of the reaction (Table 5, entries 3 and 4). Applying Fe-based catalyst a similar trend was observed.

Table 5. Hydrogenation of 1-decene.^a

Entry	Catalyst	Additive (1 equiv.)	Conversion [%] ^b
1	Co _x O _y @C	-	9
2	Co-Co ₃ O ₄ /NGr@C	-	9
3	Co _x O _y @C	Et ₃ N	11
4	Co-Co ₃ O ₄ /NGr@C	Et ₃ N	11
5	Fe _x O _y @C	-	11
6	Fe ₂ O ₃ /NGr@C	-	16
7	Fe _x O _y @C	NH ₃	12
8	Fe ₂ O ₃ /NGr@C	NH ₃	19

^a Reaction conditions: 0.5 mmol 1-decene, 0.5 mol % Co (5 mg) or 4.5 mol % Fe (42 mg). ^b GC conversions using *n*-hexadecane as internal standard

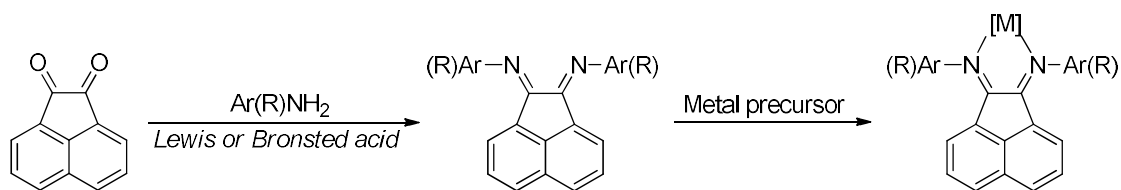
Carbonyl, cyano groups and quinolines were completely unreactive with these catalysts (see for example **2d**, **2e** and **2d** in Scheme 3). This is not surprisingly because these substrates are generally activated by Lewis acids and the catalysts herein presented are composed by a carbonaceous layer that completely lacks any acidic site. In keeping with this, Beller and co-workers recently reported that Co-based catalysts similarly prepared using ceria^[19b] or alumina^[19a, 19d] as supports instead of carbon were active in the hydrogenation of ketones to alcohols, nitriles to amines and quinolines to 1,2,3,4-tetrahydroquinolines. In comparison, the

materials prepared using Vulcan® as supports were much less active in the same kind of transformations. On the contrary, nitroarenes are unlikely to require a Lewis acid as an activator, since they are among the weakest nucleophiles known. This results in a very high selectivity towards the reduction of the nitro functionality with respect to other reducible functional groups when carbonaceous supports are employed.

4. Ar-BIANs and related α -diimine Co complexes as precursors for heterogeneous catalysts: on the role of nitrogen

4.1. Introduction

As previously mentioned, in 2013 Beller and co-workers discovered novel heterogeneous catalysts for selective nitroarenes hydrogenations. Their preparation involved the pyrolysis of carbon adsorbed metal chelates between Co, Fe or Ni and Phen. Nevertheless, from an economical point of view, Phen is an expensive compound which functionalization often requires multistep fair-yielding transformations. Thus, we were interested in using other, more easily tunable, nitrogen precursors. In this respect, chelating α -diimine (and especially Ar-BIAN ligands), are widely used in transition-metal catalysed reactions. As the starting materials are inexpensive, it is possible to prepare a large number of ligands with different electronic and/or steric properties (Scheme 4). This allows for the synthesis of tailor-made transition-metal based catalysts.^[25]



Scheme 4. General preparation of Ar-BIANs and related metal complexes.

In the second part of this project, we report for the first time the use of Ar-BIANs and related ligands as effective precursors for the generation of active Co/NGr catalysts.

4.2. Catalysts preparation and characterisation

The catalytic materials were prepared according to the standard protocol previously published by Beller and co-workers.^[16d] An in-situ prepared complex between $\text{Co}(\text{OAc})_2 \cdot 4\text{H}_2\text{O}$ and the ligand (molar ratio Co:ligand = 1:2) was wet impregnated onto Vulcan® XC 72 R carbon and pyrolysed at 800 °C for 2 hours under Ar atmosphere affording the heterogeneous material. By virtue of the synthetic versatility of the employed ligands, we synthesized a variety of catalysts (Co/L1-Co/L7) starting from seven different ligands (L1-L7) (Figure 11).

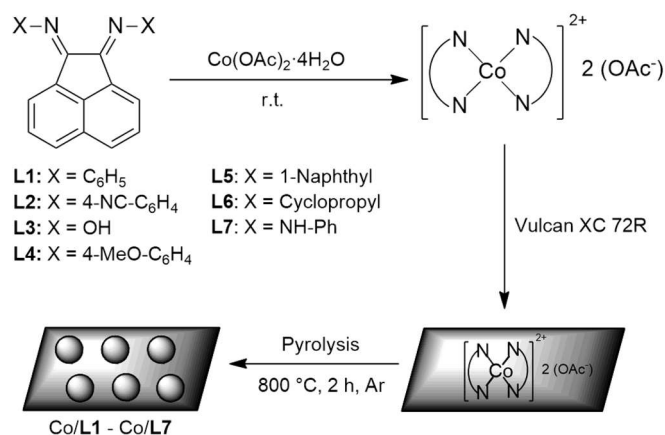


Figure 11. Catalysts preparation.

Four selected materials (Co/L1, Co/L2, Co/L3 and Co/L7) were fully characterized by using different techniques such as X-ray diffractions (XRD), X-ray photoelectron microscopy (XPS), transmission electron microscopy (TEM) and temperature programmed reduction (TPD).

Our study commenced with XRD measurements in order to identify the constituting phases of the samples (Figure 12).

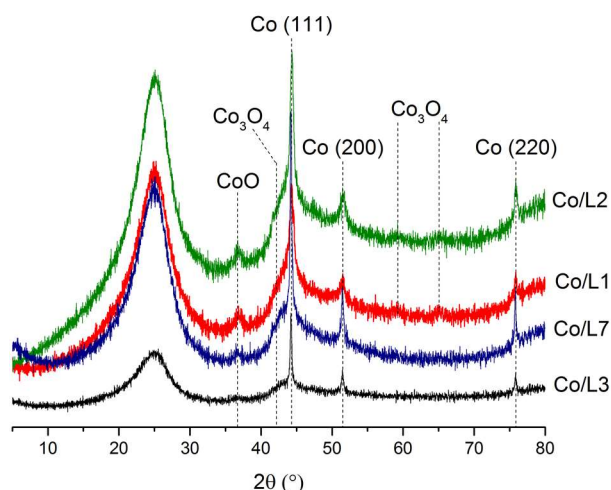


Figure 12. XRD patterns of the selected catalysts.

The XRD pattern revealed that the main specie present is metallic Co. In fact, peaks at 2θ values of 44.4, 54.7 and 76.0 corresponds to (111), (200) and (220) crystal planes of cobalt in its ground state.^[26] Minor peaks corresponding to 2θ values of 37.3, 42.5, 59.5 and 65.2 were further detected and assigned to CoO and Co₃O₄.^[27] In addition, the broad peak at around $2\theta = 25$ is ascribed to the amorphous carbon-based support.

Next, XPS was employed to investigate the surface elemental composition and electronic states of the materials. As Figure 13 demonstrated, nitrogen is successfully incorporated into the carbonaceous matrix indicating that the employed ligands participate in the generation of these materials.

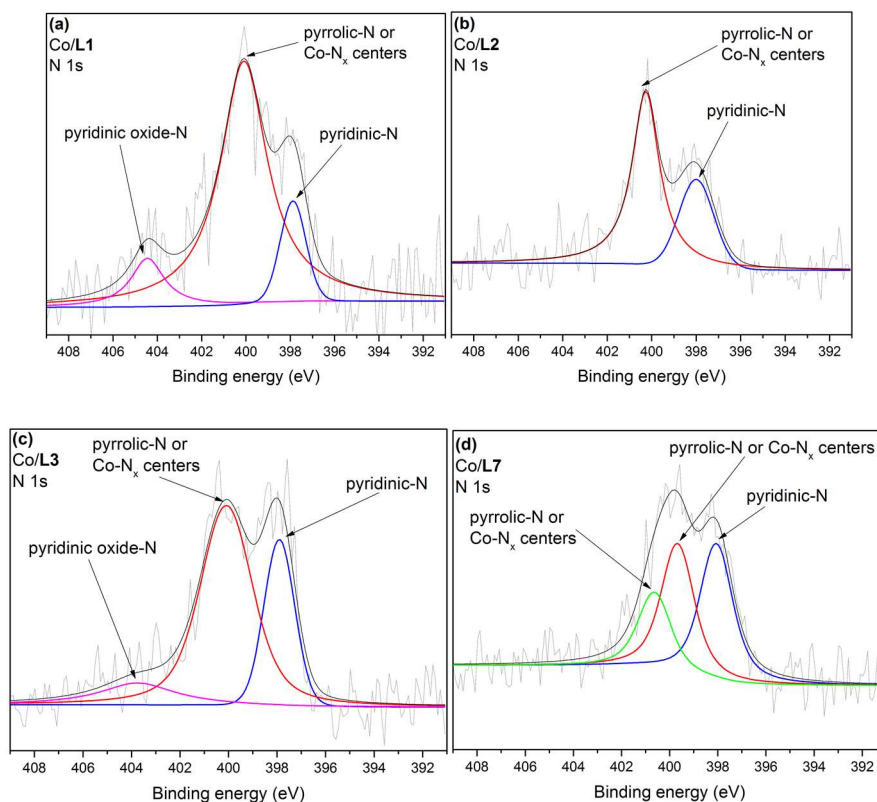
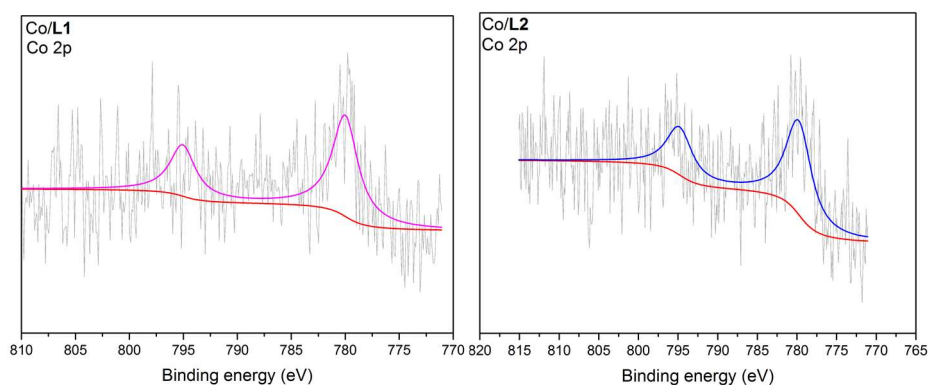


Figure 13. High resolution XPS N 1s spectra of Co/L1 (a), Co/L2 (b), Co/L3 (c) and Co/L7 (d)

Detected peaks ranging from 397.9 eV to 398.1 eV are ascribed to pyridinic-type N atoms whereas peaks at around 400 eV can be ascribed to pyrrolic configurations of the N atoms or N coordinated to Co (Co-N_x centers).^[28] Because of the expected proximity of the latter signals, it is impossible to unequivocally quantify the two independent contributions. Catalysts Co/L1 and Co/L3 exhibited two additional peaks at 404.4 eV and 403.8 eV, respectively. These can be assigned to N-oxides of the pyridinic N modifications. In the case of Co/L3, N-oxide formation upon pyrolysis is explained by the presence of oxygen atoms directly bounded to the chelating N atoms in the precursors. However, in the case of Co/L1, the N-O signals are likely to originate from traces of adventitious oxygen inside the pyrolytic oven. Co/L7 showed slightly different peak features with three states at 398.1 eV, 399.7 eV and 400.6 eV. Whereas the first state can be attributed to pyridinic N as for the other samples, the both latter ones can be correlated to the Co-N_x centers and pyrrolic N. Co 2p region was further examined (Figure 14).



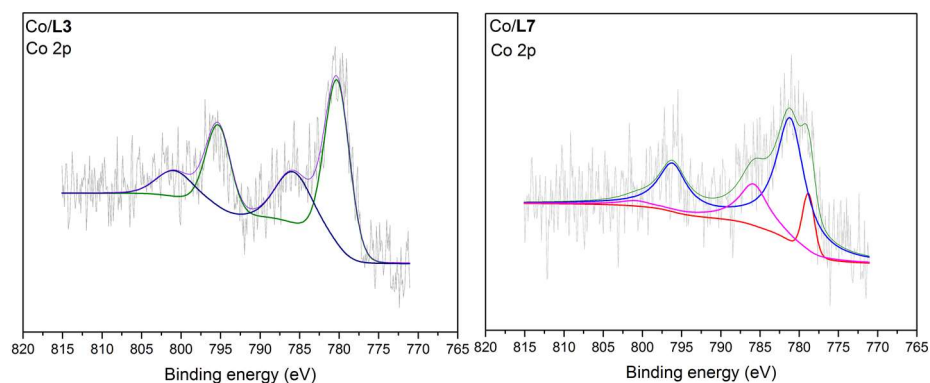


Figure 14. High resolution XPS Co 2p spectra of Co/L1 (top left), Co/L2 (top right), Co/L3 (bottom left) and Co/L7 (bottom right).

Catalysts Co/L1 and Co/L2 displayed similar peaks. For the Co/L1 and Co/L2 two peaks were observed, one at 780 eV corresponding to the $2p_{3/2}$ state and the other one at 795 eV correlated with the $2p_{1/2}$ state. Due to the low amount of Co it is not possible to distinguish between bi- and three valent Co electronic situations. Peaks at 786 eV and 800 eV (typical for CoO) were found for the other two samples.^[29] Finally, Co/L7 presented an additional peak at 778.8 eV representative of Co atoms in zero oxidation state.^[30] Furthermore, carbon and oxygen region were studied (Figure 15).

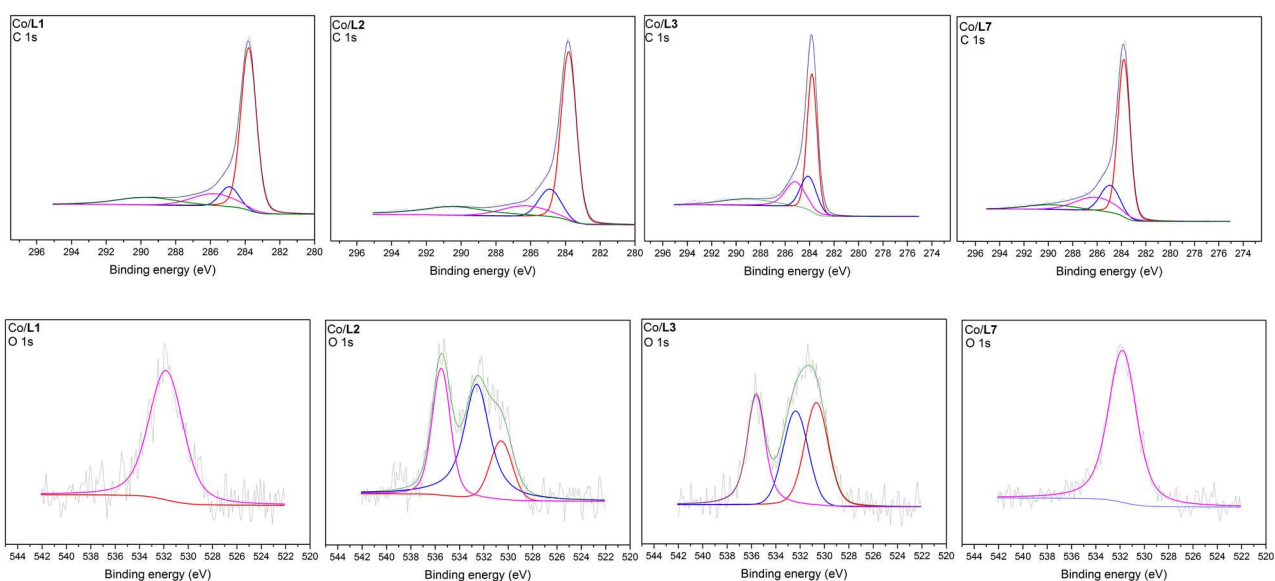


Figure 15. High resolution C 1s (first row) and O 1s (second row) XPS spectra of the selected catalysts.

Concerning the former, the four catalysts displayed an analogous pattern. The peaks at 283.8 eV, 284.9 eV and 285.2-286.3 eV can be attributed to the presence of C=C, C=N and C-N bonds confirming the enclosure of the N atoms into the graphitic matrix. Every C 1s spectra showed the shake-up feature around 290 eV arising from the π to π^* transition typical for graphitic like compounds. The interpretation of the oxygen region is not straightforward due to a multitude of possible O containing compounds, e.g. CoO, Co(OH)₂ and several organic moieties containing C-O and C=O bonds. The peaks between 530.6 eV and 533 eV can be ascribed to all these compounds.^[31]

To evaluate morphological differences caused by the use of different ligands, high resolution transmission electron microscopy (HRTEM) technique was exploited. Parallel high angle annular dark field (HAADF) and annular bright field (ABF) images were taken. The HAADF images are sensitive to differences in the atomic number (Z) of the atoms present in the sample. In the current case, oxidic cobalt phases show less contrast than metallic cobalt. In combination with EDX measurements and indexing of high resolution images, it is possible to describe the Co containing phase nature. Since HAADF prefers the imaging of heavy elements, ABF has to be used for light elements such as carbon. By using this technique, graphitic structures at the top of the NP were observed.

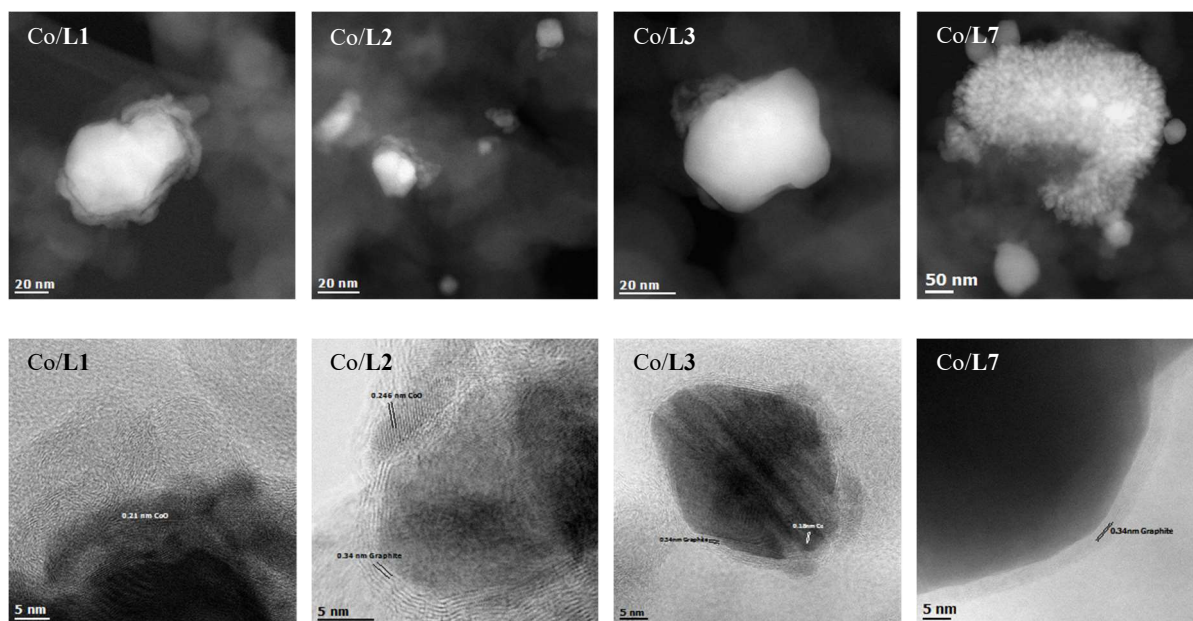


Figure 16. HRTEM images of the selected catalysts: HAADF (upper row) and ABF (lower row).

Figure 16 shows typical images for the selected catalysts. The different appearance of particles with metallic core and oxidic shells can be easily seen. Whereas Co/L1 contains completely covered particles, the oxidic coverage decreases for Co/L2 and Co/L3. Co/L7 shows a different morphology. Here, the Co-containing phase is split into agglomerates of small oxidic and bigger nearly uncovered metallic particles. As shown by the ABF images, graphitic structures (graphene layers) appear at the top of the metallic Co fractions intimately in contact with the particles. For Co/L1 no graphitic envelops were found since the metallic Co is completely embedded by cobalt oxide. From Co/L2 to Co/L7 the cobalt oxidic shell decreases and it can be observed (Co/L2) that only free metallic Co is in tight contact to the graphitic or graphene layers. The chemical composition of the four materials was further corroborated by EDX (energy dispersive X-ray) analysis (Figures S1, S2, S3 and S4). The core of the NP reveals the presence of only Co whereas the periphery is composed by Co and O indicating the formation of oxidic species.

Finally, TPR was employed to get insight into the reducibility of the catalytic materials (Figure 17). Co/L1, Co/L2 and Co/L3 showed a very similar behavior. In contrast, Co/L7 displayed a peak area much

smaller than the previous ones. This is ascribed to a greater metallic contribution in the NP. This result is in agreement with that obtained from the XPS and STEM studies for the same catalyst.

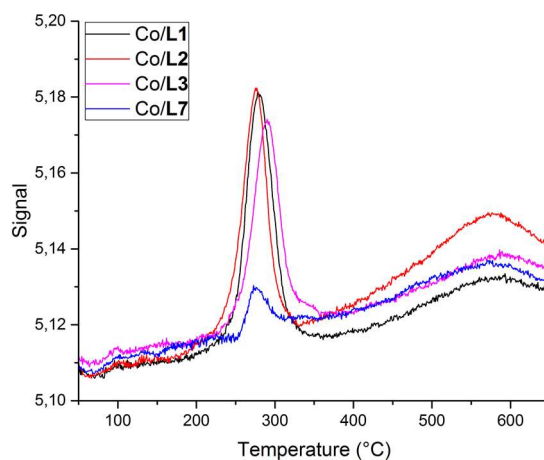


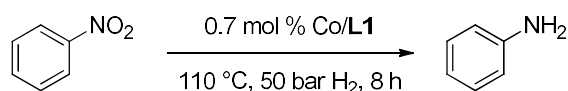
Figure 17. TPR patterns of the selected catalysts.

In conclusion, similarly to Co-Co₃O₄/NGr@C, most of the prepared materials exhibit a core-shell structure in which metallic and oxidic species coexist. In addition, nitrogen-doped graphitic and graphene-type layers in contact with these NPs are observed.

4.3. Evaluation of the catalytic activity

The catalytic performance of the prepared materials was primarily explored in the hydrogenation of nitrobenzene to aniline. Initially, Co/L1 was employed for the hydrogenation of nitrobenzene in the presence of different solvents (Table 6).

Table 6. Catalytic hydrogenation of nitrobenzene to aniline: solvent screening.^a



Entry	Solvent	Conversion [%] ^b	Selectivity [%] ^b
1	hexane	<1	-
2	toluene	<1	-
3	AcOEt	<1	-
4	AcOEt-H ₂ O	11	>99
5	THF	5	>99
6	THF-H ₂ O	15	>99
7	EtOH	21	>99
8	EtOH-H ₂ O	28	>99
9	MeOH	20	>99
10	MeOH-H ₂ O	24	>99

^a Reaction conditions: 0.5 mmol PhNO₂, 2 mL solvent (+ 100 μL H₂O if stated); ^b Conversion and selectivities are based on GC analyses, using *n*-hexadecane as an internal standard.

As expected, while apolar solvents proved to be detrimental for the reactivity, polar ones allowed for higher conversions. In particular, EtOH was found to be the best solvent. The addition of small amount of water (1:20 by volume) further increased the nitrobenzene conversion in every case. With all the tested solvents, selectivities towards the desired product were very high.

In agreement with the findings previously discussed (Project 1, first part), organic bases are beneficial for achieving higher conversions. Thus, different basic additives were tested in combination with catalyst Co/L2 (Table 7).

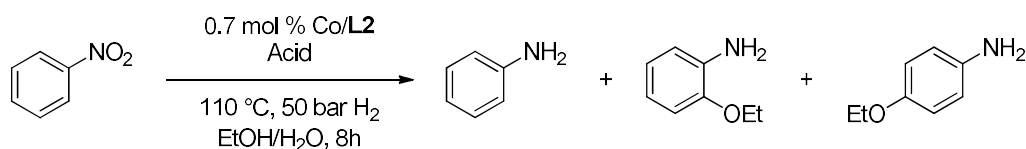
Table 7. Catalytic hydrogenation of nitrobenzene to aniline: base screening.^a

Entry	Base	Conversion [%] ^b	Selectivity PhNH ₂ [%] ^b	Selectivity azobenzene [%] ^b	Selectivity azoxybenzene [%] ^b
1	-	63	>99	-	-
2	NaOH	>99	17	59	11
3 ^c	NaOH	>99	21	36	23
4 ^d	NaOH	52	31	7	53
5	Na ₂ CO ₃	48	95	<1	<1
6	Na ₃ PO ₄ ·6H ₂ O	68	92	1	2
7	NMM ^e	79	>99	-	-
8	Pyridine	>99	95	-	-
9	DMAP ^f	>99	98	-	-
10	Et ₃ N	92	>99	-	-

^a Reaction conditions: 0.5 mmol PhNO₂, solvent: 2 mL EtOH + 100 μL H₂O; ^b Based on GC analysis using *n*-hexadecane as an internal standard; ^c Co/L3 was used instead of Co/L2; ^d No catalyst; ^e N-methylmorpholine; ^f 4-dimethylaminopyridine.

Inorganic bases led to moderate or full conversions but the selectivity into the aniline dropped owing to the formation of azobenzene and azoxybenzene as side products. As expected, when Et₃N was employed, complete conversion and full selectivity were achieved, thus avoiding the formation of undesired side products. For a complete investigation of the catalytic system, acidic additives were also tested (Table 8).

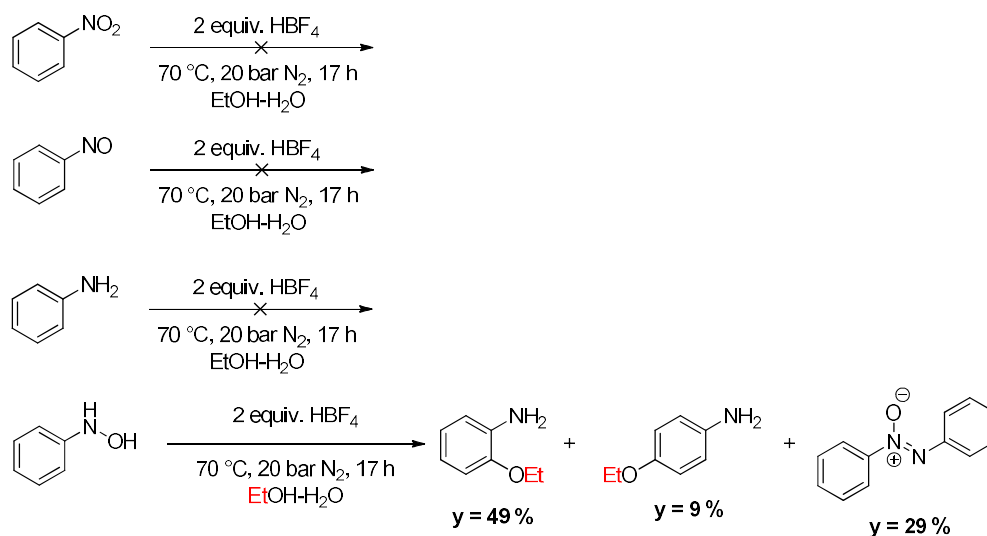
Table 8. Catalytic hydrogenation of nitrobenzene to aniline: acid screening.^a



Entry	Acid	Equivalents with respect to PhNO ₂	Conversion [%] ^b	Selectivity PhNH ₂ [%] ^b	Selectivity 2-ethoxyaniline [%] ^b	Selectivity 4-ethoxyaniline [%] ^b
1	-	-	63	>99	-	-
2	CF ₃ COOH	1	61	61	6	19
3	CF ₃ COOH	2	61	55	10	31
4	HBF ₄ ·OEt ₂	1	60	22	15	61
5	HBF ₄ ·OEt ₂	2	60	18	12	69
6	Al(OTf) ₃	1	45	23	14	54
7	Zn(OTf) ₂	1	48	73	5	21

^a Reaction conditions: 0.5 mmol PhNO₂, solvent: 2 mL EtOH + 100 μL H₂O; ^b Based on GC analysis using *n*-hexadecane as an internal standard.

Two Brønsted (HBF₄·OEt₂ and CF₃COOH) and two Lewis acids (Al(OTf)₃ and Zn(OTf)₂) were used at various concentrations. In every cases, a slight decreasing of the conversion and a drop in the selectivity were detected. The decline of the selectivity was attributed to the formation of 2-ethoxy- and 4-ethoxyaniline. Control experiments carried out under a dinitrogen atmosphere without the catalyst and in the presence of HBF₄·OEt₂ (2 equivalents) revealed that nitrobenzene, nitrosobenzene or aniline do not react. On the contrary, *N*-phenylhydroxylamine under the same conditions led to the formation of 2-ethoxyaniline, 4-ethoxyaniline and azoxybenzene in 49, 9 and 29 % yield, respectively (Scheme 5).



Scheme 5. Behavior of nitrobenzene, nitrosobenzene, aniline and *N*-phenylhydroxylamine with HBF₄ under catalytic reaction conditions.

This behavior was previously reported in the case of both Brønsted^[32] or Lewis acids.^[33] Having good conditions in our hands, the seven catalysts were tested in the benchmark hydrogenation of nitrobenzene to

aniline with and without the addition of Et₃N. In every case, the addition of the organic base led to improved performance (Figure 18).

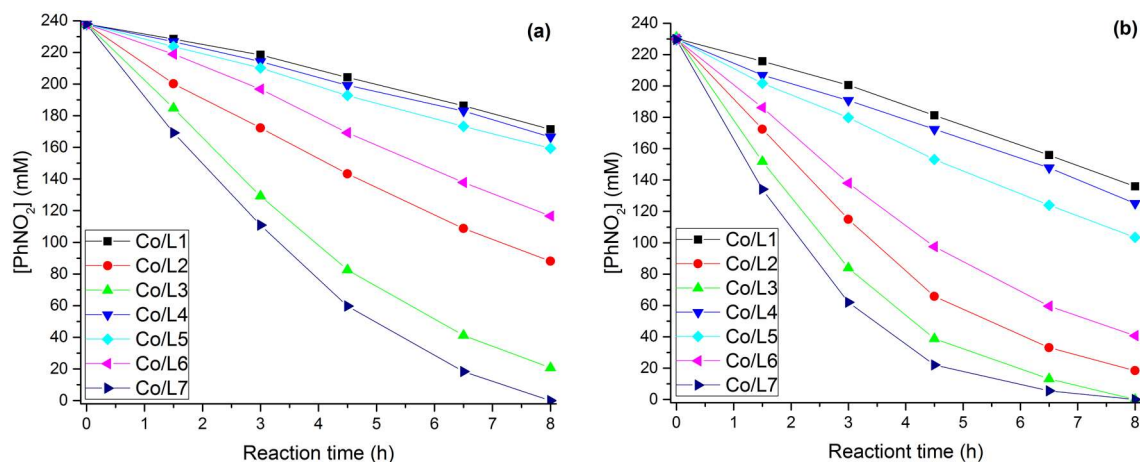


Figure 18. Variation of [PhNO₂] during the reaction without (a) and with (b) 1 equiv. of Et₃N. Reaction conditions: 0.5 mmol PhNO₂, 0.7 mol % Co, solvent: 2 mL EtOH + 100 μL H₂O, 50 bar H₂, 110 °C.

More specifically, Co/L7 displayed the maximum activity followed by Co/L3, Co/L2, Co/L6, Co/L5, Co/L4 and finally Co/L1. Interestingly, this trend is retained even if Et₃N was added, which indicates that the base acts as promoter but leaves the catalytic material unaffected. In all cases selectivities were very high and no side-products such as nitrosobenzene, azobenzene or azoxybenzene were detected at the end of the catalytic experiment. This observation, coupled with the fact that selectivities into aniline increased with increasing reaction time (Figure 19), clearly demonstrates that *N*-phenylhydroxylamine is an intermediate in the present catalytic transformation.

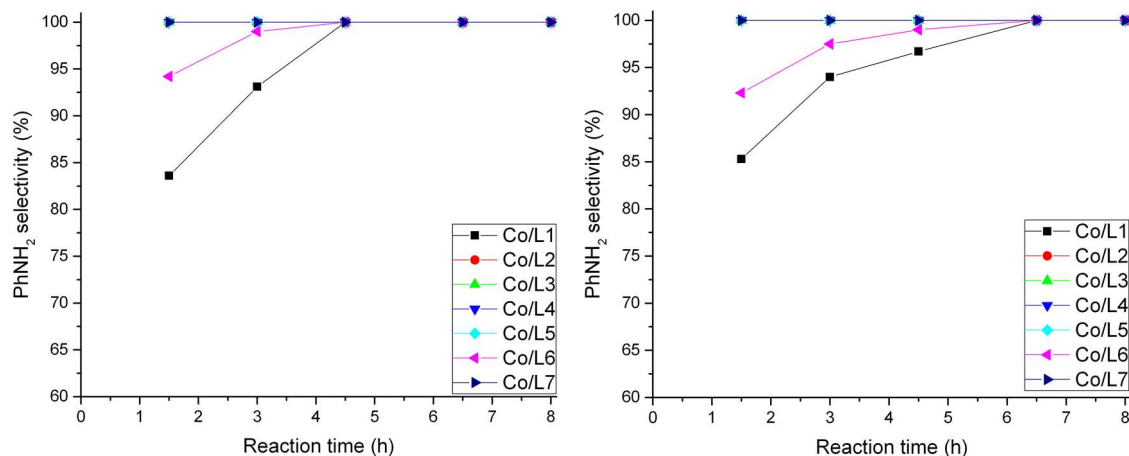


Figure 19. Variation of PhNH₂ selectivity during the reaction conducted without (left) and with (right) the addition of Et₃N. Reaction conditions: 0.5 mmol PhNO₂, 0.7 mol % Co, solvent: 2 mL EtOH + 100 μL H₂O, 50 bar H₂, 110 °C.

Next, the reusability of Co/L7 was investigated in a six-fold scaled up reaction showing a good recyclability (Figure 20). A slight decrease of the conversion was observed after the first and second recycling. However, after the second run the catalytic performance remained constant. In addition, the selectivity was completely retained at a value of > 99 % throughout the 5 recycling experiments.

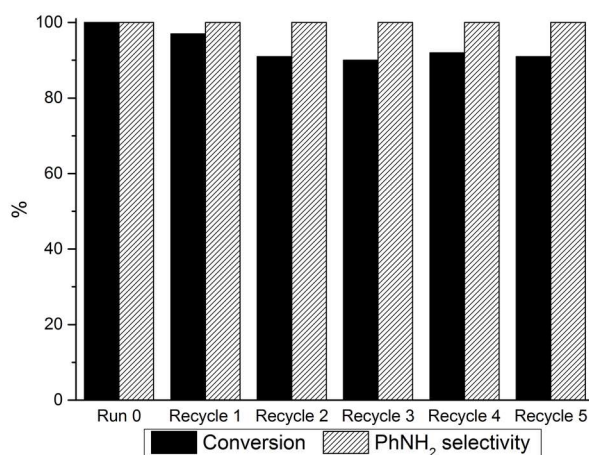
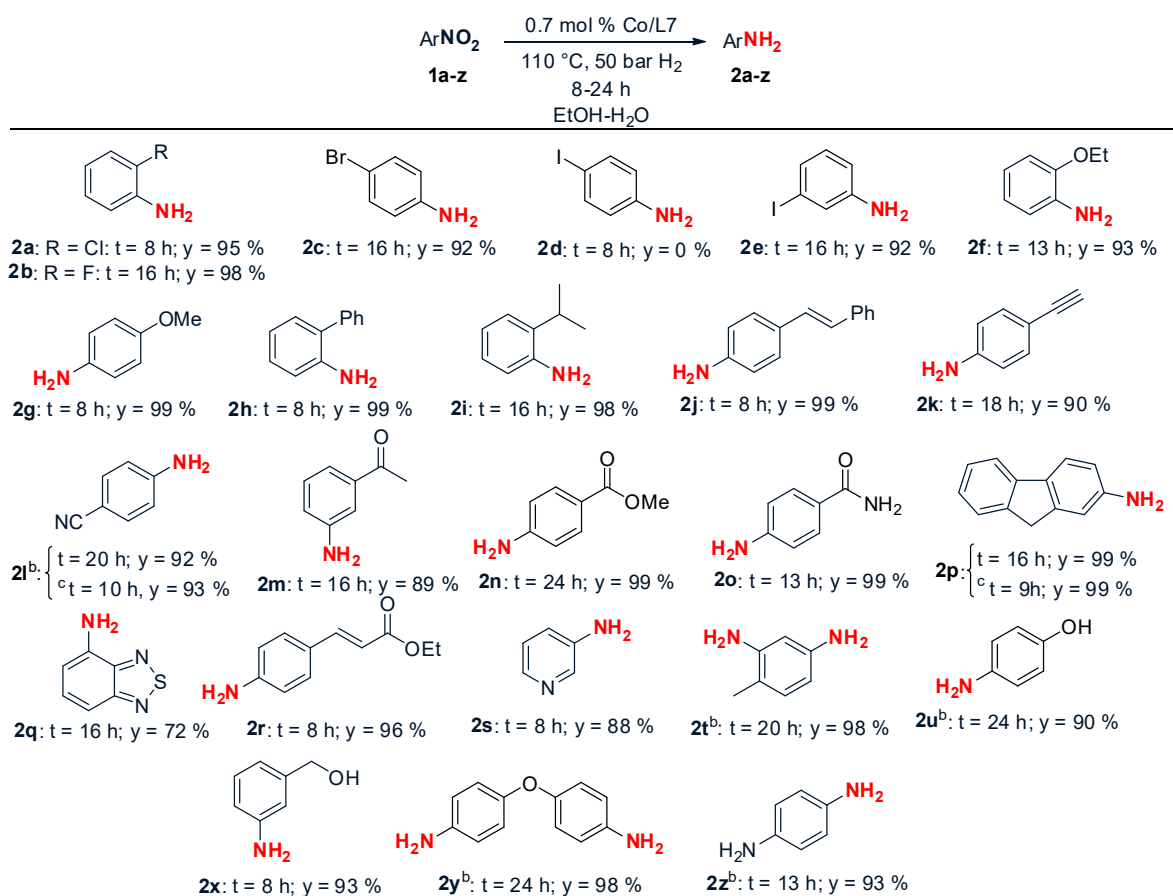


Figure 20. Recycling experiments of Co/L7. Reaction conditions: 3 mmol PhNO₂, 0.7 mol % Co/L7, solvent: 12 mL EtOH + 600 μ L H₂O, 8 h, 50 bar H₂, 110 °C.

ICP analysis of the liquid phase after each recycle indicated no Co leaching (detection limit is 0.5 ppm). In addition, Maitlis' hot filtration test was carried out in order to detect whether soluble active Co species were present to catalyse the reaction, (Table S9). The results confirmed that no active cobalt was leached. Thus, we conclude that the employed catalyst is inherently heterogeneous.

Subsequently, the reaction scope was explored employing various substituted aromatic nitro compounds as substrates (Scheme 6).



Scheme 6. Co/L7-catalysed hydrogenation of substituted nitro compounds: reaction scope.

The catalytic system is excellently tolerant to halogen containing substrates. The presence of Br, Cl or F did not affect the selectivity and the various nitro compounds were smoothly converted into the corresponding anilines (**2a**, **2b** and **2c**). Only in the case of 4-iodonitrobenzene (**1d**), dehalogenation occurred producing aniline and N-ethylaniline in 83 % and 16 % yield, respectively (Figure 21). Control experiments reveals that even 4-iodoaniline is subjected to dehalogenation under catalytic conditions. The formation of N-ethylaniline is likely to be caused by *in-situ* formation of EtI from ethanol (solvent) and HI derived from the dehalogenation followed by alkylation of the amino group (Figure 21).^[34]

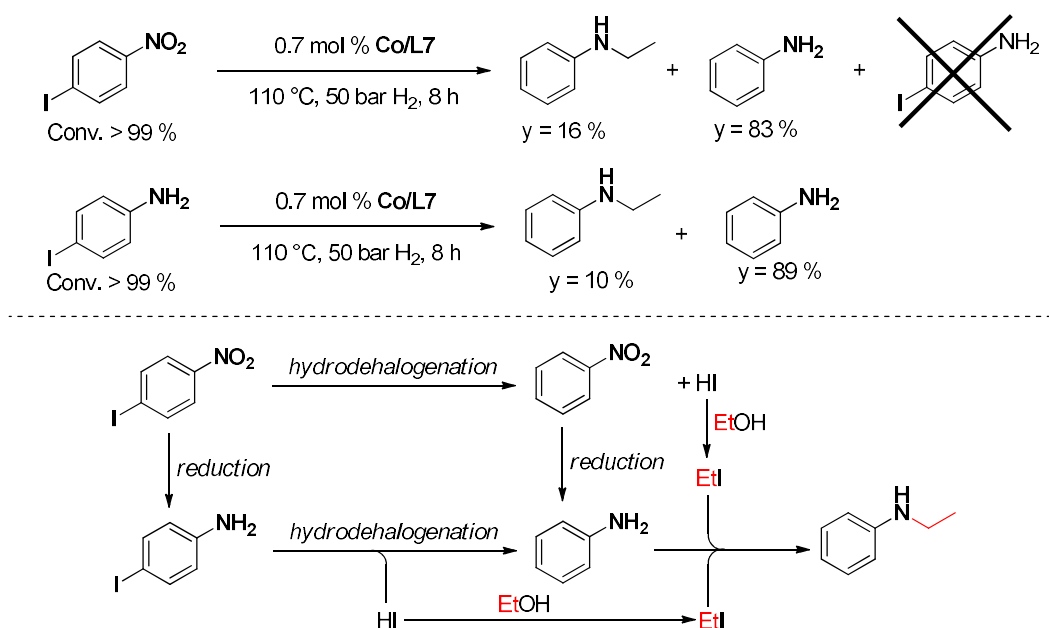


Figure 21. Co/L7-catalysed reduction of 4-iodonitrobenzene: proposed hydrodehalogenation and alkylation pathways.

Notably, 3-iodonitrobenzene (**1e**), did not show this undesired pathway affording the desired product in excellent yield. Electron donating substituents (**2f**, **2g**, **2u**, **2x**, **2y**, **2z**) and steric hindrance (**2h**, **2i**) were well tolerated. Other reduction-labile functional groups such as double (**2j**) or triple- (**2k**) carbon-carbon bonds, nitriles (**2l**), ketones (**2m**), simple and conjugated esters (**2n**, **2r**) and amides (**2o**) are well tolerated affording the corresponding anilines in very high yields. Heteroaromatic nitro compounds were hydrogenated furnishing the corresponding anilines in good (**2s**) and moderate (**2q**) yields. An excellent selectivity was also achieved in the reduction of 2,4-dinitrotoluene (**1t**) into the corresponding diamine. Such hydrogenation is currently employed yearly on a multi-million tons scale as a step in the preparation of 2,4-toluendiisocyanate. As mentioned earlier, the addition of 1 equivalent of Et₃N boosts the activity of the catalytic system (see **1l** and **1q**). The pharmaceutically important substrates nitroresorcinol (**1aa**) and Flutamide (**1ab**) were also investigated in the catalytic hydrogenation. (Figure 22)

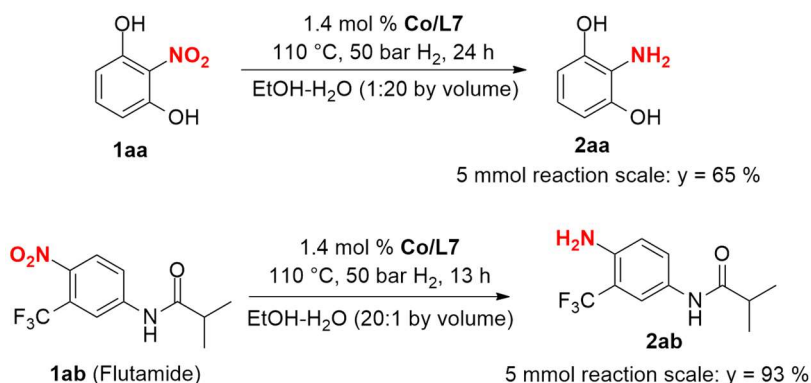


Figure 22. Co/L7-catalysed hydrogenation of pharmaceutically important substrates.

The corresponding reduction products are key-intermediates in the preparation of biologically active compounds and are valuable starting molecules in total syntheses.^[35] In the case of **1aa**, the reaction was slow using EtOH-H₂O with a volume ratio 20:1 as solvent mixture but proceeded faster in a reaction media almost exclusively composed of water. This is likely to be attributed to the very strong intramolecular H-bond between the partially positively charged H of the OH groups and the two negatively-charged oxygen atoms of the adjacent nitro group (Figure 23).^[36]

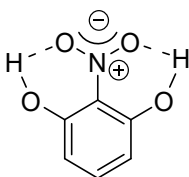


Figure 23. Intramolecular H-bond in nitroresorcinol.

Thus, a strong polar system is required to break the H-bond and facilitates the reduction step. In fact, upon shifting from a 20:1 mixture of EtOH:H₂O to a 1:20 ratio of EtOH:H₂O, the dielectric constant of the reaction medium triples (from 20 to 60 at 80 °C).^[37] However, it was not possible to conduct the catalytic transformation in pure water as the solubility of the substrate was insufficient in this case. This reaction is the first example of a non-noble metal catalysed reduction of 2-nitroresorcinol to 2-aminoresorcinol. Similarly, hydrogenation of **1ab** proceeded with excellent chemoselectivity and its purification does not require expensive and waste-producing chromatographic separation techniques. In fact, just filtration over Celite® and consecutive solvent evaporation were needed to obtain the product in a pure form at the end of the reaction.

4.4. Kinetic studies

In order to understand the different catalytic behavior of the seven employed catalysts, kinetic experiments were carried out. The collected data are in accordance with a first order kinetics in PhNO₂ (Figure 24).

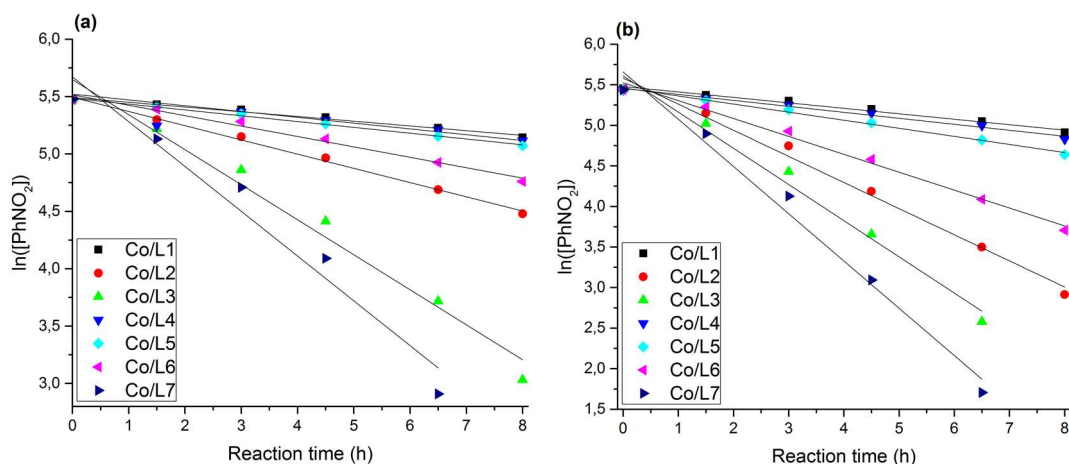


Figure 24. First order kinetic plot of the seven catalysts without (a) and with (b) 1 equiv. of Et₃N. Reaction conditions are reported in the caption of Figure 18.

Despite the structural and morphological similarity of the prepared materials, the bulk N content (wt. %) varies from catalyst to catalyst (see Table 9). Since control experiments confirmed that the catalyst prepared without any nitrogen ligand is totally inactive (Table S3, entry 5), we assumed that the activities of the catalysts correlates with the bulk nitrogen content in the final catalytic material. In fact, if one plots the first-order kinetic constant vs the nitrogen content in the final material a clear correlation is observed: the higher is the nitrogen content, the better the activity of the catalyst. Notably, the same trend is retained if the reactions were carried out in the presence of 1 equiv. of Et₃N. In this case, kinetic constants were dramatically improved (Figure 25 and Table 9).

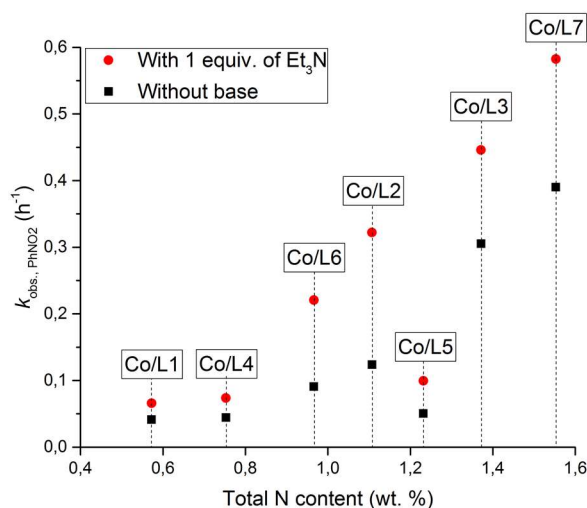


Figure 25. Correlation between first-order kinetic constant and total nitrogen content in the catalytic material.

Table 9. Comparison between kinetic constants for reactions conducted with and without Et₃N.

Catalyst	C; H; N; Co ^a [%]	Kinetic constant	Kinetic constant	$\frac{k_{Et_3N}}{k}$
		without Et ₃ N k [h ⁻¹]	with 1 equiv. Et ₃ N k_{Et_3N} [h ⁻¹]	
Co/L1	85.93; 0.13; 0.92; 3.13	0.0413	0.066	1.6
Co/L2	87.30; 0.10; 1.48; 3.00	0.1239	0.322	2.6
Co/L3	87.81; 0.14; 1.67; 3.49	0.3052	0.4461	1.5
Co/L4	85.86; 0.30; 1.05; 3.26	0.0443	0.0737	1.7
Co/L5	86.38; 0.24; 1.40; 3.20	0.0506	0.0996	2.0
Co/L6	83.48; 0.24; 1.23; 3.25	0.0907	0.2206	2.4
Co/L7	80.19; 0.28; 1.90; 3.16	0.3903	0.5825	1.5

^a C, H, N values were determined by CHN analysis; Co content was determined by AAS.

This general trend is observed for all catalysts except for Co/L5. This can be attributed to the steric hindrance of the naphthyl groups that probably negatively affect the coordination ability of the ligand to the metal center. Thus, the N atoms are equally incorporated into the carbon matrix but not close to the catalytically active site. In fact, the catalyst prepared using a 1:1 molar ratio of Co(OAc)₂ and L5 exhibited a similar activity to Co/L5. Conversely, the catalyst prepared by combining Co(OAc)₂ and L1 (less sterically hindered) in a 1:1 molar ratio showed a much lower activity (Figure 26).

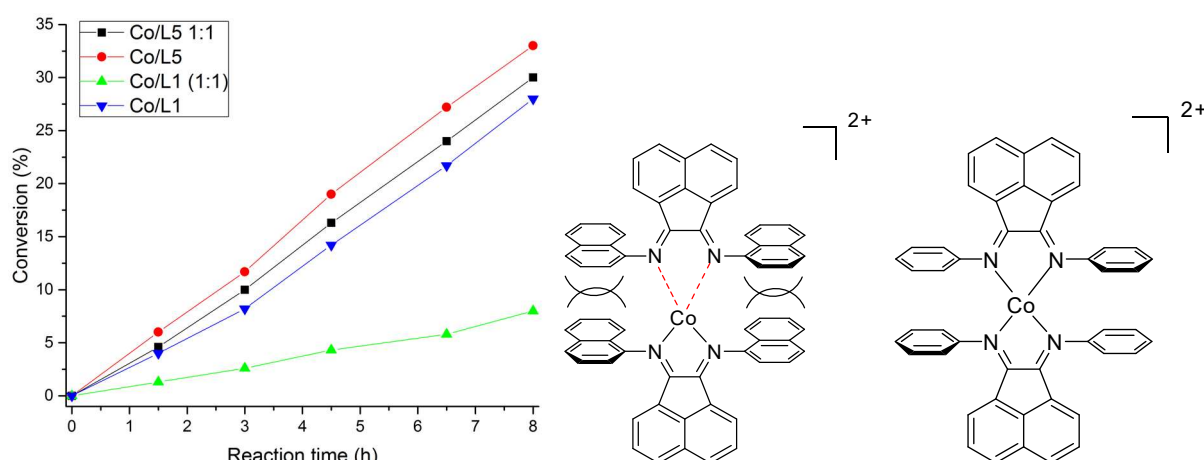


Figure 26. Comparison between the catalysts Co/L1 and Co/L5 prepared with a molar ratio metal:ligand 1:1 or 1:2.

In addition, for the selected characterized materials, a correlation with the free pyridinic N content measured by XPS was established (Figure 27 left). Since no similar correlations were observed in the case of pyrrolic/Co-N_x configurations (signals at around 400 eV in the XPS spectra), we conclude that uncoordinated pyridinic N atoms play a pivotal role in the catalytic activity (graphitic or N-oxidic configurations were not taken into account since they were not found in all the catalysts) (Figure 27 left).

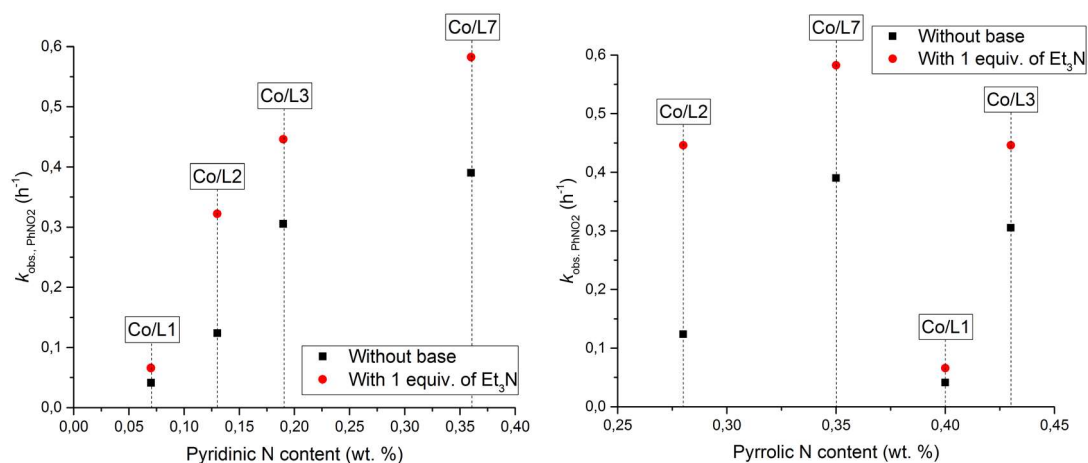


Figure 27. Correlation between first order kinetic constant and pyridinic N (left) and pyrrolic/Co-N_x configurations (right).

A related observation has been described for NGr-based catalysts for electrochemical applications.^[38] However, to the best of our knowledge, this is the first time that such a correlation is described for catalytic hydrogenation reactions. Investigations of the reaction order with respect to Et₃N and H₂ pressure using Co/L2 as the model catalyst, indicate a first-order kinetics in both the reactants (Figure 28). This latter observation is ascribed to the linear dependence of the H₂ solubility with increasing gas pressure in alcoholic solvents.^[39]

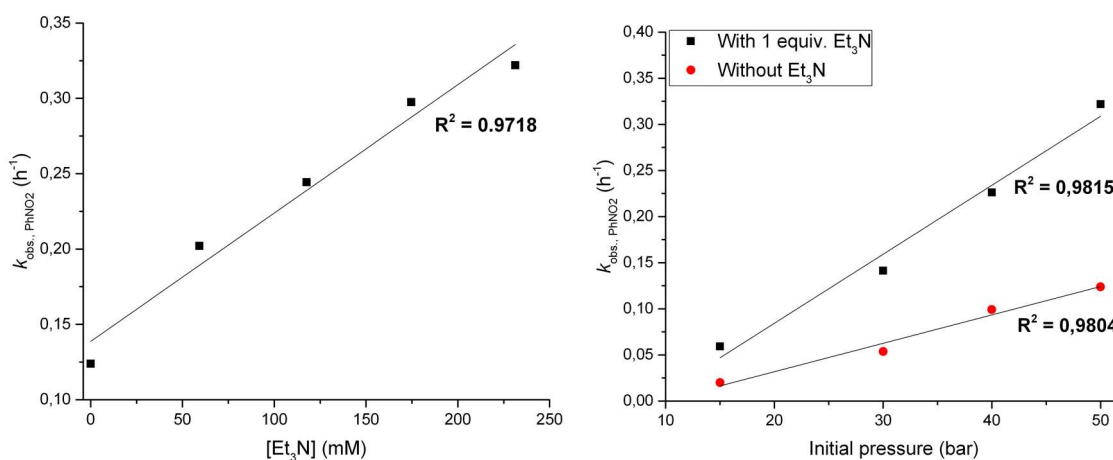
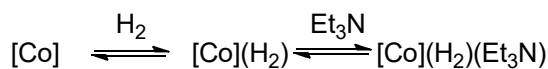


Figure 28. Evaluation of the reaction order for Et₃N (left) and H₂ pressure (right) using Co/L2 as catalyst.

First order kinetics with respect to nitrobenzene, dihydrogen and, if present, triethylamine cannot be explained by a single slow step without the existence of at least one kinetically relevant equilibrium stage before the r.d.s. Given that activation of nitrobenzene is very unlikely to be reversible (nitroarenes are among the weakest bases known and their metal complexes are extremely labile), the most likely explanation for the observed kinetic data is that reversible formation of an activated form of dihydrogen first occurs, the equilibrium being strongly shifted to the reagents side. If this were not true the kinetics would deviate from first order for both H₂ and Et₃N. The activated dihydrogen then reacts in the r.d.s. with nitrobenzene. Indeed, by indicating with [Co] the active cobalt site, with [Co](H₂) its dihydrogen adduct and with [Co](H₂)(Et₃N) the activated intermediate, the total active site concentration, [[Co]T], is given by eq. 1:

$$(eq. 1) \quad [[Co]_T] = [[Co]] + [[Co](H_2)] + [[Co](H_2)(Et_3N)]$$

Given the equilibria:



It turns out that:

$$(eq. 2) \quad K_{eq} = \frac{[[Co]] \cdot [H_2] \cdot [Et_3N]}{[[Co](H_2)(Et_3N)]}$$

Since the first irreversible step is the first hydrogen uptake by nitrobenzene (according to the first order dependence of the rate on the concentration of this reagent), the rate of nitrobenzene consumption is given by:

$$(eq. 3) \quad -\frac{d[PhNO_2]}{dt} = k[PhNO_2][[Co](H_2)(Et_3N)] = k[PhNO_2] \frac{[[Co]][H_2][Et_3N]}{K_{eq}} = k_{obs} [PhNO_2][[Co]][H_2][Et_3N]$$

where:

$$(eq. 4) \quad [[Co]] = [[Co]_T] - [[Co](H_2)] - [[Co](H_2)(Et_3N)]$$

Given the large excess of dihydrogen under the reaction conditions and the fact that triethylamine is not consumed irreversibly and surely $[Et_3N] \gg [[Co]_T]$, the values of $[H_2]$ and $[Et_3N]$ can be considered to be constant during the reaction. However, in general the concentration of free active cobalt sites, $[[Co]]$, depends on both dihydrogen and triethylamine concentrations and, according to equilibrium (2), should decrease as $[H_2]$ and $[Et_3N]$ increase. This would result in a deviation from first order dependency of the reaction rate from both H_2 and Et_3N concentrations, which is in contrast to the clean first order with respects to these reagents experimentally observed. The only situation that fits all observed kinetic data is that in which both equilibria in eq. 2 are strongly shifted on the left side through the whole range of concentrations/pressures employed in our kinetic study. Under these conditions, $[[Co](H_2)] + [[Co](H_2)(Et_3N)] \ll [[Co]]$ and $[[Co]] \cong [[Co]_T] = \text{constant}$. A similar, simplified, analysis holds for the competitive pathway in which no triethylamine is involved. The sharp intercept in the kinetic plot k_{obs} vs. $[Et_3N]$ with the Y axis ($[Et_3N] = 0$) is also a strong point supporting the conclusion that most of the active cobalt site are in the “free” form during the reaction. In fact, if this condition holds, the Et_3N -dependent and the Et_3N -independent pathways can occur at the same time without interfering with each other and the total k vs. $[Et_3N]$ kinetic plot is just the sum of a constant term and a straight line, as experimentally observed. Otherwise, a distinct curvature should be observed in proximity of the Y axis, which is not the case.

Based on reactivity data, and supported by the evidences suggested in the first part, we postulate that this kind of hydrogenations proceeds by a heterolytic activation of dihydrogen. The kinetic data obtained in this work not only confirms the general validity of this explanation for this class of catalysts, but also add further details. In particular, the linear dependence of the reaction rate on triethylamine concentration with a non-zero intercept points to a reaction scenario where two independent and competing mechanisms occur, in which either a nitrogen atom of the support or that of Et₃N is involved, but not both. Based on the kinetic investigations, we propose the pyridinic N content is crucial for the catalyst activity. The fact that the dihydrogen activation equilibrium is shifted towards the left is not only consistent with the kinetic orders observed, but also explains why the rate of the Et₃N-free reaction is not affected by triethylamine concentration. Indeed, at any given moment the active sites are virtually all available independent of the Et₃N concentration. A schematic representation of the initial steps of the reaction is shown in Figure 29.

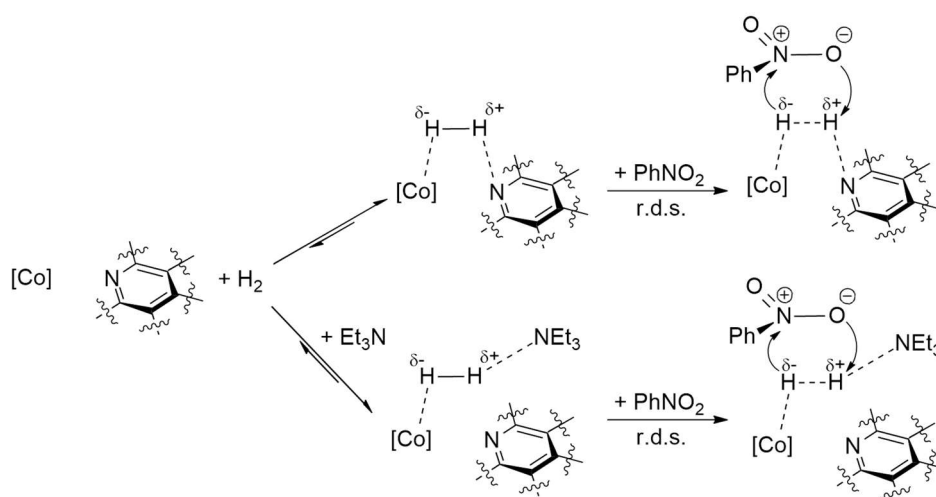


Figure 29. Proposed reaction mechanism.

Recent both experimental and theoretical works dealing with transition metal/NGr catalysts indicate that the nature of the active sites can be a M-N_x-C_y network in which the metal is present as a single atom (so-called single-atom or single-site catalysis, SAC).^[40] According to our structural characterization we postulate the involvement of either single-site Co centers or Co NP coordinated to pyridinic N atoms whose configurations are not definitely elucidated. The established correlation between non-coordinated pyridinic N configurations and activity (Figure 27 left) suggests an internal base role by the latter. The relationship between activity and amount of pyridinic N can be ascribed to its basicity. In agreement with this proposal, a recent study described that in NGr-based materials, the pyridinic N exhibits the maximum basicity among the three types of N (the other two are pyrrolic and graphitic).^[41] These conclusions are corroborated by control experiments. Indeed, it must be stressed that the contemporary presence of both a cobalt source and a nitrogen ligand before the pyrolysis step is required to obtain active catalysts.

Finally, the most active catalyst (Co/L7) was compared with commercially available noble-metal based heterogeneous catalysts (Tables 11 and 12). Two model substrates were employed for that purpose: (*E*)-4-nitrostilbene (**1j**) and 3-nitroacetophenone (**1m**). In both cases, Co/L7 showed superior chemoselectivity

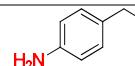
towards the formation of the desired products, while several side- and over-reduction products were detected when the reactions were carried out with standard noble-metal based catalysts. Aromatic ring hydrogenation and double bond saturation are the most frequent side reactions in the case of **1j**, whereas carbonyl hydrogenation and hydrodeoxygenation occur in the case of **1m**.

Table 10. Hydrogenation of (*E*)-4-nitrostyrene with noble-metal based commercially available heterogeneous catalysts.

Entry	Catalyst	Conv. [%] ^b	Sel. 2j [%] ^b	Other by-products detected by GC-MS
1	Co/L7	>99	>99	-
2	5 % wt. Ru/C	>99	<1	
3	10 % wt. Pd/C	>99	<1	
4	Raney®-Ni	>99	<1	
5	5 % wt. Pd/Al ₂ O ₃	>99	traces	
6	10 % wt. Pt/C	>99	traces	

Table 11. Hydrogenation of 3-nitroacetophenone with noble-metal based commercially available heterogeneous catalysts.

Entry	Catalyst	Conv. [%] ^b	Sel. [%] ^b	Other by-products detected by GC-MS
1	Co/L7	>99	89	-
2	5 % wt. Ru/C	>99	<1	
3	10 % wt. Pd/C	>99	<1	
4	Raney®-Ni	>99	<1	
5	5 % wt. Pd/Al ₂ O ₃	>99	traces	



5. Conclusion

In conclusion, in the first part of this project, an in depth investigation of reaction conditions allowed us to significantly decrease temperature and hydrogen pressure (with respect to the original published values) in the hydrogenation of nitro compounds using Co-Co₃O₄/NGr@C and Fe₂O₃/NGr@C catalysts. Key-points for achieving the proposed target was the use of polar protic solvents (EtOH and MeOH) and the addition of bases (Et₃N and NH₃) which greatly enhance the activity of both the systems. Gratefully, the chemoselectivity into the production of substituted anilines was not affected at all. In addition, control experiments and other experimental evidences set the foundations for postulating a reaction mechanism in which a heterolytic activation of the dihydrogen is likely to be involved.

In the second part of the project, we demonstrated that Ar-BIANs and related α -diimine complexes are competitive N-ligand for the generation of active Co-bases heterogeneous catalysts instead of using 1,10-phenanthroline. Structural elucidations revealed chemical and structural features very similar to the congener Co-Co₃O₄/NGr@C. Even in this case, alcoholic polar solvents and base addition were found to be crucial for the catalytic performance. Furthermore, excellent chemoselectivity in the hydrogenation of variously substituted nitro compounds were detected as well as good a recyclability of the catalyst. Straightforward kinetic investigations suggested a linear and direct correlation between the activity of the catalysts (kinetic constant) and the total amount of nitrogen in the support. An additional correlation between the activity and the free pyridinic N in the support was demonstrated. All our findings, corroborated with very recent publications in the field, are in accordance with a catalytic site composed by single Co atoms coordinated to N functionalities. Finally, supported by the results presented in the first part, herein we validate our assumption for an heterolytic activation of the dihydrogen molecule.

6. Supplementary catalytic data and experimental section

6.1. General methods – reagents, solvents and manipulations

Concerning the synthesis of the ligands, all the reactions were carried out under a nitrogen atmosphere using standard Schlenk techniques. All glassware and magnetic stirring bars were kept in an oven at 120 °C for at least two hours and were cooled to room temperature under vacuum prior to use. CDCl₃ used for the NMR experiments was filtered on basic alumina and stored under nitrogen over 4 Å molecular sieves. Concerning the catalytic experiments, all manipulations were carried out in the air. Chemicals and solvents were purchased from Sigma Aldrich, Alfa Aesar or Tokyo Chemical Industry. Carbon powder VULCAN XC 72R® (code XVC72r, CAS No. 1333-86-4) was obtained from Cabot Corporation. Pyrolysis were carried out in a Dekema-Austromat 324 oven.

6.2. General methods - analysis and characterisation

TEM measurements were performed at 200 kV with an aberration-corrected JEM-ARM200F (JEOL, Corrector: CEOS). The microscope is equipped with a JED-2300 (JEOL) energy-dispersive X-ray spectrometer (EDXS) for chemical analysis. The sample was deposited without any pre-treatment on a holey carbon supported Cu-grid (mesh 300) and transferred to the microscope. The High-Angle Annular Dark Field (HAADF) and Annular Bright Field (ABF) images were recorded with a spot size of approximately 0.1 nm, a probe current of 120 pA and a convergence angle of 30-36°. The collection semi-angles for HAADF and ABF were 70-170 mrad and 11-22 mrad, respectively.

XPS data were obtained with a VG ESCALAB220iXL (ThermoScientific) with monochromatic Al K α (1486.6 eV) radiation. The electron binding energies E_B were obtained without charge compensation. For quantitative analysis the peaks were deconvoluted with Gaussian-Lorentzian curves, the peak area was divided by a sensitivity factor obtained from the element specific Scofiled factor and the transmission function of the spectrometer.

XRD pattern of the materials were recorded on a Panalytical X'Pert Pro diffractometer in reflection mode with Cu K α radiation ($\lambda=1.5406$ Å) and a silicon strip detector (X'Celerator).

NMR spectra of ligands and isolated anilines were recorded on a Bruker Avance DRX 300 or on a Bruker Avance DRX 400 operating at 300 and 400 MHz, respectively.

CHN analyses were performed using a Leco Microanalyser TruSpec or a PerkinElmer 2400 CHN. Metal content of the catalysts was determined by atom absorption spectroscopy using a PerkinElmer AAS Analyst 300 after fusion melts and acidic dissolving of the sample.

TPR-H₂ measurements were conducted using a Micrometrics Autochem II 2920 instrument equipped with a TCD detector. The experiment run was carried out from 36 °C to 700 °C in a 5% H₂/Ar flow (20 cm³ min⁻¹) with a heating rate of 10 K min⁻¹.

6.3. General methods - catalysts preparation

For Co-based catalysts. Cobalt(II) acetate tetrahydrate was added to absolute ethanol (40 mL of EtOH for 1 mmol of Co(OAc)₂·4H₂O) and stirred until complete solubilisation (10 min., formation of a clear purple solution). Then the ligand (2 mmol) was added (color change from orange to deep red depending on the ligand) and the resulting solution was stirred at 60 °C for 2 h. Owing to their scarce solubility in EtOH, ligands **L2** and **L7** were initially solubilized in the minimum amount of inhibitor-free THF and then dropwise added to a solution of Co(OAc)₂·4H₂O in EtOH. After that, VULCAN XC 72R[®] (1.392 g for 1 mmol of Co(OAc)₂·4H₂O) was portionwise added during about 30 min and the suspension was stirred at 25 °C for 18 h. Then, the solvent was removed and the obtained solid was dried for 4 hours under vacuum, grinded to a very fine powder and finally transferred into a ceramic crucible, equipped with a lid, and placed in the pyrolysis oven. Following the same procedure but omitting the ligand Co_xO_y@C was prepared.

For Fe-based catalysts. Fe(II) acetate (stored under Ar atmosphere) was added to absolute ethanol (40 mL of EtOH for 1 mmol of Fe(OAc)₂). Then Phen (3 mmol) was added and the so-obtained brown solution was stirred at 60 °C for 2 hours. After that, VULCAN XC 72R[®] (1.392 g for 1 mmol of Co(OAc)₂·4H₂O) was portionwise added during about 30 min and the suspension was stirred at 25 °C for 18 h. Then, the solvent was removed and the obtained solid was dried for 4 hours under vacuum, grinded to a very fine powder and finally transferred into a ceramic crucible, equipped with a lid, and placed in the pyrolysis oven. Following the same procedure but omitting the ligand Fe_xO_y@C was prepared.

Pyrolysis. The oven was heated to 100 °C (25 K/min) flushing 10 mL·min⁻¹ of Ar. Once the temperature reached 100 °C, the chamber was evacuated for 5 min and flood with Ar for 60 °C. The latter operation was repeated for two times. Thus, the temperature was increased to 800 °C and maintained for 2 h. During the whole process Ar was flushed. At the end, the heating was stopped and the chamber allowed cooling down to room temperature. The lid containing the active catalyst was removed. Both the catalysts can be stored under air for months without loss of activity.

6.4. General methods –catalytic reactions in the autoclave

In an 8 mL glass vial fitted with a magnetic stirring bar and a septum cap, the catalyst (the amount depends of the catalyst) was added followed by the nitroarene (0.5 mmol), the internal standard (*n*-hexadecane, 20 mg) and the solvent. A needle was inserted in the septum cap, which allows dihydrogen to enter. The vials (up to 7) were placed into a 300 mL steel Parr autoclave which was flushed twice with dihydrogen at 20 bar and then pressurized to 50 bar. Then the autoclave was placed into an aluminum block pre-heated at the desired temperature. At the end of the reaction, the autoclave was quickly cooled down at room temperature with an ice bath and vented. Finally, the samples were removed from the autoclave,

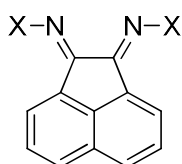
diluted with a suitable solvent, filtered using a Pasteur pipette filled with Celite® (6 cm pad) and analyzed by GC.

6.5. General methods - recycling experiments

For the catalyst recycling experiments, six-fold scaled up reactions were carried out. All the reactions were performed in glass vials set up according to the previously described procedure. After completion of the reaction the content of the vial was quantitatively transferred into a centrifuge tube. Hereafter, the reaction mixture was centrifugated and the catalyst was separated from the supernatant. The catalyst was washed three times with EtOH and dried under vacuum overnight. This material was then used for the next catalytic reaction.

6.6. Preparation of Ar-BIANs and related α -diimine complexes

6.6.1. Synthesis of Ar-BIAN^[42]



- L1:** X = C₆H₅
- L2:** X = 4-NC-C₆H₄
- L4:** X = 4-MeO-C₆H₄
- L5:** X = 1-Naphthyl

In a Schlenk flask, acenaphthenequinone (0.500 g, 2.7 mmol) and anhydrous ZnCl₂ (1.00 g, 7.3 mmol) were suspended in glacial acetic acid (7.5 mL). The flask was heated to about 60 °C and the aniline (6.3 mmol) was added. The reaction mixture was refluxed for 45 minutes and then filtered through a Buchner funnel while hot. The collected solid was washed with diethyl ether and dried under vacuum. The obtained complex was suspended in CH₂Cl₂ (20 mL for each mmol of complex) in a round-bottom flask under air. A saturated aqueous solution of potassium oxalate (5 mL for each mmol of complex) was added and the biphasic mixture stirred stirring for 15 minutes. The organic layer was washed twice with water, dried over Na₂SO₄, filtered and finally evaporated to dryness affording the pure ligand.

C₆H₅-BIAN (L1): yellow powder, 78% yield. ¹H NMR (300 MHz, CDCl₃) δ 7.89 (d, J = 8.3 Hz, 2H), 7.48 (t, J = 7.7 Hz, 4H), 7.37 (t, J = 7.8 Hz, 2H), 7.27 (t, J = 7.4 Hz, 2H), 7.14 (d, J = 7.8 Hz, 4H), 6.85 (d, J = 7.2 Hz, 2H) ppm. ¹³C NMR (75 MHz, CDCl₃) δ 161.9, 152.4, 142.4, 131.8, 130.0, 129.6, 129.1, 128.2, 125.0, 124.6, 118.8 ppm. Anal. Calcd for C₂₄H₁₆N₂ (%): C 86.72; H 4.85; N 8.43. Found: C 86.56; H 4.80; N 8.21.

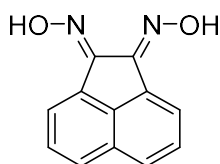
4-NC-C₆H₄-BIAN (L2): orange powder, 80% yield. ¹H NMR (400 MHz, CDCl₃) δ 8.00 (d, J = 8.3 Hz, 2H), 7.79 (d, J = 8.4 Hz, 4H), 7.47 (t, J = 7.8 Hz, 2H), 7.22 (d, J = 8.4 Hz, 4H), 6.86 (d, J = 7.3 Hz, 2H) ppm. ¹³C NMR (101 MHz, CDCl₃) δ 161.2, 155.3, 142.2, 133.9, 131.4, 130.1, 128.0, 127.7, 124.3, 119.0, 108.2 ppm. A quaternary carbon was not detected or coincided with another carbon resonance. Anal. Calcd for C₂₆H₁₄N₂ (%): C 81.66; H 3.69; N 14.65. Found: C 81.64; H 3.90; N 14.50.

4-MeO-C₆H₄-BIAN (L4): dark orange powder, 84% yield. ¹H NMR (300 MHz, CDCl₃) 7.86 (d, J = 8.2 Hz, 2H), 7.37 (t, J = 7.8 Hz, 2H), 7.09 (d, J = 8.8 Hz, 4H), 7.03 – 6.95 (m, 6H) 3.87 (s, 3H, -OCH₃) ppm. ¹³C

NMR (75 MHz, CDCl₃) δ 161.7, 157.0, 145.0, 141.8, 131.4, 129.0, 128.8, 127.7, 123.8, 119.9, 114.7, 55.6 ppm. Anal. Calcd for C₂₆H₂₀N₂O₂ (%): C 79.57; H 5.14; N 7.14. Found: C 79.45; H 5.18; N 7.02.

1-Naphthyl-BIAN (L5): The ligand and the corresponding ZnCl₂ complex were already known in the literature.^[43] The synthesis was performed following the general procedure reported above. However, in order to obtain the pure product, the intermediate zinc complex was suspended in MeOH (5 mL), stirred for 30 minutes and then filtered through a Buchner funnel. Dark red powder, 65% yield. ¹H NMR (400 MHz, CDCl₃) δ 8.09 (d, *J* = 8.4 Hz, 2H), 7.95 (d, *J* = 8.2 Hz, 2H), 7.80 (d, *J* = 8.3 Hz, 4H), 7.62 – 7.51 (m, 4H), 7.44 (ddd, *J* = 8.1, 6.8 and 1.2 Hz, 2H), 7.29 – 7.17 (m, 4H), 6.65 (d, *J* = 7.2 Hz, 2H) ppm. ¹³C NMR (75 MHz, CDCl₃) δ 162.1, 148.5, 142.0, 134.5, 131.3, 129.1, 128.8, 128.1, 127.9, 126.7, 126.2, 125.8, 125.1, 124.6, 124.0 (two overlapped CH), 112.6 ppm. Anal. Calcd. for C₃₂H₂₀N₂ (%): C 88.86; H 4.66; N 6.48. Found: C 89.08; H 4.59; N 6.03.

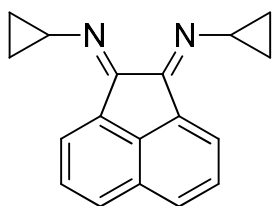
6.6.2. Synthesis of acenaphthenequinone dioxime (L3)



The ligand has been known in the literature,^[44] for more than one century; however, its NMR characterization was never reported. The synthesis was performed adapting a procedure previously described in the literature.^[45] Hydroxylamine hydrochloride (0.955 g, 13.8 mmol) was dissolved in H₂O (4 mL) and NaHCO₃ (1.18 g, 14.0 mmol) was added portionwise while stirring. MeOH (35 mL) and solid acenaphthenequinone (1.03 g, 5.6 mmol) were then added. The reaction mixture was refluxed for 1 hour, allowed to cool and filtered through a Büchner funnel. The obtained off-white solid was washed with MeOH and dried under vacuum. Although the crude was quite pure, it contained traces of the monooxime and it was further purified by column chromatography (AcOEt : Hexane = 1:9 + 1% Et₃N) which was followed by washing the product with water to eliminate residual triethylammonium salts. Yield: 0.934 mg (4.4 mmol, 79%).

¹H NMR (300 MHz, DMSO-*d*₆) δ 12.37 (s, 2H, -OH), 8.36 (d, *J* = 7.1 Hz, 2H), 8.02 (d, *J* = 8.3 Hz, 2H), 7.71 (dd, *J* = 8.2 and 7.3 Hz, 2H) ppm. ¹³C NMR (75 MHz, DMSO-*d*₆) δ 149.1, 136.3, 130.4, 129.2, 128.6, 127.6, 125.6 ppm. Anal. Calcd for C₁₂H₈N₂O₂ (%): C 67.92; H 3.80; N 13.20. Found C 67.96; H 4.01; N 12.87.

6.6.3. Synthesis of cyclopropyl-BIAN (L6)^[46]



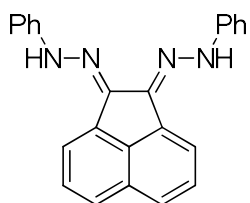
The synthesis was performed in a thick-walled glass vessel. Acenaphthenequinone (0.500 g, 2.7 mmol) was suspended in dry MeOH under a dinitrogen atmosphere, cyclopropylamine (0.570 mL, 8.2 mmol) was added and the vessel was sealed. The reaction mixture was heated to 80 °C and allowed to stir for 8 h. The volatiles were evaporated affording a light brown residue. The crude was dissolved in hot heptane (20 mL) and filtered while hot by the aid of a cannula. Upon cooling the product precipitated as pale orange needles, which were collected by filtration and washed with cold hexane (2 mL). 0.490 g, 1.9 mmol, 69 % yield.

Following this procedure, the ligand **L6** is obtained as a mixture of *syn-anti* and *anti-anti* isomers. As previously reported,^[46a] evidence of that is provided by the ¹H NMR and ¹³C NMR recorded in CDCl₃. However, we noticed that in C₆D₆ the equilibrium is almost completely shifted to the *syn-anti* isomer and the NMR spectra are more easily understandable. ¹H NMR and ¹³C NMR spectra in both solvents are reported below.

¹H NMR (300 MHz, CDCl₃) δ 8.24 (d, *J* = 7.2 Hz, 2H, *anti-anti* isomer), 8.09 (d, *J* = 7.2 Hz, 1H, *syn-anti* isomer), 7.94 (d, *J* = 8.3 Hz, 2H, *anti-anti* isomer), 7.89 (d, *J* = 8.3 Hz, 1H, *syn-anti* isomer), 7.86 -7.79 (m, 2H, *syn-anti* isomer), 7.69 – 7.52 (m, both isomers), 5.59 – 5.42 (m, 2H, *syn-anti* isomer), 3.99 – 3.77 (m, both isomers), 1.35 – 1.00 (m, both isomers) ppm. ¹³C NMR (75 MHz, CDCl₃) δ 162.8, 161.1, 159.3, 140.3, 138.8, 137.1, 131.9, 131.5, 131.3, 128.9, 128.6, 128.4, 128.0, 127.1, 124.2, 123.4, 118.2, 37.3, 36.4, 34.0, 12.2, 11.8, 11.1 ppm.

¹H NMR (400 MHz, C₆D₆) δ 8.02 (d, *J* = 6.9 Hz, 1H), 7.71 (d, *J* = 7.1 Hz, 1H), 7.54 (d, *J* = 8.3 Hz, 1H), 7.49 (d, *J* = 8.2 Hz, 1H), 7.29 (pst, *J* = 7.6 Hz, 1H), 7.22 (pst, *J* = 7.7 Hz, 1H), 6.14 – 5.62 (m, 1H), 3.59 (m, 1H), 1.38 – 1.18 (m, 2H), 1.10 – 1.00 (m, 4H), 0.95 – 0.84 (m, 2H) ppm. ¹³C NMR (101 MHz, C₆D₆) δ 160.9, 158.5, 138.7, 137.4, 131.8, 131.3, 128.6, 127.9, 127.4, 126.5, 123.0, 118.1, 36.0, 34.0, 12.1, 11.2 ppm. C₁₈H₁₆N₂ (%): C 83.04; H 6.19; N 10.76. Found: C 82.83; H 6.28; N 10.67.

6.6.4. Synthesis of acenaphthenequinone bis(phenylhydrazone) (L7)



The reaction was performed in a thick walled glass vessel. Acenaphthenequinone (1.5 g, 8.2 mmol) was suspended in EtOH (30 mL), phenylhydrazine (2.5 mL, 25 mmol) was added and the vessel was sealed. The mixture was heated to 140 °C while stirring for 2 h, allowed to cool and filtered through a Büchner funnel. The crude was washed with EtOH and dried under vacuum affording 2.4 g (6.7 mmol, 82 % yield) of the ligand as an orange powder.

^1H NMR (300 MHz, DMSO- d_6) δ 12.71 (s, 1H, NH), 10.19 (s, 1H, NH), 8.43 (d, J = 7.1 Hz, 1H), 8.00 (d, J = 8.2 Hz, 1H), 7.86 (dd, J = 8.2 and 0.6 Hz, 1H), 7.83 (dd, J = 7.0 and 0.7 Hz, 1H), 7.75 (dd, J = 8.2 and 7.2 Hz, 1H), 7.68 (dd, J = 8.1 and 7.1 Hz, 1H), 7.46 (d, J = 4.2 Hz, 4H), 7.43 – 7.26 (m, 4H), 7.07 – 6.99 (m, 1H), 6.95 (tt, 7.4 and 1.3 Hz, 1H) ppm. ^{13}C NMR (75 MHz, DMSO- d_6) δ 145.6, 144.3, 142.8, 136.0, 134.9, 134.8, 130.5, 130.1, 129.8, 129.1, 128.9, 128.4, 128.0, 125.2, 123.6, 121.8, 121.4, 116.6, 114.4, 113.4 ppm. Anal. Calcd for $\text{C}_{24}\text{H}_{18}\text{N}_4$ (%): C 79.54; H 5.01; N 15.46. Found: C 79.58; H 4.94; N 15.38.

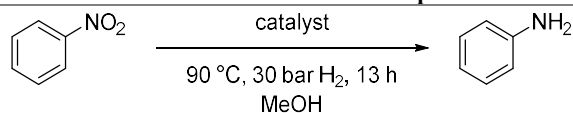
6.7. Additional catalytic data, catalysts characterisations, control experiments and characterisation of the catalytic reduction products

6.7.1. Control experiments

Table S1. Co-catalysed hydrogenation of nitrobenzene to aniline: control experiments.^a

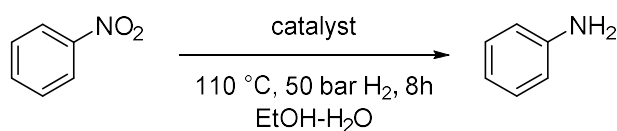
Entry	Catalyst	Conversion [%] ^b	Selectivity [%] ^b
1	0.5 mol % $\text{Co}_x\text{O}_y@\text{C}$	<1	-
2 ^c	0.5 mol % $\text{Co}_x\text{O}_y@\text{C}$	<1	-
3 ^d	0.5 mol % $\text{Co-Co}_3\text{O}_4/\text{NGr}@\text{C}$	<1	-
4 ^{c, d}	0.5 mol % $\text{Co-Co}_3\text{O}_4/\text{NGr}@\text{C}$	<1	-
5	-	<1	-
6 ^c	-	<1	-

^a Reaction conditions: 0.5 mmol PhNO_2 ; solvent = 2 mL EtOH + 100 μL H_2O ; ^b GC values using *n*-hexadecane as the internal standard; ^c 1 equiv. of Et_3N was added; ^d Reaction carried out under 20 bar of N_2 .

Table S2. Fe-catalysed hydrogenation of nitrobenzene to aniline: control experiments.^a

Entry	Catalyst	Conversion [%] ^b	Selectivity [%] ^b
1	4.5 mol % Fe _x O _y @C	<1	-
2 ^c	4.5 mol % Fe _x O _y @C	<1	-
3 ^c	4.5 mol % Fe _x O _y @C	<1	-
4 ^d	4.5 mol % Fe ₂ O ₃ /NGr@C	<1	-
5 ^{c, d}	4.5 mol % Fe ₂ O ₃ /NGr@C	<1	-
6 ^{c, d}	4.5 mol % Fe ₂ O ₃ /NGr@C	<1	-
7	-	<1	-
8 ^c	-	<1	-
9 ^c	-	<1	-

^a Reaction conditions: 0.5 mmol PhNO₂; 3 mL MeOH; ^b GC values using *n*-hexadecane as internal standard; ^c 1 equiv. of NH₃ was added; ^d Reaction carried out under 20 bar of N₂; ^e 1 equiv. of DMAP (4-dimethylaminopyridine) was added.

Table S3. Co-catalysed hydrogenation of nitrobenzene to aniline: control experiments.^a

Entry	Catalysts	Conversion [%] ^b	Selectivity [%] ^b
1	-	<1	-
2 ^c	3 mol % Co(OAc) ₂ ·4H ₂ O	2	-
3 ^c	3 mol % Co(OAc) ₂ ·4H ₂ O + L1 (2 equiv. with respect to the metal)	2	-
4	3 mol % [Co(Ph-BIAN)] ₂ [OAc] ₂ on Vulcan XC 72 R (<i>unpyrolysed material</i>)	1	-
5	3 mol % Co(OAc) ₂ ·4H ₂ O on Vulcan XC 72 R (<i>pyrolysed material</i>)	2	-
6 ^d	3 mol % Co(OAc) ₂ ·4H ₂ O on Vulcan XC 72 R (<i>pyrolysed material</i>)	1	-
7	L1 on Vulcan XC 72 R (<i>pyrolysed material</i>)	<1	-
8 ^d	L1 on Vulcan XC 72 R (<i>pyrolysed material</i>)	<1	-

^a Reaction conditions: 0.5 mmol PhNO₂, Solvent: 2 mL EtOH + 100 μL H₂O; ^b Conversion and selectivities based on GC analyses using *n*-hexadecane as an internal standard; ^c Reactions carried out under homogeneous conditions; ^d 1 equiv. of Et₃N was added.

Table S4. Co-catalysed hydrogenation of nitrobenzene to aniline: control experiments.^a

Entry	Solvent	Conversion [%] ^b	Selectivity [%] ^b
1	MeOH-H ₂ O	<1	<1
2	EtOH-H ₂ O	<1	<1
3	<i>i</i> -PrOH-H ₂ O	<1	<1
4	2-methoxyethanol-H ₂ O	<1	<1
5	2-methyl-2-butanol-H ₂ O	<1	<1
6 ^c	EtOH-H ₂ O	<1	<1
7 ^d	EtOH-H ₂ O	<1	<1
8 ^e	EtOH-H ₂ O	<1	<1
9 ^f	EtOH-H ₂ O	<1	<1

^a Reaction conditions: 0.5 mmol PhNO₂, 2 mL solvent + 100 μL H₂O; ^b Conversion and selectivities based on GC analyses using *n*-hexadecane as an internal standard; ^c 1 equiv. Et₃N was added; ^d 0.7 mol % of Co/L2 was used instead of Co/L1; [e] 0.7 mol % of Co/L3 was used instead of Co/L1; [f] 0.7 mol % of Co/L7 was used instead of Co/L1.

Table S5. Elemental analysis of the Co catalyst prepared with (first row) and without Phen (second row).

Catalyst	C [%]	H [%]	N [%]	Co [%]
Co-Co ₃ O ₄ /NGr@C	92.18	0.18	2.61	3.05
Co _x O _y @C	83.10	0.18	<0.1	4.33

Table S6. Elemental analysis of the Fe catalyst prepared with (first row) and without Phen (second row).

Catalyst	C [%]	H [%]	N [%]	Fe [%]
Fe ₂ O ₃ /NGr@C	90.94	0.28	2.79	2.95
Fe _x O _y @C	82.03	0.096	<0.1	4.53

Table S7. Elemental analysis of the Co and Fe catalysts after five recycles.

Catalyst	C [%]	H [%]	N [%]
Co-Co ₃ O ₄ /NGr@C	92.01	0.25	2.50
Fe ₂ O ₃ /NGr@C	91.01	0.23	2.77

6.7.2. Maitlis' hot filtration test for Co-Co₃O₄/NGr@C and Fe₂O₃/NGr@C

The hot filtration test was carried out following the standard procedure for a catalytic experiment. The reaction was stopped before complete conversion. A small amount of the vial contents was filtered by using Pasteur pipette filled with Celite® and an aliquot of the filtrate analysed at GC. Then, the remaining reaction mixture was quantitatively transferred into a Schlenk flask and heated up to 90 °C for 1 hour. The reaction

mixture was filtered while hot and the filtrate was transferred into a clean reaction vial and subsequently subjected to the standard reaction conditions for 13 h.

Table S8

Entry	Catalyst	Conversion before filtration	Conversion after filtration
		[%] ^c	[%] ^{c, d}
1	Co-Co ₃ O ₄ /NGr@C ^a	52.3	53.0
2	Fe ₂ O ₃ /NGr@C ^b	38.5	37.8

^a Reaction conditions for Co-Co₃O₄/NGr@C: 0.5 mmol PhNO₂, 0.5 mol % Co-Co₃O₄/NGr@C (5 mg), 70 °C, 20 bar H₂, solvent: 2 mL EtOH + 100 μL H₂O, 1 equiv. Et₃N; ^b Reaction conditions for Fe₂O₃/NGr@C: 0.5 mmol PhNO₂, 4.5 mol % Fe₂O₃/NGr@C (42 mg), 120 °C, 50 bar H₂, solvent: 3 mL MeOH, 1 equiv. NH₃; ^c Conversion determined by GC using *n*-hexadecane as internal standard; ^d After 13 h of reaction under the same reaction conditions.

6.7.3. Maitlis' hot filtration test for Co/L7

The procedure for setting up a standard catalytic experiment was followed, but the reaction was interrupted after 2 hours. Hereafter, the autoclave was cooled down to room temperature and vented. A small amount of the vial content was filtered through a Pasteur pipette filled with Celite® (6 cm pad) and an aliquot of the filtrate was analyzed by GC. Then the remaining reaction mixture was quantitatively transferred into a Schlenk flask and heated up to 90 °C for 1 h. The mixture was rapidly filtered while hot using a Pasteur pipette filled with Celite® (6 cm pad). The filtrate was quantitatively transferred into a clean reaction vial and subjected to the standard reaction conditions. In the latter case, the reaction time was prolonged to 24 h in order to take into account any soluble Co species that exhibit only low catalytic activity. The reaction mixture was finally analyzed by GC.

Table S9

Entry	Catalyst	Conversion before filtration	Conversion after filtration
		[%] ^b	[%] ^b
1	Co/L7	35.6	35.2
2 ^c	Co/L7	51.3	51.8

^a Reaction conditions: 0.5 mmol PhNO₂, 0.5 mol % Co/L7 (5.9 mg), 2 mL EtOH + 100 μL H₂O, 110 °C, 50 bar H₂; ^b Conversion based on GC analysis using *n*-hexadecane as the internal standard; ^c 1 equivalent of Et₃N was added at the beginning of the first catalytic experiments.

6.7.4. Additional characterisation data (STEM, EDX and XPS) for Co/L1, Co/L2, Co/L3 and Co/L7 catalysts

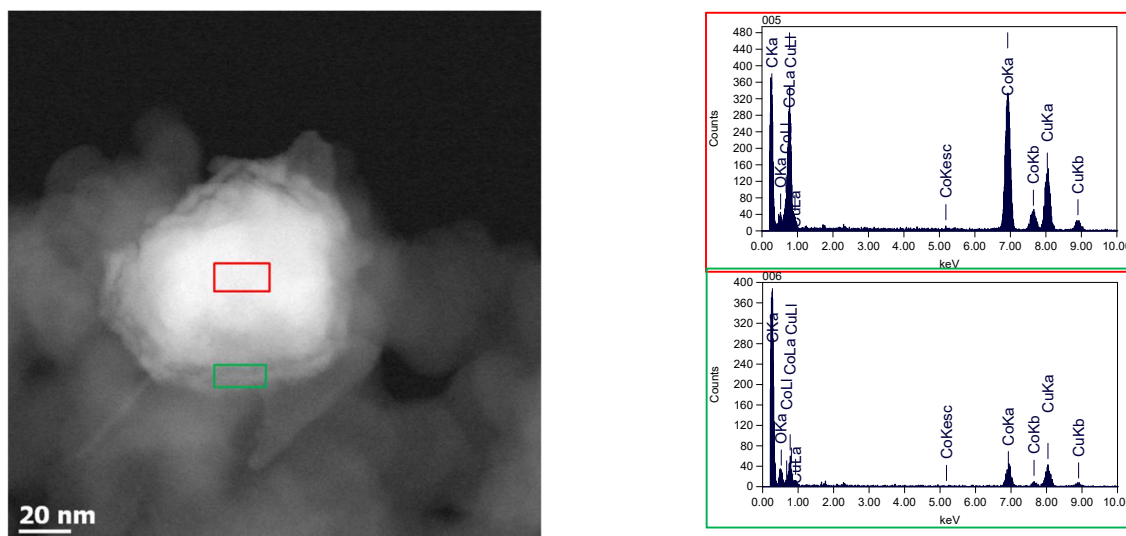


Figure S1. STEM image and EDX analysis of a selected Co/L1 NP

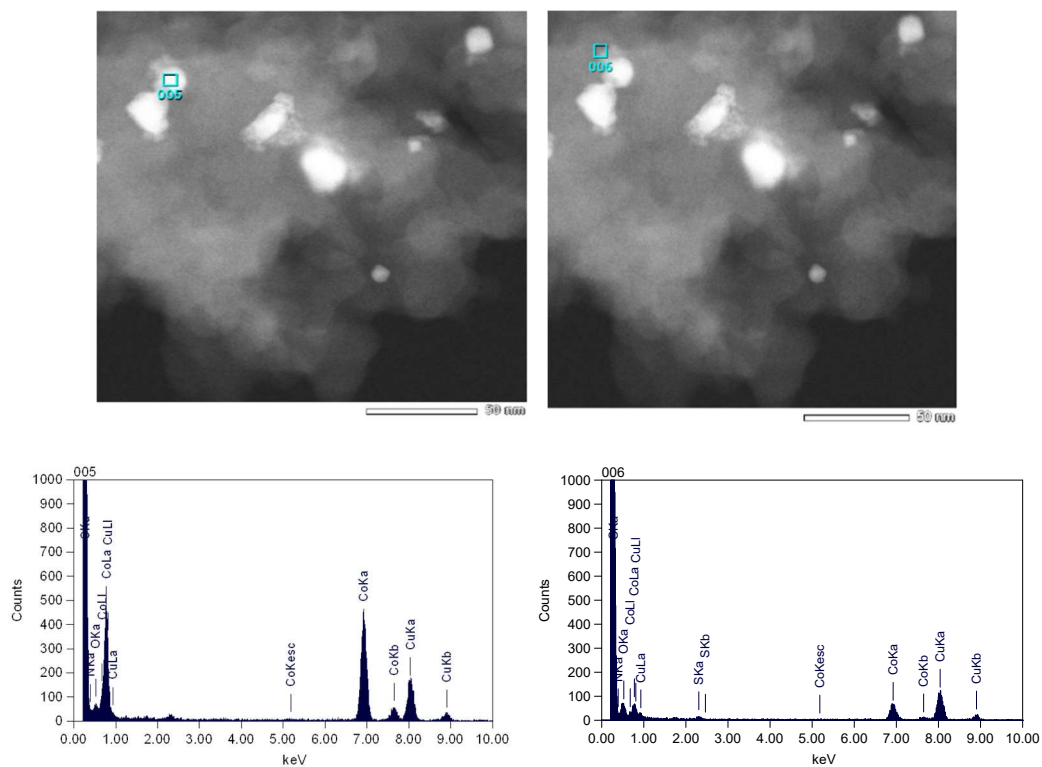


Figure S2. STEM image of a selected NP of Co/L2 (upper row) and the corresponding EDX analysis of the core (lower row, left) and the periphery (lower row, right).

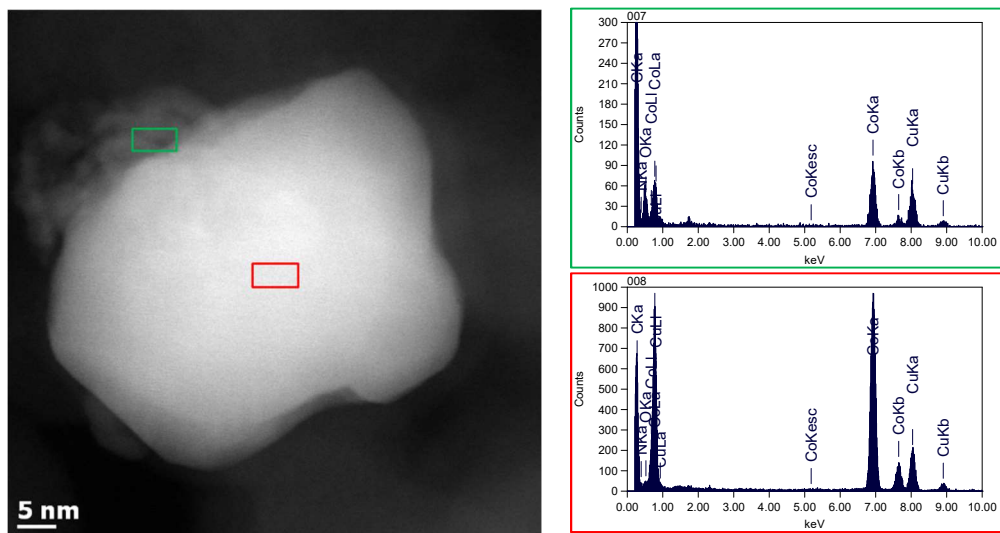


Figure S3. STEM image and EDX analysis of a selected Co/L3 NP.

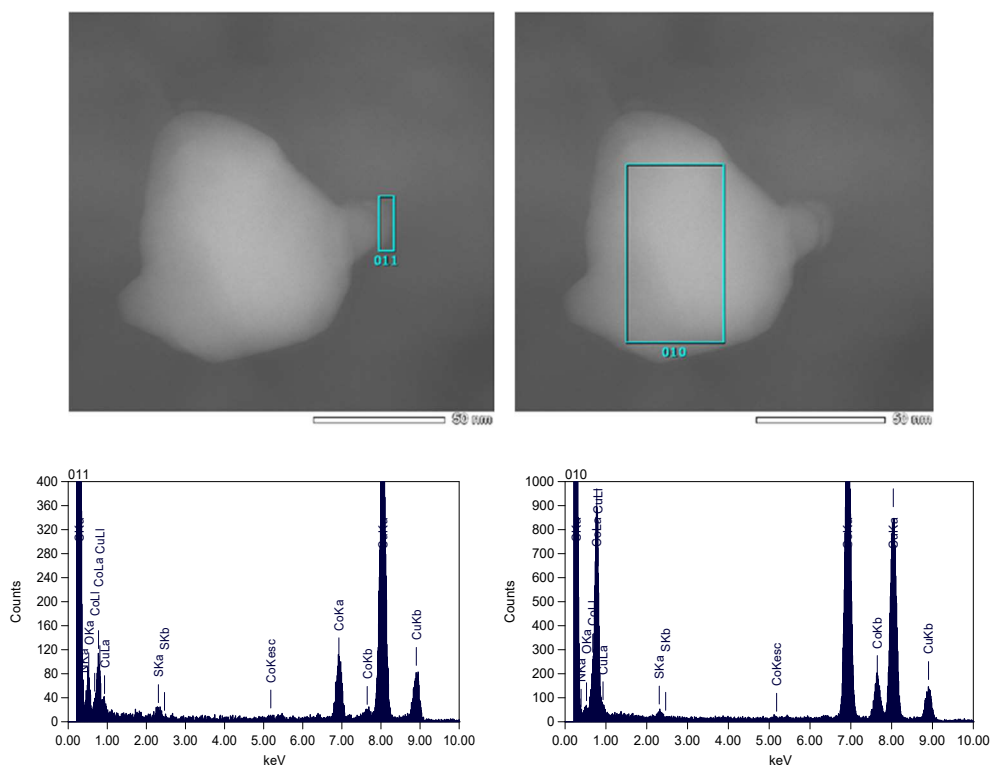
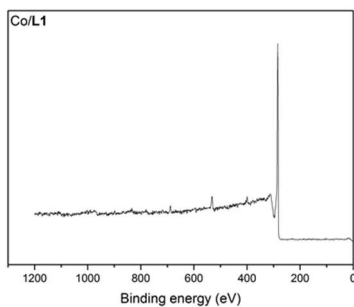
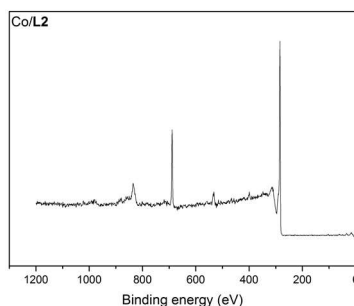


Figure S4. STEM image of a selected NP of Co/L7 (upper row) and the corresponding EDX analysis of the core (lower row, left) and the periphery (lower row, right).



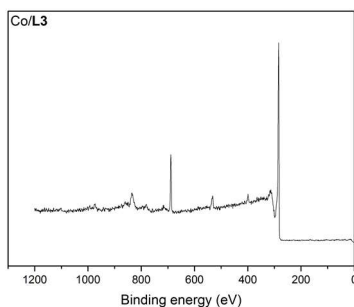
Peak name	Area/cps-eV	Ebin/eV	Sigma	Lambda	TF	Sens. Fact.	Norm. Area	Quant./at.%
C1s Peak 1	7821.963358	283.8	1	20.31	0.836	16.979	460.6845726	61.69 94.52
C1s Peak 2	1132.800582	284.9	1	20.29	0.837	16.983	66.70203039	8.93
C1s Peak 3	1627.393205	285.77	1	20.28	0.838	16.995	95.75717595	12.82
C1s Peak 4	1405.755912	289.64	1	20.23	0.84	16.993	82.72558774	11.08
Co2p Doublet 1	242.9105598	780	19.16	13.66	1.399	366.15	0.663410914	0.09 0.09
N1s Peak 1	75.61704142	397.88	1.8	18.85	0.921	31.25	2.419745325	0.32 2.49
N1s Peak 2	443.4116343	400.09	1.8	18.82	0.923	31.268	14.1810044	1.9
N1s Peak 3	62.68304512	404.44	1.8	18.77	0.926	31.286	2.003549355	0.27
O1s Peak 1	1133.176049	531.82	2.93	17.1	1.046	52.408	21.62219603	2.9 2.9

Figure S5. XPS survey (left) and overall XPS data obtained for Co/L1 catalyst



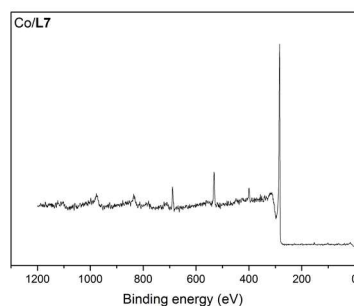
Peak name	Area/cps-eV	Ebin/eV	Sigma	Lambda	TF	Sens. Fact.	Norm. Area	Quant./at.%
C1s Peak 1	6643.213571	283.81	1	20.3	0.836	16.971	391.4450281	56.37 94.65
C1s Peak 2	1561.317172	284.9	1	20.29	0.837	16.983	91.93412072	13.24
C1s Peak 3	1261.172103	286.26	1	20.27	0.838	16.986	74.24773954	10.69
C1s Peak 4	1694.690856	290.44	1	20.22	0.841	17.005	99.65838614	14.35
Co2p Doublet 1	283.5680991	779.75	19.16	13.67	1.399	366.42	0.773883934	0.11 0.11
N1s Peak 1	131.4297417	398	1.8	18.85	0.921	31.25	4.205751735	0.61 1.9
N1s Peak 2	280.1354534	400.26	1.8	18.82	0.923	31.268	8.959174026	1.29
O1s Peak 1	197.7238651	530.58	2.93	17.11	1.044	52.338	3.777826151	0.54 3.13
O1s Peak 2	565.3460257	532.58	2.93	17.09	1.047	52.427	10.78348991	1.55
O1s Peak 3	378.1648170	535.5	2.93	17.05	1.05	52.454	7.209456229	1.04
S2p Doublet 1	38.78556517	163.14	1.677	21.8	0.762	27.858	1.392259501	0.2 0.2

Figure S6. XPS survey (left) and overall XPS data obtained for Co/L2 catalyst



Peak name	Area/cps-eV	Ebin/eV	Sigma	Lambda	TF	Sens. Fact.	Norm. Area	Quant./at.%
C1s Peak 1	6245.466503	283.81	1	20.3	0.836	16.971	368.0081612	45.57 92.64
C1s Peak 2	2466.905228	284.07	1	20.3	0.837	16.991	145.1899370	17.98
C1s Peak 3	2561.176229	285.16	1	20.29	0.837	16.983	150.8082335	18.67
C1s Peak 4	1430.388609	288.98	1	20.24	0.84	17.002	84.13060871	10.42
Co2p Doublet 1	695.4711956	780.23	19.16	13.66	1.4	366.41	1.898037191	0.24 0.35
Co2p Doublet 2	323.2535815	785.77	19.16	13.58	1.41	366.87	0.881107256	0.11
N1s Peak 1	220.7543834	397.91	1.8	18.85	0.921	31.25	7.064140270	0.87 3.24
N1s Peak 2	508.9240884	400.09	1.8	18.82	0.923	31.268	16.27619574	2.02
N1s Peak 3	87.54823730	403.75	1.8	18.78	0.926	31.303	2.796800220	0.35
O1s Peak 1	511.2679827	530.67	2.93	17.11	1.044	52.338	9.768580816	1.21 3.42
O1s Peak 2	469.0943847	532.37	2.93	17.09	1.046	52.377	8.956114033	1.11
O1s Peak 3	467.0364383	535.62	2.93	17.05	1.05	52.454	8.903733525	1.1
S2p Doublet 1	60.09669105	163.23	1.677	21.8	0.763	27.894	2.154466589	0.27 0.36
S2p Doublet 2	20.14097115	167.47	1.677	21.75	0.765	27.903	0.721820992	0.09

Figure S7. XPS survey (left) and overall XPS data obtained for Co/L3 catalyst



Peak name	Area/cps-eV	Ebin/eV	Sigma	Lambda	TF	Sens. Fact.	Norm. Area	Quant./at.%
C1s Peak 1	5485.758171	283.8	1	20.31	0.836	16.979	323.0907692	53.64 89.17
C1s Peak 2	1460.196875	284.94	1	20.29	0.837	16.983	85.97991374	14.27
C1s Peak 3	1543.889462	286.11	1	20.28	0.838	16.995	90.84374596	15.08
C1s Peak 4	632.0672699	289.74	1	20.23	0.84	16.993	37.19574353	6.18
Co2p Doublet 1	53.59376953	778.82	19.16	13.68	1.397	366.16	0.146364680	0.02 0.3
Co2p Doublet 2	477.5230135	781.14	19.16	13.65	1.401	366.40	1.303251321	0.22
Co2p Doublet 3	134.7265577	785.81	19.16	13.58	1.41	366.87	0.367230417	0.06
N1s Peak 1	322.7653598	398.06	1.8	18.85	0.921	31.25	10.32849151	1.71 4.3
N1s Peak 2	306.6502644	399.67	1.8	18.83	0.922	31.25	9.812808463	1.63
N1s Peak 3	181.4744332	400.63	1.8	18.82	0.923	31.268	5.803838852	0.96
O1s Peak 1	1963.102239	531.8	2.93	17.1	1.046	52.408	37.45806441	6.22 6.22
O1s Peak 2	0	534.12	2.93	17.07	1.048	52.416	0	0

Figure S8. XPS survey (left) and overall XPS data obtained for Co/L7 catalyst

6.7.5. MS spectra of side-products detected in the catalytic run employing 1n as substrate

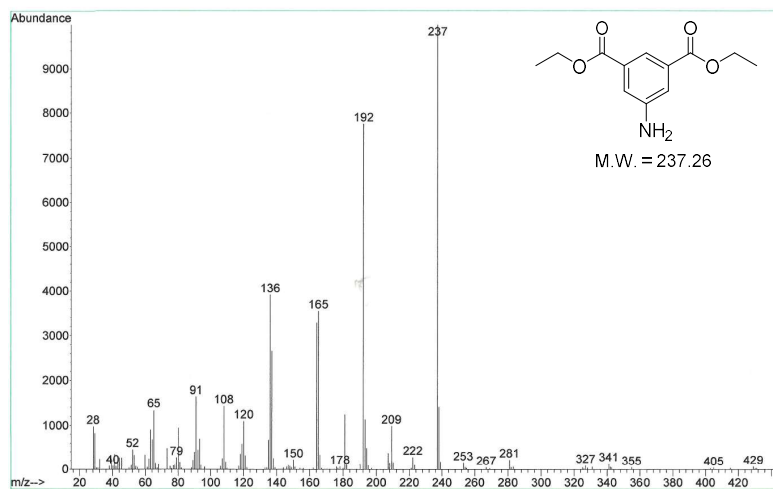


Figure S9. MS spectra of diethyl-5-aminoisophthalate

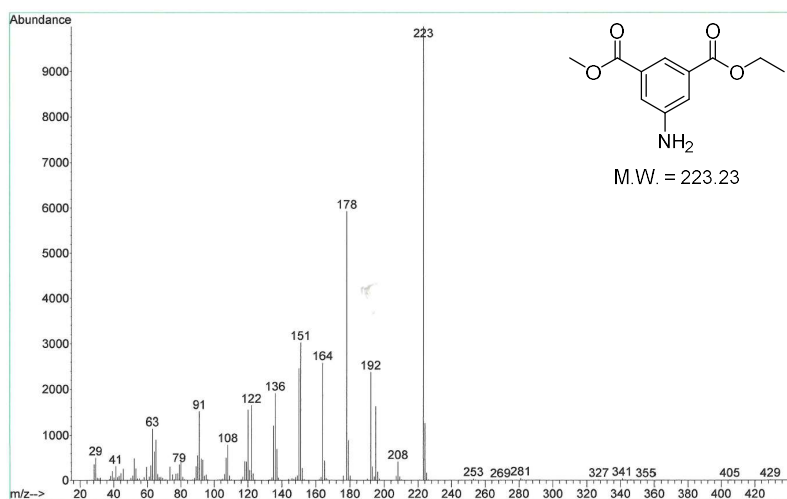
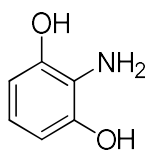


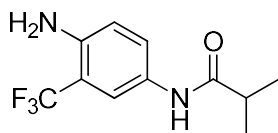
Figure S10. MS spectra of 1-methyl-3-ethyl-5-aminoisophthalate.

6.7.6. Isolated products: 2-aminoresorcinol and aminoflutamide (2aa and 2ab)



After the reaction was complete, the catalyst was separated using a Pasteur pipette filled with Celite® and the Celite® pad was washed with EtOH. The solvent was evaporated and the desired product isolated using column chromatography (AcOEt:heptane = 1:1). The product was obtained as a light brown solid.

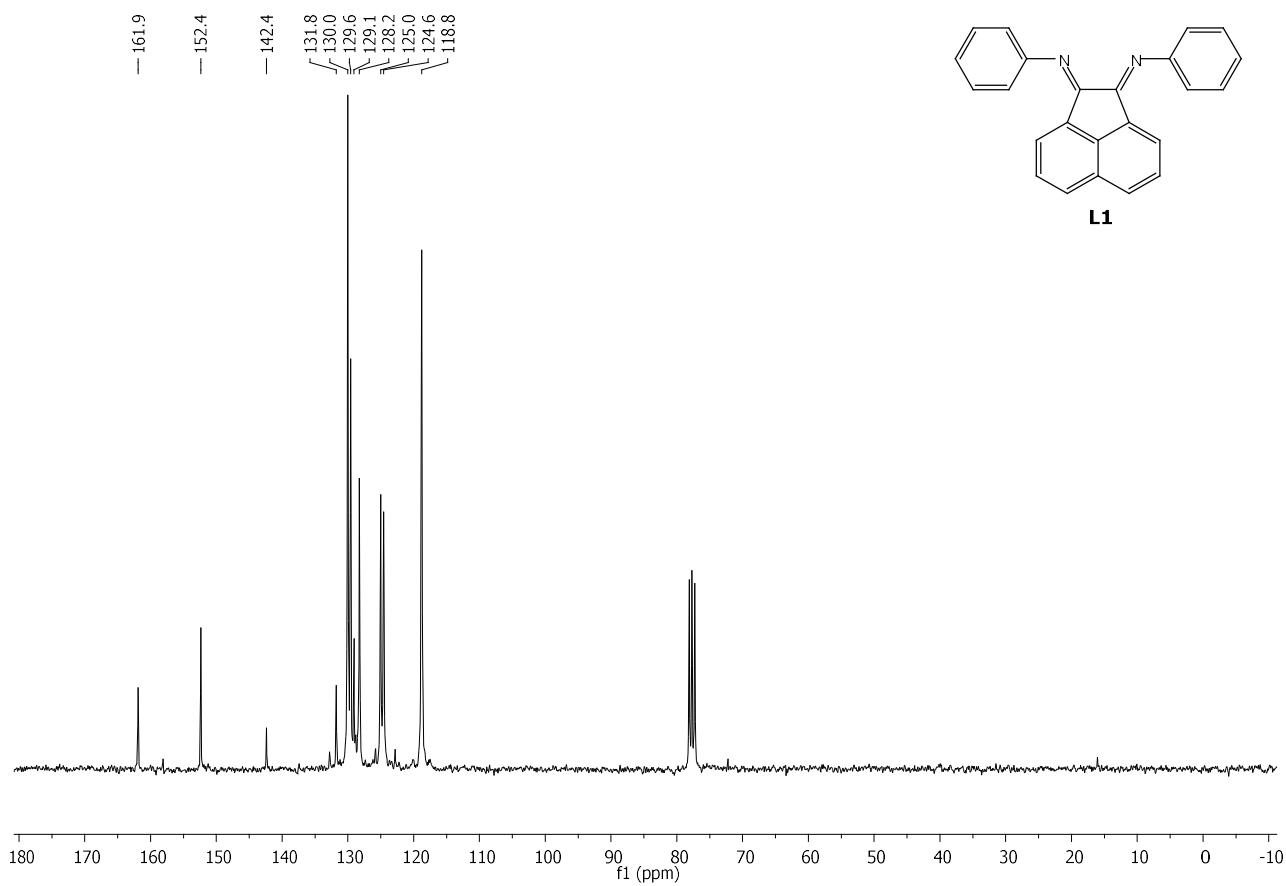
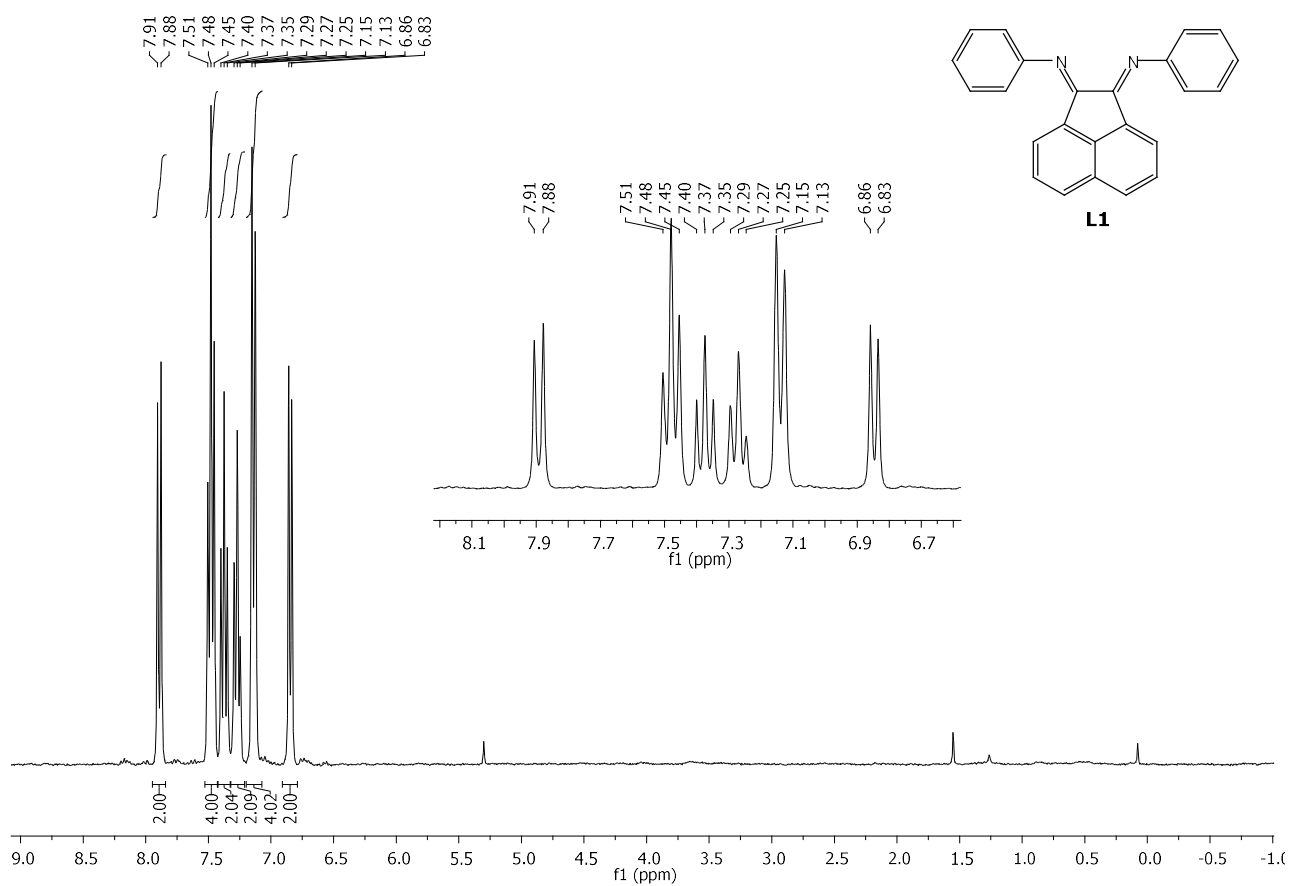
^1H NMR (300 MHz, DMSO- d_6) δ 8.82 (br, 2H), 6.29-6.20 (m, 3H), 3.82 (br, 2H) ppm. ^{13}C NMR (75 MHz, DMSO- d_6) δ 145.3, 124.3, 116.3, 107.1 ppm. Elemental analysis for $\text{C}_6\text{H}_7\text{NO}_2$ (%): C 57.59; H 5.64; N 11.19. Found: C 57.23; H 5.79; N 10.99.

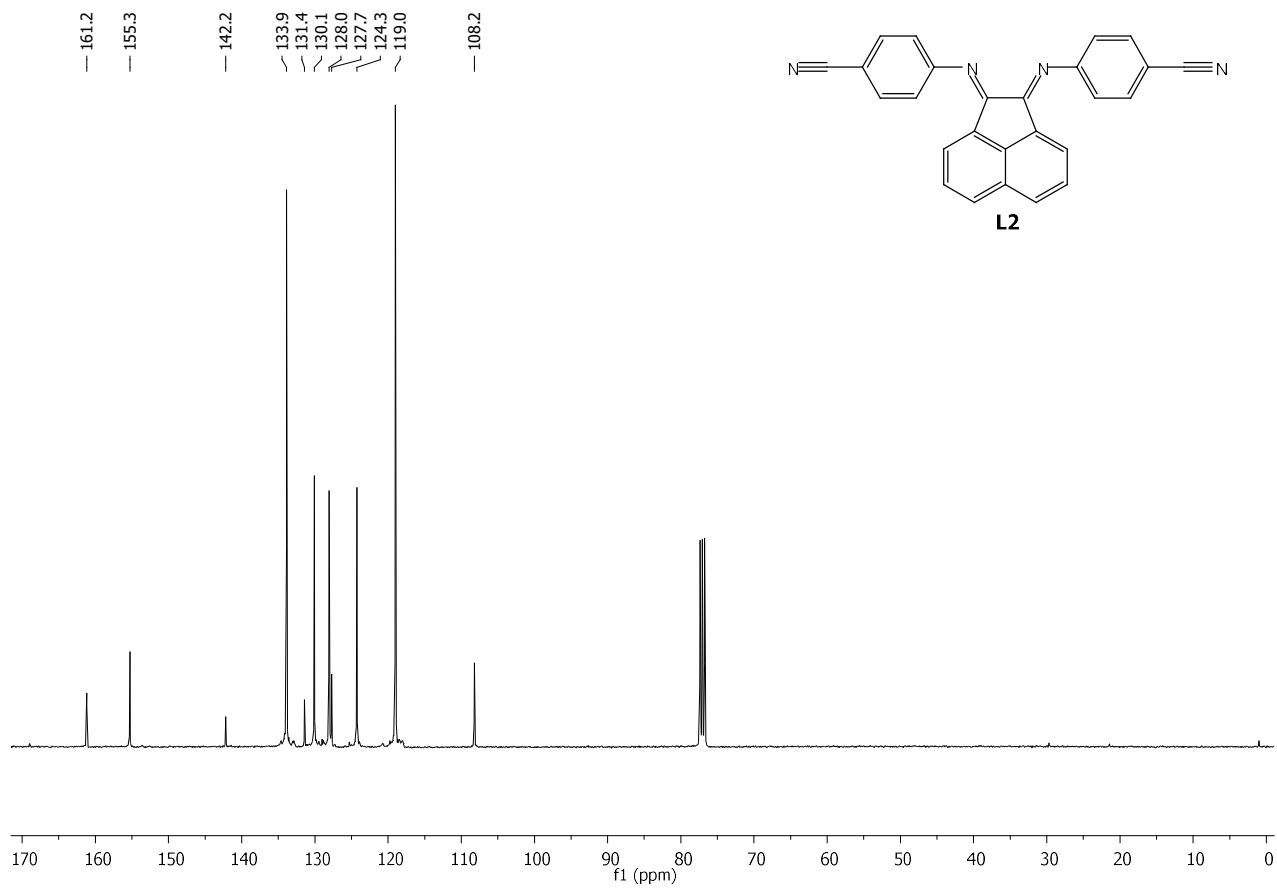
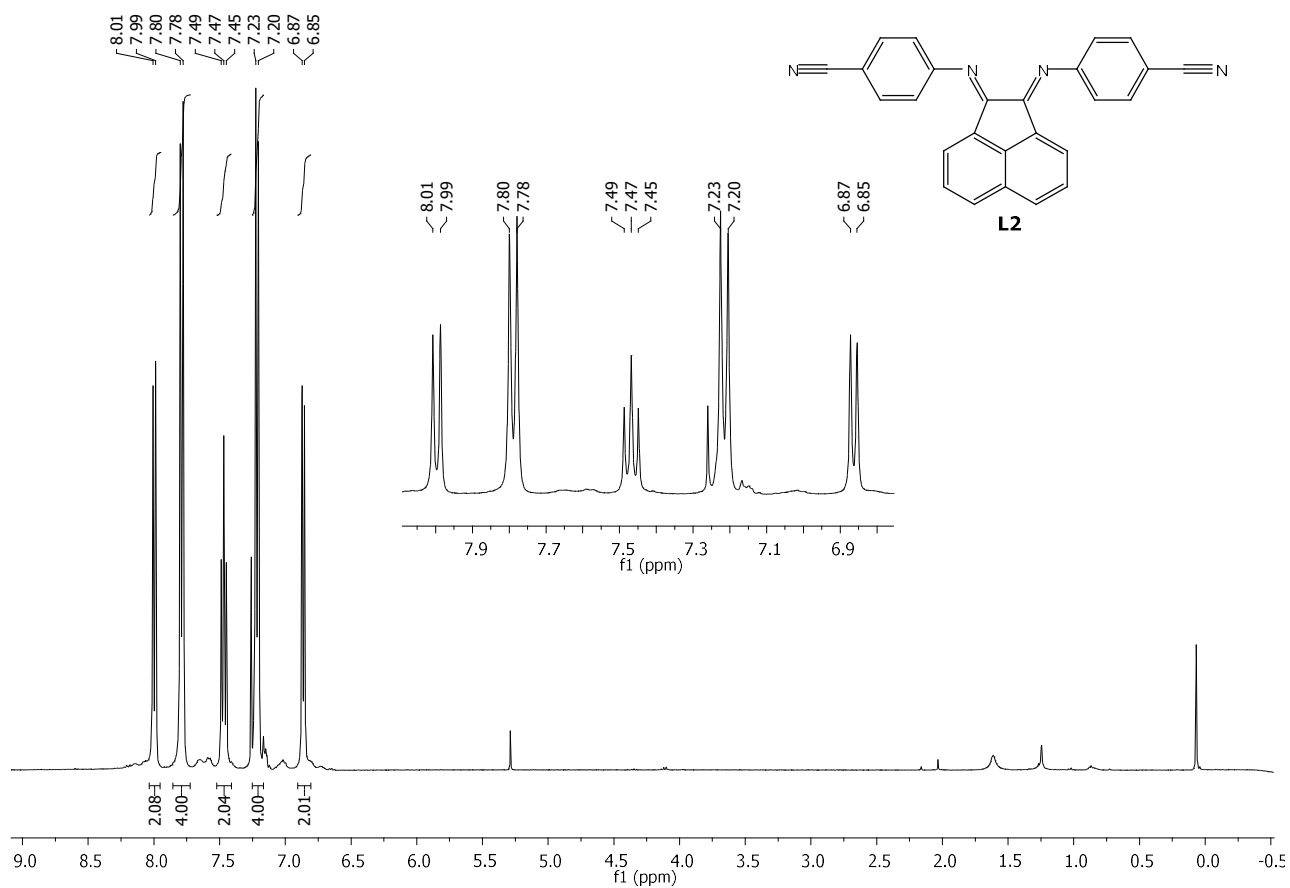


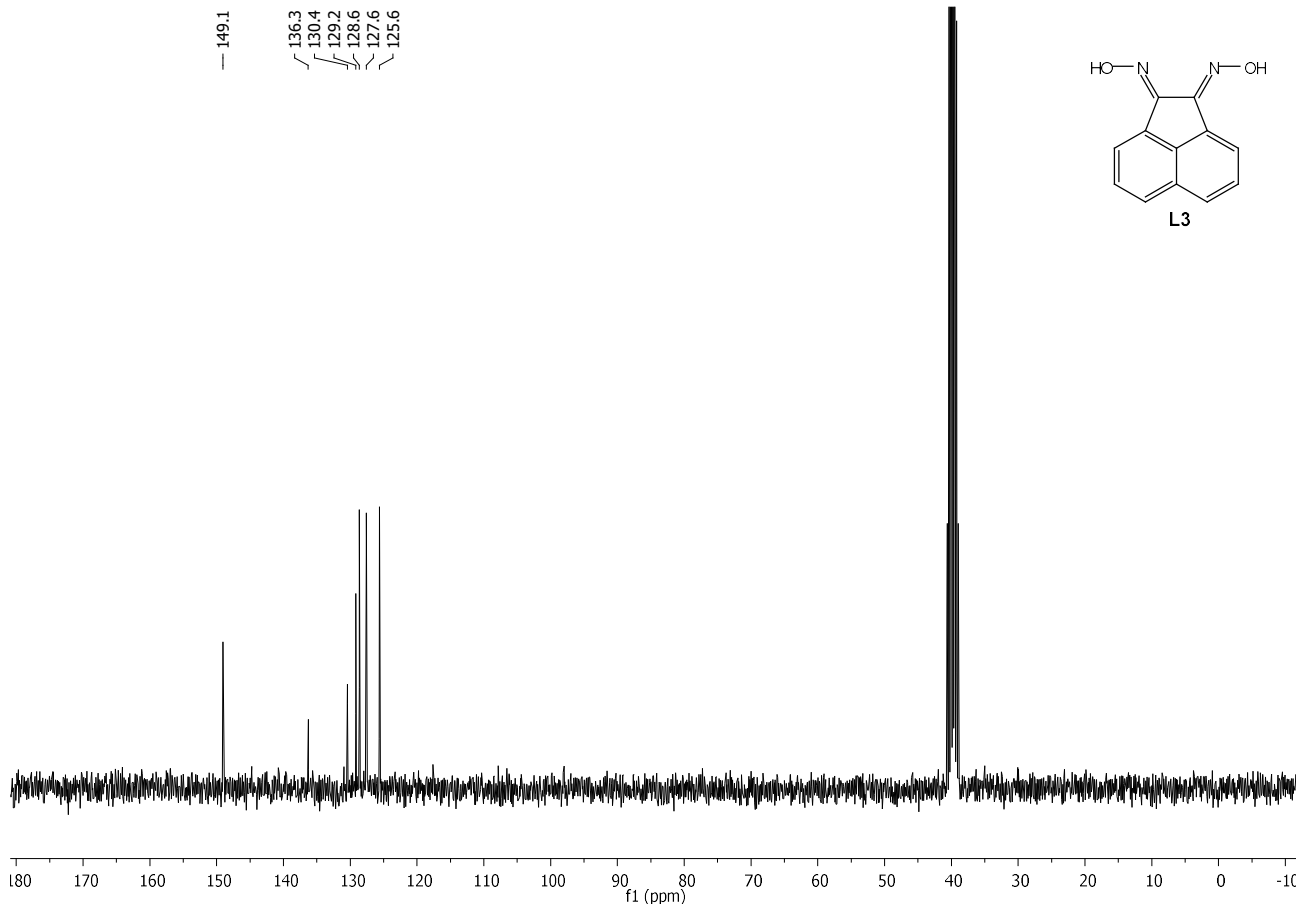
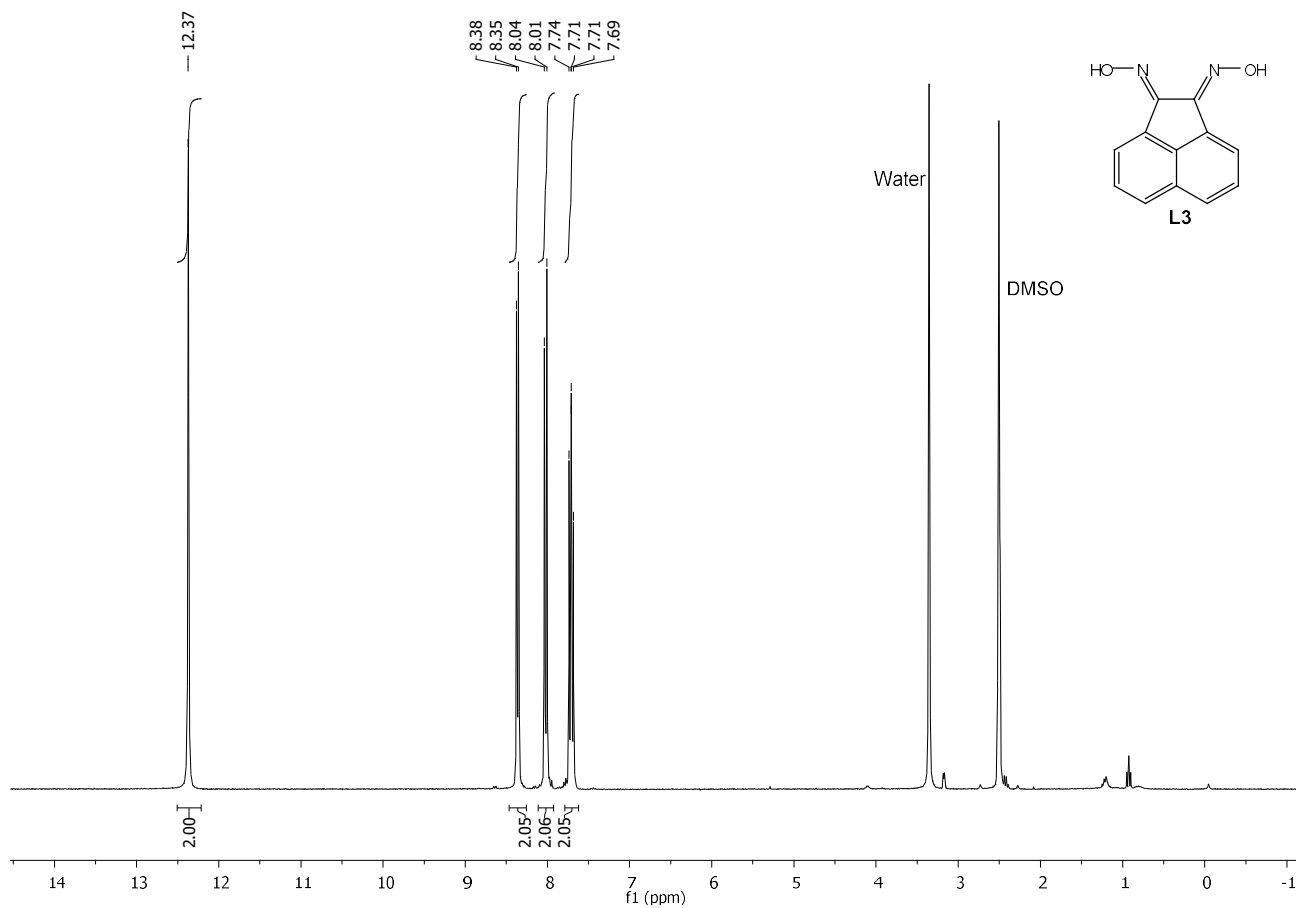
After the reaction was complete, the catalyst was separated using a Pasteur pipette filled with Celite® and the Celite® pad was washed with AcOEt. The solvent was removed in vacuo affording the product as a pale orange solid.

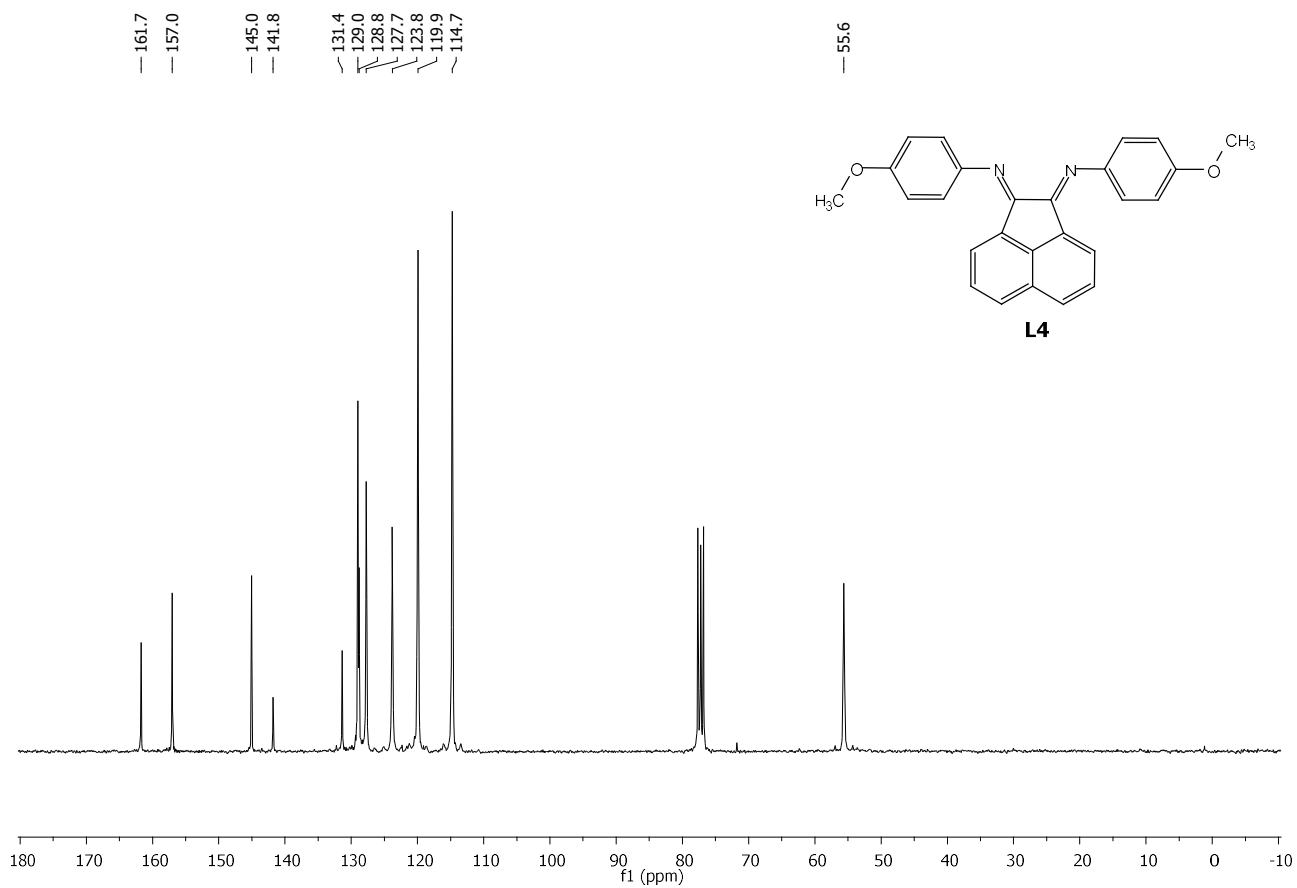
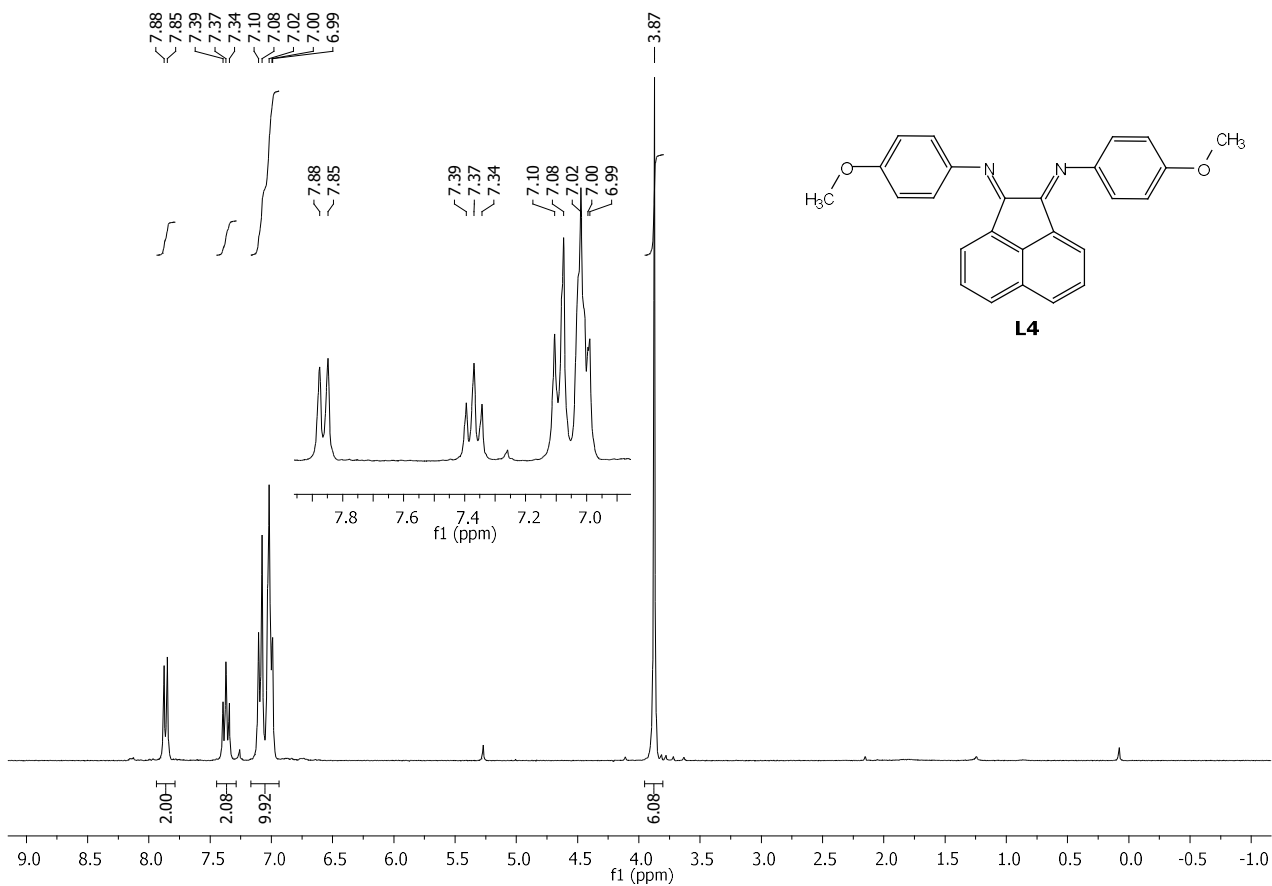
^1H NMR (300 MHz, CDCl_3) δ 7.54 (d, $J = 2.4$ Hz, 1H), 7.45 (dd, $J = 8.7, 2.3$ Hz, 1H), 7.31 (br, 1H), 6.68 (d, $J = 8.7$ Hz, 1H) 4.05 (br, 2H), 2.63 – 2.30 (sept, $J = 6.9$ Hz, 1H), 1.22 (d, $J = 6.9$ Hz, 6H) ppm. ^{13}C NMR (75 MHz, CDCl_3) δ 175.5, 141.3, 128.6, 126.0, 119.0 (q, $J = 5.2$ Hz), 117.7, 114.0, 36.3, 19.6 ppm. ^{19}F NMR (282 MHz, CDCl_3) δ -62.5. Elemental analysis for $\text{C}_{11}\text{H}_{13}\text{F}_3\text{N}_2\text{O}$ (%): C 53.66; H 5.32; N 11.38. Found: C 53.59; H 5.35; N 11.25.

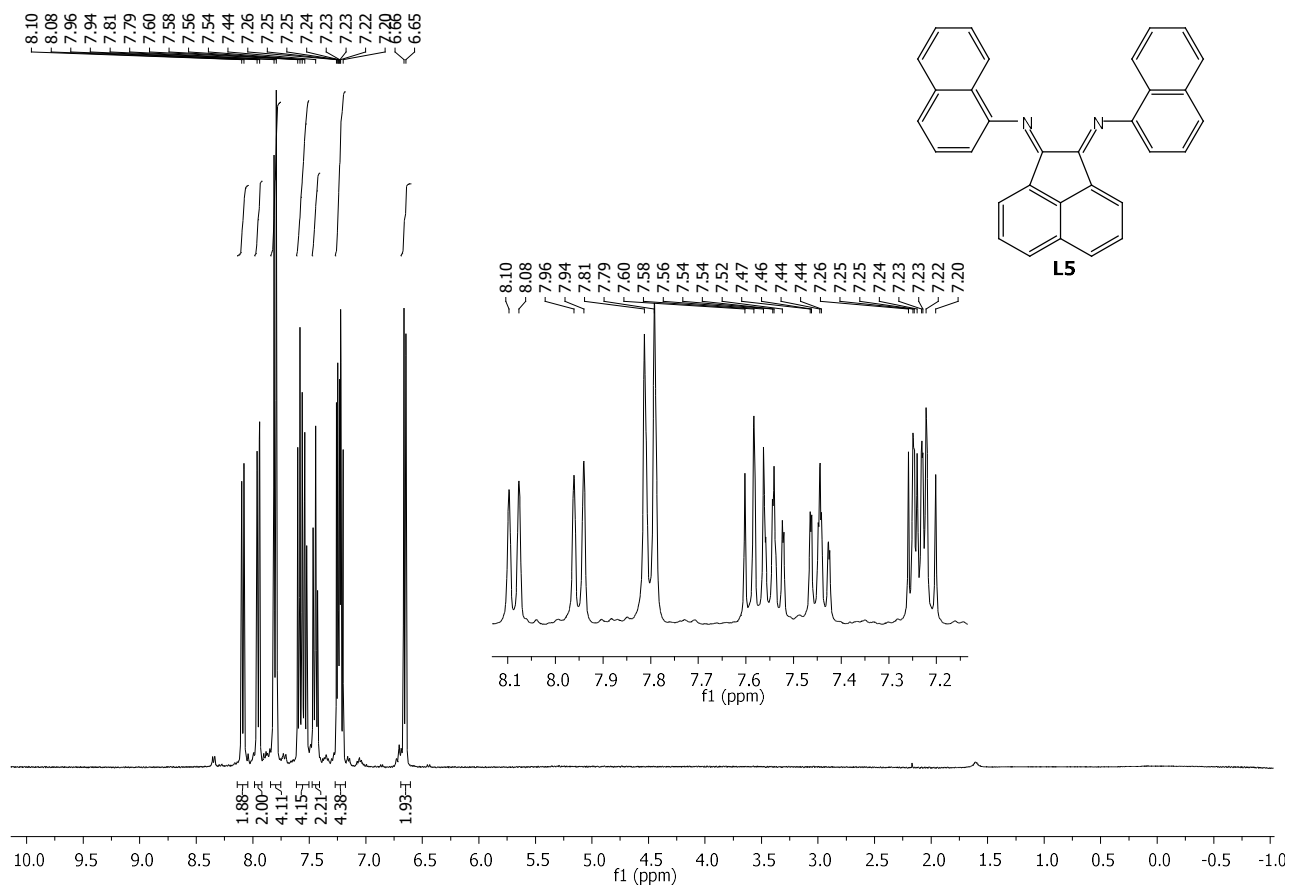
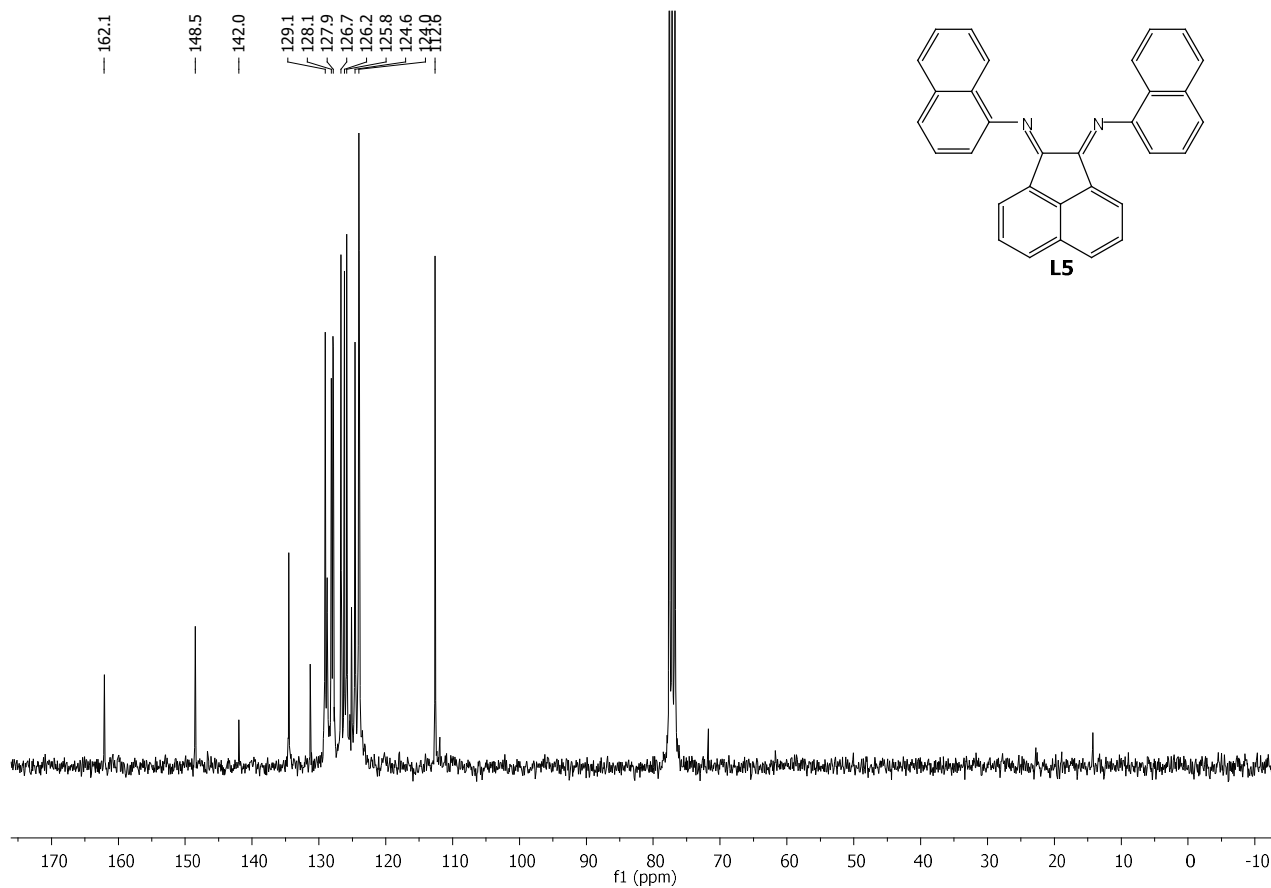
6.8. NMR

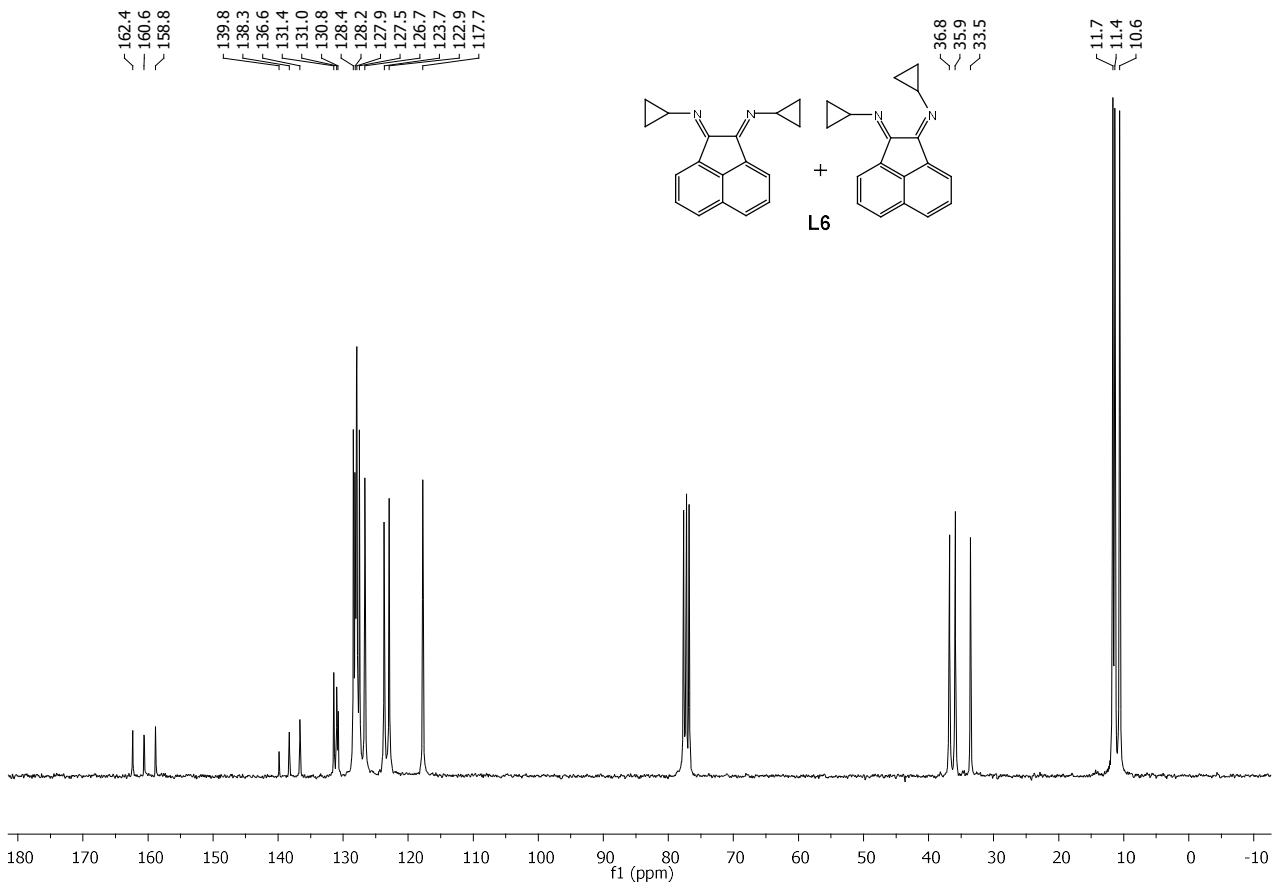
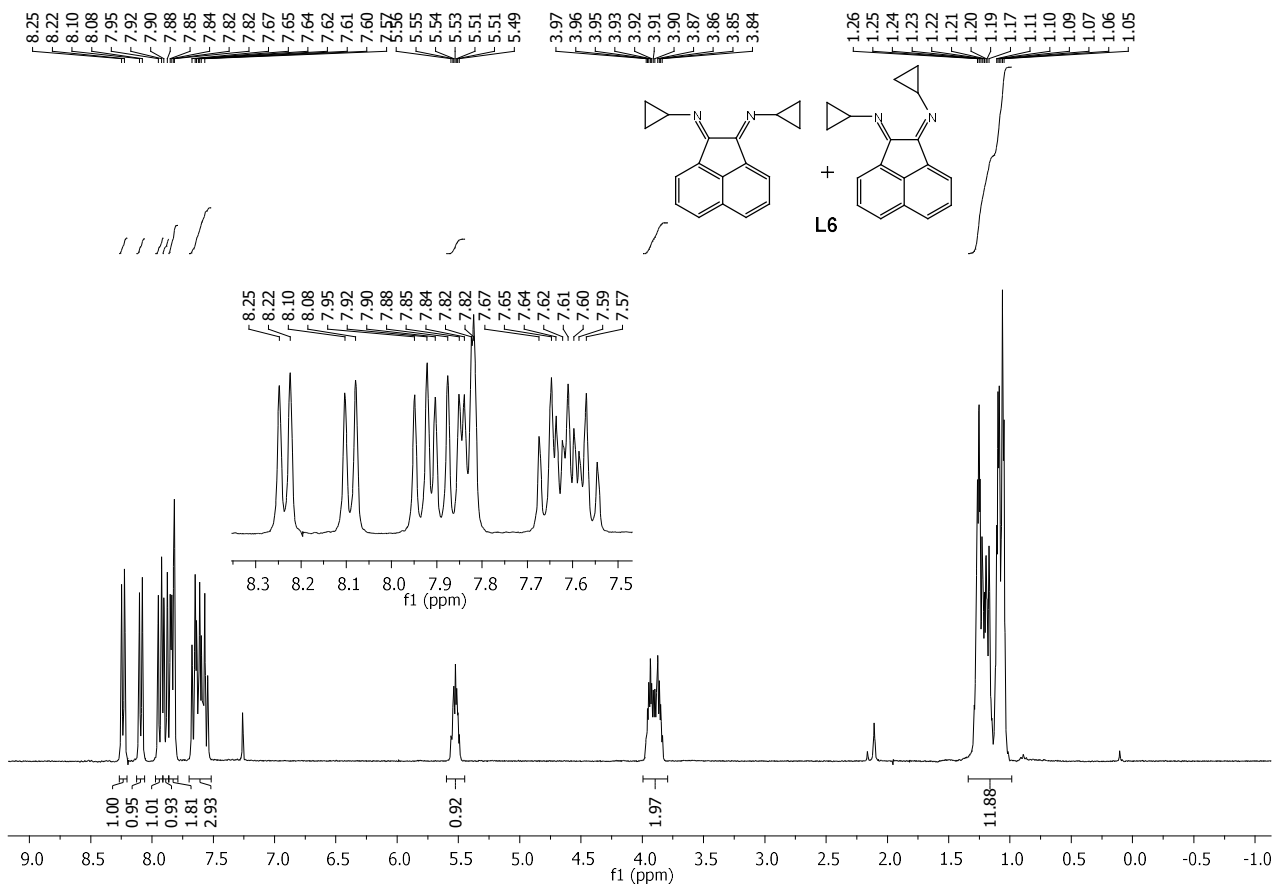


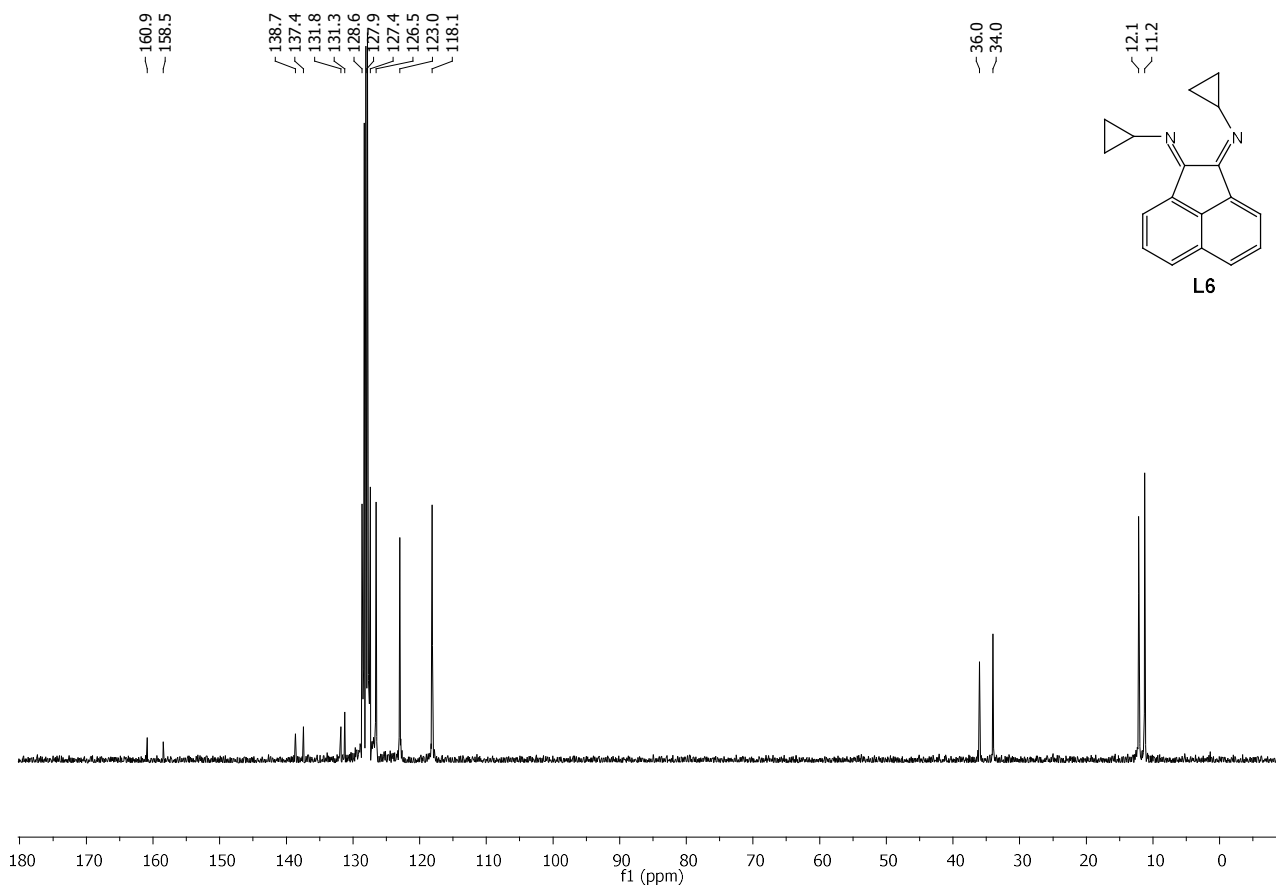
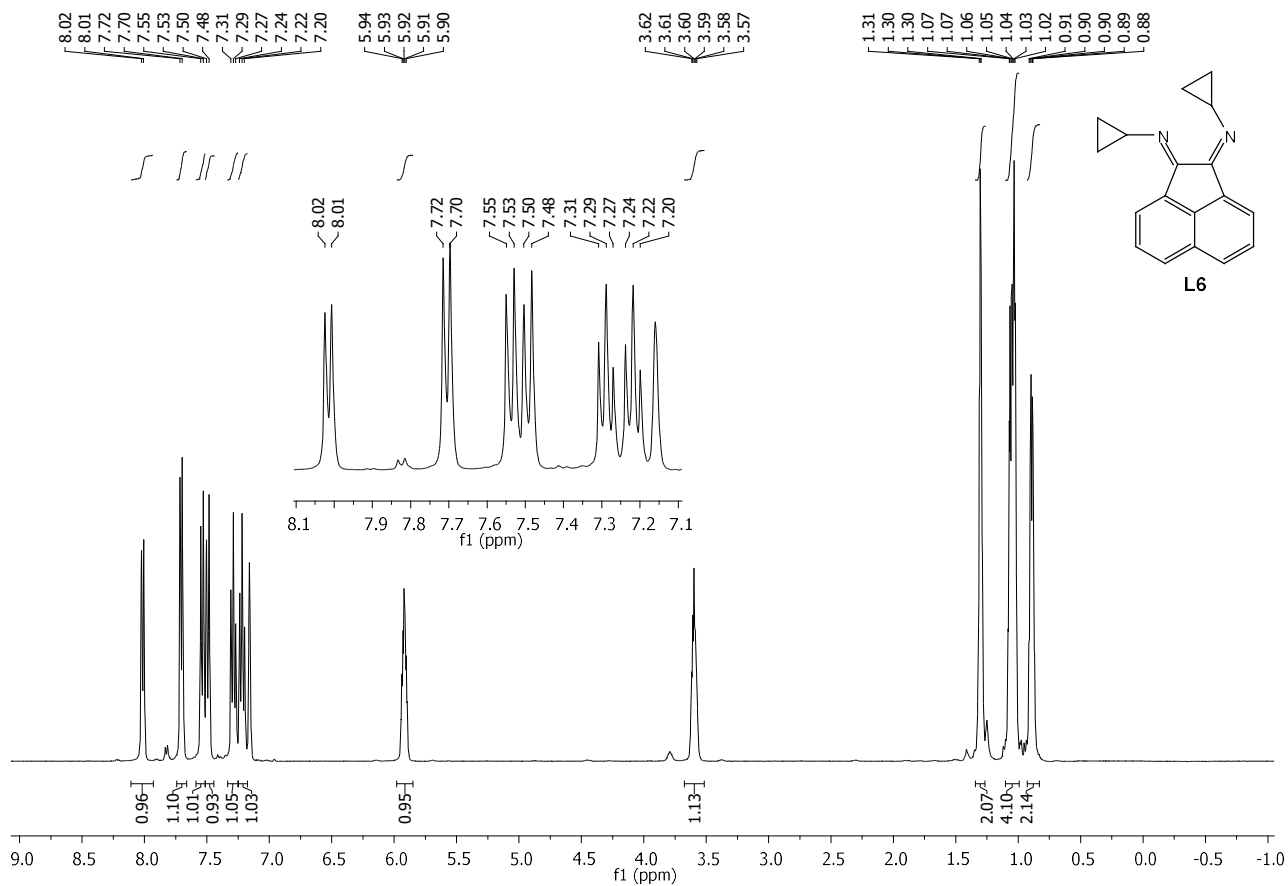


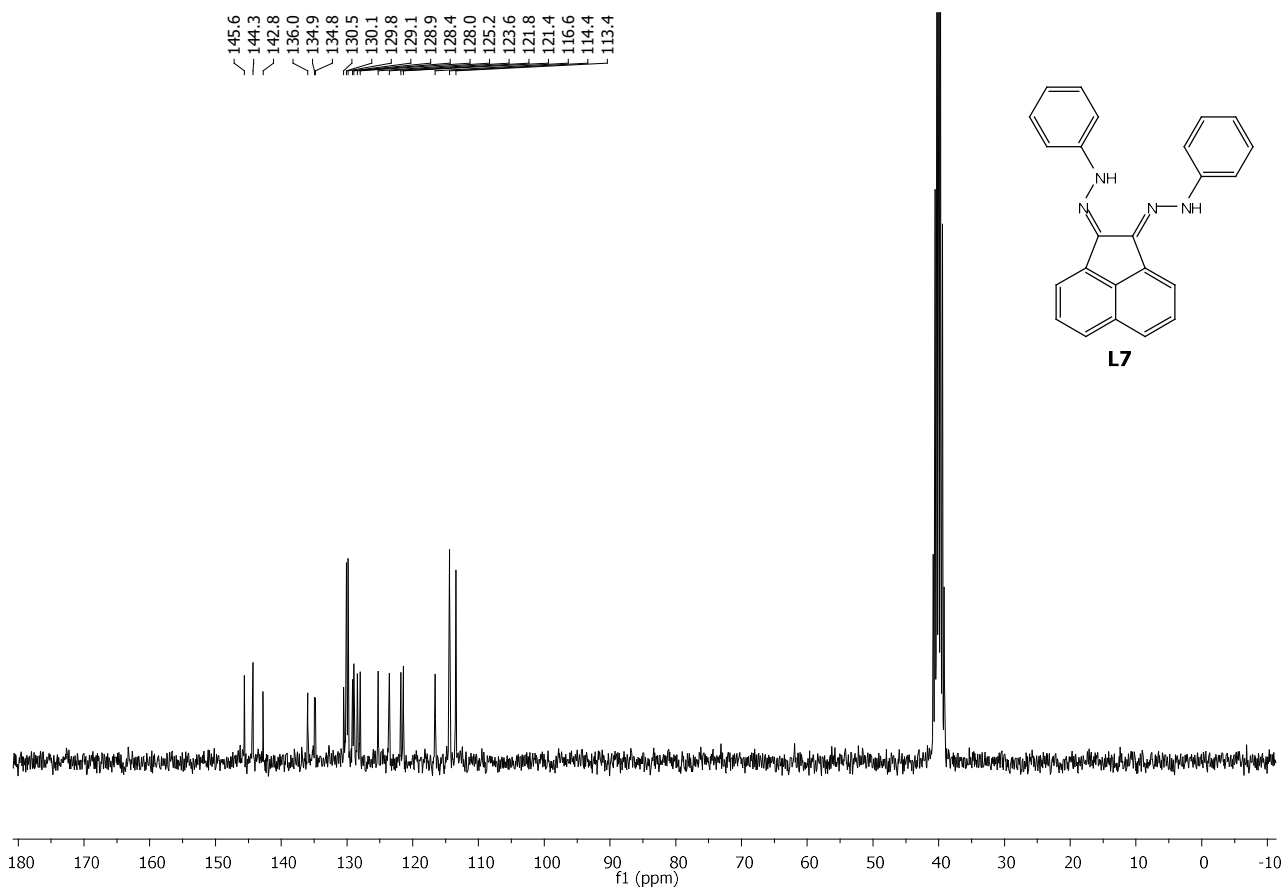
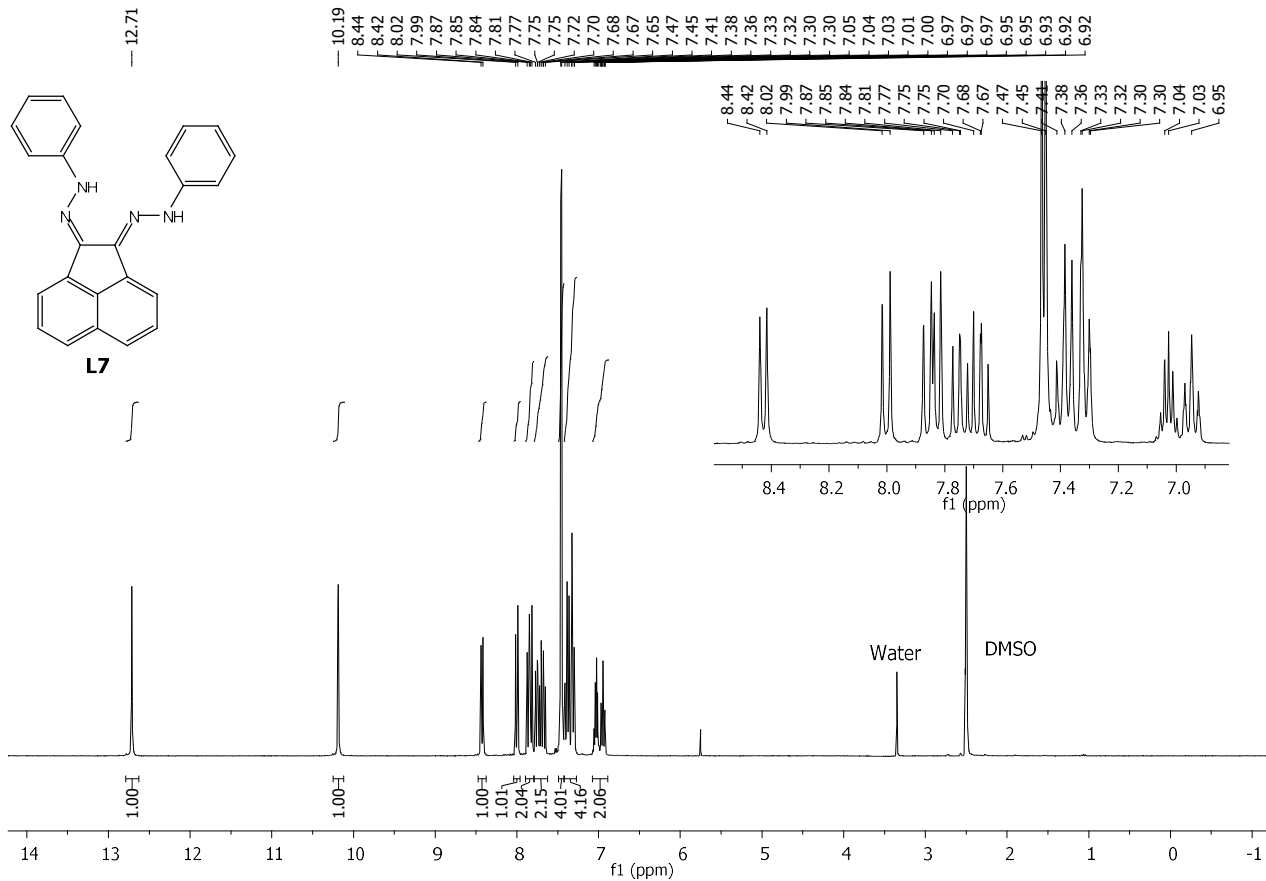


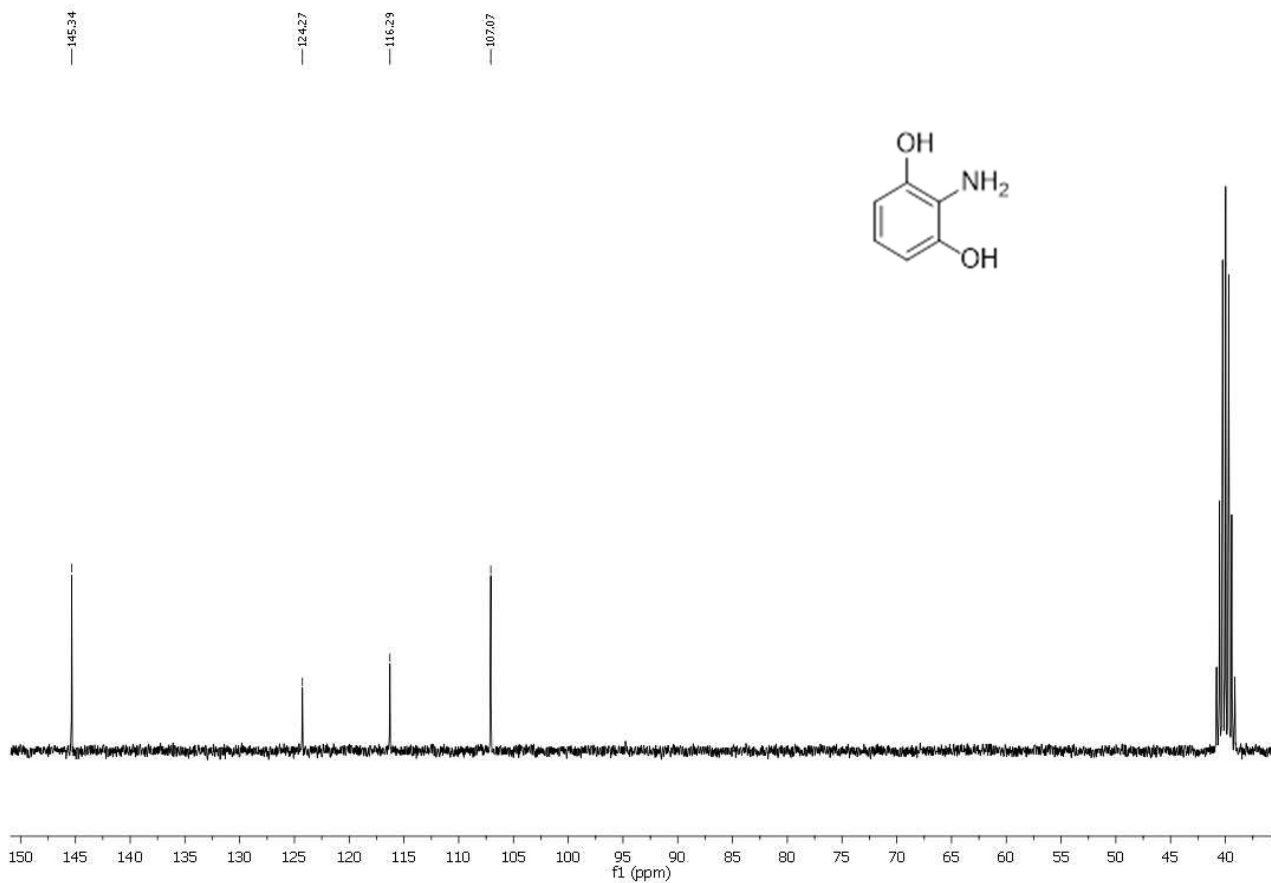
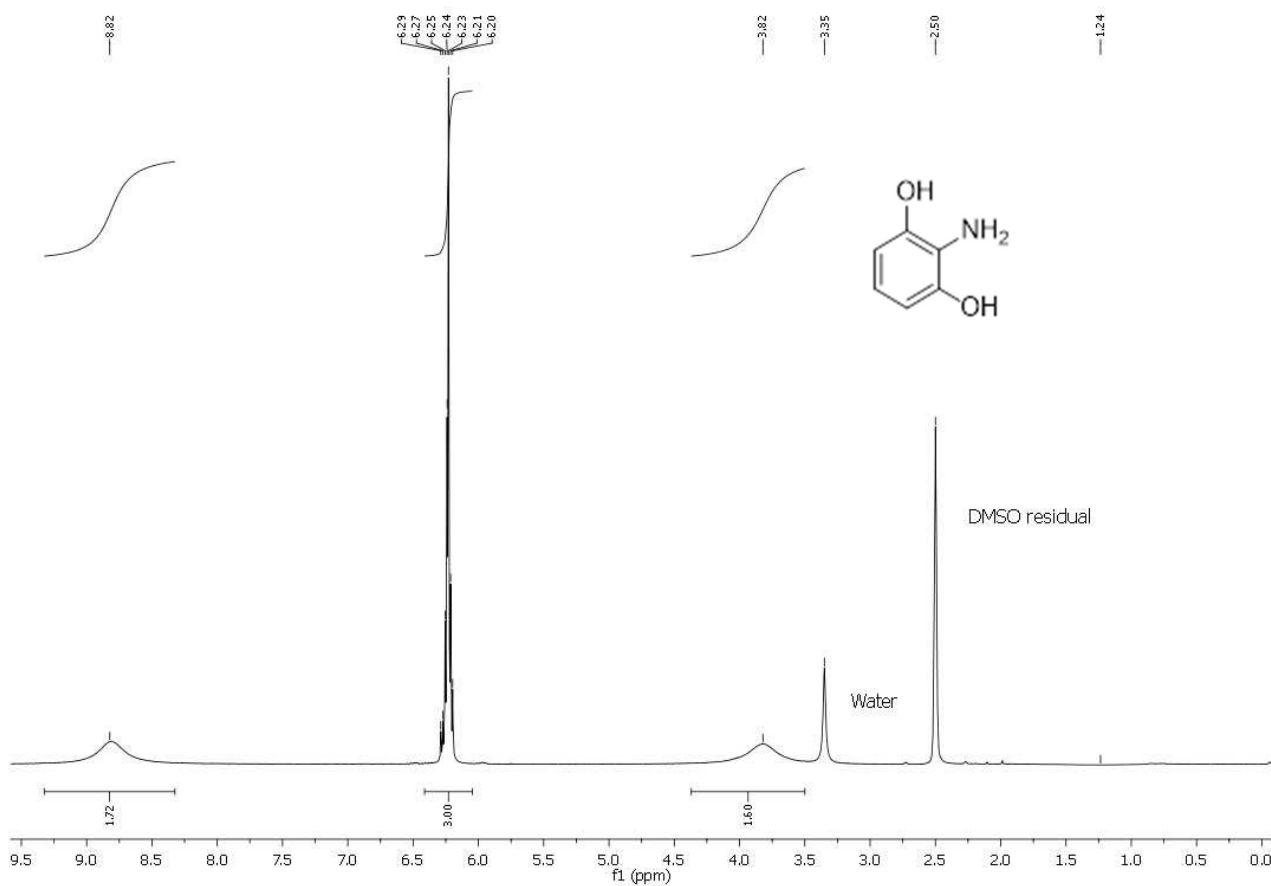


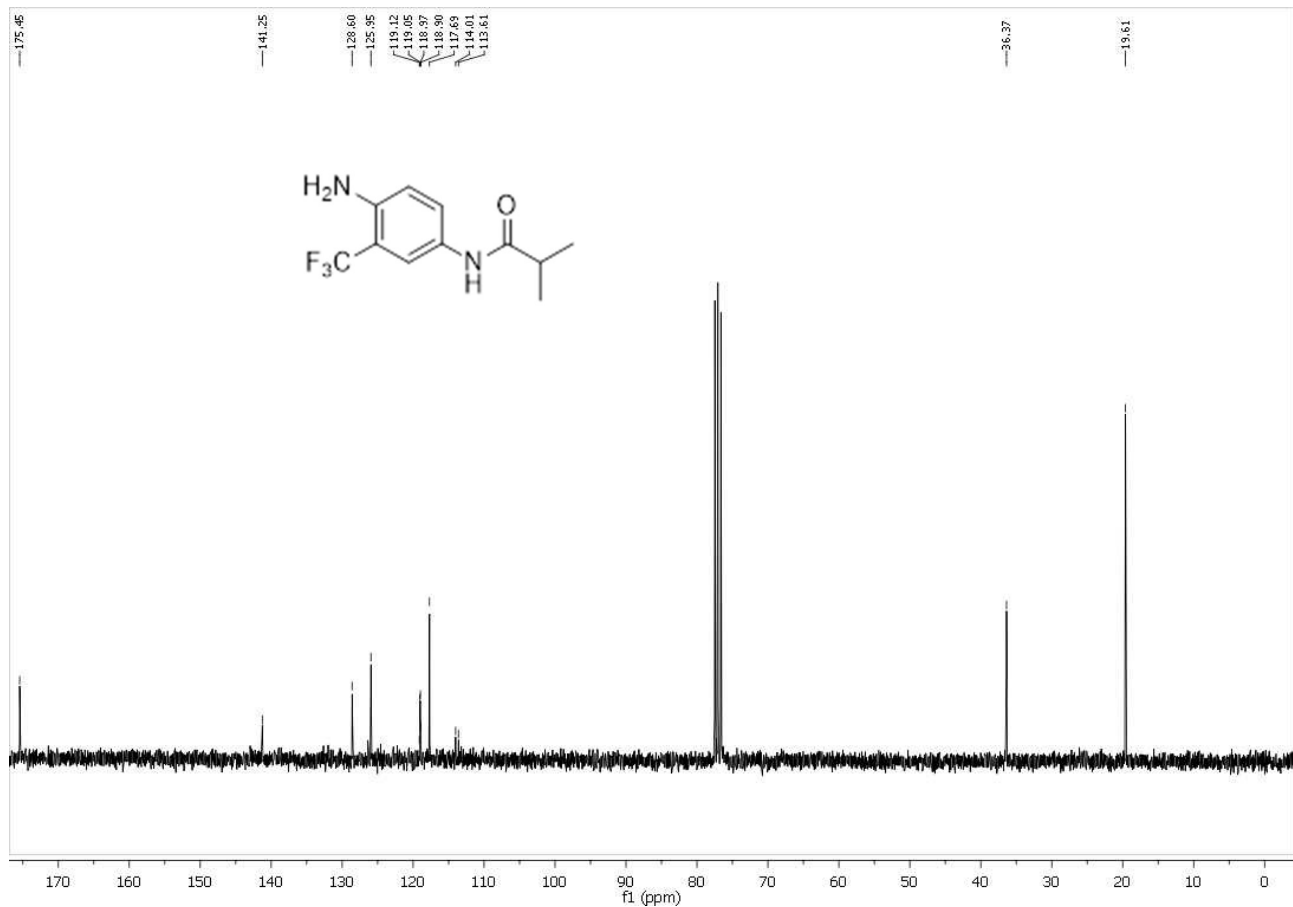
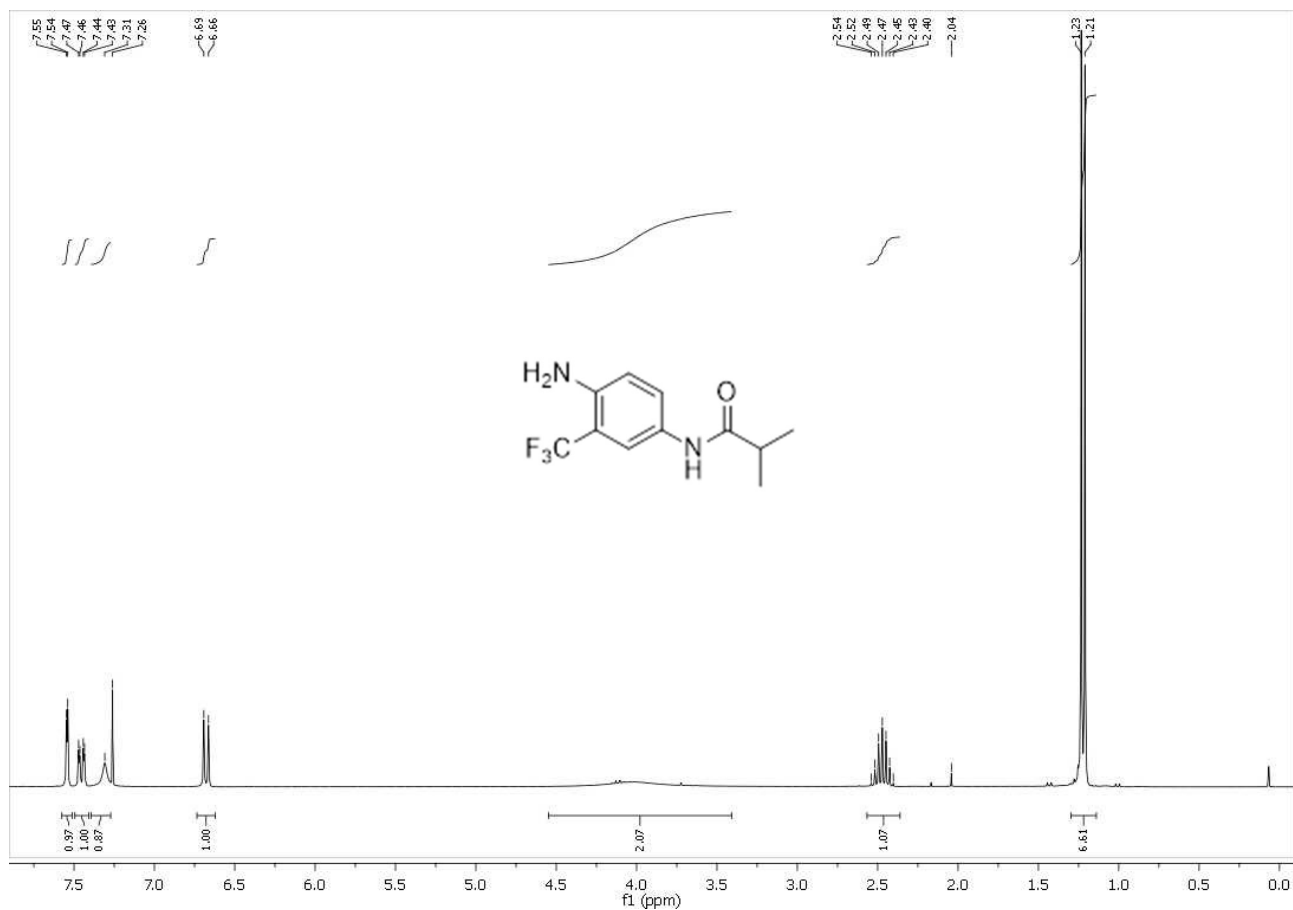












References

- [1] (a) H.-J. Arpe, *Industrial Organic Chemistry*, Wiley-VCH, **2010**; (b) T. Kahl, K.-W. Schröder, F. R. Lawrence, W. J. Marshall, H. Höke, R. Jäckh, in *Ullmann's Encyclopedia of Industrial Chemistry*, Wiley-VCH Verlag GmbH & Co. KGaA, **2000**; (c) R. S. Downing, P. J. Kunkeler, H. van Bekkum, *Catal. Today* **1997**, *37*, 121-136; (d) D. J. Dixon, O. Pando Morejón, *Recent Developments in the Reduction of Nitro and Nitroso Compounds in Comprehensive Organic Synthesis II (Second Edition)* (Ed. P. Knochel), **2014**, 479-492.
- [2] For excellent reviews in the field of selective reduction of nitro compounds see: (a) H.-U. Blaser, A. Schnyder, H. Steiner, F. Rössler, P. Baumeister, in *Handbook of Heterogeneous Catalysis*, Wiley-VCH Verlag GmbH & Co. KGaA, **2008**; (b) B. Chen, U. Dinggerdissen, J. G. E. Krauter, H. G. J. Lansink Rotgerink, K. Möbus, D. J. Ostgard, P. Panster, T. H. Riermeier, S. Seebald, T. Tacke, H. Trauthwein, *Appl. Catal., A.*, **2005**, *280*, 17-46.
- [3] A. Corma, P. Serna, *Science* **2006**, *313*, 332-334.
- [4] Y. Chen, C. Wang, H. Liu, J. Qiu, X. Bao, *Chem. Commun.* **2005**, 5298-5300.
- [5] H.-U. Blaser, H. Steiner, M. Studer, *ChemCatChem* **2009**, *1*, 210-221.
- [6] For recent reviews in the field of non-noble metal catalysts see: (a) M. S. Holzwarth, B. Plietker, *ChemCatChem* **2013**, *5*, 1650-1679; (b) B. Su, Z.-C. Cao, Z.-J. Shi, *Acc. Chem. Res.* **2015**, *48*, 886-896; (c) K. S. Egorova, V. P. Ananikov, *Angew. Chem. Int. Ed.* **2016**, *55*, 12150-12162; (d) S.-S. Wang, G.-Y. Yang, *Catal. Sci. Technol.* **2016**, *6*, 2862-2876; (e) J.-L. Renaud, S. Gaillard, *Synthesis* **2016**, *48*, 3659-3683; (f) Z. Chen, D. Higgins, A. Yu, L. Zhang, J. Zhang, *Energy Env. Sci.* **2011**, *4*, 3167-3192; (g) J. R. Carney, B. R. Dillon, S. P. Thomas, *Eur. J. Org. Chem.* **2016**, *23*, 3912-3929; (h) T. Olivier, *Org. Biomol. Chem.* **2013**, *11*, 2740-2755; (i) A. Fürstner, *ACS Cent. Sci.* **2015**, *2*, 778-789; (j) W. A. Czaplik, M. Mayer, J. Cvengros, A. J. von Wangelin, *ChemSusChem* **2009**, *2*, 396-417; (k) A. Welther, A. J. von Wangelin, *Curr. Org. Chem.* **2013**, *17*, 326-335.
- [7] K. H. Wedepohl, in *Elements and Their Compounds in the Environment*, Wiley-VCH Verlag GmbH, **2008**, pp. 2-16.
- [8] (a) A. Schaetz, M. Zeltner, W. J. Stark, *ACS Catal.* **2012**, *2*, 1267-1284; (b) B. F. Machado, P. Serp, *Catal. Sci. Technol.* **2012**, *2*, 54-75; (c) J. Alberro, H. Garcia, *J. Mol. Catal. A: Chem.* **2015**, *408*, 296-309; (d) L. Prati, C. E. Chan-Thaw, S. Campisi, A. Villa, *Chem. Rec.* **2016**, *16*, 2187-2197.
- [9] (a) R. Zhou, M. Jaroniec, S.-Z. Qiao, *ChemCatChem* **2015**, *7*, 3808-3817; (b) C. N. R. Rao, K. Gopalakrishnan, A. Govindaraj, *Nano Today* **2014**, *9*, 324-343; (c) J. Duan, S. Chen, M. Jaroniec, S. Z. Qiao, *ACS Catal.* **2015**, *5*, 5207-5234; (d) W. Zhang, L. Wu, Z. Li, Y. Liu, *RSC Adv.* **2014**, *5*, 49521-49533.
- [10] (a) X. Fan, G. Zhang, F. Zhang, *Chem. Soc. Rev.* **2015**, *44*, 3023-3035; (b) H. Liu, Y. Liu, D. Zhu, *J. Mater. Chem.* **2011**, *21*, 3335-3345.
- [11] (a) H. Wang, T. Maiyalagan, X. Wang, *ACS Catal.* **2012**, *2*, 781-794; (b) J. Masa, W. Xia, M. Muhler, W. Schuhmann, *Angew. Chem. Int. Ed.* **2015**, *54*, 10102-10120.
- [12] (a) M. Li, F. Xu, H. Li, Y. Wang, *Catal. Sci. Technol.* **2016**, *6*, 3670-3693; (b) D. W. Chang, J.-B. Baek, *Chemistry – An Asian Journal* **2016**, *11*, 1125-1137; (c) O. Y. Podyacheva, Z. R. Ismagilov, *Catal. Today* **2015**, *249*, 12-22; (d) L. He, F. Weniger, H. Neumann, M. Beller, *Angew. Chem. Int. Ed.* **2016**, *55*, 12582-12594; (e) K. N. Wood, R. O'Hayre, S. Pylypenko, *Energy Env. Sci.* **2014**, *7*, 1212-1249.
- [13] R. V. Jagadeesh, A.-E. Surkus, H. Junge, M.-M. Pohl, J. Radnik, J. Rabeah, H. Huan, V. Schünemann, A. Brückner, M. Beller, *Science* **2013**, *342*, 1073-1076.
- [14] F. A. Westerhaus, R. V. Jagadeesh, G. Wienhöfer, M.-M. Pohl, J. Radnik, A.-E. Surkus, J. Rabeah, K. Junge, H. Junge, M. Nielsen, A. Brückner, M. Beller, *Nat Chem* **2013**, *5*, 537-543. For the same kind of catalyst supported onto carbon nanotubes see: T. Baramov, P. Loos, J. Hassfeld, H. Alex, M. Beller, T. Stemmler, G. Meier, M. Gottfried, S. Roggan, *Adv. Synth. Catal.* **2016**, *358*, 2903-2911.
- [15] S. Pisiewicz, D. Formenti, A.-E. Surkus, M.-M. Pohl, J. Radnik, K. Junge, C. Topf, S. Bachmann, M. Scalone, M. Beller, *ChemCatChem* **2016**, *8*, 129-134.
- [16] (a) R. V. Jagadeesh, H. Junge, M.-M. Pohl, J. Radnik, A. Brückner, M. Beller, *J. Am. Chem. Soc.* **2013**, *135*, 10776-10782; (b) D. Banerjee, R. V. Jagadeesh, K. Junge, M.-M. Pohl, J. Radnik, A. Brückner, M. Beller, *Angew. Chem. Int. Ed.* **2014**, *53*, 4359-4363; (c) R. V. Jagadeesh, H. Junge, M.

- Beller, *Nat Commun* **2014**, *5*; (d) R. V. Jagadeesh, T. Stemmler, A.-E. Surkus, M. Bauer, M.-M. Pohl, J. Radnik, K. Junge, H. Junge, A. Bruckner, M. Beller, *Nat. Protocols* **2015**, *10*, 916-926; (e) K. Natte, R. V. Jagadeesh, M. Sharif, H. Neumann, M. Beller, *Org. Biomol. Chem.* **2016**, *14*, 3356-3359; (f) R. V. Jagadeesh, H. Junge, M. Beller, *ChemSusChem* **2015**, *8*, 92-96.
- [17] (a) R. V. Jagadeesh, D. Banerjee, P. B. Arockiam, H. Junge, K. Junge, M.-M. Pohl, J. Radnik, A. Bruckner, M. Beller, *Green Chem.* **2015**, *17*, 898-902; (b) R. V. Jagadeesh, K. Natte, H. Junge, M. Beller, *ACS Catal.* **2015**, *5*, 1526-1529.
- [18] (a) S. Pisiewicz, T. Stemmler, A.-E. Surkus, K. Junge, M. Beller, *ChemCatChem* **2015**, *7*, 62-64; (b) T. Stemmler, A.-E. Surkus, M.-M. Pohl, K. Junge, M. Beller, *ChemSusChem* **2014**, *7*, 3012-3016.
- [19] (a) F. Chen, A.-E. Surkus, L. He, M.-M. Pohl, J. Radnik, C. Topf, K. Junge, M. Beller, *J. Am. Chem. Soc.* **2015**, *137*, 11718-11724; (b) T. Stemmler, F. Chen, S. Pisiewicz, A. E. Surkus, M. M. Pohl, C. Topf, M. Beller, *J. Mater. Chem., A* **2015**, *3*, 17728-17737; (c) F. A. Westerhaus, I. Sorribes, G. Wienhöfer, K. Junge, M. Beller, *Synlett* **2015**, *26*, 313-317; (d) F. Chen, C. Topf, J. Radnik, C. Kreyenschulte, H. Lund, M. Schneider, A.-E. Surkus, L. He, K. Junge, M. Beller, *J. Am. Chem. Soc.* **2016**, *138*, 8781-8788; (e) X. Cui, Y. Li, S. Bachmann, M. Scalone, A.-E. Surkus, K. Junge, C. Topf, M. Beller, *J. Am. Chem. Soc.* **2015**, *137*, 10652-10658.
- [20] (a) D. Prat, J. Hayler, A. Wells, *Green Chem.* **2014**, *16*, 4546-4551; (b) C. M. Alder, J. D. Hayler, R. K. Henderson, A. M. Redman, L. Shukla, L. E. Shuster, H. F. Sneddon, *Green Chem.* **2016**, *18*, 3879-3890; (c) H. E. Gottlieb, G. Graczyk-Millbrandt, G. G. A. Inglis, A. Nudelman, D. Perez, Y. Qian, L. E. Shuster, H. F. Sneddon, R. J. Upton, *Green Chem.* **2016**, *18*, 3867-3878.
- [21] (a) H. S. Fry, J. L. Cameron, *J. Am. Chem. Soc.* **1927**, *49*, 864-873; (b) C. M. Suter, F. B. Dains, *J. Am. Chem. Soc.* **1928**, *50*, 2733-2739.
- [22] R. K. Henderson, A. P. Hill, A. M. Redman, H. F. Sneddon, *Green Chem.* **2015**, *17*, 945-949.
- [23] For selected examples see: (a) R. A. Sánchez-Delgado, N. Machalaba, N. Ng-a-qui, *Catal. Commun.* **2007**, *8*, 2115-2118; (b) M. Fang, N. Machalaba, R. A. Sanchez-Delgado, *Dalton Trans.* **2011**, *40*, 10621-10632; (c) M. Fang, R. A. Sánchez-Delgado, *J. Catal.* **2014**, *311*, 357-368; (d) A. Sánchez, M. Fang, A. Ahmed, R. A. Sánchez-Delgado, *Appl. Catal., A* **2014**, *477*, 117-124.
- [24] (a) T. Xu, D. Chen, X. Hu, *Coord. Chem. Rev.* **2015**, *303*, 32-41; (b) O. Eisenstein, R. H. Crabtree, *New J. Chem.* **2013**, *37*, 21-27; (c) D. W. Stephan, G. Erker, *Angew. Chem. Int. Ed.* **2015**, *54*, 6400-6441; (d) R. M. Bullock, *Chem. Eur. J.* **2004**, *10*, 2366-2374.
- [25] M. Viganò, F. Ferretti, A. Caselli, F. Ragaini, M. Rossi, P. Mussini, P. Macchi, *Chem. Eur. J.* **2014**, *20*, 14451-14464 and references cited therein.
- [26] N. A. M. Barakat, B. Kim, S. J. Park, Y. Jo, M.-H. Jung, H. Y. Kim, *J. Mater. Chem.* **2009**, *19*, 7371-7378.
- [27] L. Zhang, P. Hu, X. Zhao, R. Tian, R. Zou, D. Xia, *J. Mater. Chem.* **2011**, *21*, 18279-18283.
- [28] F. Jaouen, J. Herranz, M. Lefèvre, J.-P. Dodelet, U. I. Kramm, I. Herrmann, P. Bogdanoff, J. Maruyama, T. Nagaoka, A. Garsuch, J. R. Dahn, T. Olson, S. Pylypenko, P. Atanassov, E. A. Ustinov, *ACS Appl. Mater. Interf.* **2009**, *1*, 1623-1639.
- [29] Y. Su, Y. Zhu, H. Jiang, J. Shen, X. Yang, W. Zou, J. Chen, C. Li, *Nanoscale* **2014**, *6*, 15080-15089.
- [30] Q. He, Q. Li, S. Khene, X. Ren, F. E. López-Suárez, D. Lozano-Castelló, A. Bueno-López, G. Wu, *J. Phys. Chem. C* **2013**, *117*, 8697-8707.
- [31] M. C. Biesinger, B. P. Payne, A. P. Grosvenor, L. W. M. Lau, A. R. Gerson, R. S. C. Smart, *Appl. Surf. Sci.* **2011**, *257*, 2717-2730.
- [32] (a) E. Bamberger, J. Lagutt, *Chem. Ber.* **1898**, *31*, 1500-1508; (b) H. Lund, in *Organic Electrochemistry* (Ed.: O. H. Henning Lund), CRC Press, New York, **2000**.
- [33] E. Müller, E. Lindemann, *Angew. Chem.* **1933**, *46*, 681-685.
- [34] Y.-S. Choi, Y.-J. Kim, L.-L. Shen, Y. S. Lee, J.-H. Jeong, *Synlett* **2015**, *26*, 970-974.
- [35] (a) A. Urios, M. Llargeron, M.-B. Fleury, M. Blanco, *Free Radical Biol. Med.* **2006**, *40*, 791-800; (b) H. Gao, J. Kawabata, *Bioorg. Med. Chem. Lett.* **2008**, *18*, 812-815; (c) E. Kato, K. Oikawa, K. Takahashi, J. Kawabata, *Biosci., Biotechnol., Biochem.* **2012**, *76*, 1044-1046; (d) E. Kato, H. Tsuji, J. Kawabata, *Tetrahedron* **2015**, *71*, 1419-1424; (e) B. Wen, K. J. Coe, P. Rademacher, W. L. Fitch, M. Monshouwer, S. D. Nelson, *Chem. Res. Toxicol.* **2008**, *21*, 2393-2406; (f) W. Herath, I. A. Khan, *Chem. Pharm. Bull.* **2010**, *58*, 562-564.
- [36] K. B. Borisenko, I. Hargittai, *J. Phys. Chem.* **1993**, *97*, 4080-4084.
- [37] G. Akerlof, *J. Am. Chem. Soc.* **1932**, *54*, 4125-4139.

- [38] (a) F. Jaouen, S. Marcotte, J.-P. Dodelet, G. Lindbergh, *J. Phys. Chem. B* **2003**, *107*, 1376-1386; (b) P. H. Matter, L. Zhang, U. S. Ozkan, *J. Catal.* **2006**, *239*, 83-96; (c) G. Faubert, R. Côté, J. P. Dodelet, M. Lefèvre, P. Bertrand, *Electrochim. Acta* **1999**, *44*, 2589-2603; (d) D. Guo, R. Shibuya, C. Akiba, S. Saji, T. Kondo, J. Nakamura, *Science* **2016**, *351*, 361-365.
- [39] (a) J. V. H. d'Angelo, A. Z. Francesconi, *J. Chem. Eng. Data* **2001**, *46*, 671-674; (b) K. Radhakrishnan, P. A. Ramachandran, P. H. Brahme, R. V. Chaudhari, *J. Chem. Eng. Data* **1983**, *28*, 1-4.
- [40] (a) L. Zhang, A. Wang, W. Wang, Y. Huang, X. Liu, S. Miao, J. Liu, T. Zhang, *ACS Catal.* **2015**, 6563-6572; (b) U. I. Kramm, I. Herrmann-Geppert, J. Behrends, K. Lips, S. Fiechter, P. Bogdanoff, *J. Am. Chem. Soc.* **2016**, *138*, 635-640; (c) A. Zitolo, V. Goellner, V. Armel, M.-T. Sougrati, T. Mineva, L. Stievano, E. Fonda, F. Jaouen, *Nat. Mater.* **2015**, *14*, 937-942; (d) T. Cheng, H. Yu, F. Peng, H. Wang, B. Zhang, D. Su, *Catal. Sci. Technol.* **2016**, *6*, 1007-1015; (e) C. E. Szakacs, M. Lefevre, U. I. Kramm, J.-P. Dodelet, F. Vidal, *PCCP* **2014**, *16*, 13654-13661; (f) Y. Zhu, B. Zhang, X. Liu, D.-W. Wang, D. S. Su, *Angew. Chem. Int. Ed.* **2014**, *53*, 10673-10677; (g) W. Liu, L. Zhang, W. Yan, X. Liu, X. Yang, S. Miao, W. Wang, A. Wang, T. Zhang, *Chem. Sci.* **2016**, *7*, 5758-5764; (h) X. Zhang, P. Lu, X. Cui, L. Chen, C. Zhang, M. Li, Y. Xu, J. Shi, *J. Catal.* **2016**, *344*, 455-464; (i) F. Jaouen, F. Charreter, J. P. Dodelet, *J. Electrochem. Soc.* **2006**, *153*, A689-A698; (j) N. Ramaswamy, U. Tylus, Q. Jia, S. Mukerjee, *J. Am. Chem. Soc.* **2013**, *135*, 15443-15449; (k) Q. Jia, N. Ramaswamy, U. Tylus, K. Strickland, J. Li, A. Serov, K. Artyushkova, P. Atanassov, J. Anibal, C. Gumeci, S. Calabrese Barton, M.-T. Sougrati, F. Jaouen, B. Halevi, S. Mukerjee, *Nano Energy* **2015**, *29*, 65-82.
- [41] B. Li, X. Sun, D. Su, *PCCP* **2015**, *17*, 6691-6694.
- [42] F. Ragaini, S. Cenini, D. Brignoli, M. Gasperini, E. Gallo, *J. Org. Chem.* **2002**, *68*, 460-466.
- [43] V. Rosa, T. Avilés, G. Aullon, B. Covelo, C. Lodeiro, *Inorg. Chem.* **2008**, *47*, 7734-7744.
- [44] C. Graebe, E. Gfeller, *Just. Lieb. Ann. Chem.* **1893**, *276*, 1-20.
- [45] H. C. Rai, B. K. Rai, *Asian J. Chem.* **2001**, *13*, 264-268.
- [46] (a) F. Ragaini, M. Gasperini, E. Gallo, P. Macchi, *Chem. Commun.* **2005**, 1031-1033; (b) F. Ragaini, M. Gasperini, P. Parma, E. Gallo, N. Casati, P. Macchi, *New J. Chem.* **2006**, *30*, 1046-1057.

A part of this chapter (including figures, tables and schemes) was reproduced by permission of The Royal Society of Chemistry©.

Original citation is:

Dario Formenti, Christoph Topf, Kathrin Junge, Fabio Ragaini and Matthias Beller
Catal. Sci. Technol. **2016**, *6*, 4473-4477; DOI: 10.1039/C5CY01925G.

Chapter IV

Appendix

1. Papers published

1. F. Ragaini, M. Viganò, F. Ferretti, M. Hagar, D. Formenti, M. Villa.

The Schiff bases of BIAN chemistry. The evolution of a ligand.

La Chimica & l'Industria **2013**, 6, 133-139.

2. S. Pisiewicz, D. Formenti, A.-E. Surkus, M.-M. Pohl, J. Radnik, K. Junge, C. Topf, S. Bachmann, M. Scalone, M. Beller.

Synthesis of novel nickel nanoparticles with N-doped graphene for catalytic reductions.

ChemCatChem **2016**, 8, 129-134

3. D. Formenti, C. Topf, K. Junge, F. Ragaini, M. Beller.

Fe₂O₃/NGr@C and Co-Co₃O₄/NGr@C-catalysed hydrogenation of nitroarenes under mild conditions.

Cat. Sci. Tech. **2016**, 6, 4473-4477.

2. Papers submitted (last update December, 18th, 2016)

1. D. Formenti, F. Ferretti, C. Topf, A.-E. Surkus, M.-M. Pohl, J. Radnik, M. Schneider, K. Junge, M. Beller, F. Ragaini.

Co-Based heterogeneous catalysts from well-defined α -diimine complexes: discussing the role of nitrogen.

2. F. Ferretti, D. Formenti, F. Ragaini

The reduction of organic nitro compounds by carbon monoxide as an effective strategy for the synthesis of N-heterocyclic compounds: a personal account.

3. Communications to schools and congress

1. F. Ragaini, M. Hagar, E. Storer, F. Ferretti, D. Formenti, M. Villa

Alkyl formates as CO alternatives in nitroarenes deoxygenation to give indoles. (Oral Communication)

20th EuChemMS Conference on Organometallic Chemistry

St. Andrews, Scotland, June 30 – July 4, **2013**

2. M. El-Atawy, M. Hagar, F. Ferretti, D. Formenti, S. Muto, F. Ragaini

Carbon monoxide as a reductant: synthesis of indoles by palladium catalyzed reductive cyclization of ortho-nitrostyrenes. (Poster)

13th Sigma-Aldrich Young Chemists Symposium

Riccione, Italy, October 28-30, **2013**

3. D. Formenti, F. Ferretti, E. Storer, F. Ragaini

Formate esters as CO sources: synthesis of indoles by reductive cyclization of *ortho*-nitrostyrenes. (Poster)

XI Interdivisional Congress of Organometallic Chemistry of the Italian Chemical Society

Milano, Italy, June 24-27, **2014**

4. D. Formenti, F. Ferretti, F. Ragaini

Indole synthesis by reductive cyclization of ortho-nitrostyrenes: formate ester as CO surrogates. (Oral Communication)

14th Sigma-Aldrich Young Chemists Symposium

Riccione, Italy, October 27-29, **2014**

5. D. Formenti, F. Ferretti, C. Topf, A.-E. Surkus, K. Junge, M. Beller, F. Ragaini

Co-based heterogeneous catalysts from well-defined complexes: synthesis and applications. (Poster)

10th International School of Organometallic Chemistry

Camerino, Italy, September 5-9, **2015**

6. D. Formenti, F. Ferretti, F. Ragaini

Reductive cyclization of nitro compounds using CO surrogates: formate esters at work. (Oral Communication)

XII Interdivisional Congress of Organometallic Chemistry of the Italian Chemical Society

Genova, Italy, June 5-8, **2016**

7. D. Formenti, F. Ferretti, F. Ragaini

Reductive cyclization of nitro compounds using CO surrogates: formate esters at work. (Oral Communication)

XII Interdivisional Congress of Organometallic Chemistry of the Italian Chemical Society

Genova, Italy, June 5-8, **2016**

8. D. Formenti, F. Ferretti, F. Ragaini

Pd-Catalyzed Synthesis of Heterocycles from Nitro Compounds using Liquid CO Sources (Poster)

6th EuChemS Congress

Seville, Spain, September 11-15, **2016**

